

# MODELLING AUSTRALIAN FIRE REGIMES

By

Douglas Kelley

Supervised By  
Sandy Harrison  
Colin Prentice  
Belinda Medlyn

A THESIS SUBMITTED TO MACQUARIE UNIVERSITY  
for the degree of  
Doctor of Philosophy  
Department of Biological Sciences  
March 2015



© Douglas Kelley, 2015.

Typeset in L<sup>A</sup>T<sub>E</sub>X 2<sub>ε</sub>.

I certify that the work in this thesis entitled “Modelling Australian Fire Regimes” has not previously been submitted for a degree nor has it been submitted as part of requirements for a degree to any other university or institution other than Macquarie University. I also certify that the thesis is an original piece of research and it has been written by me. Any help and assistance that I have received in my research work and the preparation of the thesis itself have been appropriately acknowledged. In addition, I certify that all information sources and literature used are indicated in the thesis.

---

Douglas Kelley



# Contents

<b>List of Figures</b>	<b>ix</b>
<b>List of Tables</b>	<b>xiii</b>
<b>Abstract</b>	<b>xv</b>
<b>Acknowledgements</b>	<b>xvii</b>
<b>List of Publications</b>	<b>xix</b>
<b>1 Introduction</b>	<b>1</b>
1.1 The Importance of fire in the Earth System . . . . .	2
1.1.1 The influence of fire on climate . . . . .	2
1.1.2 The influence of fire on vegetation . . . . .	4
1.1.3 The impact of fire on humans . . . . .	6
1.2 Fire in Australia . . . . .	7
1.3 The controls of fire . . . . .	9
1.3.1 Global Studies of Fire . . . . .	11
1.3.2 Controls of fire in Australia . . . . .	14
1.4 Adaptations to fire . . . . .	15
1.4.1 Fire resistance traits . . . . .	16
1.4.2 Fire-recovery traits . . . . .	17
1.4.3 Traits that promote fire . . . . .	20
1.5 Modelling fire in dynamic global vegetation models . . . . .	21
1.6 LPX . . . . .	31
1.7 Fire in a Changing Climate . . . . .	33
1.7.1 Global Projections . . . . .	33
1.7.2 Australian studies . . . . .	35
1.8 Philosophy and approach in this thesis . . . . .	36
1.9 References . . . . .	39
<b>2 A comprehensive benchmarking system for evaluating global vegetation models</b>	<b>65</b>
2.1 Introduction . . . . .	66
2.2 Materials and methods . . . . .	67
2.2.1 Principles . . . . .	67
2.2.2 Benchmark datasets . . . . .	68
fAPAR . . . . .	68

Vegetation cover . . . . .	69
NPP . . . . .	70
GPP . . . . .	70
Canopy height . . . . .	71
Burnt fraction . . . . .	71
River discharge . . . . .	71
CO <sub>2</sub> concentration . . . . .	71
2.2.3 Metrics . . . . .	71
Annual average . . . . .	73
Inter-annual variability . . . . .	73
Seasonality . . . . .	73
Relative abundance . . . . .	73
Null models . . . . .	74
2.2.4 Models . . . . .	74
Simple Diagnostic Biosphere Model . . . . .	74
LPJ . . . . .	74
LPX . . . . .	75
2.2.5 Model protocol . . . . .	75
2.3 Results . . . . .	76
2.3.1 Benchmark results . . . . .	76
fAPAR . . . . .	76
Vegetation cover . . . . .	76
NPP/GPP . . . . .	76
Canopy height . . . . .	76
Burnt fraction . . . . .	76
River discharge . . . . .	78
CO <sub>2</sub> concentration . . . . .	78
2.3.2 Sensitivity tests . . . . .	81
Incorporating data uncertainties . . . . .	81
The influence of choice of dataset . . . . .	83
Benchmarking the sensitivity to parameter tuning . . . . .	83
2.4 Discussion and conclusion . . . . .	84
2.5 References . . . . .	89
<b>3 Patterns in the abundance of post-fire resprouting in Australia based on plot-level measurements.</b>	<b>95</b>
3.1 Abstract . . . . .	96
3.2 Introduction . . . . .	97
3.3 Methods . . . . .	98
3.3.1 Structure of the database . . . . .	98
3.3.2 Plot data . . . . .	98
3.3.3 Derivation of abundance scores . . . . .	100
3.3.4 Plant functional type attribution . . . . .	100
3.3.5 Fire-response attribution . . . . .	100
3.3.6 Derivation of climate and environmental data . . . . .	101

3.3.7 Statistical analyses . . . . .	102
3.4 Results . . . . .	102
3.4.1 Fire responses and PFTs . . . . .	103
3.4.2 Fire responses and climate . . . . .	108
3.4.3 Geographical patterns in fire responses . . . . .	109
3.5 Discussion and Conclusions . . . . .	112
3.6 References . . . . .	116
3.S1 Supplementary Information . . . . .	120
<b>4 Improved simulation of fire-vegetation interactions in the Land surface Processes and eXchanges dynamic global vegetation model (LPX-Mv1)</b>	<b>125</b>
4.1 Abstract . . . . .	126
4.2 Introduction . . . . .	126
4.3 LPX model description . . . . .	127
4.4 Changes to the LPX-M fire module . . . . .	129
4.4.1 Lightning ignitions . . . . .	129
4.4.2 Fuel drying . . . . .	131
4.4.3 Fuel decomposition . . . . .	131
4.4.4 Rooting depth . . . . .	132
4.4.5 Bark thickness . . . . .	132
4.4.6 Resprouting . . . . .	134
4.5 Model configuration and test . . . . .	136
4.5.1 Testing the formulation of resprouting . . . . .	137
4.6 Model performance . . . . .	139
4.6.1 LPX-Mv1-nr . . . . .	140
4.6.2 LPX-Mv1-rs . . . . .	142
4.7 Discussion . . . . .	143
4.8 Conclusions . . . . .	144
4.9 References . . . . .	144
4.S1 Supplementary Information . . . . .	149
4.S1.1 Additional data information . . . . .	150
4.S1.2 Extended results . . . . .	162
4.S1.3 Wet dat lighting sensitivity analysis . . . . .	172
4.S1.4 Derivation of parameter for grass in Eq. 36 . . . . .	174
4.S1.5 References for data used to parameterize adaptive bark thickness vs diameter at breast height. . . . .	175
4.S1.6 References . . . . .	177
<b>5 Enhanced Australian carbon sink despite increased wildfire during the 21<sup>st</sup> century</b>	<b>181</b>
5.1 Abstract . . . . .	182
5.2 Introduction . . . . .	182
5.3 Methods . . . . .	183
5.4 Results . . . . .	184

5.4.1	Simulation of present-day carbon budget of Australia . . . . .	184
5.4.2	Response to RCP4.5 climate scenarios . . . . .	185
5.4.3	Response to RCP8.5 climate scenarios . . . . .	187
5.4.4	Impact of direct CO <sub>2</sub> effects on the 21 <sup>st</sup> century carbon cycle . .	189
5.4.5	Impact of resprouting on the 21 <sup>st</sup> century carbon cycle . . . . .	189
5.5	Discussion and Conclusions . . . . .	190
5.6	References . . . . .	191
5.S1	Supplementary Information: Enhanced Australian carbon sink despite increased wildfire during the 21 <sup>st</sup> century . . . . .	193
5.S1.1	The LPX-Mv1 DGVM . . . . .	193
5.S1.2	Historical simulations . . . . .	195
5.S1.3	Inputs for the 21 <sup>st</sup> century climate simulations . . . . .	196
5.S1.4	Sensitivity Experiments . . . . .	198
5.S1.5	Evaluation of the historical simulations . . . . .	198
5.S1.6	Definition of regions . . . . .	201
5.S1.7	Results of the individual RCP4.5 simulations . . . . .	202
5.S1.8	Ensemble and individual results of the individual RCP8.5 simulations . . . . .	205
5.S2	References . . . . .	208
<b>6</b>	<b>Conclusion</b>	<b>211</b>
6.1	References . . . . .	216

# List of Figures

1.1	Global fire emissions and its effects on climate via its contribution to the inter-annual variability of CO <sub>2</sub> and radiative forcing. . . . .	3
1.2	Burnt area and carbon emissions from fire in different ecosystems. . . . .	5
1.3	Mapped annual average burnt area; timing of the fire season; and fire season length for Australia. . . . .	8
1.4	Annual cost of fire damage to infrastructure in Australia. . . . .	9
1.5	Summary of the interactions between the controls on fire occurrence on coarse scales. . . . .	13
1.6	Relative contributions of production, moisture and natural ignitions to the limitation of fire in Australia. . . . .	15
1.7	Observations of fire frequencies for different bark thickness's and tree diameters . . . . .	17
1.8	Examples of apical, epicormic and basal resprouting in Eucalyptus woodland 4–6 months after fire. . . . .	19
1.9	Description of the simulation of vegetation dynamics used in LPJ-based DGVMs, including LPX. . . . .	32
1.10	Description of the structure of the fire component in LPX. . . . .	34
1.11	Iterative model development approach used in this thesis. . . . .	38
2.1	Illustration of all the benchmark datasets used . . . . .	70
2.2	Results of bootstrap resampling of inter-annual variability in global burnt fraction from observations compared to benchmark scores for LPJ- and LPX-DGVMs. . . . .	74
2.3	Observed seasonal cycle of atmospheric CO <sub>2</sub> concentrations at 26 CO <sub>2</sub> stations compared to the simulated seasonal cycle from the Simple Diagnostic Biosphere Model; LPJ; and LPX. . . . .	75
2.4	Comparison of observed and simulated seasonal phase and seasonal concentration of fraction of absorbed photosynthetically active radiation (fAPAR). . . . .	82
2.5	Comparisons of observed and simulated NPP and GPP. . . . .	83
2.6	Comparisons of observed and: LPX simulated height; LPX simulated height scaled so that the simulated global mean height is the same as the observations; and so that the simulated height has the same global mean and variance as the observed. . . . .	84
2.7	Annual average burnt fraction from observations and as simulated by LPJ and LPX. . . . .	86
2.8	Observed inter-annual runoff compared to runoff simulated by LPJ and LPX showing with and without a one year lag. . . . .	86

2.9	Comparison of observed and simulated annual average net primary production from Simple Diagnostic Biosphere Model, LPJ and LPX . . . . .	87
2.10	Comparison of observed inter-annual variability in global atmospheric CO <sub>2</sub> concentration compared to inter-annual variability simulated by LPJ and LPX. . . . .	88
3.1	Distribution of the sites used in this study and included in the database on a topographic map . . . . .	99
3.2	The distribution of the sites used in this study in Australian climate space. . . . .	103
3.3	Abundance of resprouting and resprouting trait categories by plant functional types. . . . .	104
3.4	Distribution of different measures of resprouting abundance in climate and environmental space. . . . .	107
3.5	Abundance of resprouting trait categories in climate and environmental space. . . . .	111
3.6	Abundance of resprouting trait categories in geographic space. . . . .	113
3.S1	The distribution of the sites used in this study in Australian climate space. . . . .	121
4.1	Description of the structure of the fire component of LPX. . . . .	128
4.2	Observed relationships between: the total and cloud-to-ground lightning flashes; the percentage of dry lightning with respect to the number of wet days per month; and the percentage of dry days with lightning with respect to monthly dry lightning strikes. . . . .	130
4.3	Proportion of roots in the upper 50 cm of the soil by Plant Functional Type. . . . .	133
4.4	Bark thickness vs. diameter at breast height for each Plant Functional Type in LPX-M-v1-nr and LPX-M-v1-rs. . . . .	134
4.5	Illustration of the variable bark thickness scheme. . . . .	135
4.6	Comparison of the observed and simulated abundance of grass, tree and resprouting trees along the climatic gradient in moisture. . . . .	140
4.7	Simulated time to recovery after fire compared to observed time to recovery for above-ground resprouters (RS); a combination of other RS types and obligate seeders; and vegetation which does not display specific fire adaptations. . . . .	140
4.8	Comparison of observed tree cover and tree cover simulated by LPX-M, LPX-Mv1-nr and LPX-Mv1-rs. . . . .	141
4.9	Comparison of annual average burnt area from various remote sensed and ground observations, and as simulated by LPX, LPX-Mv1-nr, LPX-Mv1-rs. . . . .	142
4.10	The difference in simulated tree cover and burnt area between the non-resprouting (LPX- MV1-nr) and resprouting (LPX-Mv1-rs) versions of LPX. . . . .	142
4.S1	Comparison of annual average burnt area from various remote sensed and ground observations, and as simulated by individual parametrizations of LPX-Mv1. . . . .	170

---

4.S2 Comparison of the simulated abundance of resprouting tree PFTs and their non- resprouting equivalent PFTs along the climatic gradient in moisture. . . . .	171
4.S3 Simulated annual average, seasonal and inter-annual burnt area for the wet day lightning sensitivity analysis using LPX-Mv1-rs. . . . .	172
5.1 Comparison of observed and simulated components of the carbon cycle during the recent period. . . . .	185
5.2 Changes in the carbon cycle over Australia through the 21 <sup>st</sup> century in response to climate change driven by the RCP4.5 scenario. . . . .	186
5.3 Changes in the carbon cycle over Australia through the 21 <sup>st</sup> century in response to climate change driven by the RCP8.5 scenario. . . . .	188
5.4 Contribution of CO <sub>2</sub> fertilization and resprouting to the simulated changes in the carbon cycle over the 21 <sup>st</sup> century. . . . .	189
5.S1 Inter-annual variability in historic and RCP4.5 future climate inputs used to drive the LPX-Mv1 simulations. . . . .	197
5.S2 Inter-annual variability in historic and RCP8.5 future climate inputs used to drive the LPX-Mv1 simulations. . . . .	199
5.S3 Annual CO <sub>2</sub> concentrations used as input to the LPX-Mv1 model. . . .	200
5.S4 Map showing the four regions used in the final analyses. . . . .	201
5.S5 Maps of the ensemble changes in climate, vegetation and carbon cycle from the RCP4.5 and RCP8.5 experiments compared to the historic period.	204
5.S6 Changes in the carbon cycle over Australia through the 21 <sup>st</sup> century based on the RCP8.5 scenarios. . . . .	205
5.S7 Contribution of direct CO <sub>2</sub> effects and resprouting to the simulated changes in the carbon cycle over the 21 <sup>st</sup> century based on the RCP8.5 scenarios. . . . .	206



# List of Tables

1.1	Development of the processes controlling fire in coupled DGVM-fire models. . . . .	23
1.2	Development of the processes describing the impacts of fire on carbon cycling and vegetation mortality in coupled DGVM-fire models. . . . .	28
2.1	Summary description of the benchmark datasets. . . . .	69
2.2	Summary description of the benchmark metrics . . . . .	72
2.3	Mean, absolute variance and standard deviation of the annual average values of benchmark observations. . . . .	72
2.4	Scores obtained using the mean of the benchmark data, and the mean and standard deviation of the scores obtained from bootstrapping experiments. . . . .	77
2.5	Mean and variance of simulated annual averages and comparison metric scores for model simulations against observations . . . . .	79
2.6	Mean annual GPP normalised mean error comparison metrics using site-based and gridded data as alternative benchmarks. . . . .	83
2.7	Comparison metric scores for simulations with the Simple Diagnostic Biosphere Model against observations of the seasonal cycle of atmospheric CO <sub>2</sub> concentration and annual average NPP . . . . .	85
3.1	Probability matrix comparing the abundance of resprouting and non-resprouting taxa in each plant functional type. . . . .	105
3.2	Probability matrix comparing the abundance of resprouting syndromes in each woody plant functional type. . . . .	105
3.3	Regression coefficients from the generalized linear model for abundance of resprouting (and types of resprouter) with controls on productivity and fuel dryness. . . . .	109
3.S1	Definitions of the plant and fire-response traits and trait categories included in the database. . . . .	122
3.S2	Regression analysis of climate, bioclimate and environmental variables. Inputs are the gridded values of these variables for all of the 0.05° grid-cells covering Australia. . . . .	123
4.1	Plant functional type — specific values used in LPX-Mv1 . . . . .	132
4.2	Translation between LPX Plant Functional Types (PFTs) and the vegetation trait information available for sites which were used to provide rooting depths. . . . .	133
4.3	Summary description of the benchmark datasets. . . . .	137

4.4	Scores obtained using the mean of the data and the mean and standard deviation of the scores obtained from bootstrapping experiments for steps: 1 - straight comparison; 2 - comparison with the influence of the mean removed; 3 - with mean and variance removed . . . . .	138
4.5	Scores obtained for the individual parameterization experiments, and for LPX-Mv1-nr and LPX-Mv1-rs compared to the scores obtained for LPX. . . . .	139
4.S1	Allocation of species to plant functional type and to aerial resprouting, non-resprouting, and other resprouting/unknown resprouting categories for the bark thickness analyses. . . . .	151
4.S2	Information used to calculate recovery time at sites with different fire-response adaptations as shown in Fig. 4.7. . . . .	157
4.S3	Extended version of Table 4.5. . . . .	162
4.S4	Mean, variance of annual average and comparison metric scores for individual and full model simulations against observations. . . . .	165
4.S5	Comparison metric scores for LPX-Mv1-rs and LPX-Mv1-rs incorporating wet day lighting against burnt area observations taken from GFED version 4. . . . .	173
5.1	Summary of changes in individual components of the carbon cycle for Australia over the 21 <sup>st</sup> century. . . . .	186
5.S1	Summary of the simulation protocol for model spin-up and the baseline simulations. . . . .	195
5.S2	Information on the models from the CMIP5 database used to provide future climate scenarios. . . . .	196
5.S3	Summary of changes in carbon budget terms as simulated using RCP4.5 outputs from individual climate models. . . . .	204
5.S4	Summary of changes in carbon budget terms as simulated using RCP8.5 outputs from individual climate models. . . . .	207

# Abstract

Fire is an important component of the Earth System, influencing vegetation dynamics and the carbon cycle, and with feedbacks to the climate system. Fire properties (occurrence, frequency and intensity) are controlled in part by ignitions, fuel loads and fuel properties such as moisture content. Climate influences the prevalence of lightning ignitions, as well as the type and productivity of local vegetation, which in turn influences the abundance and type of fuel. The type of fuel influences the speed of drying along with climate. Fire itself, along with climate, helps control vegetation type and productivity. Unravelling the complex interactions of climate, vegetation and fire is important to assess future changes and feedback of fire, and requires both analysis of observational data and process-based modelling. This thesis focuses on improving the representation of fire and fire-vegetation interactions within dynamic global vegetation model (DGVM) LPX (Land surface Processes and eXchanges) which is used to explore carbon and vegetative impacts of fire under future climate change. Development is targeted through comparisons with observations of fire and processes that effect the simulation of fire, and parameterization is based on extensive data-analysis of weather and vegetation dynamics which influence fire.

The thesis consists of four papers. The first paper describes a system for benchmarking fire-enabled DGVMs. The benchmarking system uses standard metrics to evaluate the performance of a model against a suite of vegetation, hydrology, fire and carbon-related global data sets. The modelling community has argued for the creation and systematic use of benchmarking in vegetation-model development, but this paper is the first to present and demonstrate the use of a fully comprehensive benchmarking system to quantify differences between models. This benchmarking exercise was used to identify processes in LPX that affected the simulation of fire and needed improvement. It identified Australia as one of the regions where the simulation of fire was particularly poor, and this motivates the use of this region as a test bed for model development.

In common with many other models, post-fire recovery of vegetation in the original version of LPX took decades to centuries. Observed recovery rates, collated in this thesis, demonstrate recovery time is much faster, and is at least partially because many trees and shrubs have the ability to resprout vegetatively from above- or below-ground meristems (buds). The inclusion of resprouting behaviour is one of the improvements that I have made to LPX. The second paper in the thesis describes a data set of site-based information on the abundance of resprouting in fire prone regions of Australia, and explores the relationships between climate and resprouting abundance. I subsequently used these data for evaluation of the new LPX model.

The third paper describes the new version of LPX. This model includes a new treatment of lightning ignitions, plant functional type (PFT) and fuel-type specific

decomposition, fuel drying rates, fire resistance through adaptive bark thickness, and fire response through resprouting. The new model produces an 18% improvement in the simulation of fire and a 33% improvement in vegetation composition over Australia.

The final paper describes the application of the new model to simulate fire regimes during the 21st century, as driven by alternative future climate simulations. It shows that Australian fire regimes will alter significantly under the projected future climate, with increasing burnt area, particularly in fuel limited regions, and increased fire emissions and temperature induced respiration. Despite these increases in carbon losses, we show a continuing uptake of carbon with increasing atmospheric CO<sub>2</sub> concentrations, due to woody vegetation expansion into semi-arid, increasingly fire prone areas because of the combined affects of CO<sub>2</sub> fertilization and resprouting fire-adaptations.

# Acknowledgements

I'd like to thank Macquarie University for giving me the opportunity to study such a fascinating subject for the past 4 years and for supporting me through the Macquarie University International Research Scholarship (iMQRES). I'd also like thank the Department of Biological Sciences for supporting the last three months of my candidature and the Faculty of Science for providing funding via the postgraduate research fund award for my attendance at the American Geographical Union Conference in San Francisco at the end of last year, where I got the opportunity to present and discuss my research with ecologists and vegetation/fire modellers from across the world.

I have been very fortunate to have the opportunity to work with some of the best scientists in the field whilst studying at Macquarie. One of which, Sandy Harrison, agreed to take me on as a slightly clueless, ex-physics undergraduate who knew very little about ecology or modelling, and has dedicated a huge amount of time and effort in helping me develop an understanding of my subject area, figure out how to organise my research, and teaching me the tricks of the scientific trade. Sandy has also been fantastic at helping me with my writing, which is probably the weakest part of my work. If any of the papers in this thesis seem well written, then that is entirely down to Sandy's encouragement, "red pen", and the occasional whack around the head until I understood what I was doing wrong.

My co-supervisors have also been very supportive during my studies. Colin Prentice was very helpful at developing the direction of the thesis, and also seemed to have the magically ability of strengthening arguments in our papers with just the quickest of glances. And whenever I was confused by statistics or if we got stuck incorporating data into our modelling framework, Belinda Medlyn always seemed to know exactly what we should do next. Belinda also introduced me to her 'CAFE M' research group, who have been great for discussing ideas and for technical help, particularly Martin De Kauwe for his help with coding and latex and Melanie Zeppel for discussing plant traits and for listening to me moan when my PhD wasn't going so smoothly.

Our own research group, Biosphere and Climate Dynamics, was still very small when I started my candidature. As the only other student in the group, Wang Han very kindly took me under her wing when I first started, helping me settle in at work and helping both me and my partner, Lauren, settle into life in Sydney. There has been a lot of people who have joined the group since then, and I think all the new members have helped me along my PhD somehow. I'd particularly like to thank Sam Newton, Anna Ukkola, Rhys Whitley, Li Guangq, Kevin Willis, Dong Ning, Ines Hessler, Brad Evans, Yasmin Hageer, and Annika Herbert for helping with my spelling, keeping a 'healthy' supply of cakes and fruit in the office, and buying the drinks if I ever needed cheering up.

As with any model-based research topic, this thesis required a large amount of data processing and coding, which seemed to increase paper-by-paper. My code would not have had the necessary structure or organisation to complete most of the data analysis or model development in the last half of this thesis without two courses organised as part of the Genes to Geoscience Research Enrichment Program - the ‘Software Carpentry’ course by Greg Wilson; and the ‘Nice R code’ course run by Daniel Falster and Rich FitzJohn.

Perhaps without knowing it, many friends and family outside of work have also helped me through my thesis. My parents have been very supportive despite being the other side of the world, and even helped with a little proof reading. I’d also like to thank my running friends at Epping District Athletics Club, particularly James Palethorpe, Fred O’Conner and Mel Zeppel, for looking after me when I first arrived and for always showing an interest in my work and well-being.

Above all, I would like to thank my partner, Lauren. She was the main person who encouraged me to do the PhD in the first place, and has supported the both of us through the past four years, specially in the last few months of the PhD. I would not of been able to finish this thesis without her looking after me.

# List of Publications

The main chapters in this thesis are self-contained. Each chapter has been written as a journal article, and is either published, in review, or ready to submit.

**Chapter 2** Kelley, D.I., Prentice, I.C., Harrison, S.P., Wang, H., and Willis, K., 2013. *A comprehensive benchmarking system for evaluating dynamic global vegetation models*. *Biogeosciences Discussions* 9: 1-63. *Biogeosciences* 10: 3313-3340.

S. P. Harrison and I. C. Prentice were responsible for the design of the benchmarking system; I. C. Prentice, K. O. Willis and D. I. Kelley designed the metrics; J. B. Fisher and M. Simard provided remote-sensed datasets, and H. Wang and D. I. Kelley collated and regridded all of the datasets. D. I. Kelley ran the LPJ and LPX simulations and H. Wang ran the SDBM simulations. D.I. Kelley coded the metrics and made all the statistical analyses. D. I. Kelley, S. P. Harrison and I. C. Prentice wrote the first draft of the paper; all authors contributed to the final version of the manuscript.

**Chapter 3** Harrison, S.P., Kelley, D.I., Wang, H., Herbert, A., Li, G., Bradstock, R., Fontaine, J., Enright, N., Murphy, B.P., Pekin, B.K., Penman, T., Russell-Smith, J. and Wittkuhn, R.S. (2014). *Patterns in the abundance of post-fire resprouting in Australia based on plot-level measurements*. Submitted to *Global Ecology and Biogeography*, March 2014.

The original idea for this paper arose from discussions between S.P. Harrison, R. Bradstock, J.Fontaine, B.P. Murphy and J. Russell-Smith. R. Bradstock, J. Fontaine, N. Enright, B.P. Murphy, B.K. Pekin, T. Penman, J. Russell-Smith and R.S. Wittkuhn provided site-level abundance data sets. S.P. Harrison, D.I. Kelley, H. Wang, A. Herbert, and G. Li were responsible for the design and construction of the database. S.P. Harrison and D.I. Kelley designed the analyses. D.I. Kelley ran all the statistical analyses and produced all the figures. S.P. Harrison and D.I Kelley produced the first version of the manuscript and all the authors contributed to the final version.

**Chapter 4** Kelley, D.I., Harrison, S.P. and Prentice, I.C., 2014. *Improved simulation of fire-vegetation interactions in the Land surface Processes and eXchanges Dynamic Global Vegetation Model (LPX-Mv1)*. *Geoscientific Model Development* 7: 2411-2433.

All three authors identified areas for re-parameterization. D. I. Kelley collected lightning data; S. P. Harrison collected rooting depth data; both D. I. Kelley and S. P. Harrison were responsible for the collection of bark thickness data. The new model structure was designed by D. I. Kelley and S. P. Harrison. D. I. Kelley coded, ran

and benchmarked LPX-M1 and its individual parameterizations. D. I. Kelley and S. P. Harrison wrote the first draft of the paper; all three authors contributed to the final version of the manuscript.

**Chapter 5** *Kelley, D.I. and Harrison, S.P., 2014. Enhanced Australian carbon sink despite increased wildfire during the 21st century. Environmental Research Letters 9: 104015*

Both authors contributed to the design of this paper, the analyses of the simulations and the drafting of the paper. D.I. Kelley was responsible for running the LPX-M1 simulations.

#### Other publications obtained during candidature:

- Ciais, P., Tagliabue, a., Cuntz, M., Bopp, L., Scholze, M., Hoffmann, G., Lourantou, a., Harrison, S. P., Prentice, I. C., Kelley, D. I., Koven, C. and Piao, S. L.: Large inert carbon pool in the terrestrial biosphere during the Last Glacial Maximum, *Nat. Geosci.*, 5(1), 7479, doi:10.1038/ngeo1324, 2011.
- Prentice, I. C., Kelley, D. I., Foster, P. N., Friedlingstein, P., Harrison, S. P. and Bartlein, P. J.: Modeling fire and the terrestrial carbon balance, *Global Biogeochem. Cycles*, 25(3), 113, doi:10.1029/2010GB003906, 2011.
- Zeppel M., Harrison S. P., Adams H., Kelley D. i., Li G., Tissue D., Dawson T., Fensham R., Medlyn B., Palmer T., West A., McDowell N.: Drought-induced mortality within resprouters. *New Phytol.* In Press.

#### Conference preceeding:

- Kelley, D., Harrison, S. P. and Prentice, I. C.: Implications of introducing realistic fire response traits in a Dynamic Global Vegetation Model, in AGU Fall Meeting Abstracts, vol. 1, p. 6., 2013.



# 1

## Introduction

*Waikawa Bush Fire — Sid Mosdell*

Fire is the most prominent natural disturbance (Bowman et al., 2009; Harrison et al., 2010a). Between 310 and 377 Million hectares (around 2-2.5%) of the global land surface is burnt annually (Giglio et al., 2013), and 69% of the globe experiences fire often enough to influence local ecosystem dynamics and biodiversity (Krawchuk et al., 2009; Harrison et al., 2010a). In addition to the immediate human impacts and costs, fire also has a profound impact on climate both directly through greenhouse gas emissions, and indirectly through changes in ecosystem structure, altering albedo and the ability of vegetation to take up carbon. Fire regimes and the impacts of fire are likely to alter dramatically in the future due to projected changes in the climatic and vegetation controls on fire (Krawchuk et al., 2009; Harrison et al., 2010a; Moritz et al., 2012). Fire-enabled dynamic global vegetation models are increasingly being used to explore potential future changes in fire (e.g. Bachelet et al., 2003b; Scholze et al., 2006; Harrison et al., 2010a; Pechony and Shindell, 2010; Kloster et al., 2012; Ward et al., 2012). Although there is an improving understanding of what controls the incidence of fire, quantification of their relative importance on regional to global scales is still relatively uncertain (Bowman et al., 2009). The knock-on impact of these changes in fire on vegetation and on feedbacks to climate via the carbon cycle are even less well constrained (Sitch et al., 2008a; Harrison et al., 2010a; Arneth et al., 2010). Here, I review the impacts and controls of fire and, focusing on Australia, discuss the implication of a quantitative understanding of these controls and impacts for development

of fire-enabled Dynamic Global Vegetation Models (DGVMs). I then describe a data-driven model-development framework to improve the representation of these controls in the Land surface Processes and eXchanges (LPX) DGVM, which I use to assess changes in fire, vegetation and carbon across Australia in response to projections of future climate change.

## 1.1 The Importance of fire in the Earth System

### 1.1.1 The influence of fire on climate

Fire influences climate directly through changing the physical properties of the land surface and through emissions to the atmosphere, and also indirectly by influencing the nature of the vegetation.

The most important effect of fire on global climate is through emissions of carbon and other greenhouse gases (Randerson et al., 1997; Cofer et al., 1998; Bowman et al., 2009; Arneth et al., 2010, ; Fig. 1.1). Carbon emissions from fire over the past two decades have been estimated to be around 2.8 PgC/year (van der Werf et al., 2004, 2006; der Werf et al., 2008; van der Werf et al., 2010, ; Fig. 1.1a). This estimate of fire-related carbon emissions is probably conservative, because the satellite products on which it is based do not generally detect small fires (i.e. fires smaller than the 500m satellite pixel width). Randerson et al. (2012) have suggested that small fires could contribute a further 0.6 PgC/year. Most of the carbon emissions (83%) are from fires in tropical forests, savannas and grassland, and Mediterranean ecosystems (Fig. 1.2c). Fire associated with land clearance in the tropics (so-called deforestation fire) has contributed 19% of the anthropogenic increase in CO<sub>2</sub> concentration since 1850 (Bowman et al., 2009). Model-based estimates indicate that fire-related emissions account for 1/3 of the inter-annual variability in atmospheric CO<sub>2</sub> (Fig. 1.1b; Prentice et al., 2011). Trace gas emissions from fire have additional feedbacks on climate via changes in atmospheric chemistry (Fig. 1.1c; Bowman et al., 2009), contributing 4% of the radiative forcing associated with changes in methane (CH<sub>4</sub>), 25% of that associated with changes in nitrous oxide (NO<sub>x</sub>), and 17% of that associated with changes in tropospheric ozone (O<sub>3</sub>).

Fire-induced changes in vegetation also affect carbon fluxes through changes in vegetation productivity and in decomposition rates. Fire mortality leads to a short-term reduction in vegetation cover, but can also lead to a more permanent shift from woody to herbaceous vegetation (Menaut et al., 1995; Fensham et al., 2003). Both processes result in a reduction in ecosystem production, therefore reducing the rate of capture of CO<sub>2</sub> from the atmosphere (Beringer et al., 2007; Higgins et al., 2007; Murphy et al., 2014; Li et al., 2013a). The burning of litter during fires causes a reduction in heterotrophic respiration (the decay of litter and soil organic matter that is then fluxed to the atmosphere) from the ecosystem (Haverd et al., 2013b,a). Fire-induced vegetation changes also cause changes in the nature of litter, for example a shift to herbaceous vegetation results in the production of more fine fuel, which in

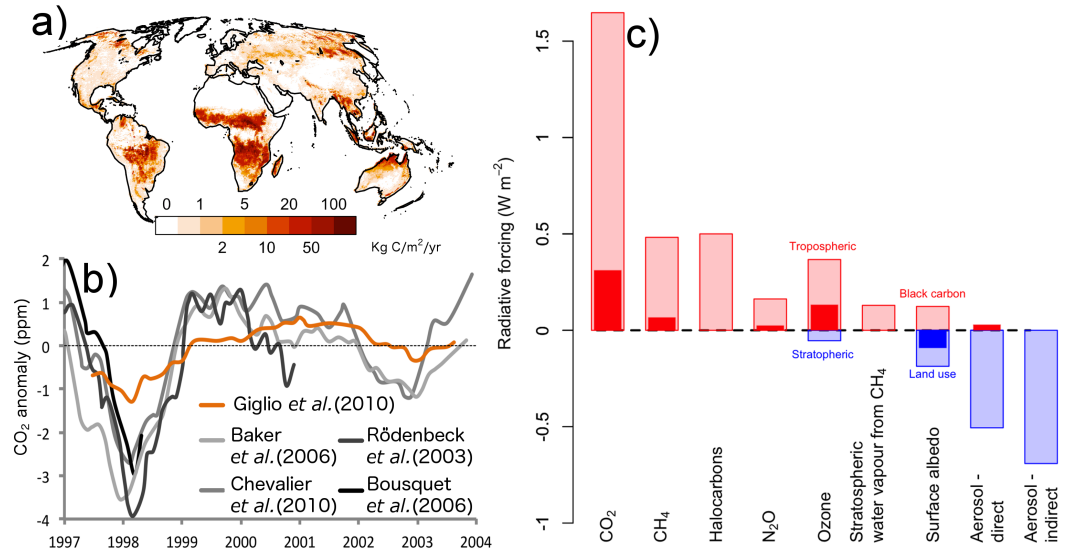


**FIGURE 1.1:** Fire emissions and its effects on climate. a) Estimated carbon release (van der Werf et al., 2010) based on remote sensed observation of global burnt area between June 1996-May 2010 from Global Fire Database version 3 (Giglio and Randerson, 2010); b) Twelve-month running mean of monthly global atmospheric CO<sub>2</sub> concentration anomalies between 1998-2005, and the contribution of fire emissions to the inter-annual variability of CO<sub>2</sub>. Concentrations taken from (black to light grey); Bousquet et al. (2000); Rödenbeck et al. (2003); LCSE Chevallier et al. (2010); and Baker et al. (2006). Fire emission (in orange) contributions calculated from total monthly flux from GFED version 3 fire carbon emissions (van der Werf et al., 2010). Reproduced from Prentice et al. (2011); c) Estimated changes in radiative forcing over the industrial era. Light coloured bars indicate total change in radiative forcing, whereas filled bars indicates the contribution of fire. Reproduced from Harrison et al. (2010a)

turn affects the rate of heterotrophic respiration because fine litter is respired more rapidly than coarse litter (Bergeron et al., 2007; Brovkin et al., 2012).

The physical impacts of fire on the radiation budget, via albedo, surface roughness and atmospheric reflectance tend to be more localized and short-lived than changes in carbon flux (Harrison et al., 2010a), but can be associated with large temperature changes (Hoffmann and Jackson, 2000). Large vegetation-destroying fires blacken the land surface through deposition of charcoal and soot (black carbon). These dark surfaces absorb more energy, which leads to surface warming. Surface fires, on the other hand, do not necessarily result in decreased albedo if the tree cover remains intact. In both cases, however, the destruction of the vegetation lowers surface roughness, affecting the partitioning of sensible and latent heat fluxes at the surface. These effects of fire on land-surface properties typically last for a few years to decades, until vegetation has recovered (Harrison et al., 2010a). Changes in atmospheric reflectance occur through increases in the absorption of incoming solar radiation by fire-produced aerosols, and through changes in cloud absorption/reflectance via increasing the number and effectiveness of cloud condensation nuclei (Hobbs and Radke, 1969; Eagan et al., 1974;

Day, 2004; Martins et al., 2009). These changes in forcing have been shown to influence regional atmospheric stability and therefore vertical motion which, combined with changes in the number of condensation nuclei (Rosenfeld, 1999; Martins et al., 2009; Lu and Sokolik, 2013), has wider implications for the hydrological cycle (Menon et al., 2002).

### 1.1.2 The influence of fire on vegetation

Fire occurs periodically in almost all terrestrial ecosystems, except some humid tropical forest and desert ecosystems (Bond and van Wilgen, 1996b; Bowman et al., 2009, Fig. 1.2a). Fire is a major structuring force for much of the world's vegetation (Bond et al., 2005; Bond and Keeley, 2005). In fire-prone ecosystems, fires often suppress tree growth in favor of quick growing herbaceous vegetation in climates that would otherwise be suitable for trees (Pickett and White, 1985; Bond and van Wilgen, 1996b; Bond et al., 2003, 2005; Bond, 2008). Bond et al. (2005) showed, through modelling experiments, that the absence of fire could potentially result in a doubling of forest cover globally (from 26.9% to 56.4%).

The influence of fire on vegetation is most prominent in warm, seasonally or annually dry ecosystems. Tropical savanna and grassland ecosystems, for example, experience more fire than any other ecosystem. Although they account for only 16% of the global land area (Fig. 1.2a), they account for 78% of the observed long-term average (1996-2012) burnt area (Fig. 1.2a), with 13% of the savanna burnt each year (Fig. 1.2b). Tropical savanna and grasslands are both dominated by C<sub>4</sub> grass (Lehmann and Archibald, 2011), which are highly productive in warm, non-shaded environments and produce large quantities of fuel. Savanna is distinguished by the presence of fire-adapted woody vegetation (Fensham et al., 2003; Hoffmann et al., 2003; Ratnam et al., 2011) which is sparse enough for the canopy to remain open allowing a grass under-story to persist (McPherson, 1997; Anderson et al., 1999; Lehmann et al., 2011). The prevalence of fire in tropical savanna and grassland ecosystems results from the highly seasonal rainfall, which allows build up of fuels during the wet season and subsequent drying of the fuel load in the long dry season which promotes burning (Lehmann and Archibald, 2011). The maintenance of open canopy savanna is often described as resulting from a positive feedback between C<sub>4</sub> grasses and fire: C<sub>4</sub> grasses produce quick-drying, highly flammable fuel, which results in more fires during the dry season, killing tree seedlings and smaller trees, and thus preventing canopy closure and allowing C<sub>4</sub> plants to persist (Cochrane et al., 1999; Beckage et al., 2009; Lehmann et al., 2011). The relative paucity of woody vegetation, combined with the regular burning, in these ecosystems means that most fires are associated with comparatively low fuel loads and tend to burn at a low intensity (Gill, 1975; Bond and Keeley, 2005; Murphy et al., 2014). Individual fires in these ecosystems therefore release less carbon than fires in other woody ecosystems with less frequent fire. However, because fire frequency is high, emissions from savannas still represent half of global emissions every year (Fig. 1.2c).

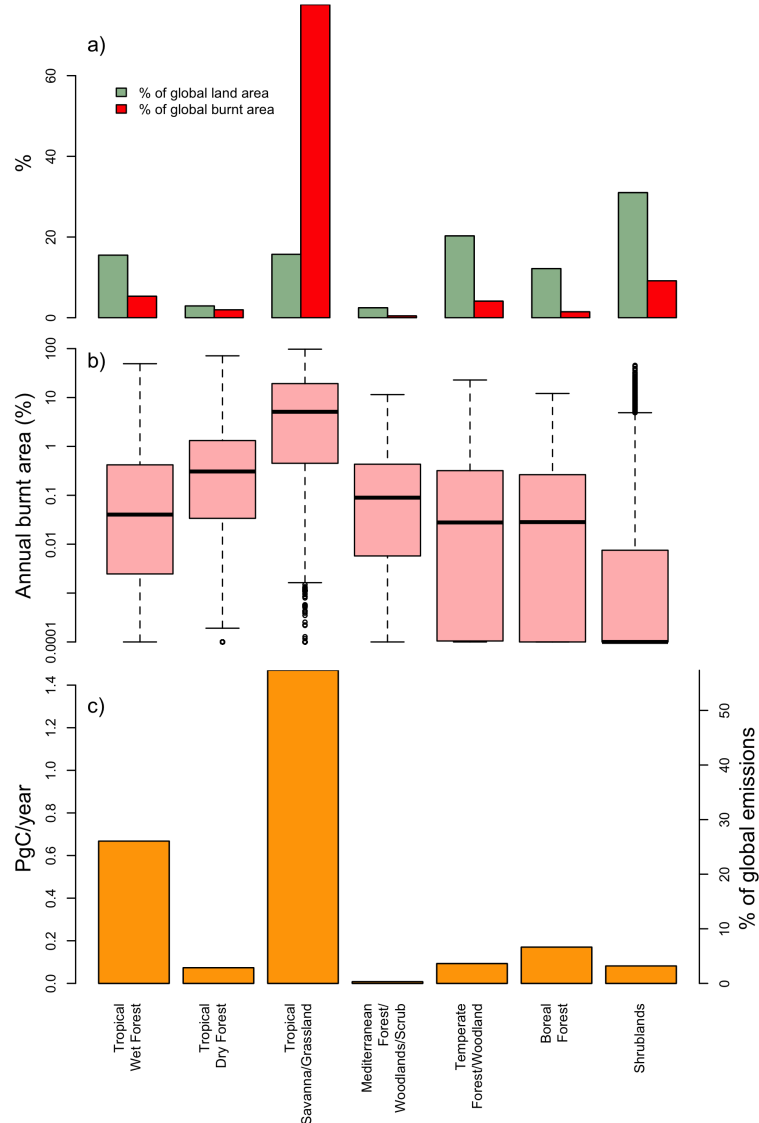


FIGURE 1.2: Burnt area and carbon emissions from different ecosystems. **a)** Fractional cover of global land area by each ecosystem and their contribution to global burnt area as defined by GFED version 4 (Giglio et al., 2013); **b)** inter-quantile range and medium burnt fraction (from GFEDv4) for areas covered by each ecosystems; **c)** contribution of each ecosystem to global fire emissions defined by GFED version 3 emission (Giglio and Randerston, 2010). Ecosystems defined by grouping vegetation types from Olson et al. (2001) where tropical wet forests is defined as tropical & Sub-tropical wet broadleaf forest, tropical and subtropical coniferous forests in Olson et al. (2001); tropical dry forest defined as tropical and sub-tropical broadleaf dry forest, tropical savanna/grassland as tropical and sub-tropical grasslands, savannas and shrublands, flooded grasslands & savannas; mediterranean forest/woodland and scrub as mediterranean forests, woodlands and scrub; temperate forest and woodland as temperate broadleaf and mixed forests, temperate grasslands, savannas & shrublands, temperate conifer forests; boreal forests as boreal forests/taiga; shrublands as montane grasslands and shrublands, tundra, deserts and xeric shrublands.

Tropical dry forests occur under somewhat wetter conditions than savanna, but are still characterized by highly seasonal climates and therefore are characterized by regular fires (Murphy et al., 2013). Tropical dry forests cover 4% of the land surface and have ca. 4% of the observed long-term average (1996-2012) global burnt area (Fig. 1.2a). Tropical dry forests are dominated by fire-adapted drought deciduous trees, but C<sub>4</sub> grasses occur in the understorey (Murphy and Lugo, 1986). Tropical dry forests are highly sensitive to changes in fire regimes: increases in fire can result in a shift from closed canopy forest to more open canopy forest or savanna (e.g. Menaut et al., 1995; Fensham et al., 2003). Tropical dry forests are more productive and have less frequent fuel-removing fires than savanna (Fig. 1.2b). However, when fire does occur, it is generally more intense Murphy et al. (2014) and associated with more emissions (Fig. 1.2c) than savanna and grassland fires. Tropical dry forests contribute 7% of the global annual emissions from fire – almost twice what might be expected given their limited area.

Mediterranean climates are also characterized by highly seasonal rainfall and temperature, with cool, wet winters and hot, dry summers. While the dry summers provide ideal conditions for fuel drying (Swetnam and Betancourt, 1990; Trabaud, 1994; Whelan, 1995; Keeley et al., 2012; Keeley, 2012), fire is not as common in Mediterranean ecosystems as in other seasonal climate regimes. Areas characterized by Mediterranean climate occupy ca. 2.8% (Fig. 1.2a) of the land surface, and on average only 0.5% of this area burns each year (Fig. 1.2b). This is partially because low growing-season precipitation reduces overall productivity, especially at the drier end of the precipitation gradient (Keeley, 2012), but may also reflect anthropogenic fire suppression (Gill and Williams, 1996; Archibald et al., 2009; Loepfe et al., 2010). Abandonment of agricultural areas in southern Europe, for example, has led to an increase in fire in recent decades (Pausas and Vallejo, 1999; Vallejo et al., 2006). Almost all Mediterranean plants show some form of adaptation to fire (Trabaud, 1994; Moreno and Oechel, 1994), with many depending on fire for reproduction (Keeley et al., 2012).

Fire also occurs in climates with non-seasonal precipitation, both in tropical and extratropical regions of the world, but fire events are much less frequent. When fires do occur, however, they tend to be large and of high severity because of the build up of fuel load (Cochrane, 2003). They also have a more damaging effect on the vegetation because plants in these ecosystems generally lack adaptations allowing them to survive fire. The infrequency of fires, coupled with the high biomass, results in high carbon emissions from individual fires. For example, wet tropical forests contribute 0.7Pg of carbon a year to the atmosphere (26% of global carbon emissions: Fig. 1.2c) despite the fact that only 7% of the long-term average global burnt area occurs in this biome (Fig. 1.2a). Similarly, boreal forests contribute 0.17 Pg/C/year to the atmosphere (7% of global carbon emissions: Fig. 1.2c) despite the fact that only 1.3% of the long-term average global burnt area occurs in this biome (Fig. 1.2a).

### 1.1.3 The impact of fire on humans

Fire-induced changes in climate and vegetation clearly affect humans. However, fire also has more direct impacts on humans, associated with the cost of fighting or managing

fires, the loss of life and infrastructure during fires, and health problems associated with particulate matter released during fires.

Over the last 30 years, fires have led to almost 2000 deaths worldwide and affected another 6 million people (Doerr and Santin, 2013). The cost associated with the loss of infrastructure during this period has been estimated as ca. \$52.3 billion (based on the disasters reported in the International Disaster Database: <http://www.emdat.be>). These estimates are conservative, because they only include the costs from reported large fires that are classified as disasters and ignore the costs of smaller fires that are not categorized as disasters. Furthermore, these estimates do not include loss of potential economic growth in areas affected by large fires.

In many developed countries, the costs of fire fighting are large. The USA, for example, spent US\$2.5 billion on active fire suppression between 2001 and 2010, with spending increasing in real terms by 3.1% per year (Gebert and Schuster, 2008; Department of the Wildland Interior, 2012). The loss of life associated with fire fighting is also increasing. In the USA, there have been 786 deaths from fire since 1950, with 169 deaths occurring in the last ten years alone (NIFC, 2013) — an increase in the number of deaths of ca. 20% per year. Deaths are particularly high in states that rely more heavily on volunteer fire fighters than professionals (NIFC, 2013), and could cause higher mortality in countries, such as Australia, which rely completely non-volunteer rural fire services (NIFC, 2013).

However, the largest costs of fires result from health problems associated with the release of particulate matter (PM). Johnston et al. (2012) estimated that exposure to PM released by fire resulted in between 260,000 and 600,000 deaths per year globally between 1997-2006. These deaths occur mainly in urban areas, where PM from fire can be many times higher than background urban pollution (Johnston et al., 2006; Dennekamp and Abramson, 2011), and mainly in less developed economies without health service infrastructure to cope with the respiratory problems associated with PM (Dennekamp and Abramson, 2011). However, there are still major health implications in developed economies, where PM released by fires results in increases in hospitalization associated with aggravation of long-term health problems, complications with respiratory infections, and non-respiratory illnesses such as conjunctivitis (Sasaki, 2002b; Doerr and Santin, 2013).

## 1.2 Fire in Australia

Around 6.4% of the Australian continent burns annually and ca. 91% of the area experiences fires periodically – more than any other continent (Bradstock et al., 2012). Only the most arid parts of the continental interior do not experience periodic fire (Fig. 1.3a). Much of northern Australia is covered by tropical savanna, shifting to grassland towards the continental interior (NVIS, 2007; Murphy et al., 2013), and experiences highly seasonal precipitation. Fire frequency is high, with most areas experiencing a fire every 1-5 years, although the fire intensity is generally low (e.g. Gill et al., 2000; Williams et al., 2002; Bradstock, 2010; Murphy et al., 2011, 2013). Fires tend to be concentrated in the dry winter and early spring months (Fig. 1.3b Mooney

et al., 2012; Murphy et al., 2014) but can occur at other times in the year. The northeastern and southeastern coastal regions are characterized by flammable moist tropical or subtropical forest and dry forest with rare litter fires and infrequent ( $>100$  years) but severe larger fires (Lehmann et al., 2011; Murphy et al., 2014, 2013). Further inland, the vegetation changes to dry forest or woodland and eventually grassland or shrubland in the interior. Fires are relatively frequent ( $\sim 10$  years Gill and Catling, 2002) in the dry woodland regions, but become increasingly rare with increasing aridity (Murphy et al., 2013). Fires occur over much of the year in the northeast (Fig. 1.3c), but become more seasonal in the southeast with the largest fires occurring during summer (Fig. 1.3b). Southwestern Australia is characterized by Eucalyptus forests/woodland and kwongan shrub/scrubland with reasonably frequent ( $\sim 10$  years) fires concentrated in the hot, dry summers (Fig. 1.3b; McCaw and Hanstrum, 2003). However, seasonal timing of fires in many of these coastal regions are often altered by prescribed burning used in much of the populated and agricultural regions of Australia to prevent mid season, catastrophic fires (see for example Boer et al., 2009; Bradstock et al., 2012)). The arid and semi-arid areas of the interior are fire prone (Allan and Southgate, 2002; Russell-Smith et al., 2007) although lack of fuel limits the occurrence of regular fire. Much of the Australian vegetation is highly adapted to fire, through strategies that promote fast recovery of biomass or rapid re-establishment (e.g. Hoffmann and Solbrig, 2003; Chatto et al., 2003; Lawes et al., 2011a; He et al., 2011; Bradstock et al., 2012).

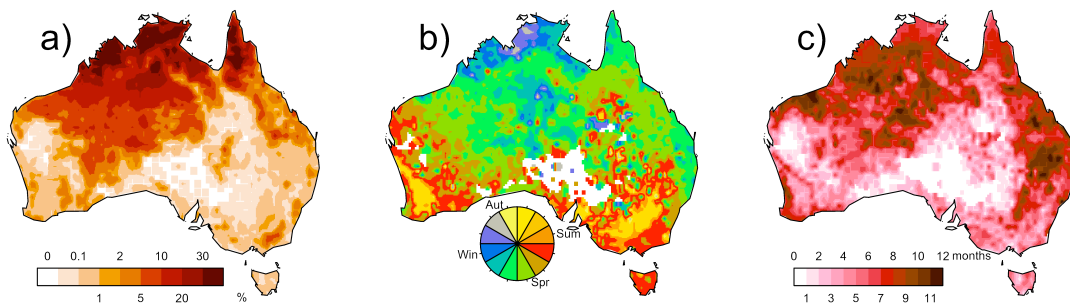


FIGURE 1.3: Fire observations in Australia based on GFED version 4 (Giglio et al., 2013) burnt area product, June 1995–May 2012. **a)** Annual average burnt area; **b)** Timing of the fire season calculated as per Chapter 2 (Kelley et al., 2013), with fires occurring in: summer (red); Autumn (yellow); winter (blue); and spring (green) and **c)** fire season length (in months), defined as the number of months that contain 99% of the annual average burnt areas.

Fire has a large impact on the inhabitants of Australia. Fires have caused almost 1000 fatalities and 10,000 serious injuries since 1850 (Romsey, 2009, – compiled from Australian Emergency Management database <http://www.em.gov.au/>), and costs of \$6.9 billion have been incurred since 1967 (inflation corrected to March 2014 values: ICA (2014); E. Scandrett pers. comm.). Despite advances and investment in fire management (Penman et al., 2011), the cost of fire has increased since 2000, with an average cost of \$400 million per year over the last 5 years (Fig. 1.4). Escalating costs are partly because of the expansion of the wildland-urban interface — the boundary

between flammable natural vegetation and urban infrastructure (Safford et al., 2009; Mell et al., 2010b,a; Price and Bradstock, 2013) — which has been linked to rapidly increasing urban populations in Australia (Hughes and Mercer, 2009). Settlement adjacent to areas of flammable natural vegetation provides a way in which wildfire can encroach on populated areas (Bradstock and Gill, 2001; Price and Bradstock, 2013). Most of the fire-related costs are incurred in southeastern and southwestern Australia, because although these regions experience less fire than areas in northern Australia, they are more densely populated, with a mixture of rural and urban environments and greater investment in infrastructure (Russell-Smith et al., 2007; Chuvieco et al., 2014). Furthermore, although fires in southern Australia occur less often than in northern Australia, the vegetation type and the lower fire frequency promote larger and less controllable fires (Bradstock et al., 2012; Murphy et al., 2013, 2014). Thanks to well-developed health infrastructure, respiratory deaths from fire emissions are much lower than in other parts of the world (e.g. Dennekamp and Abramson, 2011), but PM-related hospitalizations rise noticeably during the fire season in many southern Australian cities (Johnston et al., 2002, 2006; Tham et al., 2009; Morgan et al., 2010).

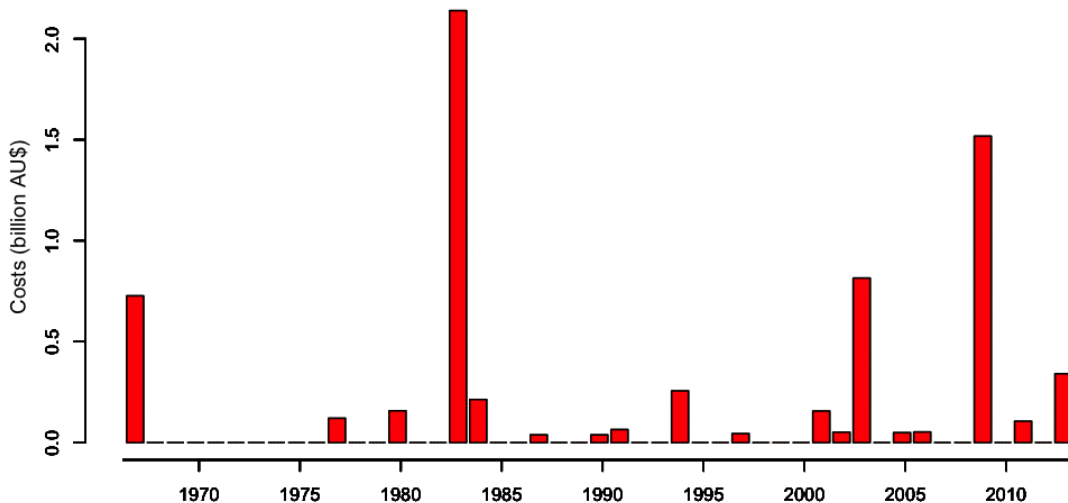


FIGURE 1.4: Annual cost of fire damage to infrastructure in Australia, adjusted for inflation to 2014 values. Data obtained from E. Scandrett (personal comms.) of Willis Re, based on (ICA, 2014).

### 1.3 The controls of fire

The geographic distribution of fire is driven by complex interactions between climate and vegetation (Fig. 1.5). Fire is also influenced by human activities, which in turn are influenced by and also impact on climate and vegetation properties. Many of these interactions are temporally and spatially scale-dependent (Parisien and Moritz, 2009; Falk et al., 2011), and before the advent of satellite observation of fire, our

understanding of these controls has typically been based on local-scale studies. Thus, atmospheric circulation patterns and moisture advection on meteorological time scales (i.e. minutes to days) determine the location, incidence and intensity of lightning storms that produce fire ignitions (Flannigan and Wotton, 1991; Rorig and Ferguson, 1999; Mitchener and Parker, 2005; Bartlein et al., 2008; Duncan et al., 2010). Weather and vegetation state also determine surface wind speeds and vapor-pressure gradients, and hence the rates of fuel drying, which in turn affect the probability of combustion (McArthur, 1969; Rothermel, 1972; Albini, 1976; Kauffman and Uhl, 1990; Beer, 1991, 1993; Viegas et al., 1999) as well as fire spread (McArthur, 1967; Rothermel, 1972; Bradshaw et al., 1983). The impact of wind on fire spread is particularly strong in flat regions. However, topographic complexity also affects the spread of fire. Fire fronts travel faster uphill because of upward convection of heat (Heyerdahl et al., 2001; Rollins et al., 2002; Sharples, 2008; Gill and Taylor, 2009), while the probability of spread downhill is reduced (Sharples, 2008). Ridge tops often act as a natural barrier to fire fronts (Rothermel, 1972; Heyerdahl et al., 2001; Stambaugh and Guyette, 2008; Archibald et al., 2009). Topographic complexity often gives rise to a mosaic of small fires, but topography is less influential when fires are large and intense (Liu et al., 2013).

On longer time scales (i.e. seasons to years), temperature and precipitation exert a major effect on fire because these climate variables govern net primary productivity, vegetation type and the abundance, composition, and structure of fuels (Archibald et al., 2009). Warmer temperatures are associated with increased burning through increasing vegetation productivity (and hence fuel production) as well as through creating climate conditions that promote burning (Kauffman and Uhl, 1990; Viegas et al., 1999; Drobyshev et al., 2012). This can be seen both in terms of geographic patterns and in changes through time in response to climate variability. The influence of precipitation is more complex: in dry regions fuel is a limiting factor for fire spread but the wetness of the fuel controls the incidence of fire in wet regions. Increases in precipitation, in space or time, will therefore lead to more fire at the arid end of the climate gradient, but less fire under wetter conditions (Veblen and Kitzberger, 2002; Archibald et al., 2009; Lehmann et al., 2011; Bradstock et al., 2012). Arid conditions are also likely to limit the size of fire, as fuel loads typically become discontinuous in dry environments, when vegetation is clumped due to e.g. grazing, or in topographically complex locations (Kerby et al., 2007; Viedma et al., 2009a; Finney et al., 2010).

People influence fire in multiple ways: through ignitions, changing land use, and through fire suppression. Anthropogenic ignitions may be accidental, deliberately set for agricultural purposes or for fire management (Bradstock et al., 1998; Vázquez and Moreno, 1998; Chuvieco, 1999; Guyette et al., 2002; Archibald et al., 2009; Padilla and Vega-García, 2011; Price and Bradstock, 2013; Penman et al., 2013). The influence of land use operates through two processes: removal of fuel through crop harvesting or forestry, and fragmentation of natural vegetation which affects the rate of fire spread (Syphard and Radeloff, 2007; Archibald et al., 2009). Landscape fragmentation is one way in which people suppress fire, but they also actively suppress fire in heavily populated areas.

Recent studies have suggested that climate, vegetation properties and human activities can have different effects on different aspects of the fire regime — the timing of the fire season, the prevalent fire type (crown versus ground fires), the number of fires, and the area burnt (Lavorel et al., 2006; Archibald et al., 2009). In general, humans have a more noticeable impact on the number and timing of fires than on the type of fire or the area burnt (Chuvieco et al., 2008; Archibald et al., 2009).

### 1.3.1 Global Studies of Fire

Global assessment of the controls on fire has only been possible since the advent of satellite remotely-sensed data in the late 1990s. Products from the Advanced Very High Resolution Radiometer (AVHRR: Levine, 1991) or Moderate-resolution Imaging Spectroradiometer (MODIS: Justice et al., 2002) have been used to produce continental- (e.g. Russell-Smith et al., 2002; Craig et al., 2002) and global-scale fire products (e.g. Randerson et al., 1997; Carmona-Moreno et al., 2005; Randerson et al., 2005; Tansey et al., 2008; Giglio et al., 2013). Studies using global burnt area products to explore the controls on fire fall into two categories: those looking for correlation between individual factors and burnt area, and those that examine the influences and co-variance of multiple potential controls.

Several studies have examined the global correlation between geographic variability in burnt area and individual potential controls. For example, Bistinas et al. (2013) used weighted regression to explore the correlation between population density and burnt area. This relationship is unimodal: burnt area initially increases with population density and then decreases. Bistinas et al. (2013) showed that the location of peak burnt area varied somewhat on different continents and with different types of land use. Daniau et al. (2012) showed that burnt area increases monotonically with increases in temperature, such that an additional 0.8% of the land area is burnt for each degree temperature increase above 20°C. Daniau et al. (2012) also showed that there is a unimodal relationship between burnt area and precipitation minus evaporation ( $P-E$ ). Harrison et al. (2010a) showed similar unimodal relationships between net primary productivity (NPP) and the ratio actual to potential evapotranspiration ( $\alpha$  — measure of availability of water for plants, and a good index for fuel moisture content — Prentice et al., 1993b), with the biggest burnt area occurring when NPP values were between 0.4 and 1 kg C/m<sup>2</sup> and  $\alpha$  values were between 0.3-0.8. van der Werf et al. (2008) compared inter-annual variability in burnt area across the tropics and climate variables related to either fuel accumulation (rainfall in the growing season) or fuel drying (rainfall during the fire season). They showed that increased fire was either correlated with fuel accumulation and anti-correlated with dry season rainfall or vice versa. This suggests that the unimodal relationships of burnt area with factors such as  $P-E$  or NPP may be emergent system properties. Thus, in drier areas (which will also have low NPP) fuel availability is the factor limiting the amount of fire; in these regions increasing precipitation leads to increased NPP, increased fuel and hence increased fire. In wetter areas (which will also have higher NPP), fuel is abundant but burning can be limited by fuel wetness; in such areas, increases in rain will further decrease the amount of burning whereas decreases in rain would increase the amount of burning.

Several recent studies have used statistical modelling to explore the impacts of multiple controls on fire (Fig. 1.5). Aldersley et al. (2011), for example, used a regression-tree and random-forest approach to examine the influence of climate, vegetation and human impact on monthly burnt area. They found that climate and vegetation properties were the most important controls on burnt area: for e.g. fires occurred almost exclusively in months with temperatures  $> 28^{\circ}\text{C}$  and the highest burnt areas occurred at precipitation levels between 350–1100mm. Whereas cumulative precipitation and lightning were important variables in determining burnt area, variables related to human impacts were generally unimportant. Gross domestic product (GDP) was the most significant of the human impact variables, but was monotonically and negatively correlated with burnt area. The regression-tree approach initially uses single variable comparisons to construct the branching structure. Thus, while it allows combinations of variables to be considered together, it only partially deals with co-correlation between these variables. Furthermore, the use of variables that display unimodal relationships with burnt area (e.g. Mean Annual Precipitation — MAP) strongly suggests that these variables are surrogates for the actual controls.

Krawchuk et al. (2009) and Moritz et al. (2012) used Generalized Additive Models (GAMs) to explore relationships between burnt area and 17 climate variables, NPP and two measures of human impact. Different subsets of the variables were found to be important in different GAMs, but overall NPP (used as a measure of fuel availability) was the most important variable in determining the amount of burning, with variables controlling fuel moisture (in particularly seasonal temperature variables) being the next most important. Moritz et al. (2012) further demonstrated that the relative importance of specific controls varied geographically and with biome. In the tropics and warm-temperate regions, NPP was the strongest control on the amount of burning in desert, temperate grassland, temperate savanna and Mediterranean ecosystems, whereas factors influencing fuel drying, specifically dry season precipitation and temperature seasonality, were the strongest controls on the amount of burning in tropical and subtropical dry/moist forests.

Knorr et al. (2014) optimized a non-linear statistical model of fire focusing on the potential human influences on burnt area by using a set of pre-defined but parameterized relationships describing the important natural controls. Thus, they described the influence of fuel production using a positive monotonic relationship between fraction of Absorbed Photosynthetic Radiation (fAPAR) and burnt area, and the influence of fuel dryness using a positive monotonic relationship between the Nesterov Index (NI) and burnt area. They then tested relationships between population density amongst different land cover types/socio-economic development regions and fire frequency (roughly the inverse of burnt area). Using non-linear parameter optimization, they showed that increases in human population result in a significant exponential decrease in fire in all but the most sparsely populated ( $<0.1 \text{ people/km}^2$ ) areas.

Bistinas et al. (2014) used Generalized Linear Modelling (GLM) to examine the relationships between 11 variables representing vegetation, land use, climate and potential ignition rates (tree cover, grass/shrub cover, NPP, number of dry days, diurnal temperature range, maximum monthly temperature, the ratio of actual to equilibrium

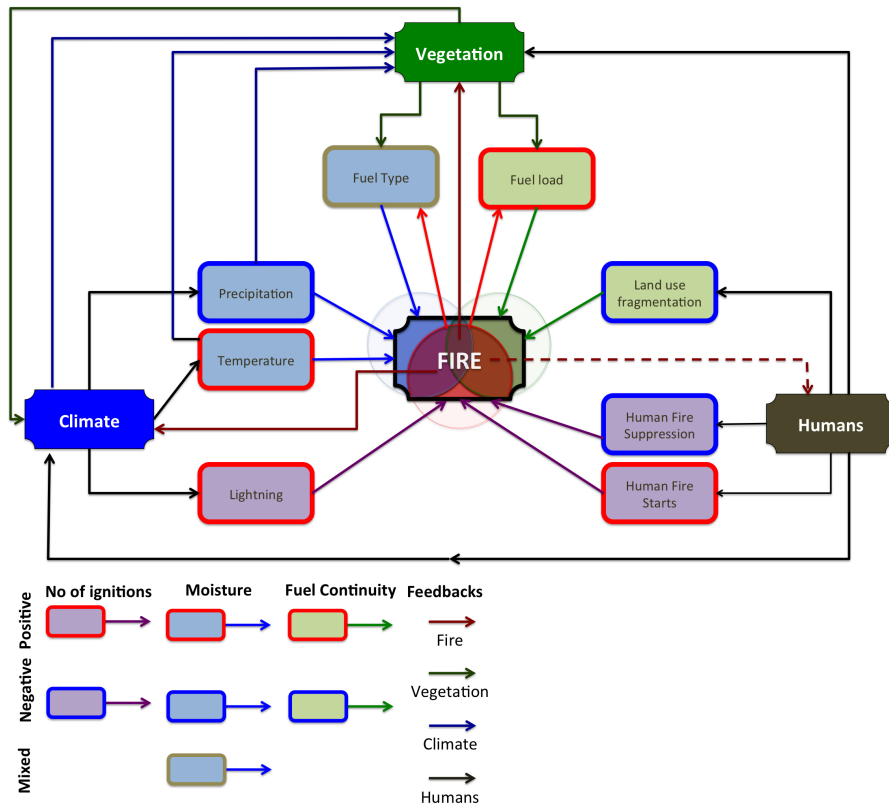


FIGURE 1.5: Summary of the interactions between the controls on fire occurrence on coarse scales. Green boxes show controls influencing fuel; blue influencing moisture; and purple influencing ignitions. Red box indicates positive influence on fire; blue a negative influence, and brown a mixed response. Brown arrows indicate interactions between people and other controls; dark green between vegetation and other controls; and dark blue from climate. Red arrows show feedback from fire.

evapotranspiration  $\alpha$ , lightning number, crop area, grazing land area, population density). The choice of environmental predictor variables was guided by explicit hypotheses about the potential controls of burnt area, and the GLM approach was adopted so as to be able to take account of potential interactions or co-variations between the controls in order to identify the underlying relationships. Bistinas et al. (2014) showed that burnt area increases with NPP, number of dry days, maximum monthly temperature, grazing-land area, grass/shrub cover and diurnal temperature range, and decreases with  $\alpha$ , cropland area and population density. They further showed that there is no significant relationship with the number of lightning strikes or with tree cover. Fuel production (NPP) is the most important determinant of burnt area, with factors affecting the rate of fuel curing (e.g.  $\alpha$ ) and fuel dryness (diurnal temperature range) and fire risk (number of dry days, maximum monthly temperature) next in importance, along with factors that influence fuel type (grass/shrub cover). The simple monotonic

relationships between these predictor variables and burnt area are nevertheless sufficient to give rise to complex behavior. Specifically, Bistinas et al. (2014) show that the unimodal relationships that have been shown between e.g. mean annual temperature, mean annual precipitation, population density and gross domestic product are secondary consequences of correlations among predictor variables. Thus, the unimodal relationship between population density and burnt areas results from the co-variance of population with production and moisture: arid conditions, where fire is limited by productivity and fuel availability, typically support only low population densities.

Thus, a consensus is emerging from these global analyses about the importance of specific controls on fire. All of the studies show that vegetation productivity is the most important control on burnt area, closely followed by factors that influence fuel drying or curing, but with the relative importance of each depending on local environmental conditions. Ignitions, whether natural or anthropogenic appear to be non-limiting to burnt area — effectively, there are always enough potential fire starts and fire spread is therefore determined by other controls. As demonstrated very clearly by Knorr et al. (2014) and Bistinas et al. (2014), the most significant human impact on fire is through suppression with burnt area decreasing with population density.

### 1.3.2 Controls of fire in Australia

I have explored the spatial variability in the relative importance of different controls on fire across Australia, using a GLM approach similar to Bistinas et al. (2014). The independent variables are NPP (as a surrogate for fuel load), the ratio of actual to equilibrium evapotranspiration during the driest month of the year ( $\alpha$ ) as a surrogate for fuel drying, lightning flash count in the driest month as a surrogate for natural ignitions. The dependent variable is burnt area from GFED version 4 (Giglio et al., 2013), regridded to a  $0.5^\circ$  resolution grid. All variables are averages from the period 1997-2012. In the GLM framework, I computed the inverse of the component + residual (as in Fig. 1 in Bistinas et al., 2014) for each variable (designated  $\beta_{NPP}$ ;  $\beta_\alpha$ ;  $\beta_{Lightn}$ ) in each grid cell using R (R Core Team, 2013). This is the inverse of the contribution of each variable to the glm result and represents the relative limitation of the variable. The relative importance of the controls on fire was assessed as:

$$\bar{\beta}_i = \frac{\beta_i}{\beta_{NPP} + \beta_\alpha + \beta_{Lightn}} \quad (1.1)$$

Moisture is the most important limiting factor on fire over most of coastal areas in Eucalyptus woodland/forest and rainforests of southeastern and southwestern Australia (Fig. 1.6), consistent with local studies which indicate that moisture is important in these areas (e.g. Ellis et al., 2004; Verdon et al., 2004). Moisture limitation is still important in the coastal eastern Eucalyptus woodlands, but variability in fuel loads also has an impact (Fig. 1.6). Again, the fact that fuel load is more important in these woodlands than other eastern forests has been highlighted in multiple local studies (e.g. Walker, 1981; Raison et al., 1983; Bradstock, 2010). Fuel limitation is almost exclusively important in ecosystems in the interior of the continent, in agreement with findings from local studies (Allan and Southgate, 2002). Some of the most arid ‘heath’

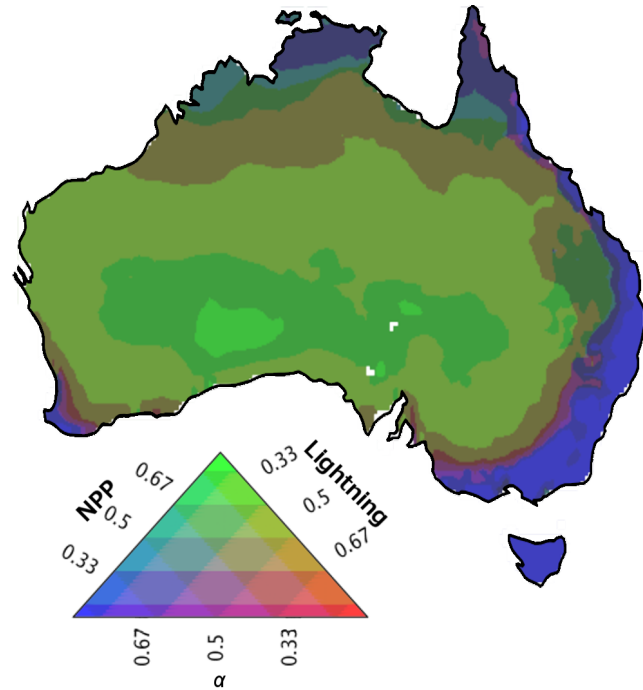


FIGURE 1.6: Relative contributions of production, moisture and natural ignitions to the limitation of fire in Australia. Green indicates areas limited by net primary production (NPP); blue indicates dry season moisture ( $\alpha$ ) limited; and red indicates dry season lightning limited areas. Mixed limitation between production and lightning occurs in yellow-brown areas; mixed limitation between Lightning and moisture in purple areas. Equal limitation (or no limitation) in grey areas.

is exclusively fuel limited, but there is still a small ( 20%) contribution of moisture limitation in regions associated with grassland and shrubland in the semi-arid ecosystems of the interior. Moisture limitation becomes increasingly important in ecosystems in northern Australia (Fig. 1.6). The transitions from fuel limitation (in the interior) to moisture limitation (in the north) correspond to the transitions from woodland/savanna to shrubland/grassland. There are no areas of Australia where ignitions are the major limitation on fire.

## 1.4 Adaptations to fire

In ecosystems that experience periodic fires, many plants display adaptations that either increase the chances of an individual surviving a fire or allow rapid recovery of either the individual or the ecosystem after a fire. These characteristics are generally referred to as fire-resistance traits or fire-response traits respectively (Clarke et al., 2013). It has also been argued that some plants have adaptations that promote fire.

### 1.4.1 Fire resistance traits

The main cause of mortality from fire in woody plants is through damage to the trunk and, if the flame is carried into the canopy, via damage to the crown (Dickinson and Johnson, 2001; Michaletz et al., 2012). Trunk damage can cause mortality in two ways: cambium damage and embolism. Mortality through necrosis of phloem and vascular tissue occurs when the cambium is heated above 60° C (Dickinson and Johnson, 2004; Bova and Dickinson, 2005; Dickinson et al., 2005; Jones et al., 2006). Cambium damage inhibits transportation of photosynthesized carbon, and causes mortality through carbon starvation (Kramer and Kozlowski, 1960; Ryan and Frandsen, 1991; Nobel, 2005). Depending on the size of available carbon stores, starvation can take months to decades (Ryan and Frandsen, 1991; Tyree and Zimmermann, 2002; Nobel, 2005). Heating of the trunk can also lead to embolism in the xylem tissues, resulting in loss of xylem conductivity (Schoonenberg, 2003; Balfour and Midgley, 2006; Michaletz et al., 2012). Mortality from embolism occurs within weeks (Ducrey et al., 1996; Michaletz et al., 2012), much faster than mortality from cambium damage. Bark helps to protect the cambium and xylem from the effects of fire (Vines, 1968; Hoffmann and Solbrig, 2003; Climent et al., 2004; Lawes et al., 2011a; Uhl and Kauffman, 1990) by buffering against heat transfer. Heat transfer is largely independent of the density and moisture content of bark, and therefore the thickness of the bark is the major determinant of resistance to trunk damage (Vines, 1968; Lawes et al., 2011), with thicker bark providing longer protection against more intense fires (Gill and Ashton, 1968; Peterson and Ryan, 1986; Lawes et al., 2011a). There is an overall increase in bark thickness (for a given tree diameter) as fire frequency increases (Fig. 1.7, based on bark thickness data collected and discussed in Chapter 4, Kelley et al., 2014 and fire frequency data from GFED4: Giglio et al., 2013).

High growth rate is also considered a fire-resistance trait. Rapid growth allows trees to grow above the characteristic flame height (Gignoux et al., 1997; Higgins et al., 2000; Archibald and Bond, 2003; Bond, 2008) thus ensuring that individual specimens suffer minimal fire damage. It has also been suggested that high growth rates allow some species to emerge from the canopy, thus minimizing the impact of fires that spread through the canopy on these emergent trees (Johnson, 1996).

Traits such as high growth rates and thick bark may increase resilience, but they also have a cost. Investment in growing thick bark, for example, uses carbon that would otherwise be used to increase tree height and thus trees with thick bark tend to have slow juvenile growth rates (Archibald and Bond, 2003; Balfour and Midgley, 2006; Lawes et al., 2011a). There is also evidence that trees with thick bark have lower wood density, and are therefore more susceptible to wind damage, drought, insect attack and herbivory in the juvenile stage (Hacke et al., 2001; King et al., 2006; Curran et al., 2008; Chave et al., 2009; Baraloto et al., 2011). Optimal resource theory has been used to explain trade-offs involved in adopting different trait strategies depending on environmental conditions (Medlyn et al., 2011; Prentice et al., 2014). However, the trade-offs involved in fire-related strategies, and their relationship with climate

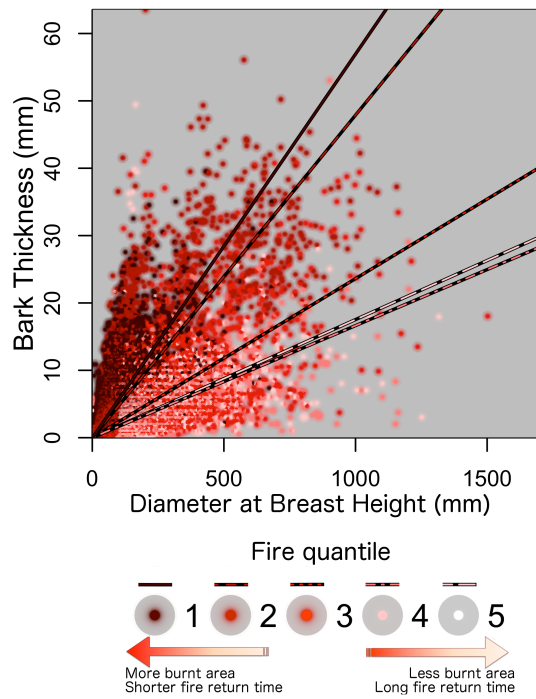


FIGURE 1.7: Site based observations of bark thickness vs tree diameter (measure at breast height) taken from the bark thickness dataset in Chapter 4 (Kelley et al., 2014). The intensity of red indicates the frequency of fires based on annual burnt area from GFED version 4 (Giglio et al., 2013) Jun 1995-May 2012 split into 5 equally distributed quantiles.

and environmental controls on vegetation, have not yet been quantified (Lawes et al., 2011a).

### 1.4.2 Fire-recovery traits

There are two types of mechanism that promote rapid recovery after fire: resprouting and timed re-seeding (Hilbert, 1987; Gignoux et al., 1997; Pausas, 2001; Bond and Midgley, 2001; Fensham et al., 2003; Miller and Chesson, 2009; Clark et al., 2013; Tucker and Cadotte, 2013). 1.8 Resprouting plants regenerate rapidly after severe loss of biomass via sprouting from meristem tissue located either in above-ground stems and branches or in below-ground tissues. The ability to resprout is largely confined to angiosperms; few gymnosperms can resprout (Del Tredici, 2001; Paula et al., 2009; Lunt et al., 2011). Several types of resprouting are recognized (Clark et al., 2013) depending on the location of the meristem tissue (Fig. 1.8). Aerial resprouters include plants that resprout from apical buds (apical resprouters in the terminology of Clark et al., 2013) and from meristems located under the bark on stems or branches (epicormic resprouters). Epicormic resprouters generally have relatively thick bark, which protects the meristem from damage in fires. However, some resprouting eucalypt species have thin bark because the meristem tissue is located deep within the heartwood rather than just below the bark, making bark protection less important (Lawes et al., 2011a;

Clarke et al., 2013). Some plants resprout from stem tissue close to or just below ground level (basal or collar resprouters) or from roots or rhizomes underground (underground resprouters). Underground resprouters and, to a lesser extent, basal/collar resprouters, capitalize on the protection offered by the soil against fire damage.

Resprouting plants must allocate carbon to roots and non-structural carbohydrate stores that are utilized during resprouting (Bell and Ojeda, 1999; Paula and Ojeda, 2009; Clark et al., 2013). This diverts resources away from other purposes, particularly reproduction. Resprouting plants often take longer to reach sexual maturity (Clarke et al., 2013) and generally produce less seeds or seeds with lower recruitment rates (Lamont and Wiens, 2003). Clarke et al. (2013) have put forward a conceptual model in which the occurrence of resprouters is driven by resource availability (i.e. nutrients, light and moisture) and disturbance. Both resprouters and non-resprouting plants can occur in regularly disturbed, nutrient poor ecosystems (Clarke et al., 2005). However, resprouting plants are more able to produce non-structural carbohydrates when nutrient availability increases, and thus they have a competitive advantage over non-resprouters in nutrient-rich, disturbed environments (Clarke and Knox, 2009). According to this conceptual model, the type of resprouting reflects the strength of disturbance. Thus, aerial resprouters occur in relatively moist environments in which carbon uptake is high, and fires are not sufficiently severe to deplete above-ground non-structural carbon stores but nevertheless frequent enough to convey a competitive advantage over non-resprouters. As fire severity (or frequency) increases, the likelihood of above-ground non-structural carbon stores being destroyed also increases and thus the competitive advantage lies with underground or basal or collar resprouters compared to epicormic or apical resprouters (Bellingham and Sparrow, 2000; Morrison and Renwick, 2000; Keeley, 2006).

Many species have developed strategies to ensure that seed release is timed to coincide with fire. Post-fire seedling establishment can provide optimal conditions for germination (Bond et al., 1984; Keeley et al., 2012) including reduced competition, optimum substrate, and maximum time to grow before the next disturbance. The two main mechanisms are timed release of seeds retained on the mother plant (serotiny: Lamont and Maitre, 1991) and induced germination of seeds retained in the soil seed bank. Induced germination can be triggered by a variety of chemical, physical or environmental signals caused by burning (Keeley and Fotheringham, 2000; Wills and Read, 2002). Serotiny is common in *Pinus* spp. in the northern hemisphere (Thomas et al., 2010) (Thomas 2010) and in evergreen hardwoods such as Banksia in Australia (Cowling and Lamont, 1985; He et al., 2011). Induced germination appears to be most common in low nutrient shrublands with intermediate fire return intervals and high burn severity (Clarke et al., 2012). Serotiny can occur in ecosystems that have very low fire frequency. For example, *Pinus contorta* is serotinous and occurs in boreal forests where fire return time may be as long as 150 years (Thomas et al., 2010). Timed re-seeding is not common in fire regimes where the fire return time is very short, when there is not enough time to build up a seed bank (Enright et al., 1998; Clarke et al., 2012). Nor is it common when the fire interval is longer than the lifespan of the soil



FIGURE 1.8: Examples of resprouting: **a)** a single apical shoot on *Xanthorrhoea sp.*, 6 months after fire disturbance; **b)** apical resprouting of understory *Xanthorrhoea*, 4 months after fire disturbance; **c)** epicormic shoot on *Eucalyptus sp.*, 4 months after fire; **d)** multiple epicormic shoots on *Eucalyptus sp.*, 8 months after fire; **e)** basal resprouting on *Eucalyptus sp.*, 6 months after fire; **f)** basal resprouting in Eucalyptus woodland 4 months after fire. a)-e) taken in Lane Cove National Park, New South Wales; f) taken in Kingslake, Victoria courtesy of Caufield (2009)

seed bank (in the case of induced germination) or the parent plant (in the case of serotiny).

Individual species can display both resprouting and reseeding responses. Although there is a general tendency for continuous variation in the relative expression of the two in response to most kinds of disturbance, this is less obvious in the case of the response to fire (Verdon et al., 2004; Vesk, 2006; Cowan, 2010). In general, plants are either resprouters or non-sprouters. The ability to resprout is an important characteristic in fire-prone ecosystems because it ensures that the ecosystem recovers within a few years after the fire. Timed germination also ensures a more rapid ecosystem recovery after disturbance than could be achieved through non-triggered germination of seeds in the soil, but nevertheless full recovery will be slower than achieved through resprouting because of the time it takes to regrow mature trees.

### 1.4.3 Traits that promote fire

Many plants have traits that encourage fire. Grasses produce finer, more flammable fuel than woody plants, which dries quicker, making those ecosystems that contain abundant grasses more susceptible to fire. Woody plants also display a number of traits that increase fire. These include the presence of volatile compounds in leaves or bark that increase flammability (Scarff and Westoby, 2006; Ormeño et al., 2009), small leaf size which affects aeration and thus the flammability of the fuel bed (Schwilke and Ackerly, 2001; Scarff and Westoby, 2006; Kane et al., 2008; Murray et al., 2013), and retention of dead biomass, particularly deciduous bark which acts as “ladder fuel” to transfer fire into the crown (Keeley et al., 2011). It has been argued that some species have evolved traits to actively promote fire, either because they themselves require fire for regeneration or to reduce competition. Gagnon et al. (2010) have suggested that it is an advantage for plants that resprout to display traits that increase flammability because this leads to the fire spreading more rapidly. This results in shorter fire residence time, which means that there is less time for cambial damage (in the case of epicormic resprouters) or overheating of the soil (in the case of underground resprouters) and thus an increased chance of resprouting occurring. Similarly, it has been argued that the presence of ladder fuel is particularly common in serotinous species that require fire to initiate seed release (Schwilke and Ackerly, 2001; Thomas et al., 2010; Cowan and Ackerly, 2010; Saura-Mas et al., 2010). Bond and Midgley (1995) have suggested that the evolution of traits to promote fire is a mechanism to enhance the success of the trait-bearing species by reducing competition from other species, the so-called ‘kill thy neighbor’ hypothesis. Fire-promoting species benefit from the death of co-occurring species because reduced competition for light and other resources allows successful colonization by their own propagules. However, Midgley (2013) argues that the conditions that require kin-selective evolution of flammability — which include very localized seed dispersal, a limited number of close neighbors, and high post-fire fitness — are too restrictive to be a common cause of the flammability found in many ecosystems. This suggests that flammability is an emergent property of an ecosystem.

## 1.5 Modelling fire in dynamic global vegetation models

Dynamic Global Vegetation Models (DGVMs) are used to simulate vegetation and biogeochemical cycles at a regional to global scale at relatively coarse resolution (Prentice et al., 2007). DGVMs simulate the dynamic competition for resources (i.e. light, water, nutrients) between a small number of plant functional types (PFTs) which can occur in a given climate space. PFTs are generally distinguished by a combination of life form (e.g. tree, grass, shrub), leaf and/or hydraulic architecture (e.g. broadleaf or needleleaf, angiosperm or gymnosperm), phenological response to cold or drought (e.g. cold-deciduous, drought-deciduous, evergreen), photosynthetic pathway ( $C_3$  or  $C_4$ ) and climate range (e.g. boreal, temperate, tropical). DGVMs simulate photosynthesis and the transfer of carbon between live biomass (typically split into sapwood/heartwood, leafmass and rootmass) and dead biomass (litter pool, soil carbon) and the atmosphere (including heterotrophic respiration). DGVMs have been widely used to explore changes in vegetation, hydrology or carbon cycling as a result of historic and future changes in climate (Cramer et al., 1999; Scholze et al., 2006; Sitch et al., 2008a; Scheiter and Higgins, 2009; Prentice et al., 2011; Murray et al., 2012; Ukkola and Prentice, 2013)

Early DGVMs generally include a generic treatment of disturbance on plant mortality (see e.g. TRIFFID: (Cox, 2001); SLAVE: (Friedlingstein and Bopp, 2001); ED: (Moorecroft et al., 2001); BIOME-BGC: (Thornton, 1998); IBIS: (Foley and Prentice, 1996; Kucharik et al., 2000)). The CASA model (Potter and Klooster, 1999) is routinely used to assess the contribution of fire to the atmospheric carbon burden, but the incidence and timing of fire is prescribed from satellite observations converted to burnt area (e.g. van der Werf et al., 2003, 2004, ; Table 1.1) with carbon emissions described using a biomass/litter type combustibility parameter (Table 1.2). This approach avoids introducing model uncertainties in fire occurrence into the emissions estimates, but cannot be used to investigate the response of fire to climate changes. The importance of fire in the carbon cycle, as well as in controlling the distribution of savanna and grassland vegetation, underpins the development of a more explicit treatment of fire disturbance.

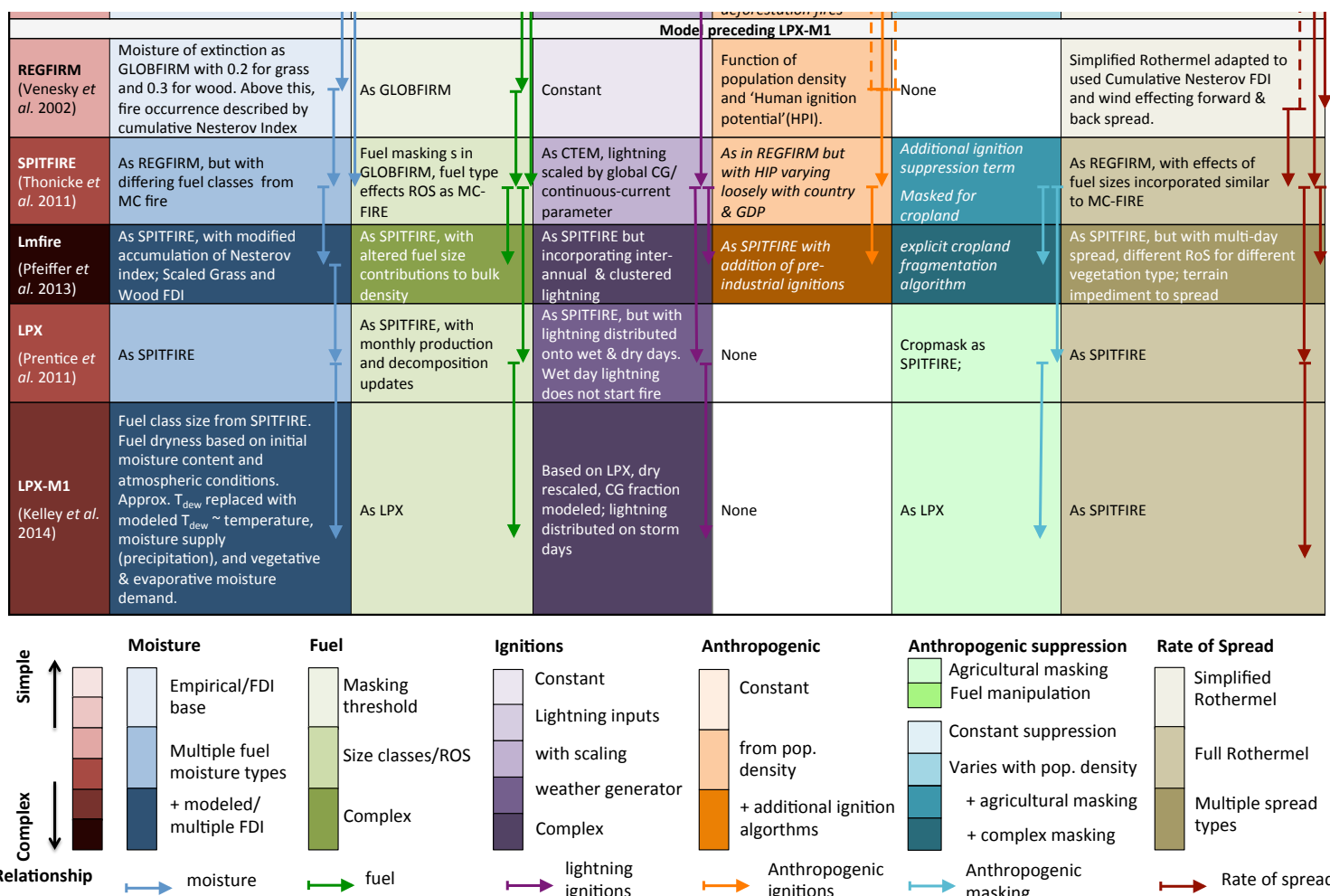
The GLOBal FIRE Model (GLOBFIRM Thonicke et al., 2001) was one of the earliest representations of fire for use in a DGVM (Table 1.1). In GLOBFIRM, burnt area is an exponential function of annual fire season length, based on the idea that the longer burning conditions persist (i.e. the longer the fire season) the larger fires can grow. Fire season length is calculated as the summed daily ‘probability of fire’, which is an exponential power function of fuel moisture and the moisture of extinction (i.e. the point at which latent heat demand of moisture becomes too great for a fire to occur). Fuel moisture is considered to be equivalent to the moisture content of the upper part of the soil (explicitly simulated by the DGVM) and the moisture of extinction level is set to 30% saturation. The functions relating moisture, season length and burnt area were calibrated using site-based observations. In addition, GLOBFIRM has a threshold value of 200 gC/m<sup>2</sup> to represent the point at which fuel becomes discontinuous and

the probability of fire occurring is therefore zero. In order to calculate emissions, it is assumed that all the aboveground litter/biomass is burnt and this is converted to carbon flux using a PFT-specific emission factor. GLOBFIRM was initially developed for inclusion in the Lund-Potsdam-Jena DGVM (LPJ: Thonicke et al., 2001) (Sitch et al., 2003), but has since been coupled into several other DGVMs including the Common Land Model (Dai et al., 2003; Chen, 2008, CDLM) and the Community Land Model (Levis et al., 2004; Oleson et al., 2010; Lawrence et al., 2011; Castillo et al., 2012, CLM) and, with some slight modification, into the ORganizing Carbon and Hydrology in Dynamic EcosystEms (Krinner et al., 2005, ORCHIDEE) and Biosphere Energy-Transfer Hydrology (Kelley, 2008; Kaminski and Knorr, 2013) models.

Subsequent fire-model developments drew on concepts identified through local-scale studies (Venevsky et al., 2002) and in particular tried to link the four components of fire risk or environmental susceptibility to fire, ignitions, suppression and fire spread in a modelling framework. (Pechony and Shindell, 2009), for example, developed a fire algorithm that incorporated fire susceptibility, natural and anthropogenic ignitions and fire suppression (Table 1.1) in order to calculate the number of fires. Fire susceptibility is a function of Leaf Area Index (LAI), which is a proxy for fuel load, precipitation which is a proxy for fuel moisture and vapor pressure deficit (VPD) which is a proxy for the drying power of the atmosphere. Natural ignitions are prescribed from remote sensed observed lightning, scaled by latitude to account for a higher fraction of cloud-to-ground strikes (CG) as opposed to cloud-to-cloud flashes at lower latitudes (Prentice and Mackerras, 1977). Anthropogenic fire starts are modeled as a function of population density multiplied by a global parameter representing the probability of a person starting a fire. This approach, originally developed by Venevsky et al. (2002), produces an increase in the number of fires starts with increasing population but with a gradient that decreases as the opportunities for fire starts become saturated. The model also includes anthropogenic suppression, which increases with population, again saturating at high population densities. The model itself is not designed to calculate burnt area, but simulated number of fire starts have been converted into burnt area using an “expected fire size” scaling algorithm used to derive CASA burnt area (Pechony and Shindell, 2009). The human ignition and suppression relationships described by (Pechony and Shindell, 2009) have been used in several other fire models (Kloster et al., 2010; Thonicke et al., 2010; Li et al., 2012; Pfeiffer et al., 2013).

TABLE 1.1: Development of the processes controlling fire in coupled DGVM-fire models. Shade of colour represents the complexity of the description of the process. Red describes the complexity of the model as a whole: light red being the simplest; dark red being the most complex. Blue represents the complexity of description of moisture control on fire susceptibility ranging from: simple statistical relationships/ fire danger indices (FDIs) of fuel as a whole (light blue); description of moisture in multiple fuel size classes; fully modelled or specifically chosen FDIs for specific fuel moisture (dark blue). Green represents the complexity of fuel controlled fire susceptibility: simple masking at a specified fuel threshold (light green); fuel structure effects on ignition probability and rate of spread; and complex modelling of fuel bulk density (dark green). Purple shows complexity of natural ignition schemes: no specified/ assumed ignitions (white); constant ignition source (light purple); prescribed ignitions - normally through lightning climatology inputs; prescribed lightning with additional scaling for e.g. latitude dependent cloud-ground lightning (CG); daily distributed lightning via a weather generator; and with additional complex ignition simulation (dark purple). Orange represents anthropogenic ignitions: none (white); constant background ignition source (light orange); human population density varying ignitions based on a ‘human ignition potential’ (HIP) and/or gross domestic product (GDP); inclusion of additional, complex human ignition schemes such as pre-historic human behaviour (dark orange). Cyan and lime green represent inclusion of human ignitions suppression and agriculture: none (white); constant suppression (light cyan); increasing suppression with population (medium cyan); simple agricultural masking of fire (light lime green); fuel load manipulation from agriculture (lime green); a mix of agricultural and ignition suppression (dark cyan). Italicize text under ‘human ignitions’ and ‘human suppression’ denote models where the combined influence of human ignitions and suppression result in a unimodal description of fire relative to population density (see section 1.3.1). Brown shows complexity of the calculation of fire sizes, typically through a rate of spread model (RoS):. None (white); simplified RoS model (light brown); full Rothermel RoS; multiple RoS models (dark brown). Arrows demonstrate the exchange of components between models. Arrows start in the model containing the original process description.

Model	Moisture	Fuel	Natural Ignitions	Anthropogenic Ignitions	Anthropogenic Suppression	Rate of Spread (ROS) & Wind
<b>CASA/GFED</b>	None. Fire translated to burnt area from satellite fire counts.					
<b>GLOBFIRM</b> (Thonikke et al. 2001)	Increasing probability of fire for moisture <30%	No fire < 200 g/m <sup>2</sup>	Assumed	None		None
<b>ORCHIDEE</b> (Krimmer et al. 2005)	As in GLOBFIRM	As in GLOBFIRM	As in GLOBFIRM	As in GLOBFIRM	Reduced fuel from grazing	As in GLOBFIRM
<b>P&amp;S</b> (Pechony & Shindell, 2009)	Function of VPD representing ambient atmospheric conditions (temperature, relative humidity & precipitation)	Fire scaled by vegetation density based on LAI	Input lightning. Latitude dependent CG lightning	Ignitions as in REGFIRM	Suppression Increases with population	No fire spread: Model only calculates fire counts. Burnt area calculated as in CASA.
<b>Rate of Spread Models</b>						
<b>Rothermel RoS</b> (Rothermel 1972)	Effects RoS	Fuel size ratios effected RoS	-	-	-	Oval fire spread, scaled by Canadian Fine Fuel (Van Wagner, 1987); National System (Bradshaw et al. 1983) FDIs. stretched by wind
<b>MC-FIRE</b> (Lenihan et al. 1998)	Fuel moisture from live fuel & 4 dead size classes. Effects RoS & fire start	As Rothermel	Fire occurrence when 1000hr fuel moisture content goes below 14.2%	None		Simplified Rothermel with constant wind
<b>CTEM</b> (Arora and Boar 2005)	Fuel moisture represented by soil moisture. Reduces rate of spread & effects prob. fire occurrence	No fire below 200 gC/m <sup>2</sup> ; Fuel limitation to 1000 gC/m <sup>2</sup>	Lightning inputs	Constant	Constant suppression	MC-FIRE minus FDI. Addition of differing fuel types. Variable Wind treated as in REGFIRM
<b>Li</b> (Li et al. 2012)	No fire for Rh >70%; No suppression from moisture for Rh<30%. In-between, moisture limits fire based on surface soil wetness.	As CTEM but with values 155 & 1050 gC/m <sup>2</sup>	As P & S	As in P & S. HIP parameter re-tuned for global use	As in P & S	As CTEM
<b>Kloster</b> (Kloster et al. 2012)	As CTEM	As CTEM	Input lightning. Latitude dependent CG lightning similar to P & S	As P & S with HIP dependent on population density such that prob. of ignition = 100% at 300 people/m <sup>2</sup> Inclusion of deforestation fires	As in P & S	As CTEM



MC-FIRE (Lenihan et al., 1998) was the first attempt to link number of fires to burnt area via an explicit Rate of Spread (RoS) model. MC-FIRE simulates fire on a daily timestep but takes information about the vegetation from the DGVM simulations only once a year. Fuel load is equivalent to the litter produced in the previous year, and divided into four size classes (1hr, 10hr 100hr and 1000hr fuel classes) corresponding to the size-dependent time constant of drying to equilibrate with the surroundings. Total fuel moisture is the sum of these four dead fuel classes and the moisture content of live fuel. Dead fuel moisture is estimated using the Canadian Fine Fuel Moisture Code (Van Wagner, 1987) and the National Fire Danger Rating System (Bradshaw et al., 1983). Fire starts occur when the moisture content of 1000hr fuel falls below 14.2% and the probability of fire spread according to a simple ignition index (Bradshaw et al., 1983). MC-FIRE thus only simulates the largest and most intense fires (Lenihan et al., 1998). The rate of spread model is a simplified version of the Rothermel (1972) model, with winds set at a constant value and fires allowed to burn for a maximum of 1 day. Canopy fires are initiated using the (Wagner, 1993) equations. Burnt leaves from crown fires and scorched leaves from tall ground fires provide a source of carbon emissions to the atmosphere, while other scorched material enters the dead litter carbon pool. MC-FIRE inspired the development of several RoS based models and many modern DGVM-driven fire models still use a similar basic framework (e.g. Venevsky et al., 2002; Arora and Boer, 2005; Thonicke et al., 2010; Kloster et al., 2010; Prentice et al., 2011; Li et al., 2012; Pfeiffer et al., 2013).

In the Canadian Terrestrial Ecosystem Model (CTEM) model (Arora and Boer, 2005), the pre-defined FDI in MC-FIRE to determine fire occurrence is replaced by an explicit calculation of susceptibility as the product of the probabilities associated with fuel and moisture constraints on fire (Table 1.1). The probability of fire is zero when fuel is less than  $200 \text{ gC/m}^2$  and increases to 1 as fuel loads increase to  $1 \text{ kgC/m}^2$ . Fuel does not limit fire above this threshold. The probability of fire as moisture increases follows a relationship similar to that used in GLOBFIRM (Table 1.1).

CTEM simulates ignitions in a more explicit way than MC-FIRE. Ignitions are calculated as a combination of natural and anthropogenic ignitions. Natural ignitions are prescribed using a spatially and monthly varying climatology of lightning strikes, and scaled using a simple linear transformation. The probability of anthropogenic ignition is 0.5 globally. The number of fire starts is simply the probability of fire susceptibility by the probability of an ignition source. CTEM then uses a RoS model similar to MC-FIRE to define the area burnt of an individual fire. It differs from MC-FIRE by including variable winds and by allowing wind direction to determine the shape of fire spread. CTEM includes fire suppression via a ‘fire extinguishing’ probability to account for suppression by natural and man-made barriers, as well as deliberate human suppression of fires. However, this probability is set to 0.5 everywhere. Fire fluxes to the atmosphere are defined by PFT and wood type combustibility parameters. Fluxes to other carbon pools follow the same process as CASA (van der Werf et al., 2003, ;Table 1.2).

The Li et al. (2012) fire model uses the same basic concept as CTEM, but borrows elements from other fire models (Table 1.1). Thus it employs the same fuel-fire

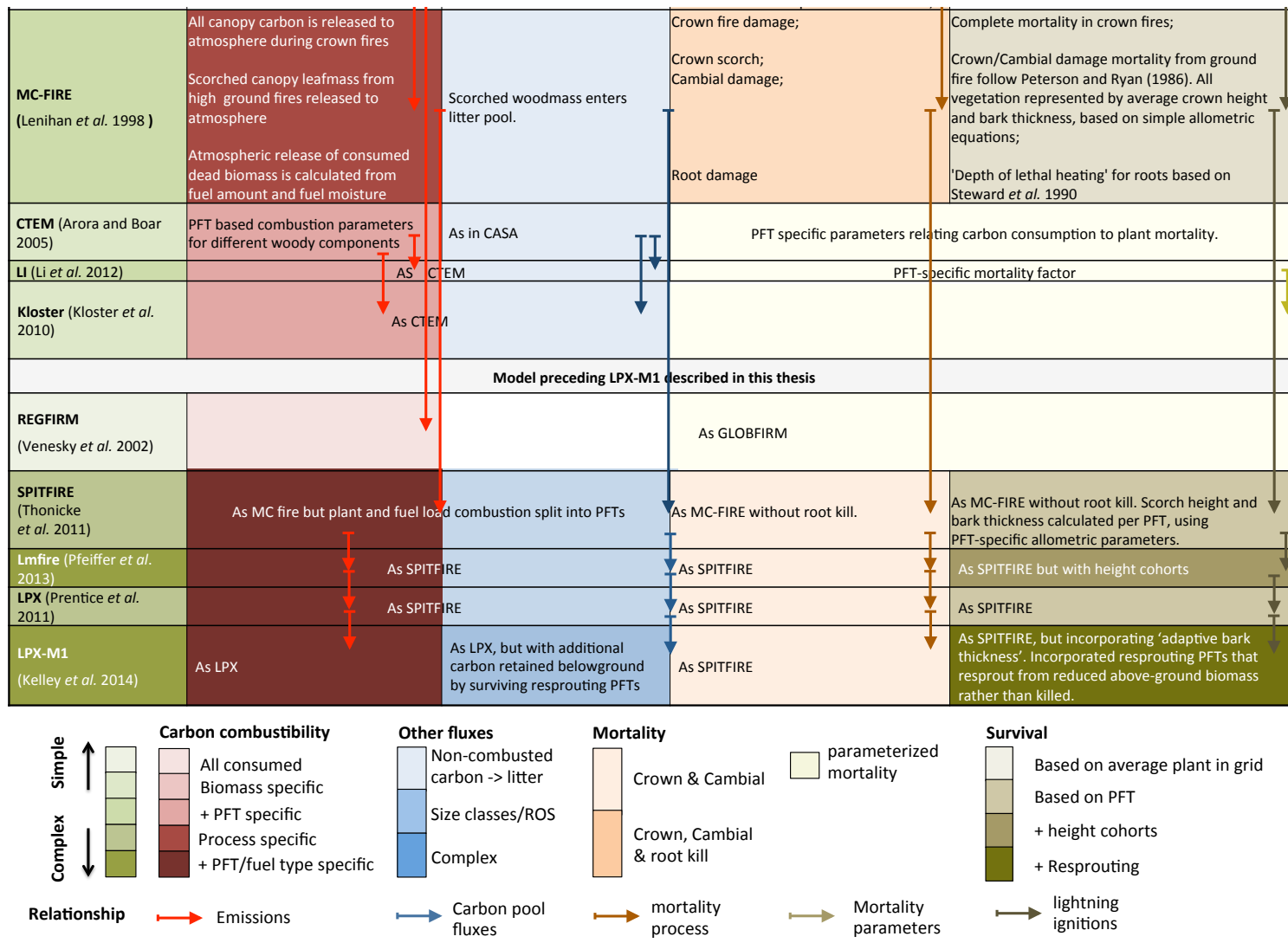
probability approach as CTEM, but the lower fuel threshold is 155 gC/m<sup>2</sup> and the upper threshold above which fuel is not limiting is 1050gC/m<sup>2</sup>. The impact of moisture on the probability of fire is recast to include relative humidity thresholds: the probability of fire is zero when the relative humidity is >70% but when relative humidity levels drop to <30% there is no moisture limitation on fire. Between these values, the probability of fire is defined by surface soil wetness in the same way as in CTEM (Table 1.1). Li et al. (2012) use the natural and anthropogenic ignition scheme from (Pechony and Shindell, 2009) (Table 1.1), but with the human ignitions re-tuned based on comparison of MODIS active fire counts, modeled fire susceptibility and natural ignitions, and population densities from wildland areas in the US. They also use the same suppression algorithm as Pechony and Shindell (2009), giving rise to a unimodal relationship between population density and fire as in Pechony and Shindell (2009) (Table 1.1). However, the RoS model is the same as in CTEM (Table 1.1). Li et al. (2012) calculate carbon fluxes as in CTEM.

Kloster et al. (2010) adopt a similar approach of combining elements from CTEM and Pechony and Shindell (2009) in the construction of a fire model for use in Community Land Model (Table 1.1). Thus, the ignition and suppression schemes follow Pechony and Shindell (2009) except that the anthropogenic ignitions vary such that the probability of ignition is 1 when population density is 300 people/km<sup>2</sup> (Table 1.1) while other elements of the model follow CTEM. Carbon fluxes are calculated as in CTEM, except that Kloster et al. (2010) include the impacts of prescribed land use change on fire fluxes via a simple set of ‘land conversion flux’ parameters. A fraction of this lost carbon is released as fire emission, calculated from the same fire susceptibility function used in the fire component of the model. Kloster et al. (2010) tested different parameterizations of human ignition and suppression and demonstrated that the unimodal relationship for human fire starts introduced from Pechony and Shindell (2009) translates into a unimodal relationship between population density and burnt area and fire flux.

There has been a succession of RoS-based fire models developed for use within the Lund-Potsdam-Jena (LPJ) DGVM. The first, REGional FIRe Model (REGFIRM Venevsky et al., 2002) adopted the discontinuous fuel load threshold of 200 gC/m<sup>2</sup> used by GLOBFIRM to prevent fires occurring in regions of low productivity. Outside these regions, fire susceptibility is calculated from fuel moisture using the Cumulative Nestroff Fire Danger Index (NI Nesterov, 1949) to describe the cumulative drying power of the atmosphere. REGFIRM uses monthly climate data interpolated to daily values. Daily temperature and dew point temperature as used to estimate relative humidity (as described by Running et al., 1987) and dew point temperature ( $T_{dew}$ ) are approximated from the daily minimum temperature ( $T_{min}$ ). With each precipitation event, defined as a day with >3 mm precipitation, NI is set to zero on the assumption that the fuel has become saturated. Between precipitation events, the cumulative NI is calculated over each dry day with a minimum temperature >0°C and upper soil moisture values >30% saturation. The probability of fire start is influenced by overall fuel moisture content and NI, which is considered to approximate the inherent latent heat requirement the atmosphere (Nesterov, 1949; Venevsky et al., 2002). Natural ignitions are prescribed from observations. REGFIRM is the source of the anthropogenic fire starts scheme

TABLE 1.2: Development of the impacts of fire in coupled DGVM-fire models. Shade of colour represents the complexity of the description of the component. Green indicates complexity of the representation of fire impacts. Red describes the complexity of the description of atmospheric fluxes from fire: flux is equivalent to all consumed biomass (light red); consumption based on biomass specific combustion parameters; inclusion of PFT combustion parameters; process based; biomass/PFT parameterized process-based (dark red). Blue represents the complexity of carbon fluxes to other carbon pools: no additional fluxes (white); non-combusted dead carbon flux (light blue); carbon fluxes based on fire spread properties; fire-adapted vegetation carbon retention (dark blue). Orange represents complexity of simulated mortality processes: parameterized morality(yellow); mortality from crown and cambial damage (light orange); additional root damage mortality (dark orange). Brown represents complexity of plant adaptation to fire when mortality processes are included: mortality based on a grid cell's 'average plant' properties of fire resistant traits (light brown); PFT based average traits; inclusion and height cohorts; inclusion of dynamic/complex adaptions such as resprouting (RS)(dark brown). Arrows demonstrate the exchange of components between models, starting in the model containing the original description.

Model (main citation)	Carbon Emission	Other carbon feedbacks	Plant mortality type	Plant resistance
CASA/GFED	Combustibility dependent on fuel type (leaf, stem and root, dead) and life-form (wood or grass)	Killed but not consumed plant material enters litter pool.	Fraction of woody plants killed dependent on % woody to grass cover. In high wood cover, most trees killed. Low tree and high grass cover, few trees killed. All above-ground grass biomass killed; 90% belowground grass biomass survive	
GLOBFIRM (Thonicke <i>et al.</i> 2001)	All aboveground litter & living biomass consumed and released to atmosphere (Sitch <i>et al.</i> 2003)	None	PFT based mortality parameter	
ORCHIDEE (Krimmer <i>et al.</i> 2005)	As GLOBFIRM	Includes 'Black carbon' (i.e. inert carbon for 1,000s years).	As GLOBFIRM	
P&S (Pechony & Shindell, 2009)			None	
Rate of Spread Models				
Peterson and Ryan (Peterson and Ryan 1986)			Crown scorch mortality based on 'lethal scorch height' of fire and canopy height; Cambial mortality based on fire residence time and plant bark thickness;	



used by Pechony and Shindell (2009), but fire suppression is not included in REGFIRM. The RoS model is a simplified form of the Rothermel (1972) model described in Telitsyn (1988, 1996). Only one fuel class is considered. Fire spread is assumed to occur only in the driest part of the day, and daily fire size is therefore calculated based on 241 minutes of burning. Fire carbon fluxes are calculated in the same way as in GLOBFIRM. The SPread and InTensity of FIRE (SPITFIRE: Table 1.1) model (Thonicke et al., 2010) was developed from REGFIRM, but incorporated the idea of using multiple dead fuel classes and live fuel from the MC-FIRE model. The moisture content of the fuel is estimated from NI using an exponential scaling factor that was tuned to observed burnt area. Seasonally-varying lightning ignitions are prescribed from observations, as in CTEM, but a globally constant parameter was used to scale the observations to derive the number of continuous current strikes (i.e. strikes that have sufficient continuous energy to heat fuel to the ignition point: Latham and Schlieter, 1989; Latham and Williams, 2001). Anthropogenic ignitions are a function of population density and the potential number of ignitions per person per day. The potential number of ignitions is a spatially varying parameter, derived using data on numbers of human caused fire and population density, designed to capture socio-economic and cultural influences on the use of fire. The influence of population density per se is unimodal, with increases in fire up to a density of 10 people/km<sup>2</sup> and decreases again thereafter. Fire suppression follows the approach in (Pechony and Shindell, 2009), but an additional mechanism was included by not allowing fire to occur in agricultural areas. Fire fluxes are calculated as in MC-FIRE, but with the introduction of a PFT-specific combustibility parameter to determine the proportion of carbon moved between pools (Table 1.2).

The SPITFIRE model was the basis for the development of the Last Millennium fire model (LMfire: Pfeiffer et al., 2013). LMfire introduced modifications related to susceptibility, ignitions and RoS. Modifications of fire susceptibility include applying the moisture of extinction values for live fuel to other fine fuel categories including organic litter. This is the only value used in calculating the FDI in grass-dominated systems. A further modification is the introduction of gradual wetting on days with precipitation rather than resetting the NI to zero. LMFire includes a substantial modification to the SPITFIRE ignition scheme. Inter-annual variability of lightning is introduced by scaling the lightning climatology using convective available potential energy. Lightning ignitions at each time step are then scaled by the fraction of land burnt up to that date, in order to deal with the tendency for lightning to occur in the same locations. Fires are allowed to burn for more than a single day without requiring a new ignition source. Potential differences in the number of anthropogenic ignitions associated with different cultural groups (specifically hunter-gatherers, pastoralists, farming communities) were introduced based on tuning against observations of historic fire patterns. Fire suppression in agricultural areas was also modified: in addition to not allowing burning in cropland areas, a cellular-automata fire spread model was used to parameterize the impact of cropland masking within a grid cell where the distribution of cropland is assumed to be random. There were also changes to the RoS component of the model, chiefly focused on improving the simulation of fire in specific environments. A new RoS equation was included for grasslands based on Mell et al. (2005). The gridcell RoS is

then the average of the RoS values for grass and woody vegetation. A reduction of fire spread in boreal regions was achieved through scaling fuel bulk density by the length of the growing season in order to increase the density in colder regions. To account for the constraints on fire spread in areas of complex topography, a “terrain impedance” factor is included. Although all these modifications were based on some form of data analysis or tuning against observations, the analyses were only based on regional data sets and largely conducted independently.

The treatment of post-fire plant mortality in fire-enabled DGVMs is relatively simple and has changed comparatively little over time (Table 1.2). CASA and GLOBFIRM represent tree mortality after fire by scaling the fraction of a cell burnt by mortality parameters that vary with fractional wood cover (CASA) or with PFT (GLOBFIRM). CTEM, REGFIRM and the models described by Li et al. (2012) and Kloster et al. (2012) follow a similar approach but replace burnt area by carbon consumption. MCFIRE has a more explicit treatment of mortality, in which fire intensity and residence time influence mortality from ground fires via crown scorching and cambial damage. Canopy height relative to flame height (which is a function of fire intensity) determines the extent of crown scorching. Bark thickness, which scales with tree diameter, protects against damage to the trunk, such that thicker barked trees have more chance of surviving a fire of a given residence time. LPJ-SPITFIRE uses a similar approach except that the bark thickness scalar with tree diameter is a PFT-specific parameter and canopy height is also defined for each PFT. LMfire includes a simple representation of size cohorts within each PFT, with the bark thickness scalar being defined explicitly for each size cohort. None of these models allows for the variability in bark thickness that occurs between species within a PFT or between individuals of similar height. As a result, simulated fires do not lead to the selection for thicker-barked species that is observed in the real world and which provides a mechanism for tree survival in regions with relatively high fire frequency (see section 1.4.1). Furthermore, all of the models assume that a sufficiently severe fire will kill the tree completely. None of the models incorporate the resprouting response that allows trees in savannas and other fire-prone regions to recover rapidly after fire (see section 1.4.2).

## 1.6 LPX

The Land surface Processes and eXchanges model (LPX: Prentice et al., 2011), the starting point for the model development described in this thesis, was also developed from LPJ-SPITFIRE. The vegetation component of LPX (Fig. 1.9) is based on LPJ (Sitch et al., 2003) and uses nine PFTs: tropical broadleaf evergreen tree (TBE), tropical broadleaf deciduous tree (TBD), temperate needleleaf evergreen (tne), temperate broadleaf evergreen tree (tbe), temperate broadleaf deciduous tree (tbd), boreal needleleaf evergreen tree (bne), boreal broadleaf deciduous tree (bdd), C<sub>3</sub> grass (C<sub>3</sub>) and C<sub>4</sub> grass (C<sub>4</sub>). PFT specific properties (e.g. establishment, mortality and growth) are updated annually, but water and carbon exchange processes (such as production and respiration) are simulated on a monthly time step.

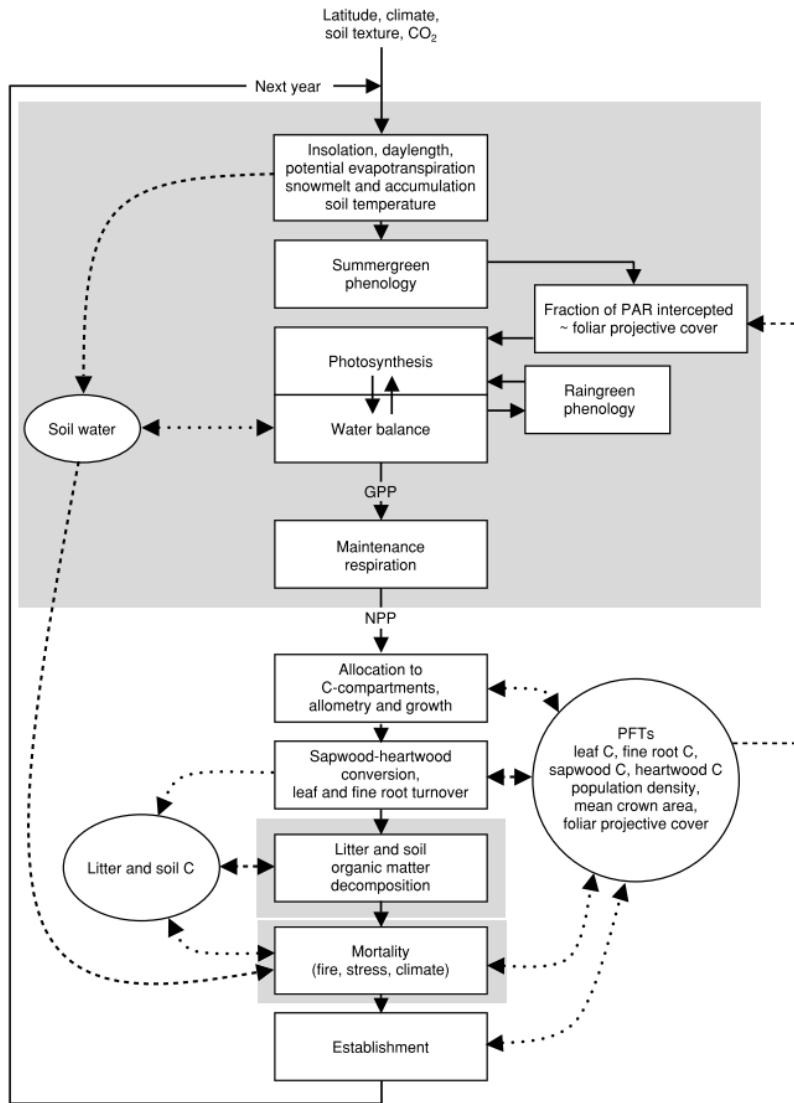


FIGURE 1.9: Description of the simulation of vegetation dynamics used in LPJ-based DGVMs, including LPX. Individual process representations in boxes are performed in all grid cells once per year. The dashed lines show exchange of information between vegetation/soil state variables and vegetation processes. Arrows indicate the direction of information flow. Processes with shaded background run on sub-annual (i.e., monthly or daily) timestep, but are still linked annually. Reproduced from Sitch et al. (2003).

The structure of the fire component of LPX is shown in Fig. 1.10. LPX does not include anthropogenic ignitions. Natural ignition rates are derived from a monthly lightning climatology, and scaled for CG and continuous current as in LPJ-SPITFIRE. A simple inverse power function is used to preferentially allocate lightning to days with precipitation (wet lightning) as opposed to days without precipitation (dry lightning), depending on the number of wet days as determined by the weather generator used by LPJ. This describes the association of lightning with precipitation events: the fewer wet days in the month, the higher the fraction of dry lightning. Only dry day lightning is considered as an ignition source. In another departure from the LPJ-SPITFIRE model, the live and dead fuel loads are calculated on a daily basis in order to capture seasonal fluctuations in fuel load as a result of litter production and decomposition. However, fire susceptibility and spread is modeled in the same way as in LPJ-SPITFIRE (Table 1.1). The fire and carbon components of LPX were tested against seasonal and inter-annual burnt area, the seasonal cycle of CO<sub>2</sub> concentration at individual measurement locations, and the inter-annual variability of fire flux to the atmosphere (Prentice et al., 2011). Model performance globally, and particularly the simulation of fire in tropical regions, is good. However, LPX does not produce a good simulation of Australian vegetation and fire regimes. This discrepancy provides the motivation for model development work in my thesis.

## 1.7 Fire in a Changing Climate

The rising costs of fire (section 1.1.3), along with the particularly early and devastating fires in southern and eastern Australia during 2013/2014 (Shane et al., 2013; NSWRFS, 2013; CFS, 2014), has stimulated public debate in Australia over links between climate change and changing fire regimes (e.g Boer, 2013). Whether the recent increases in fire are linked to climate or not, the climatic controls on fire (section 1.3) are very likely to change in the future (Bowman et al., 2009; Harrison et al., 2010a) with large implications for fire regimes, vegetation composition, and carbon balance. There have been several studies exploring future changes in fire regimes, both globally and for Australia. Global projections have been made using both statistical relationships between climate and burnt area, and with fire-enabled DGVMs. However, the projections for Australia have focused on changes in climate-based susceptibility to fire using fire danger indices.

### 1.7.1 Global Projections

The GAMs derived from exploration of the relative importance of various controls on burnt area (see section 1.3.1) can be applied for future projections (Krawchuk et al., 2009; Moritz et al., 2012). Krawchuk et al. (2009) examined the fire response to simulated changes in climate derived from the GFDL climate model driven by the SRES B1 and A2 emissions scenarios. B1 is equivalent to a scenario that stabilizes CO<sub>2</sub> at ca. 550ppm by the end of the century, whereas A2 is a mid-high emission scenario in which CO<sub>2</sub> concentrations reach 830 ppm by 2100. Overall, there was no change in fire

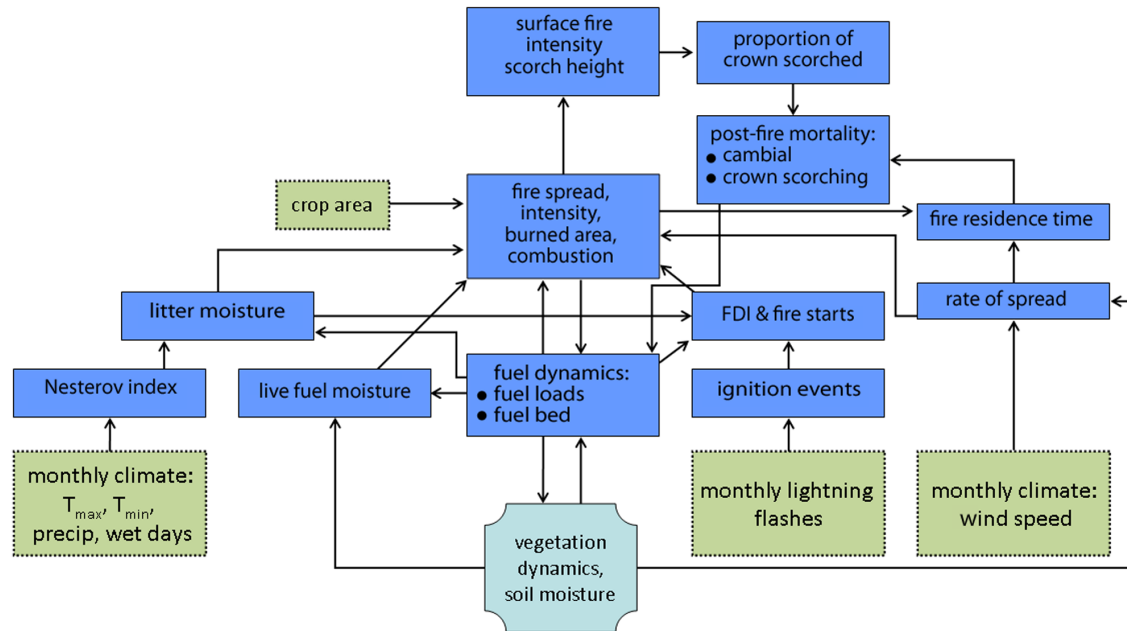


FIGURE 1.10: Description of the structure of the fire component of LPX. Inputs to the model are identified by green boxes, outputs from the vegetation dynamics component of the model are identified by light blue boxes, and internal processes and exchanges that are explicitly simulated by the fire component of the model are identified by blue boxes. Arrows indicate the direction of flow of information between processes. Reproduced from Prentice et al. (2011)

because large increases in some regions were compensated by equally large decreases in other regions, reflecting the interaction between changes in temperature and precipitation at a regional scale. Moritz et al. (2012) extended this analysis by examining the response of fire to climate changes as simulated by 16 different climate models driven by the A2 scenario. They highlight the large uncertainties in fire projections with differences in the sign of the change in fire activity for over 50% of the global land area. The inter-model consistency of predictions increases through the century. In general, temperate biomes show an increase in fire activity at the end of the century, while projections indicate a decrease in fire in tropical forest and savanna areas. The regional increases in fire largely reflect changes in temperature, while the decrease in fire in tropical ecosystems (including tropical savannas) reflects increases in precipitation which prevent fuel drying. Both Krawchuk et al. (2009) and Moritz et al. (2012) identified NPP as a major control on fire under modern conditions (see section 1.3.1), but the impact of changes in NPP on future fire regimes is only considered implicitly through the co-variation of NPP and climate. However, shifts in vegetation will not necessarily be a linear function of climate (Burkett et al., 2005; Fischlin et al., 2007; Cook et al., 2012; Knight and Harrison, 2013) and CO<sub>2</sub> fertilization could also lead to

increases in productivity and hence on fuel loads independently from climate changes (Torn and Fried, 1992; Crutzen et al., 1993; Sage, 1996).

Pechony and Shindell (2010) examined the impact of changing vegetation distribution, and hence fuel loads, by including land-cover changes in their statistical estimates of future changes using the Pechony and Shindell (2009) fire algorithm. They showed increases in fire in arid regions that are fuel limited today. However, this study does not take account of possible interactions between vegetation and fire because the vegetation changes are prescribed. Furthermore, they do not take account of the direct effects of CO<sub>2</sub> on vegetation productivity and fuel loads.

DGVM-based projections can potentially take account both of changes in vegetation boundaries and the impact of CO<sub>2</sub> fertilization. Although DGVMs have been used for regional studies (e.g. Bachelet et al., 2008; Lenihan et al., 2008), there have been few DGVM studies of the response of fire to future climate change scenarios. Scholze et al. (2006) examined the changes in fire, amongst other things, during the 21<sup>st</sup> century in response to 52 climate scenarios using the LPJ-GLOBFIRM DGVM (Thonicke et al., 2001; Sitch et al., 2003). They showed significant changes in fire risk at a regional level, exacerbated by changes in fuel loads through CO<sub>2</sub> fertilization and changes in vegetation distribution. Harrison et al. (2010a) also showed large changes in regional fire regimes over the 21<sup>st</sup> century using simulations with the LPX model driven by output from the HadCM3 coupled climate model pattern-scaled to produce either a 2°C or a 4°C warming by 2050. However, the magnitude of the regional shifts shown in these two sets of simulations differ, and both show very different patterns from those shown by statistical modelling. In Australia, for example, Scholze et al. (2006) predicted a significant increase in fire in the interior (with high inter-model agreement), as did Harrison et al. (2010a). In contrast, both Krawchuk et al. (2009) and Moritz et al. (2012) predict reduced fire in this region. Indeed Krawchuk et al. (2009) predicted a decrease in fire over most of Australia except in the northwestern part of the country.

In principle, since DGVM simulations take account of potential changes in vegetation productivity and vegetation shifts, as well as interactions between climate, vegetation and fire, DGVM predictions should provide a more reliable guide to future changes in fire regimes. Unfortunately, the existing global simulations were made with DGVMs in which the realism of the fire model — particularly for Australia — is limited. This motivates my interest in improving the LPX fire model and then applying it to predict future changes in fire across Australia (Chapter 5).

### 1.7.2 Australian studies

A number of studies have examined changes in fire danger indices (FDI) across Australia in response to climate change projections. Hennessy et al. (2005) (updated by Lucas et al., 2007) used output from the CCAM model (Mcgregor and Dix, 2001) to estimate changes in the McArthur forest FDI and grassland FDI (McArthur, 1967, 1969). They showed that the number of days with ‘extreme’ fire weather increased by 15–70% in New South Wales and Victoria by 2050, and the number of days with ‘intermediate’ fire weather that are used for control burning decreased correspondingly. Beer and Williams (1995) and Williams et al. (2001) used the McArthur forest FDI to examine

the response of fire across Australia to a doubled CO<sub>2</sub> simulation with the CSIRO 9-level model (McGregor et al., 1993). Again, both studies show an increase in the number of days with very high or extreme fire danger, reflecting increases in temperature and corresponding decreases in relative humidity. Pitman et al. (2007) examined the response of the forest and grassland FDI in summer using output from a transient simulation driven by an intermediate and a high emissions scenario. Again, this showed an overall increase in fire risk over Australia, driven primarily by increases in summer temperatures and decreases in relative humidity, with the biggest increases occurring in northwestern and southeastern Australia. Although the focus on the summer season precluded a detailed analysis of changes in northern Australia, where fires occur predominantly in winter — the FDI calculations suggest the fire season in the north will be longer. Although all these studies suggest the fire risk will increase in Australia during the 21<sup>st</sup> century, it is not clear that this will translate into an increase in burnt area. The only study that has attempted to link changes in fire weather to changes in burnt area is that of Cary et al. (2002), which used a landscape-scale fire model to examine changes in southeastern Australia. Cary et al. (2002) suggested that, at least in this region, the predicted increase in fire weather would result in large increases in burnt area. However, this study cannot take account of the impact of changes in vegetation productivity and cover on fire regimes, caused by climate changes or increased CO<sub>2</sub>.

## 1.8 Philosophy and approach in this thesis

The goal of my thesis was to develop a fire model that would be capable of realistically predicting future changes in fire regimes across Australia. I was motivated by the fact that previous estimates of how fire might change in Australia during the 21<sup>st</sup> century were either based solely on fire risk (Section 1.7.2), or were extracted from unreliable statistical models or DGVM simulations using fire models (GLOBFIRM, LPX) that perform poorly for the Australian continent (Section 1.7.1).

The starting point was the LPX fire model (Prentice et al., 2011). This model produces good predictions of fire behavior globally but performs poorly for Australia. I focused on improving processes that benchmarking exercises showed contributed to the poor performance of the LPX model (Chapter 2). Despite international calls for the development of a rigorous benchmarking system for DGVMs (e.g Randerson et al., 2009; Luo et al., 2012), there was no comprehensive system available. My first focus was therefore to develop such a system and to demonstrate that it allowed discrimination between models and the identification of sources of model error (Chapter 2).

The second chapter in the thesis (Kelley, D.I., Prentice, I.C., Harrison, S.P., Wang, H., and Willis, K., 2013. A comprehensive benchmarking system for evaluating dynamic global vegetation models. *Biogeosciences* 10: 3313–3340) describes the comprehensive benchmarking system developed to allow quantitative evaluation of the LPX model. The need for a comprehensive benchmarking system has been widely recognized in the vegetation modelling community (Randerson et al., 2009; Luo et al., 2012). However, my paper is the first to (a) bring together sufficient observational data sets

to test multiple processes related to the simulation of vegetation properties, surface hydrology and fire regimes, (b) develop appropriate metrics that allow quantitative comparisons, including comparisons taking account of the effect of biases in mean and variability, (c) develop appropriate null models for each data set that allows models to be critically compared, and (d) demonstrated that the benchmarking system was able to discriminate between different models and to allow diagnosis of the cause of data-model disagreements. The original applications of the benchmarking system was global, but I then went on to use this system to diagnose several reasons why the original LPX model produced a poor simulation of vegetation and fire across Australia.

The increasing availability of data on vegetation and fire processes now makes data-driven model development possible, and I have capitalized on this during the development of the new model.

A major focus of model improvement was on the treatment of fire-resistance (bark thickness) and fire-response (resprouting) traits (Sections 1.4.1 and 1.4.2). Specifically, I wanted to replace the simple treatment of bark thickness as a single fixed PFT-specific parameter in LPX by a treatment that allows for within-PFT variability in bark thickness. My underlying hypothesis here is that the distribution of bark thickness within a given ecosystem will change depending on the fire regime, where more frequent fires will lead to selection for trees with thicker bark, and that the model should be capable of simulating this emergent ecosystem property given within-PFT variability in bark thickness. I also wanted to include a treatment of resprouting in the model, in part because it is typical of much of the Australian flora and in part because it clearly plays a major role in the post-fire carbon cycle. No other DGVM allows for the variability in bark thickness that occurs between species within a PFT or between individuals of similar height (Table 1.2. As a result, simulated fires do not lead to the selection for thicker-barked species that is observed in the real world and which provides a mechanism for tree survival in regions with relatively high fire frequency (see section 1.4.1). Furthermore, all of the models assume that a sufficiently severe fire will kill the tree completely. None of the existing DGVMs incorporate the resprouting response that allows trees in savannas and other fire-prone regions to recover rapidly after fire (see section 1.4.1). There is a considerable amount of literature on both of these traits, and many site-based measurements have been made. However, large data sets sampling a reasonable diversity of environments are required to facilitate the analyses required to develop new model parameterizations, and thus I became involved in an effort to acquire and analyse such data.

The third chapter of the thesis (Harrison, S.P., Kelley, D.I., Wang, H., Herbert, A., Li, G., Bradstock, R., Fontaine, J., Enright, N., Murphy, B.P., Pekin, B.K., Penman, T., Russell-Smith, J. and Wittkuhn, R.S. Patterns in the abundance of post-fire resprouting in Australia based on plot-level measurements. March 2014). represents a community effort to compile a data base on the abundance of fire-response traits from sites across Australia motivated the ACEAS Working Group on “Ecosystem vulnerability to changing fire regimes”. The analyses of these data allowed me to develop a PFT-specific parameterization of resprouting within LPX. Furthermore, it provided me with data on the abundance of resprouting across climate gradients and geographically, which I could use as a test of the performance of the new model. The analyses in this

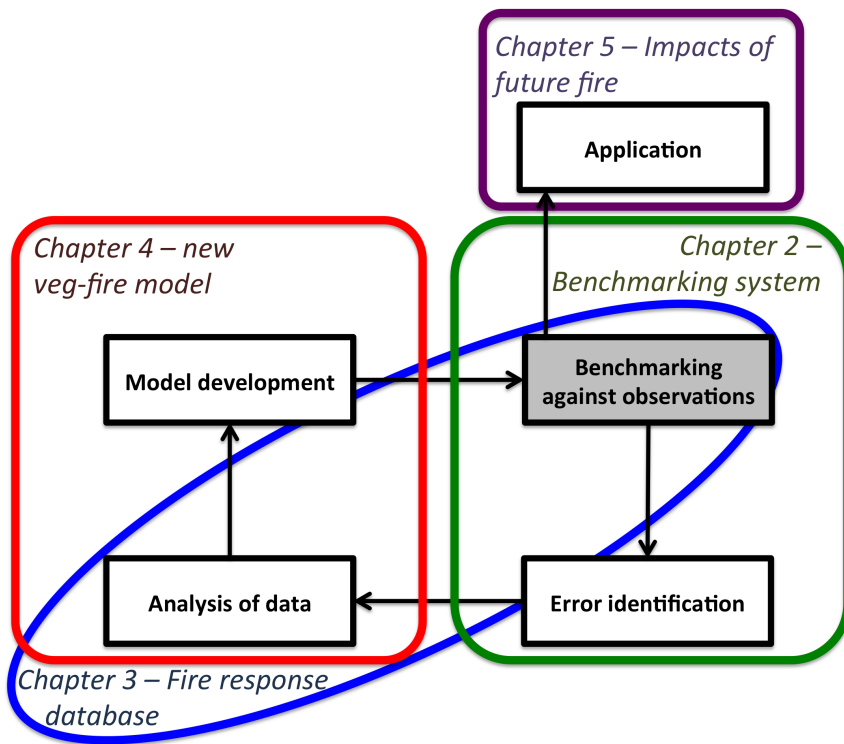


FIGURE 1.11: Iterative model development approached used in this thesis. Benchmarking (grey box) is the starting point. Arrows indicate the order of implementation. Boxes indicate the main focus of various chapters in the thesis.

paper also allow a test of existing conceptual models of resprouting, and will lead to the refinement of these models and a better understanding of resprouting behaviour.

My approach has been iterative (Fig. 1.11): I have used benchmarking procedures to identify specific areas for improvement, new algorithms were developed through extensive data analyses, these algorithms were incorporated into the fire model and benchmarked (first separately and then together) to ensure that the changes do not result in overall model degradation, this benchmarking then served as the basis for further data analyses and model developments. Once I had established that the new model produces a better simulation of Australian vegetation and fire regimes (Chapter 4), I ran the model using multiple scenarios of potential future climate changes to investigate the impact of these changes on fire regimes and the carbon cycle.

The fourth chapter of the thesis (Kelley, D.I., Harrison, S.P. and Prentice, I.C., 2014. Improved simulation of fire-vegetation interactions in the Land surface Processes and eXchanges Dynamic Global Vegetation Model (LPX-Mv1). Geoscientific Model Development Discussions 7: 1-70) describes the new model. I focused on improving lightning ignitions, introducing fuel decomposition rates that varied by PFT and litter-size, incorporating realistic PFT-specific rooting depths, improving the treatment of dead fuel drying rates, incorporating an adaptive bark thickness algorithm and introducing resprouting in tropical and temperate trees. The areas for improvement

were identified as a result of benchmarking. The new parameterizations were all based on extensive data analysis, some of which (e.g. bark thickness data) were specifically compiled for this purpose. The effects of introducing each change in the model was assessed against the observational benchmarks from Chapter 2, as well as local observational data on vegetation occurrence and production and fire: in some cases improving a specific process in the model led to a degradation of some aspects of the simulations because so many of the original parameters were tuned. However, one aspect of the benchmarking system is that it allows different aspects of the simulated patterns to be evaluated. For example, I was able to distinguish where changed parameterizations produced better simulations of the geographic patterns in a variable even where there was a significant bias in the mean state because of removing one tuning parameter but leaving others untouched. I was able to demonstrate that the final version of the model (LPX-Mv1), in which the parameterizations are based on data analysis and not tuned to match observations, produces a much better simulation of Australian fire regimes than previous versions of the LPJ-family of models.

Chapter 5 (Kelley, D.I. and Harrison, S.P. Enhanced Australian carbon sink despite increased wildfire during the 21st century) describes the application of LPX-Mv1 to examine the implication of future changes in Australian fire regimes as a consequence of projected changes in climate and CO<sub>2</sub> for the carbon cycle. I use multiple climate-model simulations driven by two of the RCP (representative concentration pathway) scenarios: RCP 4.5 which corresponds to a change in radiative forcing of 4.5W/m<sup>2</sup> by the end of the 21<sup>st</sup> century (Thomson et al., 2011) and the high-end RCP8.5 scenario which corresponds to a change in radiative forcing of 8.5W/m<sup>2</sup> by the end of the century (Riahi et al., 2011). Previous assessments for Australia have focused on changes in fire risk and shown that fire risk will increase substantially and everywhere (e.g. Pitman et al., 2007). However, my simulations show that fire will decrease in northern Australia while increasing in southern Australia. Paradoxically, although the simulations do show a small increase for the continent as a whole, carbon uptake and the terrestrial carbon stock increases significantly. I show that this occurs largely because fire-adapted resprouting trees become more abundant in areas where fire increased either through increased productivity or increased fuel drying. The quick recovery after fire ensures rapid carbon uptake and increases the standing biomass overall.

In Chapter 6, I summarize the main conclusions of my thesis and discuss some possible directions for future research in fire modelling.

## 1.9 References

Albini, F.: Estimating wildfire behavior and effects, Tech. rep., USDA Forest Service, U. S. Department of Agriculture, Ogden, Utah, URL [http://www.firemodels.org/downloads/behaveplus/publications/Albini\\_INT-30\\_1976.pdf](http://www.firemodels.org/downloads/behaveplus/publications/Albini_INT-30_1976.pdf), 1976.

Aldersley, A., Murray, S. J., and Cornell, S. E.: Global and regional analysis of climate and human drivers of wildfire., *The Science of the total environment*, 409, 3472–81, doi:10.1016/j.scitotenv.2011.05.032, 2011.

Allan, G. E. and Southgate, R. I.: Fire regimes in the spinifex landscapes of Australia, Flammable Australia: the fire regimes and biodiversity of a continent, pp. 145–176, 2002.

Anderson, R. C., Bowles, M. L., Fralish, J. S., and Baskin, J. M.: Deep-soil savannas and barrens of the Midwestern United States, Savannas, Barrens, and Rock Outcrop Plant Communities of North America., pp. 155–170, 1999.

Archibald, S. and Bond, W. J.: Growing tall vs growing wide: tree architecture and allometry of *Acacia karroo* in forest, savanna, and arid environments, *Oikos*, 102, 3–14, 2003.

Archibald, S., Roy, D. P., van Wilgen, B. W., and Scholes, R. J.: What limits fire? An examination of drivers of burnt area in Southern Africa, *Global Change Biology*, 15, 613–630, doi:10.1111/j.1365-2486.2008.01754.x, 2009.

Arneth, A., Harrison, S. P., Zaehle, S., Tsigaridis, K., Menon, S., Bartlein, P. J., Feichter, J., Korhola, A., Kulmala, M., O'Donnell, D., Schurgers, G., Sorvari, S., and Vesala, T.: Terrestrial biogeochemical feedbacks in the climate system, *Nature Geoscience*, 3, 525–532, doi:10.1038/ngeo905, 2010.

Arora, V. K. and Boer, G. J.: Fire as an interactive component of dynamic vegetation models, *Journal of Geophysical Research*, 110, G02 008, doi:10.1029/2005JG000042, 2005.

Bachelet, D., Neilson, R. P., Hickler, T., Drapek, R. J., Lenihan, J. M., Sykes, M. T., Smith, B., Sitch, S., and Thonicke, K.: Simulating past and future dynamics of natural ecosystems in the United States, *Global Biogeochemical Cycles*, 17, 2003b.

Bachelet, D., Lenihan, J. M., Drapek, R. J., and Neilson, R. P.: VEMAP vs VIN-CERA: A DGVM sensitivity to differences in climate scenarios, *Global and Planetary Change*, 64, 38–48, doi:10.1016/j.gloplacha.2008.01.007, 2008.

Baker, D. F., Doney, S. C., and Schimel, D. S.: Variational data assimilation for atmospheric CO<sub>2</sub>, *Tellus B*, 58, 359–365, 2006.

Balfour, D. A. and Midgley, J. J.: Fire induced stem death in an African acacia is not caused by canopy scorching, *Austral Ecology*, 31, 892–896, doi:10.1111/j.1442-9993.2006.01656.x, 2006.

Baraloto, C., Rabaud, S., Molto, Q., Blanc, L., Fortunel, C., Hérault, B., Dávila, N., Mesones, I., Rios, M., Valderrama, E., and Fine, P. V. A.: Disentangling stand and environmental correlates of aboveground biomass in Amazonian forests, *Global Change Biology*, 17, 2677–2688, doi:10.1111/j.1365-2486.2011.02432.x, 2011.

Bartlein, P. J., Hostetler, S. W., Shafer, S. L., Holman, J. O., and Solomon, A. M.: Temporal and spatial structure in a daily wildfire-start data set from the western United States (1986–96), *International Journal of Wildland Fire*, 17, 8–17, 2008.

- Beckage, B., Platt, W. J., and Gross, L. J.: Vegetation, Fire, and Feedbacks: A Disturbance-Mediated Model of Savannas, *The American Naturalist*, 174, 805–818, 2009.
- Beer, T.: The interaction of wind and fire, *Boundary-Layer Meteorology*, 54, 287–308, 1991.
- Beer, T.: The speed of a fire front and its dependence on wind-speed, *International Journal of Wildland Fire*, 3, 193–202, 1993.
- Beer, T. and Williams, A.: Estimating Australian forest fire danger under conditions of doubled carbon dioxide concentrations, *Climatic Change*, 29, 169–188, 1995.
- Bell, T. L. and Ojeda, F.: Underground starch storage in Erica species of the Cape Floristic Region—differences between seeders and resprouters, *The New Phytologist*, 144, 143–152, 1999.
- Bellingham, P. J. and Sparrow, A. D.: Resprouting as a life history strategy in woody plant communities, *Oikos*, 89, 409–416, 2000.
- Beringer, J., Hutley, L. B., Tapper, N. J., and Cernusak, L. A.: Savanna fires and their impact on net ecosystem productivity in North Australia, *Global Change Biology*, 13, 990–1004, 2007.
- Bistinas, I., Oom, D., Sá, A. C. L., Harrison, S. P., Prentice, I. C., and Pereira, J. M. C.: Relationships between Human Population Density and Burned Area at Continental and Global Scales., *PloS one*, 8, e81188, doi:10.1371/journal.pone.0081188, 2013.
- Bistinas, I., Harrison, S. P., Prentice, I. C., and Pereira, J. M. C.: Causal relationships versus emergent patterns in the global controls of burnt area, *Biogeosciences Discussions*, 11, 3865–3892, 2014.
- Boer, M. M.: Are the NSW bushfires linked to climate change, URL <http://theconversation.com/are-the-nsw-bushfires-linked-to-climate-change-19480>, 2013.
- Boer, M. M., Sadler, R. J., Wittkuhn, R. S., McCaw, L., and Grierson, P. F.: Long-term impacts of prescribed burning on regional extent and incidence of wild-firesEvidence from 50 years of active fire management in SW Australian forests, *Forest Ecology and Management*, 259, 132–142, doi:10.1016/j.foreco.2009.10.005, URL <http://linkinghub.elsevier.com/retrieve/pii/S0378112709007294>, 2009.
- Bond, W. J.: What Limits Trees in C 4 Grasslands and Savannas?, *Annual Review of Ecology, Evolution, and Systematics*, 39, 641–659, doi:10.1146/annurev.ecolsys.39.110707.173411, 2008.

Bond, W. J. and Keeley, J. E.: Fire as a global 'herbivore': the ecology and evolution of flammable ecosystems., *Trends in Ecology & Evolution*, 20, 387–94, doi:10.1016/j.tree.2005.04.025, 2005.

Bond, W. J. and Midgley, J. J.: Kill thy neighbour: an individualistic argument for the evolution of flammability, *Oikos*, 73, 79–85, 1995.

Bond, W. J. and Midgley, J. J.: Ecology of sprouting in woody plants: the persistence niche., *Trends in Ecology & Evolution*, 16, 45–51, 2001.

Bond, W. J. and van Wilgen, B. W.: Fire and Plants (Population and Community Biology Series 14), 1996b.

Bond, W. J., Volk, J., and Viviers, M.: Variation in seedling recruitment of Cape Proteaceae after fire, *The Journal of Ecology*, 72, 209–221, 1984.

Bond, W. J., Midgley, G. F., and Woodward, F. I.: What controls South African vegetation-climate or fire?, *South African Journal of Botany*, 69, 79–91, 2003.

Bond, W. J., Woodward, F. I., and Midgley, G. F.: The global distribution of ecosystems in a world without fire., *The New Phytologist*, 165, 525–37, doi:10.1111/j.1469-8137.2004.01252.x, 2005.

Bousquet, P., Peylin, P., Ciais, P., Le Quéré, C., Friedlingstein, P., and Tans, P. P.: Regional changes in carbon dioxide fluxes of land and oceans since 1980, *Science*, 290, 1342–1346, 2000.

Bova, A. S. and Dickinson, M. B.: Linking surface-fire behavior, stem heating, and tissue necrosis, *Canadian Journal of Forest Research*, 35, 814–822, 2005.

Bowman, D. M. J. S., Balch, J. K., Artaxo, P., Bond, W. J., Carlson, J. M., Cochrane, M. A., D'Antonio, C. M., Defries, R. S., Doyle, J. C., Harrison, S. P., Johnston, F. H., Keeley, J. E., Krawchuk, M. A., Kull, C. A., Marston, J. B., Moritz, M. A., Prentice, I. C., Roos, C. I., Scott, A. C., Swetnam, T. W., van der Werf, G. R., and Pyne, S. J.: Fire in the Earth system., *Science* (New York, N.Y.), 324, 481–484, doi:10.1126/science.1163886, 2009.

Bradshaw, L. S., Deeming, J. E., Burgan, R. E., and Cohen, J. D.: The 1978 national fire danger rating system, Gen. Tech. Rep. INT-169. Ogden, UT: USDA Forest Service, Intermountain Forest and Range Experiment Station, 1983.

Bradstock, R. A.: A biogeographic model of fire regimes in Australia: current and future implications, *Global Ecology and Biogeography*, 19, 145–158, doi:10.1111/j.1466-8238.2009.00512.x, 2010.

Bradstock, R. A. and Gill, A. M.: Living with fire and biodiversity at the urban edge: in search of a sustainable solution to the human protection problem in southern Australia, *Journal of Mediterranean Ecology*, 2, 179–196, 2001.

- Bradstock, R. A., Gill, A. M., Kenny, B., and Scott, J.: Bushfire risk at the urban interface estimated from historical weather records: consequences for the use of prescribed fire in the Sydney region of south-eastern Australia, *Journal of Environmental Management*, 52, 259–271, 1998.
- Bradstock, R. A., Williams, R. J., and Gill, A. M.: Flammable Australia: fire regimes, biodiversity and ecosystems in a changing world, CSIRO PUBLISHING, 2012.
- Brovkin, V., van Bodegom, P. M., Kleinen, T., Wirth, C., Cornwell, W. K., Cornelissen, J. H. C., and Kattge, J.: Plant-driven variation in decomposition rates improves projections of global litter stock distribution, *Biogeosciences*, 9, 565–576, doi:10.5194/bg-9-565-2012, 2012.
- Burkett, V. R., Wilcox, D. A., Stottlemyer, R., Barrow, W., Fagre, D., Baron, J., Price, J., Nielsen, J. L., Allen, C. D., Peterson, D. L., Ruggerone, G., and Doyle, T.: Nonlinear dynamics in ecosystem response to climatic change: Case studies and policy implications, *Ecological Complexity*, 2, 357–394, doi:10.1016/j.ecocom.2005.04.010, 2005.
- Carmona-Moreno, C., Belward, A., Malingreau, J.-P., Hartley, A., Garcia-Alegre, M., Antonovkiy, M., Buchshtaber, V., and Pivovarov, V.: Characterizing interannual variations in global fire calendar using data from Earth observing satellites, *Global Change Biology*, 11, 1537–1555, doi:10.1111/j.1365-2486.2005.001003.x, 2005.
- Cary, G. J., Bradstock, R. A., Williams, J. E., and Gill, A. M.: Importance of a changing climate for fire regimes in Australia., Flammable Australia: the fire regimes and biodiversity of a continent, pp. 26–46, 2002.
- Castillo, G., Kendra, C., Levis, S., and Thornton, P. E.: Evaluation of the New CNDV Option of the Community Land Model: Effects of Dynamic Vegetation and Interactive Nitrogen on CLM4 Means and Variability., *Journal of Climate*, 25, 2012.
- Caufield, S.: Kinglake, Australia, June 2009., URL <http://www.flickr.com/photos/hradcanska/3687594561>, 2009.
- CFS: Bangor Fire, Community Newsletter, p. 2014, URL [www.cfs.sa.gov.au](http://www.cfs.sa.gov.au), 2014.
- Chatto, K., Kellas, J. D., and Bell, T. L.: Effects of repeated low-intensity fire on tree growth and bark in a mixed eucalypt foothill forest in south-eastern Australia, Fire Management, Department of Sustainability and Environment, 2003.
- Chave, J., Coomes, D., Jansen, S., Lewis, S. L., Swenson, N. G., and Zanne, A. E.: Towards a worldwide wood economics spectrum., *Ecology letters*, 12, 351–66, doi:10.1111/j.1461-0248.2009.01285.x, 2009.
- Chen, M.: Couple the common land model with the dynamic global vegetation model, Ph.D. thesis, MS thesis, Institute of Atmospheric physics, Chinese Academy of Sciences, 43pp.(in Chinese), 2008.

Chevallier, F., Ciais, P., Conway, T. J., Aalto, T., Anderson, B. E., Bousquet, P., Brunke, E. G., Ciattaglia, L., Esaki, Y., Fröhlich, M., Gomez, A., Gomez-Pelaez, A. J., Haszpра, L., Krummel, P. B., Langenfelds, R. L., Leuenberger, M., Machida, T., Maignan, F., Matsueda, H., Morguí, J. A., Mukai, H., Nakazawa, T., Peylin, P., Ramonet, M., Rivier, L., Sawa, Y., Schmidt, M., Steele, L. P., Vay, S. A., Vermeulen, A. T., Wofsy, S. C., and Worthy, D.: CO<sub>2</sub> surface fluxes at grid point scale estimated from a global 21 year reanalysis of atmospheric measurements, *Journal of Geophysical Research: Atmospheres*, 115, 2010.

Chuvieco, E.: Remote sensing of large wildfires in the European Mediterranean Basin, Springer-Verlag, Berlin, Heidelberg, 1999.

Chuvieco, E., Giglio, L., and Justice, C.: Global characterization of fire activity: toward defining fire regimes from Earth observation data, *Global Change Biology*, 14, 1488–1502, doi:10.1111/j.1365-2486.2008.01585.x, 2008.

Chuvieco, E., Martínez, S., Román, M. V., Hantson, S., and Pettinari, M. L.: Integration of ecological and socio-economic factors to assess global vulnerability to wildfire, *Global Ecology and Biogeography*, 23, 245–258, doi:10.1111/geb.12095, URL <http://doi.wiley.com/10.1111/geb.12095>, 2014.

Clark, M. R., Lee, D. S., and Legg, T. P.: A comparison of screen temperature as measured by two Met Office observing systems, *International Journal of Climatology*, doi:10.1002/joc.3836, 2013.

Clarke, P. J. and Knox, K. E. J.: Trade-offs in resource allocation that favour resprouting affect the competitive ability of woody seedlings in grassy communities, *Journal of ecology*, 97, 1374–1382, 2009.

Clarke, P. J., Knox, K. E. J., Wills, K. E., and Campbell, M.: Landscape patterns of woody plant response to crown fire: disturbance and productivity influence sprouting ability, *Journal of Ecology*, 93, 544–555, 2005.

Clarke, P. J., Knox, K. E. J., and Butler, D.: Fire, soil fertility and delayed seed release: a community analysis of the degree of serotiny, *Evolutionary Ecology*, 27, 429–443, doi:10.1007/s10682-012-9604-0, 2012.

Clarke, P. J., Lawes, M. J., Midgley, J. J., Lamont, B. B., Ojeda, F., Burrows, G. E., Enright, N. J., and Knox, K. E. J.: Resprouting as a key functional trait: how buds, protection and resources drive persistence after fire., *The New Phytologist*, 197, 19–35, doi:10.1111/nph.12001, 2013.

Climent, J., Tapias, R., Pardos, J. A., and Gil, L.: Fire adaptations in the Canary Islands pine (*Pinus canariensis*), *Plant Ecology*, 171, 185–196, 2004.

Cochrane, M. A.: Fire science for rainforests., *Nature*, 421, 913–9, doi:10.1038/nature01437, 2003.

- Cochrane, M. A., Alencar, A., and Schulze, M.: Positive feedbacks in the fire dynamic of closed canopy tropical forests, *Science*, 284, 1832–1835, 1999.
- Cofer, W. R., Winstead, E. L., Stocks, B. J., Goldammer, J. G., and Cahoon, D. R.: Crown fire emissions of CO<sub>2</sub>, CO, H<sub>2</sub>, CH<sub>4</sub>, and TNMHC from a dense jack pine boreal forest fire, *Geophysical Research Letters*, 25, 3919–3922, 1998.
- Cook, B., Zeng, N., and Yoon, J.-H.: Will Amazonia Dry Out? Magnitude and Causes of Change from IPCC Climate Model Projections, *Earth Interactions*, 16, 1–27, doi:10.1175/2011EI398.1, 2012.
- Cowan, P.: Flammability, physiology and coexistence in fire prone environments, Ph.D. thesis, URL <http://escholarship.org/uc/item/84k1t1gh.pdf>, 2010.
- Cowan, P. and Ackerly, D.: Post-fire regeneration strategies and flammability traits of California chaparral shrubs, *International journal of wildland fire*, 19, 984–989, 2010.
- Cowling, R. M. and Lamont, B. B.: Variation in serotiny of three Banksia species along a climatic gradient, *Australian Journal of Ecology*, 10, 345–350, 1985.
- Cox, P. M.: Description of the TRIFFID dynamic global vegetation model, Tech. Rep. January, Hadley Centre, Met Office, URL [http://www.metoffice.gov.uk/media/pdf/9/h/HCTN\\_24.pdf](http://www.metoffice.gov.uk/media/pdf/9/h/HCTN_24.pdf), 2001.
- Craig, R., Heath, B., Raisbeck-Brown, N., Steber, M., Marsden, J., and Smith, R. W.: The distribution, extent and seasonality of large fires in Australia, April 1998–March 2000, as mapped from NOAA-AVHRR imagery, in: Australian fire regimes: contemporary patterns (April 1998 – March 2000) and changes since European settlement, 2002.
- Cramer, W., Kicklighter, D. W., Bondeau, A., Iii, B. M., Churkina, G., Nemry, B., Ruimy, A., Schloss, A. L., Intercomparison, T., and Model, P. O. F. T. P. N.: Comparing global models of terrestrial net primary productivity (NPP): overview and key results, *Global Change Biology*, 5, 1–15, 1999.
- Crutzen, P. J., Goldammer, J. G., and Others: Fire in the environment: the ecological, atmospheric and climatic importance of vegetation fires. Report of the Dahlem Workshop, Berlin, 15–20 March, 1992., in: Fire in the environment: the ecological, atmospheric and climatic importance of vegetation fires. Report of the Dahlem Workshop, Berlin, 15–20 March, 1992., John Wiley & Sons, 1993.
- Curran, T. J., Gersbach, L. N., Edwards, W., and Krockenberger, A. K.: Wood density predicts plant damage and vegetative recovery rates caused by cyclone disturbance in tropical rainforest tree species of North Queensland, Australia, *Austral Ecology*, 33, 442–450, doi:10.1111/j.1442-9993.2008.01899.x, 2008.
- Dai, Y., Zeng, X., Dickinson, R. E., Baker, I., Bonan, G. B., Bosilovich, M. G., Denning, a. S., Dirmeyer, P. A., Houser, P. R., Niu, G., Oleson, K. W., Schlosser, C. A.,

and Yang, Z.-L.: The Common Land Model, *Bulletin of the American Meteorological Society*, 84, 1013–1023, doi:10.1175/BAMS-84-8-1013, 2003.

Daniau, A.-L., Bartlein, P. J., Harrison, S. P., Prentice, I. C., Brewer, S., Friedlingstein, P., Harrison-Prentice, T. I., Inoue, J., Izumi, K., Marlon, J. R., Mooney, S. D., Power, M. J., Stevenson, J., Tinner, W., Andrič, M., Atanassova, J., Behling, H., Black, M., Blarquez, O., Brown, K. J., Carcaillet, C., Colhoun, E. A., Colombaroli, D., Davis, B. A. S., D'Costa, D., Dodson, J., Dupont, L., Eshetu, Z., Gavin, D. G., Genries, A., Haberle, S., Hallett, D. J., Hope, G., Horn, S. P., Kassa, T. G., Katamura, F., Kennedy, L. M., Kershaw, P., Krivonogov, S., Long, C., Magri, D., Marinova, E., McKenzie, G. M., Moreno, P. I., Moss, P., Neumann, F. H., Norström, E., Paitre, C., Rius, D., Roberts, N., Robinson, G. S., Sasaki, N., Scott, L., Takahara, H., Terwilliger, V., Thevenon, F., Turner, R., Valsecchi, V. G., Vannière, B., Walsh, M., Williams, N., and Zhang, Y.: Predictability of biomass burning in response to climate changes, *Global Biogeochemical Cycles*, 26, GB4007, doi:10.1029/2011GB004249, 2012.

Day, C.: Smoke from burning vegetation changes the coverage and behavior of clouds, *Physics Today*, 57, 24–26, 2004.

Del Tredici, P.: Sprouting in temperate trees: a morphological and ecological review, *The Botanical Review*, 67, 121–140, 2001.

Dennekamp, M. and Abramson, M. J.: The effects of bushfire smoke on respiratory health., *Respirology* (Carlton, Vic.), 16, 198–209, doi:10.1111/j.1440-1843.2010.01868.x, 2011.

Department of the Wildland Interior, U.: Wildland Fire Management Program Benefit-Cost Analysis A Review of Relevant Literature, Tech. Rep. June, Office of Policy Analysis, 2012.

der Werf, G. R., Dempewolf, J., Trigg, S. N., Randerson, J. T., Kasibhatla, P. S., Giglio, L., Murdiyarso, D., Peters, W., Morton, D. C., Collatz, G. J., Dolman, A. J., and Defries, R. S.: Climate regulation of fire emissions and deforestation in equatorial Asia, *Proceedings of the National Academy of Sciences*, 105, 20350–20355, 2008.

Dickinson, M. B. and Johnson, E. A.: Fire effects on trees, in: *Forest fires: behavior and ecological effects*, edited by Johnson, E. and Miyanishi, K., chap. 14, Academic Press, New York, 2001.

Dickinson, M. B. and Johnson, E. A.: Temperature-dependent rate models of vascular cambium cell mortality, *Canadian Journal of Forest Research*, 34, 546–559, 2004.

Dickinson, M. B., Jolliff, J., and Bova, A. S.: Vascular cambium necrosis in forest fires: using hyperbolic temperature regimes to estimate parameters of a tissue-response model, *Australian journal of botany*, 52, 757–763, 2005.

Doerr, S. and Santin, C.: Wildfire: A Burning issue for Insurers?, Tech. Rep. 11, Lloyd's, doi:10.1037/021722, URL <http://content.apa.org/reviews/021722>, 2013.

- Drobyshev, I., Niklasson, M., and Linderholm, H. W.: Forest fire activity in Sweden: Climatic controls and geographical patterns in 20th century, *Agricultural and Forest Meteorology*, 154–155, 174–186, doi:10.1016/j.agrformet.2011.11.002, 2012.
- Ducrey, M., Duhoux, F., Huc, R., and Rigolot, E.: The ecophysiological and growth responses of Aleppo pine (*Pinus halepensis*) to controlled heating applied to the base of the trunk, *Canadian Journal of Forest Research*, 26, 1366–1374, 1996.
- Duncan, B. W., Adrian, F. W., and Stolen, E. D.: Isolating the lightning ignition regime from a contemporary background fire regime in east-central Florida, USA, *Canadian Journal of Forest Research*, 40, 286–297, doi:10.1139/X09-193, 2010.
- Eagan, R., Hobbs, P. V., and Radke, L. F.: Measurements of cloud condensation nuclei and cloud droplet size distributions in the vicinity of forest fires, *Journal of Applied Meteorology*, 13, 553–557, 1974.
- Ellis, S., Kanowski, P., and Whelan, R. J.: National inquiry on bushfire mitigation and management, Tech. Rep. March, Commonwealth of Australia, Canberra., URL <http://ro.uow.edu.au/scipapers/4/>, 2004.
- Enright, N. J., Marsula, R., Lamont, B. B., and Wissel, C.: The ecological significance of canopy seed storage in fire-prone environments: a model for nonsprouting shrubs, *Journal of Ecology*, 86, 946–959, 1998.
- Falk, D. A., Heyerdahl, E. K., Brown, P. M., Farris, C., Fulé, P. Z., McKenzie, D., Swetnam, T. W., Taylor, A. H., and Van Horne, M. L.: Multi-scale controls of historical forest-fire regimes: new insights from fire-scar networks, *Frontiers in Ecology and the Environment*, 9, 446–454, doi:10.1890/100052, 2011.
- Fensham, R. J., Fairfax, R., Butler, D., and Bowman, D. M. J. S.: Effects of fire and drought in a tropical eucalypt savanna colonized by rain forest, *Journal of Biogeography*, 30, 1405–1414, 2003.
- Finney, M. A., Cohen, J. D., Grenfell, I. C., and Yedinak, K. M.: An examination of fire spread thresholds in discontinuous fuel beds, *International Journal of Wildland Fire*, 19, 163, doi:10.1071/WF07177, 2010.
- Fischlin, A., Midgley, G. F., Price, J., and Leemans, R.: Ecosystems , their properties , goods and services, in: Climate Change 2007: Impacts, Adaptation and Vulnerability. Contribution of Working Group II to the Fourth Assessment Report of the Intergovernmental Panel on Climate Change, edited by Parry, M., Canziani, O., Palutikof, J., van der Linden, P., and Hanson, C., chap. Ecosystems, pp. 211–272, Cambridge University Press, Cambridge, UK, 2007.
- Flannigan, M. D. and Wotton, B. M.: Lightning ignited forest fires in northwestern Ontario, *Canadian Journal of Forest Research*, 21, 277–287, 1991.

- Foley, J. A. and Prentice, I. C.: An integrated biosphere model of land surface processes, terrestrial carbon balance, and vegetation dynamics, *Global Biogeochemical Cycles*, 10, 603–628, 1996.
- Friedlingstein, P. and Bopp, L.: Positive feedback between future climate change and the carbon cycle, *Geophysical Research Letters*, 28, 1543–1546, 2001.
- Gagnon, P., Passmore, H., and Platt, W. J.: Does pyrogenicity protect burning plants?, *Ecology*, 91, 3481–3486, 2010.
- Gebert, K. and Schuster, E.: Forest service fire suppression expenditures in the Southwest, in: General Technical Report Pacific Southwest Research Station, pp. 227–236, USDA Forest Service, URL [http://gis.fs.fed.us/psw/publications/documents/psw\\_gtr189/psw\\_gtr189\\_227-236\\_gebert.pdf](http://gis.fs.fed.us/psw/publications/documents/psw_gtr189/psw_gtr189_227-236_gebert.pdf), 2008.
- Giglio, L. and Randerson, J. T.: Assessing variability and long-term trends in burned area by merging multiple satellite fire products, *Biogeosciences*, 7, 1171–1186, 2010.
- Giglio, L., Randerson, J. T., and van der Werf, G. R.: Analysis of daily, monthly, and annual burned area using the fourth-generation global fire emissions database (GFED4), *Journal of Geophysical Research: Biogeosciences*, 118, 317–328, 2013.
- Gignoux, J., Cloibert, J., and Menaut, J. C.: Alternative fire resistance strategies in savanna trees, *Oecologia*, 110, 576–583, 1997.
- Gill, A. M.: Fire and the Australian flora: a review, *Australian forestry*, 38, 4–25, 1975.
- Gill, A. M. and Ashton, D.: The role of bark type in relative tolerance to fire of three central Victorian eucalypts, *Australian Journal of Botany*, 16, 491–498, 1968.
- Gill, A. M. and Catling, P. C.: Fire regimes and biodiversity of forested landscapes of southern Australia, Flammable Australia. The fire regimes and biodiversity of a continent (eds RA Bradstock, JE Williams & AM Gill), pp. 351–369, 2002.
- Gill, A. M. and Williams, J. E.: Fire regimes and biodiversity: the effects of fragmentation of southeastern Australian eucalypt forests by urbanisation, agriculture and pine plantations, *Forest Ecology and Management*, 85, 261–278, doi: 10.1016/S0378-1127(96)03763-2, 1996.
- Gill, A. M., Ryan, P. G., Moore, P. H. R., and Gibson, M.: Fire regimes of World Heritage Kakadu National Park., Australia, *Austral Ecology*, 25, 616–625, 2000.
- Gill, L. and Taylor, A. H.: Top-down and Bottom-up Controls on Fire Regimes Along an Elevational Gradient on the East Slope of the Sierra Nevada, California, USA, *Fire Ecology*, 5, 57–75, doi:10.4996/fireecology.0503057, 2009.
- Guyette, R. P., Muzika, R., and Dey, D.: Dynamics of an anthropogenic fire regime, *Ecosystems*, 5, 472–486, doi:10.1007/s10021-002-0115-7, 2002.

- Hacke, U. G., Sperry, J. S., Pockman, W. T., Davis, S. D., and McCulloh, K. A.: Trends in wood density and structure are linked to prevention of xylem implosion by negative pressure, *Oecologia*, 126, 457–461, doi:10.1007/s004420100628, 2001.
- Harrison, S. P., Marlon, J. R., and Bartlein, P. J.: Fire in the Earth system, in: *Changing climates, earth systems and society*, edited by Dodson, J., pp. 21–48, Springer, Dordrecht, Netherlands, doi:10.1007/978-90-481-8716-4, 2010a.
- Haverd, V., Raupach, M. R., Briggs, P. R., Canadell, J. G., Isaac, P., Pickett-Heaps, C., Roxburgh, S. H., van Gorsel, E., Viscarra Rossel, R. A., and Wang, Z.: Multiple observation types reduce uncertainty in Australia's terrestrial carbon and water cycles, *Biogeosciences*, 10, 2011–2040, doi:10.5194/bg-10-2011-2013, 2013a.
- Haverd, V., Raupach, M. R., Briggs, P. R., Davies, S. J., Law, R. M., Meyer, C. P., Peters, G. P., Pickett-Heaps, C., and Sherman, B.: The Australian terrestrial carbon budget, *Biogeosciences*, 10, 851–869, doi:10.5194/bg-10-851-2013, 2013b.
- He, T., Lamont, B. B., and Downes, K. S.: Banksia born to burn., *The New Phytologist*, 191, 184–96, doi:10.1111/j.1469-8137.2011.03663.x, 2011.
- Hennessy, K., Bathols, C., Lucas, N., Nicholls, J., Suppiah, R., and Ricketts, J.: Climate change impacts on fire-weather in south-east Australia, Tech. rep., CSIRO Marine and Atmospheric Research, 2005.
- Heyerdahl, E. K., Brubaker, L., and Agee, J.: Spatial controls of historical fire regimes: a multiscale example from the interior west, USA, *Ecology*, 82, 660–678, 2001.
- Higgins, S. I., Bond, W. J., and Trollope, W. S. W.: Fire, resprouting and variability: a recipe for grass-tree coexistence in savanna, *Journal of Ecology*, 88, 213–229, doi:10.1046/j.1365-2745.2000.00435.x, 2000.
- Higgins, S. I., Bond, W. J., and February, E.: Effects of four decades of fire manipulation on woody vegetation structure in savanna, *Ecology*, 88, 1119–1125, 2007.
- Hilbert, D. W.: A model of life history strategies of chaparral shrubs in relation to fire frequency, *NATO ASI series. Series G: ecological sciences*, 15, 597–606, 1987.
- Hobbs, P. V. and Radke, L. F.: Cloud Condensation Nuclei from a Simulated Forest Fire, *Science*, 163, 279–280, 1969.
- Hoffmann, W. A. and Jackson, R.: Vegetation–Climate Feedbacks in the Conversion of Tropical Savanna to Grassland., *Journal of Climate*, 13, 1593–1602, 2000.
- Hoffmann, W. A. and Solbrig, O. T.: The role of topkill in the differential response of savanna woody species to fire, *Forest Ecology and Management*, 180, 273–286, doi:10.1016/S0378-1127(02)00566-2, 2003.
- Hoffmann, W. A., Orthen, B., Kielse, P., and Nascimento, V. D.: Comparative fire ecology of tropical savanna and forest trees, *Functional Ecology*, 17, 720–726, doi:10.1111/j.1365-2435.2003.00796.x, 2003.

- Hughes, R. and Mercer, D.: Planning to reduce risk: the wildfire management overlay in Victoria, Australia, *Geographical Research*, 47, 124–141, 2009.
- ICA: Insurance Council of Australia - Historical Disaster Statistics, URL <http://www.insurancecouncil.com.au/industry-statistics-data/disaster-statistics/historical-disaster-statistics>, 2014.
- Johnson, E. A.: Fire and Vegetation Dynamics: Studies from the North American Boreal Forest, Cambridge Studies in Ecology, Cambridge University Press, 1996.
- Johnston, F. H., Kavanagh, A. M., Bowman, D. M. J. S., and Scott, R. K.: Exposure to bushfire smoke and asthma: an ecological study., *The Medical journal of Australia*, 176, 535–8, 2002.
- Johnston, F. H., Webby, R. J., Pilotto, L. S., Bailie, R. S., Parry, D. L., and Halpin, S. J.: Vegetation fires, particulate air pollution and asthma: a panel study in the Australian monsoon tropics., *International journal of environmental health research*, 16, 391–404, doi:10.1080/09603120601093642, 2006.
- Johnston, F. H., Henderson, S. B., Chen, Y., Randerson, J. T., Marlier, M., Defries, R. S., Kinney, P., Bowman, D. M. J. S., and Brauer, M.: Estimated global mortality attributable to smoke from landscape fires., *Environmental health perspectives*, 120, 695–701, doi:10.1289/ehp.1104422, 2012.
- Jones, J. L., Webb, B. W., Butler, B. W., Dickinson, M. B., Jimenez, D., Reardon, J., and Bova, A. S.: Prediction and measurement of thermally induced cambial tissue necrosis in tree stems, *International Journal of Wildland Fire*, 15, 3, doi:10.1071/WF05017, 2006.
- Justice, C., Giglio, L., Korontzi, S., Owens, J., Morisette, J., Roy, D. P., Descloitres, J., Alleaume, S., Petitcolin, F., and Kaufman, Y.: The MODIS fire products, *Remote Sensing of Environment*, 83, 244–262, doi:10.1016/S0034-4257(02)00076-7, 2002.
- Kaminski, T. and Knorr, W.: The BETHY/JSBACH Carbon Cycle Data Assimilation System: experiences and challenges, *Journal of Geophysical Research: Biogeosciences*, 118, 1414–1426, 2013.
- Kane, J. M., Varner, J. M., and Hiers, J. K.: The burning characteristics of south-eastern oaks: discriminating fire facilitators from fire impeders, *Forest Ecology and Management*, 256, 2039–2045, 2008.
- Kauffman, J. B. and Uhl, C.: Interactions of anthropogenic activities, fire, and rain forests in the Amazon Basin, in: *Fire in the tropical biota*, pp. 117–134, Springer, 1990.
- Keeley, J. E.: Fire severity and plant age in postfire resprouting of woody plants in sage scrub and chaparral, *Madrono*, 53, 373–379, 2006.
- Keeley, J. E.: *Fire in mediterranean ecosystems*, Cambridge University Press, 2012.

- Keeley, J. E. and Fotheringham, C.: Role of fire in regeneration from seed, in: Seeds: The ecology of regeneration in plant communities 2, pp. 311–330, 2000.
- Keeley, J. E., Pausas, J. G., Rundel, P. W., Bond, W. J., and Bradstock, R. A.: Fire as an evolutionary pressure shaping plant traits., *Trends in plant science*, 16, 406–11, doi:10.1016/j.tplants.2011.04.002, 2011.
- Keeley, J. E., Bond, W. J., Bradstock, R. A., Pausas, J. G., and Rundel, P. W.: Fire adapted trait evolution, in: *Fire in Mediterranean Ecosystems*, edited by Keeley, J. E., Bond, W. J., Bradstock, R. A., Pausas, J. G., and Rundel, P. W., chap. 9, p. 253, Cambridge University Press, Cambridge, 1 edn., 2012.
- Kelley, D. I.: Wildfires as part of the global carbon cycle: quantitative analysis using data assimilation, Masters thesis, University of Bristol, UK, 2008.
- Kelley, D. I., Prentice, I. C., Harrison, S. P., Wang, H., Simard, M., Fisher, J. B., and Willis, K. O.: A comprehensive benchmarking system for evaluating global vegetation models, *Biogeosciences*, 10, 3313–3340, doi:10.5194/bg-10-3313-2013, 2013.
- Kelley, D. I., Harrison, S. P., and Prentice, I. C.: Improved simulation of fire-vegetation interactions in the Land surface Processes and eXchanges Dynamic Global Vegetation Model (LPX-Mv1), *Geoscientific Model Development Discussions*, 7, 931–1000, 2014.
- Kerby, J. D., Fuhlendorf, S. D., and Engle, D. M.: Landscape heterogeneity and fire behavior: scale-dependent feedback between fire and grazing processes, *Landscape Ecology*, 22, 507–516, 2007.
- King, D. A., Davies, S. J., Tan, S., and Noor, N. U. R. S.: The role of wood density and stem support costs in the growth and mortality of tropical trees, *Journal of Ecology*, 94, 670–680, 2006.
- Kloster, S., Mahowald, N. M., Randerson, J. T., Thornton, P. E., Hoffman, F. M., Levis, S., Lawrence, P. J., Feddema, J. J., Oleson, K. W., and Lawrence, D. M.: Fire dynamics during the 20th century simulated by the Community Land Model, *Biogeosciences*, 7, 1877–1902, doi:10.5194/bg-7-1877-2010, 2010.
- Kloster, S., Mahowald, N. M., Randerson, J. T., and Lawrence, P. J.: The impacts of climate, land use, and demography on fires during the 21st century simulated by CLM-CN, *Biogeosciences*, 9, 509–525, doi:10.5194/bg-9-509-2012, 2012.
- Knight, J. and Harrison, S.: The impacts of climate change on terrestrial Earth surface systems, *Nature Climate Change*, 3, 24–29, doi:10.1038/NCLIMATE1660, 2013.
- Knorr, W., Kaminski, T., Arneth, A., and Weber, U.: Impact of human population density on fire frequency at the global scale, *Biogeosciences*, 11, 1085–1102, doi:10.5194/bgd-10-15735-2013, 2014.
- Kramer, P. J. and Kozlowski, T. T.: *Physiology of trees.*, 1960.

Krawchuk, M. A., Moritz, M. A., Parisien, M.-A., Van Dorn, J., and Hayhoe, K.: Global pyrogeography: the current and future distribution of wildfire., PloS one, 4, e5102, doi:10.1371/journal.pone.0005102, 2009.

Krinner, G., Viovy, N., de Noblet-Ducoudré, N., Ogée, J., Polcher, J., Friedlingstein, P., Ciais, P., Sitch, S., and Prentice, I. C.: A dynamic global vegetation model for studies of the coupled atmosphere-biosphere system, Global Biogeochemical Cycles, 19, doi:10.1029/2003GB002199, 2005.

Kucharik, C. J., Foley, J. A., Delire, C., Fisher, V. A., Coe, M. T., Lengers, J. D., Young-Molling, C., Ramankutty, N., Norman, J. M., and Gower, S. T.: Testing the performance of a dynamic global ecosystem model: Water balance, carbon balance, and vegetation structure, Global Biogeochemical Cycles, 14, 795–825, doi:10.1029/1999GB001138, 2000.

Lamont, B. B. and Maitre, D. L.: Canopy seed storage in woody plants, The Botanical Review, 57, 277–317, 1991.

Lamont, B. B. and Wiens, D.: Are seed set and speciation rates always low among species that resprout after fire, and why?, Evolutionary Ecology, 17, 277–292, 2003.

Latham, D. J. and Schlieter, J. A.: Ignition probabilities of wildland fuels based on simulated lightning discharges, US Department of Agriculture, Forest Service, Intermountain Research Station, 1989.

Latham, D. J. and Williams, E.: Lightning and forest fires, Forest fires: Behavior and ecological effects, pp. 375–418, 2001.

Lavorel, S., Flannigan, M. D., Lambin, E. F., and Scholes, M. C.: Vulnerability of land systems to fire: Interactions among humans, climate, the atmosphere, and ecosystems, Mitigation and Adaptation Strategies for Global Change, 12, 33–53, doi: 10.1007/s11027-006-9046-5, 2006.

Lawes, M. J., Adie, H., Russell-Smith, J., Murphy, B. P., and Midgley, J. J.: How do small savanna trees avoid stem mortality by fire? The roles of stem diameter, height and bark thickness, Ecosphere, 2, doi:10.1890/ES10-00204.1, 2011a.

Lawes, M. J., Richards, A., Dathe, J., and Midgley, J. J.: Bark thickness determines fire resistance of selected tree species from fire-prone tropical savanna in north Australia, Plant Ecology, 212, 2057–2069, doi:10.1007/s11258-011-9954-7, 2011b.

Lawrence, D. M., Oleson, K. W., Flanner, M. G., Thornton, P. E., Swenson, S. C., Lawrence, P. J., Zeng, X., Yang, Z.-L., Levis, S., Sakaguchi, K., Gordon B Bonan, and Slater, A. G.: Parameterization improvements and functional and structural advances in version 4 of the Community Land Model, Journal of Advances in Modeling Earth Systems, 3, 2011.

Lehmann, C. E. R. and Archibald, S.: Deciphering the distribution of the savanna biome, *The New Phytologist*, 191, 1469–8137, doi:10.1111/j.1469-8137.2011.03689.x, 2011.

Lehmann, C. E. R., Archibald, S., Hoffmann, W. A., and Bond, W. J.: Deciphering the distribution of the savanna biome., *The New Phytologist*, 191, 197–209, doi: 10.1111/j.1469-8137.2011.03689.x, 2011.

Lenihan, J. M., Daly, C., Bachelet, D., and Neilson, R. P.: Simulating broad-scale fire severity in a dynamic global vegetation model, *Northwest Science*, 72, 91–103, 1998.

Lenihan, J. M., Bachelet, D., Neilson, R. P., and Drapek, R. J.: Simulated response of conterminous United States ecosystems to climate change at different levels of fire suppression, CO<sub>2</sub> emission rate, and growth response to CO<sub>2</sub>, *Global and Planetary Change*, 64, 16–25, doi:10.1016/j.gloplacha.2008.01.006, 2008.

Levine, J. S.: Global biomass burning: atmospheric, climatic, and biospheric implications, MIT press, 1991.

Levis, S., Bonan, G. B., Vertenstein, M., and Oleson, K. W.: Technical Documentation and Users Guide to the Community Land Models Dynamic Global Vegetation Model, Tech. rep., Terrestrial Sciences Section, Climate and Global Dynamics Division, National Center for Atmospheric Research, Boulder, Colorado, 2004.

Li, F., Zeng, X. D., and Levis, S.: A process-based fire parameterization of intermediate complexity in a Dynamic Global Vegetation Model, *Biogeosciences*, 9, 2761–2780, doi:10.5194/bg-9-2761-2012, 2012a.

Li, F., Bond-Lamberty, B., and Levis, S.: Quantifying the role of fire in the Earth system Part 2: Impact on the net carbon balance of global terrestrial ecosystems for the 20th century, *Biogeosciences Discussions*, 10, 17309–17350, doi: 10.5194/bgd-10-17309-2013, 2013a.

Liu, Z., Yang, J., and He, H. S.: Identifying the threshold of dominant controls on fire spread in a boreal forest landscape of Northeast China., *PloS one*, 8, e55618, doi:10.1371/journal.pone.0055618, 2013.

Loepfe, L., Martinez-Vilalta, J., Oliveres, J., Piñol, J., and Lloret, F.: Feedbacks between fuel reduction and landscape homogenisation determine fire regimes in three Mediterranean areas, *Forest Ecology and Management*, 259, 2366–2374, doi:10.1016/j.foreco.2010.03.009, 2010.

Lu, Z. and Sokolik, I. N.: The effect of smoke emission amount on changes in cloud properties and precipitation: A case study of Canadian boreal wildfires of 2007, *Journal of Geophysical Research: Atmospheres*, 118, 11,777–11,793, doi: 10.1002/2013JD019860, 2013.

Lucas, C., Hennessy, K., Mills, G., and Bathols, J.: Bushfire Weather in Southeast Australia : Recent Trends and Projected Climate Change Impacts Bushfire CRC and Australian Bureau of Meteorology, CSIRO Marine and Atmospheric Research September 2007 Consultancy Report prepared for The Climate Institute of, Tech. Rep. September, CSIRO, 2007.

Lunt, I. D., Zimmer, H. C., and Cheal, D. C.: The tortoise and the hare? Post-fire regeneration in mixed Eucalyptus–Callitris forest, *Australian Journal of Botany*, 59, 575–581, 2011.

Luo, Y. Q., Randerson, J. T., Abramowitz, G., Bacour, C., Blyth, E., Carvalhais, N., Ciais, P., Dalmonech, D., Fisher, J. B., Fisher, R., Friedlingstein, P., Hibbard, K., Hoffman, F. M., Huntzinger, D., Jones, C. D., Koven, C., Lawrence, D. M., Li, D. J., Mahecha, M., Niu, S. L., Norby, R., Piao, S. L., Qi, X., Peylin, P., Prentice, I. C., Riley, W., Reichstein, M., Schwalm, C., Wang, Y. P., Xia, J. Y., Zaehle, S., and Zhou, X. H.: A framework for benchmarking land models, *Biogeosciences*, 9, 3857–3874, doi:10.5194/bg-9-3857-2012, 2012.

Martins, J. A., Gonçalves, F. L. T., Morales, C. A., Fisch, G. F., Pinheiro, F. G. M., Leal Júnior, J. a. B. V., Oliveira, C. J., Silva, E. M., Oliveira, J. C. P., Costa, A. A., and Silva Dias, M. A. a. F.: Cloud condensation nuclei from biomass burning during the Amazonian dry-to-wet transition season, *Meteorology and Atmospheric Physics*, 104, 83–93, doi:10.1007/s00703-009-0019-6, 2009.

McArthur, A. G.: Fire behaviour in eucalypt forests, in: Department of National Development, Forestry and Timber Bureau Leaflet, vol. 107, Canberra : Forestry and Timber Bureau, 1967.

McArthur, A. G.: The fire control problem and fire research in Australia, in: Proceedings of the 1966 Sixth world forestry congress, vol. 2, pp. 1986–1991, 1969.

McCaw, L. and Hanstrum, B.: Fire environment of Mediterranean south-west Western Australia., in: Fire in ecosystems of south-west Western Australia: impacts and management. Symposium proceedings (Volume I), pp. 87–106, Backhuys Publishers, Leiden, 2003.

Mcgregor, J. L. and Dix, M. R.: The CSIRO conformal-cubic atmospheric GCM, in: IUTAM Symposium on Advances in Mathematical Modelling of Atmosphere and Ocean Dynamics, pp. 197–202, Springer, 2001.

McGregor, J. L., Gordon, H. B., Watterson, I. G., Dix, M. R., and Rotstain, L. D.: The CSIRO 9-level atmospheric general circulation model, CSIRO Division of Atmospheric Research technical paper, 1, 1993.

McPherson, G. R.: Ecology and management of North American savannas, University of Arizona Press, 1997.

- Medlyn, B. E., Duursma, R. A., Eamus, D., Ellsworth, D. S., Prentice, I. C., Barton, C. V. M., Crous, K. Y., de Angelis, P., Freeman, M., and Wingate, L.: Reconciling the optimal and empirical approaches to modelling stomatal conductance, *Global Change Biology*, 17, 2134–2144, 2011.
- Mell, W. E., Charney, J. J., Jenkins, M. A., Cheney, P., and Gould, J.: Numerical simulations of grassland fire behavior from the LANL-FIRETEC and NIST-WFDS models, in: EastFIRE Conference, vol. 2005, 2005.
- Mell, W. E., Manzello, S. L., Maranghides, A., Butry, D., and Rehm, R. G.: The wildland–urban interface fire problem—current approaches and research needs, *International Journal of Wildland Fire*, 19, 238–251, 2010a.
- Mell, W. E., McNamara, D., Maranghides, A., McDermott, R., Forney, G., Hoffman, C., and Ginder, M.: COMPUTER MODELLING OF WILDLAND-URBAN INTERFACE FIRES, 2010b.
- Menaut, J. C., Lepage, M., and Abbadie, L.: Savannas, woodlands and dry forests in Africa, Seasonally dry tropical forests, pp. 64–92, 1995.
- Menon, S., Hansen, J., Nazarenko, L., and Luo, Y.: Climate effects of black carbon aerosols in China and India, *Science*, 297, 2250–2253, 2002.
- Michaletz, S. T., Johnson, E. A., and Tyree, M. T.: Moving beyond the cambium necrosis hypothesis of post-fire tree mortality: cavitation and deformation of xylem in forest fires., *The New Phytologist*, 194, 254–63, doi:10.1111/j.1469-8137.2011.04021.x, 2012.
- Midgley, J. J.: Flammability is not selected for, it emerges, *Australian Journal of Botany*, 61, 102, doi:10.1071/BT12289, 2013.
- Miller, A. D. and Chesson, P.: Coexistence in Disturbance-Prone Communities: How a Resistance-Resilience Trade-Off Generates Coexistence via the Storage Effect, *The American Naturalist*, 173, 417–417, doi:10.1086/597669, 2009.
- Mitchener, L. J. and Parker, A. J.: CLIMATE , LIGHTNING , AND WILDFIRE IN THE NATIONAL FORESTS OF THE SOUTHEASTERN UNITED STATES : 1989 1998, *Physical Geography*, 26, 147–162, 2005.
- Mooney, S. D., Harrison, S. P., Bartlein, P. J., and Stevenson, J.: The prehistory of fire in Australasia, Flammable Australia: Fire Regimes, Biodiversity and Ecosystems in a Changing World, pp. 3–25, 2012.
- Moorcroft, P., Hurt, G., and Pacala, S.: A method for scaling vegetation dynamics: the ecosystem demography model (ED), *Ecological Monographs*, 71, 557–585, 2001.
- Moreno, J. M. and Oechel, W. C.: Fire intensity as a determinant factor of postfire plant recovery in southern California chaparral, in: The role of fire in Mediterranean-type ecosystems, pp. 26–45, Springer, 1994.

- Morgan, G. G., Sheppard, V., Khalaj, B., Ayyar, A., Lincoln, D., Jalaludin, B., Beard, J., Corbett, S., and Lumley, T.: Effects of bushfire smoke on daily mortality and hospital admissions in Sydney, Australia., *Epidemiology*, 21, 47–55, 2010.
- Moritz, M. A., Parisien, M.-A., Batllori, E., Krawchuk, M. A., Van Dorn, J., Ganz, D. J., and Hayhoe, K.: Climate change and disruptions to global fire activity, *Eco-sphere*, 3, 1–22, 2012.
- Morrison, D. A. and Renwick, J. A.: Effects of variation in fire intensity on regeneration of co-occurring species of small trees in the Sydney region, *Australian Journal of Botany*, 48, 71–79, 2000.
- Murphy, B. P., Williamson, G. J., and Bowman, D. M. J. S.: Fire regimes: moving from a fuzzy concept to geographic entity., *The New Phytologist*, 192, 316–8, doi: 10.1111/j.1469-8137.2011.03893.x, 2011.
- Murphy, B. P., Bradstock, R. A., Boer, M. M., Carter, J., Cary, G. J., Cochrane, M. A., Fensham, R. J., Russell-Smith, J., Williamson, G. J., and Bowman, D. M. J. S.: Fire regimes of Australia: a pyrogeographic model system, *Journal of Biogeography*, 40, 1048–1058, doi:10.1111/jbi.12065, 2013.
- Murphy, B. P., Lehmann, C. E. R., Russell-Smith, J., and Lawes, M. J.: Fire regimes and woody biomass dynamics in Australian savannas, *Journal of Biogeography*, 41, 133–144, doi:10.1111/jbi.12204, 2014.
- Murphy, P. G. and Lugo, A. E.: Ecology of tropical dry forest, *Annual review of ecology and systematics*, pp. 67–88, 1986.
- Murray, B. R., Hardstaff, L. K., and Phillips, M. L.: Differences in Leaf Flammability, Leaf Traits and Flammability-Trait Relationships between Native and Exotic Plant Species of Dry Sclerophyll Forest, *PloS one*, 8, e79205, 2013.
- Murray, S. J., Foster, P. N., and Prentice, I. C.: Future global water resources with respect to climate change and water withdrawals as estimated by a dynamic global vegetation model, *Journal of Hydrology*, 448, 14–29, doi:10.1016/j.jhydrol.2012.02.044, 2012.
- Nesterov, V. G.: Combustibility of the forest and methods for its determination, Moscow: Goslesbumaga, 1949.
- NIFC: Historical Wildland Firefighter Fatality Reports, URL [http://www.nifc.gov/safety/safety\\_HistFatality\\_report.html](http://www.nifc.gov/safety/safety_HistFatality_report.html), 2013.
- Nobel, P. S.: Physicochemical and Environmental Plant Physiology, Physicochemical and Environmental Plant Physiology Series, Elsevier Science, 2005.
- NSWRFS: Update Damage assessment and fire investigation, Tech. Rep. October, New South Wales Rural Fire Service, New South Wales, URL [www.rfs.nsw.gov.au](http://www.rfs.nsw.gov.au), 2013.

NVIS: Australia's native vegetation — A summary of Australia's major vegetation groups 2, 2007.

Oleson, K. W., Lawrence, D. M., Gordon, B., Flanner, M. G., Kluzek, E., Peter, J., Levis, S., Swenson, S. C., Thornton, E., and Feddema, J.: Technical description of version 4.0 of the Community Land Model (CLM), 2010.

Olson, D. M., Dinerstein, E., Wikramanayake, E. D., Burgess, N. D., Powell, G. V. N., Underwood, E. C., D'amico, J. A., Itoua, I., Strand, H. E., Morrison, J. C., Loucks, C. J., Allnutt, T. F., Ricketts, T. H., Kura, Y., Lamoreux, J. F., Wettengel, W. W., Hedao, P., and Kassem, K. R.: Terrestrial Ecoregions of the World: A New Map of Life on Earth A new global map of terrestrial ecoregions provides an innovative tool for conserving biodiversity, *BioScience*, 51, 933–938, 2001.

Ormeño, E., Céspedes, B., Sánchez, I. A., Velasco-García, A., Moreno, J. M., Fernández, C., and Baldy, V.: The relationship between terpenes and flammability of leaf litter, *Forest Ecology and Management*, 257, 471–482, doi:10.1016/j.foreco.2008.09.019, 2009.

Padilla, M. and Vega-García, C.: On the comparative importance of fire danger rating indices and their integration with spatial and temporal variables for predicting daily human-caused fire occurrences in Spain, *International Journal of Wildland Fire*, 20, 46–58, 2011.

Parisien, M.-A. and Moritz, M. A.: Environmental controls on the distribution of wildfire at multiple spatial scales, *Ecological Monographs*, 79, 127–154, 2009.

Paula, S. and Ojeda, F.: Belowground starch consumption after recurrent severe disturbance in three resprouter species of the genus *Erica*, *Botany*, 87, 253–259, 2009.

Paula, S., Arianoutsou, M., Kazanis, D., Tavsanoglu, c., Lloret, F., Buhk, C., Ojeda, F., Luna, B., Moreno, J. M., Rodrigo, A., J. M. Espelta, Palacio, S., Fernández-Santos, B., Fernandes, P. M., and Pausas, J. G.: Fire-related traits for plant species of the Mediterranean Basin: Ecological Archives E090-094, *Ecology*, 90, 1420, 2009.

Pausas, J. G.: Resprouting vs seeding—a Mediterranean perspective, *Oikos*, 94, 193–194, 2001.

Pausas, J. G. and Vallejo, V.: The role of fire in European Mediterranean ecosystems, in: Remote sensing of large wildfires in the European Mediterranean basin, edited by E., C., pp. 3–16, Springer-Verlag, 1999.

Pechony, O. and Shindell, D. T.: Fire parameterization on a global scale, *Journal of Geophysical Research*, 114, D16115, doi:10.1029/2009JD011927, 2009.

Pechony, O. and Shindell, D. T.: Driving forces of global wildfires over the past millennium and the forthcoming century., *Proceedings of the National Academy of Sciences of the United States of America*, 107, 19167–70, doi:10.1073/pnas.1003669107, 2010.

Penman, T. D., Christie, F. J., Andersen, A. N., Bradstock, R. A., Cary, G. J., Henderson, M. K., Price, O., Tran, C., Wardle, G. M., Williams, R. J., and York, A.: Prescribed burning: how can it work to conserve the things we value?, *International Journal of Wildland Fire*, 20, 721–733, 2011.

Penman, T. D., Bradstock, R. A., and Price, O. F.: Modelling the determinants of ignition in the Sydney Basin, Australia: implications for future management, 2013.

Peterson, D. L. and Ryan, K. C.: Modeling postfire conifer mortality for long-range planning, *Environmental Management*, 10, 797–808, doi:10.1007/BF01867732, 1986.

Pfeiffer, M., Spessa, A., and Kaplan, J. O.: A model for global biomass burning in preindustrial time: LPJ-LMfire (v1.0), *Geoscientific Model Development*, 6, 643–685, doi:10.5194/gmd-6-643-2013, 2013.

Pickett, S. T. and White, P. S.: The ecology of natural disturbance and patch dynamics, Academic press, 1985.

Pitman, A. J., Narisma, G. T., and McAneney, J.: The impact of climate change on the risk of forest and grassland fires in Australia, *Climatic Change*, 84, 383–401, doi:10.1007/s10584-007-9243-6, 2007.

Potter, C. S. and Klooster, S. A.: Dynamic global vegetation modelling for prediction of plant functional types and biogenic trace gas fluxes, *Global Ecology and Biogeography*, 8, 473–488, doi:10.1046/j.1365-2699.1999.00152.x, 1999.

Prentice, I. C., Sykes, M. T., and Cramer, W.: A simulation model for the transient effects of climate change on forest landscapes, *Ecological Modelling*, 65, 51–70, 1993b.

Prentice, I. C., Bondeau, A., Cramer, W., Harrison, S. P., Hickler, T., Lucht, W., Sitch, S., Smith, B., and Sykes, M. T.: Dynamic global vegetation modeling: quantifying terrestrial ecosystem responses to large-scale environmental change, in: *Terrestrial ecosystems in a changing world*, pp. 175–192, Springer, 2007.

Prentice, I. C., Kelley, D. I., Foster, P. N., Friedlingstein, P., Harrison, S. P., and Bartlein, P. J.: Modeling fire and the terrestrial carbon balance, *Global Biogeochemical Cycles*, 25, 1–13, doi:10.1029/2010GB003906, 2011.

Prentice, I. C., Dong, N., Gleason, S. M., Maire, V., and Wright, I. J.: Balancing the costs of carbon gain and water transport: testing a new theoretical framework for plant functional ecology., *Ecology letters*, 17, 82–91, doi:10.1111/ele.12211, URL <http://www.ncbi.nlm.nih.gov/pubmed/24215231>, 2014.

Prentice, S. and Mackerras, D.: The ratio of cloud to cloud-ground lightning flashes in thunderstorms, *Journal of Applied Meteorology*, 16, 545–550, 1977.

Price, O. F. and Bradstock, R. A.: The spatial domain of wildfire risk and response in the Wildland Urban Interface in Sydney, Australia, *Natural Hazards and Earth System Sciences Discussions*, 1, 4539–4564, doi:10.5194/nhessd-1-4539-2013, 2013.

R Core Team: R: A Language and Environment for Statistical Computing, R Foundation for Statistical Computing, Vienna, Austria, URL <http://www.r-project.org/>, 2013.

Raison, R. J., Woods, P. V., and Khanna, P. K.: Dynamics of fine fuels in recurrently burnt eucalypt forests, *Australian Forestry*, 46, 294–302, 1983.

Randerson, J. T., Thompson, M. V., Conway, T. J., Fung, I. Y., and Field, C. B.: The contribution of terrestrial sources and sinks to trends in the seasonal cycle of atmospheric carbon dioxide, *Global Biogeochemical Cycles*, 11, 535–560, 1997.

Randerson, J. T., Kasibhatla, P. S., Kasischke, E. S., Hyer, E. J., Giglio, L., Collatz, G. J., and van der Werf, G. R.: Global fire emissions database (GFED), version 1, Data set, available online /from , Tennessee, USA, 2005.

Randerson, J. T., Hoffman, F. M., Thornton, P. E., Mahowald, N. M., Lindsay, K., Lee, Y.-H., Nevison, C. D., Doney, S. C., Bonan, G. B., Stöckli, R., Covey, C., Running, S. W., and Fung, I. Y.: Systematic assessment of terrestrial biogeochemistry in coupled climate-carbon models, *Global Change Biology*, 15, 2462–2484, doi:10.1111/j.1365-2486.2009.01912.x, 2009.

Randerson, J. T., Chen, Y., van der Werf, G. R., Rogers, B. M., and Morton, D. C.: Global burned area and biomass burning emissions from small fires, *Journal of Geophysical Research*, 117, G04 012, doi:10.1029/2012JG002128, 2012.

Ratnam, J., Bond, W. J., Fensham, R. J., Hoffmann, W. A., Archibald, S., Lehmann, C. E. R., Anderson, M. T., Higgins, S. I., and Sankaran, M.: When is a forest a savanna, and why does it matter?, *Global Ecology and Biogeography*, 20, 653–660, doi:10.1111/j.1466-8238.2010.00634.x, 2011.

Riahi, K., Rao, S., Krey, V., Cho, C., Chirkov, V., Fischer, G., Kindermann, G., Nakicenovic, N., and Rafaj, P.: RCP 8.5 — A scenario of comparatively high greenhouse gas emissions, *Climatic Change*, 109, 33–57, doi:10.1007/s10584-011-0149-y, 2011.

Rödenbeck, C., Houweling, S., Gloor, M., and Heimann, M.: CO<sub>2</sub> flux history 1982–2001 inferred from atmospheric data using a global inversion of atmospheric transport, *Atmospheric Chemistry and Physics*, 3, 1919–1964, 2003.

Rollins, M., Morgan, P., and Swetnam, T. W.: Landscape-scale controls over 20th century fire occurrence in two large Rocky Mountain (USA) wilderness areas, *Landscape Ecology*, 17, 539–557, 2002.

Romsey: Climate Historical Alerts Interactive Information Historical Bushfires and Wildfires in Australia., 2009.

Rorig, M. L. and Ferguson, S. A.: Characteristics of lightning and wildland fire ignition in the Pacific Northwest, *Journal of Applied Meteorology*, 38, 1565–1575, 1999.

Rosenfeld, D.: TRMM observed first direct evidence of smoke from forest fires inhibiting rainfall, *Geophysical research letters*, 26, 3105–3108, 1999.

Rothermel, R. C.: A mathematical model for predicting fire spread in wildland fuels, USFS, 1972.

Running, S. W., Nemani, R. R., and Hungerford, R. D.: Extrapolation of synoptic meteorological data in mountainous terrain and its use for simulating forest evapotranspiration and photosynthesis, *Canadian Journal of Forest Research*, 17, 472–483, 1987.

Russell-Smith, J., Craig, R., Gill, A. M., Smith, R. W., and Williams, J. E.: Australia State of the Environment Second Technical Paper Series (Biodiversity), Tech. rep., Department of the Environment and Heritage, Canberra, 2002.

Russell-Smith, J., Yates, C. P., Whitehead, P. J., Smith, R., Craig, R., Allan, G. E., Thackway, R., Frakes, I., Cridland, S., Meyer, M. C. P., and Gill, A. M.: Bushfires 'down under': patterns and implications of contemporary Australian landscape burning, *International Journal of Wildland Fire*, 16, 361, doi:10.1071/WF07018, 2007.

Ryan, K. C. and Frandsen, W. H.: Basal Injury From Smoldering Fires in Mature [*Pinus ponderosa*] Laws, *International Journal of Wildland Fire*, 1, 107–118, 1991.

Safford, H. D., Schmidt, D. A., and Carlson, C. H.: Effects of fuel treatments on fire severity in an area of wildland–urban interface, *Angora Fire, Lake Tahoe Basin, California, Forest Ecology and Management*, 258, 773–787, 2009.

Sage, R. F.: Modification of Fire Disturbance by Elevated CO<sub>2</sub>, Carbon Dioxide, Populations, and Communities, p. 231, 1996.

Sasaki, N.: Forest Fires, Air Pollution, and Mortality in Southeast Asia, *Demography*, 39, 1–23, 2002b.

Saura-Mas, S., Paula, S., Pausas, J. G., and Lloret, F.: Fuel loading and flammability in the Mediterranean Basin woody species with different post-fire regenerative strategies, *International Journal of Wildland Fire*, 19, 783, doi:10.1071/WF09066, 2010.

Scarff, F. R. and Westoby, M.: Leaf litter flammability in some semi-arid Australian woodlands, *Functional Ecology*, 20, 745–752, 2006.

Scheiter, S. and Higgins, S. I.: Impacts of climate change on the vegetation of Africa: an adaptive dynamic vegetation modelling approach, *Global Change Biology*, pp. 2224–2246, doi:10.1111/j.1365-2486.2008.01838.x, 2009.

Scholze, M., Knorr, W., Arnell, N. W., and Prentice, I. C.: A climate-change risk analysis for world ecosystems., *Proceedings of the National Academy of Sciences of the United States of America*, 103, 13 116–20, doi:10.1073/pnas.0601816103, 2006.

- Schoonenberg, T.: Responses to mechanical wounding and fire in tree species characteristic of seasonally dry tropical forest of Bolivia, *Canadian Journal of Forest Research*, 33, 330–338, doi:10.1139/X02-172, 2003.
- Schwilk, D. W. and Ackerly, D.: Flammability and serotiny as strategies: correlated evolution in pines, *Oikos*, 2, 326–336, 2001.
- Shane, F., Parker, K., Shackleton, C., and Davis, S.: BUSH FIRE bulletin no 3, vol. 35, NSW Rural Fire service, New South Wales, 4 edn., 2013.
- Sharples, J.: Review of formal methodologies for windslope correction of wildfire rate of spread, *International Journal of Wildland Fire*, 17, 179–193, 2008.
- Sitch, S., Smith, B., and Prentice, I. C.: Evaluation of ecosystem dynamics, plant geography and terrestrial carbon cycling in the LPJ dynamic global vegetation model, *Global Change Biology*, 9, 161–185, 2003.
- Sitch, S., Huntingford, C., Gedney, N., Levy, P. E., Lomas, M. R., Piao, S. L., Betts, R. A., Ciais, P., Cox, P. M., Friedlingstein, P., C. D. Jones, Prentice, I. C., and Woodward, F. I.: Evaluation of the terrestrial carbon cycle, future plant geography and climate-carbon cycle feedbacks using five Dynamic Global Vegetation Models (DGVMs), *Global Change Biology*, 14, 2015–2039, 2008a.
- Stambaugh, M. C. and Guyette, R. P.: Predicting spatio-temporal variability in fire return intervals using a topographic roughness index, *Forest Ecology and Management*, 254, 463–473, 2008.
- Swetnam, T. W. and Betancourt, J. L.: Fire-southern oscillation relations in the southwestern United States., *Science*, 249, 1017–1020, 1990.
- Syphard, A. D. and Radeloff, V. C.: Human influence on California fire regimes, *Ecological Applications*, 17, 1388–1402, 2007.
- Tansey, K., Grégoire, J.-M., Defourny, P., Leigh, R., Pekel, J.-F., van Bogaert, E., and Bartholomé, E.: A new, global, multi-annual (20002007) burnt area product at 1 km resolution, *Geophysical Research Letters*, 35, L01401, doi:10.1029/2007GL031567, 2008.
- Telitsyn, G. P.: Forest Fires, their Prevention and Suppression in Khabarovsk Territory, Khabarovsk, 1988.
- Telitsyn, H. P.: A Mathematical Model of Spread of High-Intensity Forest Fires, in: Fire in ecosystems of boreal Eurasia, pp. 314–325, Springer, 1996.
- Tham, R., Erbas, B., Akram, M., Dennekamp, M., and Abramson, M. J.: The impact of smoke on respiratory hospital outcomes during the 2002-2003 bushfire season, Victoria, Australia., *Respirology (Carlton, Vic.)*, 14, 69–75, doi:10.1111/j.1440-1843.2008.01416.x, 2009.

Thomas, P. A., McAlpine, R. S., Hirsch, K., and Hobson, P.: How Plants Cope with Crown Fire, in: *Fire in the Forest*, edited by Thomas, P. A. and McAlpine, R. S., chap. 5.4, pp. 98–109, Cambridge University Press, Cambridge, 2010.

Thomson, A. M., Calvin, K. V., Smith, S. J., Kyle, G. P., Volke, A., Patel, P., Delgado-Arias, S., Bond-Lamberty, B., Wise, M. a., Clarke, L. E., and Edmonds, J. a.: RCP4.5: a pathway for stabilization of radiative forcing by 2100, *Climatic Change*, 109, 77–94, doi:10.1007/s10584-011-0151-4, 2011.

Thonicke, K., Venevsky, S., Sitch, S., and Cramer, W.: The role of fire disturbance for global vegetation dynamics: coupling fire into a Dynamic Global Vegetation Model, *Global Ecology and Biogeography*, 10, 661–677, doi:10.1046/j.1466-822X.2001.00175.x, 2001.

Thonicke, K., Spessa, A., Prentice, I. C., Harrison, S. P., Dong, L., and Carmona-Moreno, C.: The influence of vegetation, fire spread and fire behaviour on biomass burning and trace gas emissions: results from a process-based model, *Biogeosciences*, 7, 1991–2011, doi:10.5194/bg-7-1991-2010, 2010.

Thornton, P. E.: Regional ecosystem simulation: combining surface-and satellite-based observations to study linkages between terrestrial energy and mass budgets, 1998.

Torn, M. and Fried, J.: Predicting the impacts of global warming on wildland fire, *Climatic Change*, 21, 257–274, doi:10.1007/BF00139726, 1992.

Trabaud, L.: Postfire plant community dynamics in the Mediterranean Basin, in: *The role of fire in Mediterranean-type ecosystems*, pp. 1–15, Springer, 1994.

Tucker, C. M. and Cadotte, M. W.: Fire variability, as well as frequency, can explain coexistence between seeder and resprouter life histories, *Journal of Applied Ecology*, 50, 594–602, 2013.

Tyree, M. T. and Zimmermann, M. H.: Xylem structure and the ascent of sap, Springer, 2002.

Uhl, C. and Kauffman, J. B.: Deforestation, fire susceptibility, and potential tree responses to fire in the eastern Amazon, *Ecology*, 71, 437–449, 1990.

Ukkola, A. M. and Prentice, I. C.: A worldwide analysis of trends in water-balance evapotranspiration, *Hydrology and Earth System Sciences*, 17, 4177–4187, doi:10.5194/hess-17-4177-2013, 2013.

Vallejo, R., Aronson, J., Pausas, J. G., and Cortina, J.: Restoration of Mediterranean woodlands, *Restoration ecology. The new frontier*, 2006.

van der Werf, G. R., Randerson, J. T., Collatz, G. J., and Giglio, L.: Carbon emissions from fires in tropical and subtropical ecosystems, *Global Change Biology*, 9, 547–562, doi:10.1046/j.1365-2486.2003.00604.x, 2003.

- van der Werf, G. R., Randerson, J. T., Collatz, G. J., Giglio, L., Kasibhatla, P. S., Arellano, A. F., Olsen, S. C., and Kasischke, E. S.: Continental-scale partitioning of fire emissions during the 1997 to 2001 El Nino/La Nina period, *Science*, 303, 73–76, 2004.
- van der Werf, G. R., Randerson, J. T., Giglio, L., Collatz, G. J., Kasibhatla, P. S., and Arellano, A. F.: Interannual variability of global biomass burning emissions from 1997 to 2004, *Atmospheric Chemistry and Physics Discussions*, 6, 3175–3226, doi: 10.5194/acpd-6-3175-2006, 2006.
- van der Werf, G. R., Randerson, J. T., Giglio, L., Gobron, N., and Dolman, A. J.: Climate controls on the variability of fires in the tropics and subtropics, *Global Biogeochemical Cycles*, 22, GB3028, doi:10.1029/2007GB003122, 2008.
- van der Werf, G. R., Randerson, J. T., Giglio, L., Collatz, G. J., Mu, M., Kasibhatla, P. S., Morton, D. C., Defries, R. S., van Jin, Y., and van Leeuwen, T. T.: Global fire emissions and the contribution of deforestation, savanna, forest, agricultural, and peat fires (1997–2009), *Atmospheric Chemistry and Physics*, 10, 11 707–11 735, 2010.
- Van Wagner, C. E.: Development and structure of the Canadian forest fire weather index system, vol. 35, 1987.
- Vázquez, A. and Moreno, J. M.: Patterns of lightning-, and people-caused fires in peninsular Spain, *International Journal of Wildland Fire*, 8, 103–115, 1998.
- Veblen, T. T. and Kitzberger, T.: Inter-hemispheric comparison of fire history: the Colorado front range, USA, and the northern Patagonian Andes, Argentina, *Plant Ecology*, 163, 187–207, 2002.
- Venevsky, S., Thonicke, K., Sitch, S., and Cramer, W.: Simulating fire regimes in human-dominated ecosystems: Iberian Peninsula case study, *Global Change Biology*, 8, 984–998, doi:10.1046/j.1365-2486.2002.00528.x, 2002.
- Verdon, D., Kiem, A., and Franks, S.: Multi-decadal variability of forest fire risk-eastern Australia, *International Journal of Wildland Fire*, 13, 165–171, 2004.
- Vesk, P. a.: Plant size and resprouting ability: trading tolerance and avoidance of damage?, *Journal of Ecology*, 94, 1027–1034, doi:10.1111/j.1365-2745.2006.01154.x, 2006.
- Viedma, O., Angeler, D. G., and Moreno, J. M.: Landscape structural features control fire size in a Mediterranean forested area of central Spain, 2009a.
- Viegas, D. X., Bovio, G., and Ferreira, A.: Comparative study of various methods of fire danger evaluation in southern Europe, *International Journal of Wildland Fire*, 9, 235–246, 1999.
- Vines, R. G.: Heat transfer through bark, and the resistance of trees to fire., *Australian Journal of Botany*, 16, 499, doi:10.1071/BT9680499, 1968.

Wagner, C. E. V.: Prediction of crown fire behavior in two stands of jack pine, Canadian Journal of Forest Research, 23, 442–449, 1993.

Walker, J.: Fuel dynamics in Australian vegetation, Fire and the Australian biota, pp. 101–127, 1981.

Ward, D. S., Kloster, S., Mahowald, N. M., Rogers, B. M., Randerson, J. T., and Hess, P. G.: The changing radiative forcing of fires: global model estimates for past, present and future, Atmospheric Chemistry and Physics, 12, 10 857–10 886, doi:10.5194/acp-12-10857-2012, 2012.

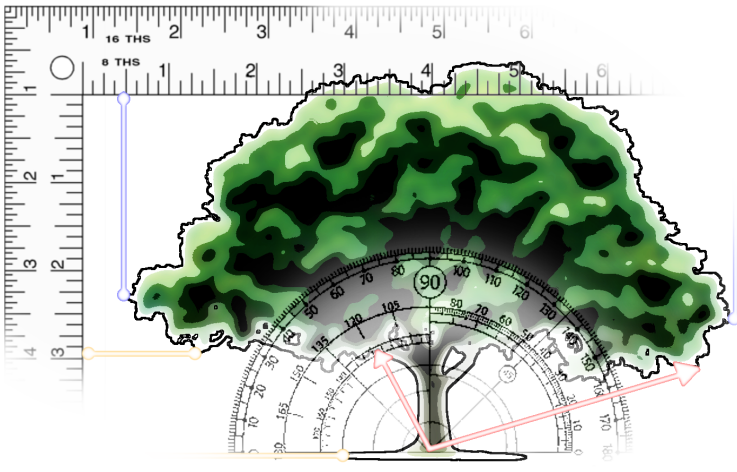
Whelan, R. J.: The ecology of fire, Cambridge University Press, 1995.

Williams, A., Karoly, D., and Tapper, N. J.: The sensitivity of Australian fire danger to climate change, Climatic Change, pp. 171–191, 2001.

Williams, R. J., Griffiths, A. D., and Allan, G. E.: northern Australia, Flammable Australia: the fire regimes and biodiversity of a continent, p. 281, 2002.

Wills, T. J. and Read, J.: Effects of heat and smoke on germination of soil-stored seed in a south-eastern Australian sand heathland, Australian Journal of Botany, 50, 197–206, 2002.

# 2



## A comprehensive benchmarking system for evaluating global vegetation models

---

D. I. Kelley<sup>1</sup>, I. C. Prentice,<sup>1,2</sup>, S. P. Harrison<sup>1,3</sup>, H. Wang<sup>1,4</sup>, M. Simard<sup>5</sup>, J. B. Fisher<sup>5</sup>, and K. O. Willis<sup>1</sup>

<sup>1</sup>Biological Sciences, Macquarie University, North Ryde, NSW 2109, Australia

<sup>2</sup>Grantham Institute for Climate Change, and Department of Life Sciences, Imperial College, Silwood Park Campus, Ascot SL5 7PY, UK

<sup>3</sup>Geography & Environmental Sciences, School of Human and Environmental Sciences, Reading University, Whiteknights, Reading, RG6 6AB, UK

<sup>4</sup>State Key Laboratory of Vegetation and Environmental Change, Institute of Botany, Chinese Academy of Science, Xiangshan Nanxincun 20, 100093 Beijing, China

<sup>5</sup>JPL, California Institute of Technology, Pasadena, CA 91109, USA

---

This chapter is presented as the published journal article:

Kelley, D. I., Prentice, I. C., Harrison, S. P., Wang, H., Simard, M., Fisher, J. B. and Willis, K. O.: A comprehensive benchmarking system for evaluating global vegetation models, *Biogeosciences*, 10(5), doi:10.5194/bg-10-3313-2013, 2013.

---

Reproduced under Creative Commons Attribution 3.0 License courtesy of Copernicus Publications on behalf of the European Geosciences Union (EGU).

Biogeosciences, 10, 3313–3340, 2013  
[www.biogeosciences.net/10/3313/2013/](http://www.biogeosciences.net/10/3313/2013/)  
doi:10.5194/bg-10-3313-2013  
© Author(s) 2013. CC Attribution 3.0 License.



Biogeosciences  
Open Access



## A comprehensive benchmarking system for evaluating global vegetation models

D. I. Kelley<sup>1</sup>, I. C. Prentice<sup>1,2</sup>, S. P. Harrison<sup>1,3</sup>, H. Wang<sup>1,4</sup>, M. Simard<sup>5</sup>, J. B. Fisher<sup>5</sup>, and K. O. Willis<sup>1</sup>

<sup>1</sup>Department of Biological Sciences, Macquarie University, North Ryde, NSW 2109, Australia

<sup>2</sup>Grantham Institute for Climate Change, and Department of Life Sciences, Imperial College, Silwood Park Campus, Ascot SL5 7PY, UK

<sup>3</sup>Geography & Environmental Sciences, School of Human and Environmental Sciences, Reading University, Whiteknights, Reading, RG6 6AB, UK

<sup>4</sup>State Key Laboratory of Vegetation and Environmental Change, Institute of Botany, Chinese Academy of Science, Xiangshan Nanxincun 20, 100093 Beijing, China

<sup>5</sup>Jet Propulsion Laboratory, California Institute of Technology, Pasadena, CA 91109, USA

Correspondence to: D. I. Kelley (douglas.kelley@students.mq.edu.au)

Received: 20 July 2012 – Published in Biogeosciences Discuss.: 9 November 2012

Revised: 5 March 2013 – Accepted: 7 March 2013 – Published: 17 May 2013

**Abstract.** We present a benchmark system for global vegetation models. This system provides a quantitative evaluation of multiple simulated vegetation properties, including primary production; seasonal net ecosystem production; vegetation cover; composition and height; fire regime; and runoff. The benchmarks are derived from remotely sensed gridded datasets and site-based observations. The datasets allow comparisons of annual average conditions and seasonal and inter-annual variability, and they allow the impact of spatial and temporal biases in means and variability to be assessed separately. Specifically designed metrics quantify model performance for each process, and are compared to scores based on the temporal or spatial mean value of the observations and a “random” model produced by bootstrap resampling of the observations. The benchmark system is applied to three models: a simple light-use efficiency and water-balance model (the Simple Diagnostic Biosphere Model: SDBM), the Lund-Potsdam-Jena (LPJ) and Land Processes and eXchanges (LPX) dynamic global vegetation models (DGVMs). In general, the SDBM performs better than either of the DGVMs. It reproduces independent measurements of net primary production (NPP) but underestimates the amplitude of the observed CO<sub>2</sub> seasonal cycle. The two DGVMs show little difference for most benchmarks (including the inter-annual variability in the growth rate and seasonal cycle of atmospheric CO<sub>2</sub>), but LPX represents burnt fraction

demonstrably more accurately. Benchmarking also identified several weaknesses common to both DGVMs. The benchmarking system provides a quantitative approach for evaluating how adequately processes are represented in a model, identifying errors and biases, tracking improvements in performance through model development, and discriminating among models. Adoption of such a system would do much to improve confidence in terrestrial model predictions of climate change impacts and feedbacks.

### 1 Introduction

Dynamic global vegetation models (DGVMs) are widely used in the assessment of climate change impacts on ecosystems, and feedbacks through ecosystem processes (Cramer et al., 1999; Scholze et al., 2006; Sitch et al., 2008; Scheiter and Higgins, 2009). However, there are large differences in model projections of the vegetation response to scenarios of future changes in atmospheric CO<sub>2</sub> concentration and climate (Friedlingstein et al., 2006; Denman et al., 2007; Sitch et al., 2008). Assessing the uncertainty around vegetation-model simulations would provide an indicator of confidence in model predictions under different climates. Such a system would serve several functions, including the following: comparing the performance of different models; identifying

3314

**D. I. Kelley et al.: Benchmarking system for evaluating global vegetation models**

processes in a particular model that need improvement; and checking that improvements in one part of a model do not compromise performance in another.

Benchmarking is a routine component in the assessment of climate-model performance, including investigation of parameter uncertainties (e.g. Murphy et al., 2004; Piani et al., 2005) and multi-model comparison (Randall et al., 2007; Reichler and Kim, 2008), and is used both to inform model development (e.g. Jackson et al., 2008) and to interpret the reliability of projections of future climate (e.g. Shukla et al., 2006; Hall and Qu, 2006). In recent years, there has been considerable effort spent on the development of standard metrics for climate-model evaluation (Taylor, 2001; Gleckler et al., 2008; Lenderink, 2010; Moise and Delage, 2011; Yokoi et al., 2011). In comparison, there has been little quantitative assessment of DGVM performance under recent conditions. Although most studies describing vegetation-model development provide some assessment of the model's predictive ability by comparison with observational datasets (e.g. Sitch et al., 2003; Woodward and Lomas, 2004; Prentice et al., 2007), such comparisons often focus just on one aspect of the model where recent development has taken place (e.g. Gerten et al., 2004; Arora and Boer, 2005; Zeng et al., 2008; Thonicke et al., 2010; Prentice et al., 2011). It has not been standard practice to track improvements in (or degradation of) general model performance caused by new developments.

A benchmarking system should facilitate more comprehensive model evaluation, and help to make such tracking routine. The land modelling community has recently recognized the need for such a system (e.g. the International Land Model Benchmarking Project, ILAMB: <http://www.ilamb.org/>), and some recent studies have designed and applied benchmarking systems. Blyth et al. (2009, 2011) compared results of the JULES land-surface model with site-based water and CO<sub>2</sub> flux measurements and satellite vegetation indices, quantifying the difference between model output and observations using root mean squared error (RMSE) as a metric. Beer et al. (2010) used a gridded dataset of gross primary productivity (GPP), derived from up-scaling GPP from the FLUXNET network of eddy covariance towers (Jung et al., 2009, 2010) to assess and compare the Lund-Potsdam-Jena (LPJ), LPJmL, ORCHIDEE, CLM-CN and SDGVM models. Bonan et al. (2011) evaluated latent heat fluxes with the tower-derived gridded GPP dataset (Beer et al., 2010) to evaluate the calibration of the CLM4 model. Cadule et al. (2010) used the model-to-data deviation, normalised standard deviation and Pearson's correlation to quantify the "distance" between simulated and observed CO<sub>2</sub> concentration and applied these to compare three coupled climate–vegetation models that incorporate two DGVMs: TRIFFID and ORCHIDEE. All of these studies focus on a very limited number of simulated processes, and use metrics that are difficult to interpret across processes and models. Randerson et al. (2009) introduced a more systematic framework to as-

sess and compare the performance of two biogeochemical models (CLM-CN and CASA') against net primary production (NPP) and CO<sub>2</sub> concentration data, including the definition of comparison metrics tailored to the benchmark observations and a composite skill score that combined metric scores for each observation into an overall measure of model performance. The Randerson et al. (2009) composite score was a weighted combination of scores across different metrics, where the weights were based on a qualitative and necessarily somewhat subjective assessment of the "importance" and uncertainty of each process (Randerson et al., 2009). Luo et al. (2012) recommended the development of a working benchmarking system for vegetation models that incorporates some of the approaches used in these various studies including a set of standard target datasets for benchmarks, a scoring system; and a way of comparing across model processes in order to evaluate model strengths and weaknesses to guide model development. Luo et al. (2012) reject the idea of a single composite metric because of the subjectivity involved in choices of relative weightings.

Our purpose here is to demonstrate a benchmarking system including multiple observational datasets and transparent metrics of model performance with respect to individual processes. We have tested the system on three vegetation models to demonstrate the system's capabilities in comparing model performance, assigning a level of confidence to the models' predictions of key ecosystem properties, assessing the representation of different model processes and identifying deficiencies in each model.

## 2 Materials and methods

### 2.1 Principles

The benchmarking system consists of a collection of datasets, selected to fulfil certain criteria and to allow systematic evaluation of a range of model processes, and metrics, designed with the characteristics of each benchmark dataset in mind. We selected site-based and remotely sensed observational datasets that, as far as possible, fulfil the following requirements:

- They should be global in coverage or, for site-based data, they should sample reasonably well the different biomes on each continent. This criterion excludes "campaign mode" measurements, and datasets assembled only for one continent or region.
- They should be independent of any modelling approach that involves calculation of vegetation properties from the same driving variables as the vegetation models being tested. This criterion allows remotely sensed fraction of absorbed photosynthetically active radiation (fAPAR) products but excludes the MODIS NPP product

used by Randerson et al. (2009), or remotely sensed evapotranspiration (e.g. Fisher et al., 2008, 2011; Mu et al., 2011). It allows use of flux measurements and CO<sub>2</sub> inversion products, but excludes, for example, the up-scaled GPP used by Beer et al. (2010).

- They should be available for multiple years and seasonal cycles to allow assessment of modelled seasonal and inter-annual variation, for variables that change on these time scales.
- Datasets should be freely available, so that different modelling groups can evaluate their models against the same benchmarks.

The selected datasets (Table 1) provide information for the following: fAPAR, the fractional coverage of different plant life and leaf forms, GPP and NPP, height of the canopy, fire, as burnt fraction; runoff, as river discharge, and seasonal and inter-annual variation in atmospheric CO<sub>2</sub> concentration (Fig. 1):

- fAPAR is the fundamental link between primary production and available energy (Monteith, 1972). It measures the seasonal cycle, inter-annual variability and trends of vegetation cover. Of all ecosystem properties derived from spectral reflectance measurements, fAPAR is closest to the actual measurements.
- Fractional cover of different life forms and leaf forms provides basic information about vegetation structure and phenology.
- GPP and NPP are the two fundamental measures of primary production.
- Vegetation height is a key variable for characterising vegetation structure, function and biomass.
- Remotely sensed data on fire (as fractional burnt area) have been available for a few years (e.g. Carmona-Moreno et al., 2005; Giglio et al., 2006). The latest dataset (Giglio et al., 2010; van der Werf et al., 2010) is derived from active fire counts and involves empirical (biome-dependent) modelling to translate between active fire counts and burned area. Our criteria exclude the use of the accompanying fire CO<sub>2</sub> emissions product (van der Werf et al., 2010), however, as this depends strongly on the use of a particular biogeochemical model.
- Annual runoff is an indicator of ecosystem function, as it represents the spatial integration of the difference between precipitation and evapotranspiration – the latter primarily representing water use by vegetation. It is a sensitive indicator, because a small proportional error in modelled evapotranspiration translates into a larger proportional error in runoff (Raupach et al., 2009). Runoff

is measured independently of meteorological data by gauges in rivers.

- Atmospheric CO<sub>2</sub> concentration is measured at high precision at a globally distributed set of stations in remote locations (distant from urban and transport centres of CO<sub>2</sub> emission). The pattern of the seasonal cycle of atmospheric CO<sub>2</sub> concentration at different locations provides information about the sources and sinks of CO<sub>2</sub> in the land biosphere (Heimann et al., 1998), while the inter-annual variability of the increase in CO<sub>2</sub> provides information about CO<sub>2</sub> uptake at the global scale. Ocean impacts on the seasonal cycle are small (Nevison et al., 2008). For inter-annual variability we use inversion products which selectively remove the ocean contribution (about 20 % of the signal: Le Quéré et al., 2003).

All remotely sensed data were re-gridded to a 0.5° resolution grid and masked to a land mask common to all three models.

Data-model comparison metrics were designed to be easy to implement, intuitive to understand, and comparable across multiple benchmarked processes. Metric scores for comparison of models with these datasets were compared against scores from two null models: one corresponding to the observational mean and the other obtained by randomly resampling the observations.

To demonstrate whether the benchmark system fulfilled the functions of evaluating specific modelled processes and discriminating between models, we applied it to three global models: a simple light-use efficiency and water-balance model introduced by Knorr and Heimann (1995), known as the Simple Diagnostic Biosphere Model (SDBM: Heimann et al., 1998) and two DGVMs. The SDBM is driven by observed precipitation, temperature and remotely sensed observations of fAPAR. The model has two tunable global parameters representing light-use efficiency under well-watered conditions, and the shape of the exponential temperature dependence of heterotrophic respiration. The DGVMs are the Lund-Potsdam-Jena (LPJ) model (version 2.1: Sitch et al., 2003, as modified by Gerten et al., 2004) and the Land surface Processes and eXchanges (LPX) model (Prentice et al., 2011). LPX was developed from LPJ-SPITFIRE (Thonicke et al., 2010), and represents a further refinement of the fire module in LPJ-SPITFIRE.

## 2.2 Benchmark datasets

### 2.2.1 fAPAR

fAPAR data (<http://oceancolor.gsfc.nasa.gov/SeaWiFS/>; Table 1) were derived from the SeaWiFS remotely sensed fAPAR product (Gobron et al., 2006), providing monthly data for 1998–2005. fAPAR varies between 0 and 1, and the average uncertainty for any cell/month is 0.05 with highest uncertainties in forested areas. Reliable fAPAR values cannot be

3316

D. I. Kelley et al.: Benchmarking system for evaluating global vegetation models

**Table 1.** Summary description of the benchmark datasets.

Dataset	Variable	Type	Period	Comparison	Reference
SeaWiFS	Fraction of absorbed photosynthetically active radiation (fAPAR)	Gridded	1998–2005	Annual average, seasonal phase and concentration, inter-annual variability	Gobron et al. (2006)
ISLSCP II vegetation continuous fields	Vegetation fractional cover	Gridded	Snapshot – 1992/1993	Fractional cover of bare ground, herbaceous and tree; comparison of tree cover split into evergreen or deciduous, and broadleaf or needleleaf	DeFries and Hansen (2009)
Combined net primary production	Net primary production (NPP)	Site	Various 1950–2006	Direct comparison with grid cell in which site falls	Luyssaert et al. (2007), Olson et al. (2001)
Luyssaert gross primary production	Gross primary production (GPP)	Site	Various 1950–2006	Direct comparison with grid cell in which site falls	Luyssaert et al. (2007)
Canopy height	Annual average height	Gridded	2005	Direct comparison	Simard et al. (2011)
GFED3	Fractional burnt area	Gridded	1997–2006	Annual average, seasonal phase and concentration, inter-annual variability	Giglio et al. (2010)
River discharge	River discharge (at or near river mouths)	Site	1950–2005 for LPJ and LPX; 1998–2005 for all models	Annual average discharge per river basin, inter-annual variability in global runoff	Dai et al. (2009)
CDIAC atmospheric CO <sub>2</sub> concentration	Atmospheric CO <sub>2</sub> concentration	Site	1998–2005	Seasonal phase and concentration	CDIAC: <a href="http://cdiac.ornl.gov">cdiac.ornl.gov</a>
CO <sub>2</sub> inversions	Atmospheric CO <sub>2</sub> concentration	Site	1980–2006	Inter-annual comparisons	Keeling (2008), Bousquet et al. (2000), Rödenbeck et al. (2003), Baker et al. (2006), Chevalier et al. (2010)

obtained for times when the solar incidence angle is  $> 50^\circ$ . This limitation mostly affects cells at high latitudes, or with complex topography, during winter. Cells where fAPAR values could not be obtained for any month were excluded from all comparisons. Annual fAPAR, which is the ratio of total annual absorbed to total annual incident PAR, is not the same as the average of the monthly fAPAR. True annual fAPAR was obtained by averaging monthly values weighted by PAR. Monthly PAR values were calculated using Clime Research Unit (CRU) TS3.1 monthly fractional cloud cover (Jones and Harris, 2012) as described in Gallego-Sala et al. (2010). Monthly and annual fAPAR values were used for annual average, inter-annual variability and seasonality comparisons. The monthly fAPAR data are used as a driver for the SDBM, but as a benchmark for the DGVMs.

### 2.2.2 Vegetation cover

Fractional cover data (Table 1) were obtained from International Satellite Land-Surface Climatology Project (ISLSCP) II vegetation continuous field (VCF) remotely sensed product (Hall et al., 2006; DeFries and Hansen, 2009 and refer-

ences therein). The VCF product provides separate information on life form, leaf type and leaf phenology at  $0.5^\circ$  resolution for 1992–1993. There are three categories in the life-form dataset: tree (woody vegetation  $> 5$  m tall), herbaceous (grass/herbs and woody vegetation  $< 5$  m), and bare ground cover. Leaf type (needleleaf or broadleaf) and phenology (deciduous or evergreen) is only given for cells that have some tree cover. Tree cover greater than 80 % is not well delineated due to saturation of the satellite signal, whereas tree cover of less than 20 % can be inaccurate due to the influence of soil and understorey on the spectral signature (DeFries et al., 2000).

The  $0.5^\circ$  dataset was derived from a higher resolution (1 km) dataset (DeFries et al., 1999). Evaluation of the 1 km dataset against ground observations shows it reproduces the distribution of the major vegetation types: the minimum correlation is for bare ground at high latitudes ( $r^2 = 0.79$ ) whereas grasslands and forests have an  $r^2$  of 0.93.

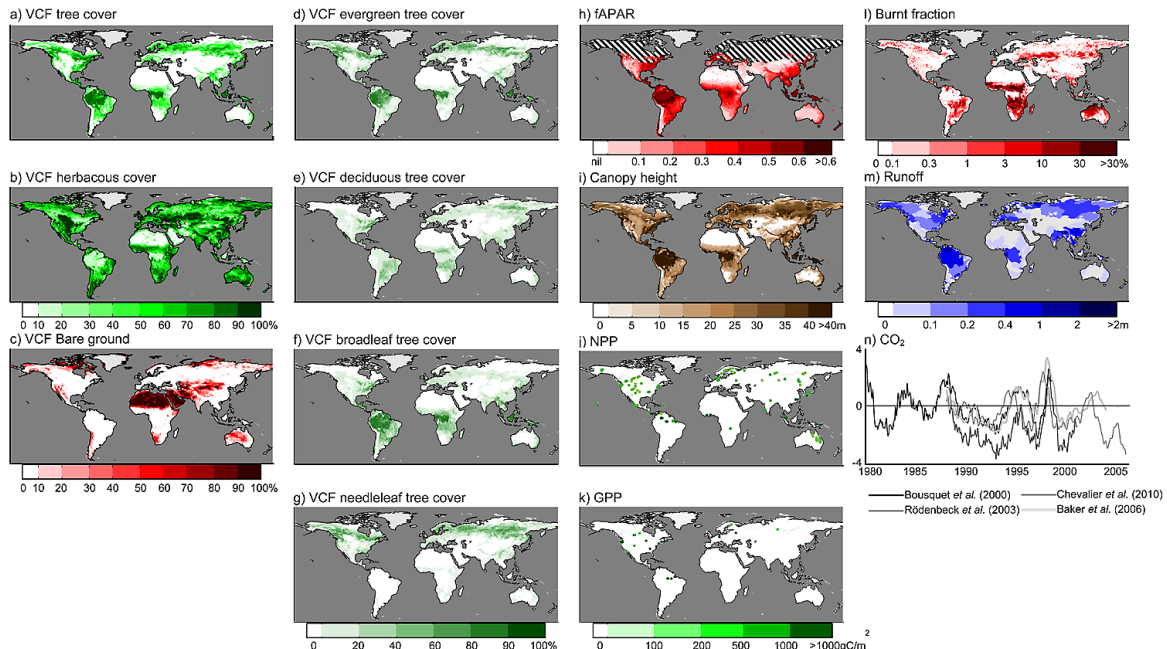


**Fig. 1.** Illustration of the benchmark datasets: ISLSCP II continuous vegetation fields based on a snapshot for 1992–1993 (DeFries and Hansen, 2009) give the proportions of (**a**) woody vegetation > 5 m in height (tree), (**b**) grass/herb and woody vegetation < 5 m (herbaceous), and (**c**) bare ground; for areas with tree cover, the datasets also give the proportion of (**d**) evergreen, (**e**) deciduous, (**f**) broadleaf and (**g**) needleleaf; (**i**) annual average fAPAR value for 1998–2005 from SeaWiFS (Gobron et al., 2006); (**j**) annual average burnt fraction for 1997–2006 from the GFED3 dataset (Giglio et al., 2010); (**k**) sites with measurements of net primary production, NPP and (**l**) measurements of gross primary production, GPP are both from the Luyssaert et al. (2007) dataset; (**m**) global atmospheric CO<sub>2</sub> concentrations for 1980–2005 based on inversion datasets (Bousquet et al., 2000; Rödenbeck et al., 2003; Baker et al., 2006; Chevalier et al., 2010); (**n**) annual average river runoff from 1950–2005 from the Dai et al. (2009) dataset, displayed over associated GRDC basins (<http://www.bafg.de/GRDC>); and (**m**) vegetation height based on a snapshot from 2005 (Simard et al., 2011). Hashed area in (**g**) shows areas without comparison data.

### 2.2.3 NPP

The NPP dataset (Table 1) was created by combining site data from the Luyssaert et al. (2007) and the Ecosystem Model/Data Intercomparison (EMDI: Olson et al., 2001) databases. We exclude sites from managed or disturbed environments; i.e. we do not use class B records from EMDI, and we exclude sites classified as “managed”, “recently burnt”, “recently cut clear”, “fertilized” or “irrigated” in Luyssaert et al. (2007). The Luyssaert et al. (2007) data used here are all from woody biomes, and all but two of the EMDI data used are from grasslands. The NPP estimates in Luyssaert et al. (2007) were obtained by summing direct measurements of the following: (a) year-round leaf litter collection, (b) stem and branch NPP (from measurements of basal area, scaled using allometric equations), (c) fine root NPP from soil coring, isotopic turnover estimates or upscaling of root length production as observed in mini-rhizotrons, or indirectly via soil respiration, and (d) understorey NPP through destructive harvests. The uncertainty in the NPP estimate is provided for each site, and ranges from 110–656 g C m<sup>-2</sup> depending on

the latitude, data collection and analysis methods. The NPP estimates in the EMDI database were collected from the published literature, and therefore derived using a similar variety of methodologies as used in the Luyssaert et al. (2007) compilation. The individual studies were divided into 2 classes based on an assessment of data quality. Here, we use only the top class (class A), which represents sites that are geolocated, have basic environmental metadata, and have NPP measurements on both above- and below-ground components. The EMDI database does not include estimates of the uncertainties associated with individual sites.

### 2.2.4 GPP

GPP data were obtained from the Luyssaert et al. (2007) database, and are estimated from flux tower (eddy covariance) measurements. The sites used here are, again, only representative of woody biomes. The uncertainty of the site-based estimates ranges from 75–677 g C m<sup>-2</sup>, again depending on latitude, data collection and analysis methods.

### 2.2.5 Canopy height

The forest canopy height dataset (Table 1; Simard et al., 2011) is derived from Ice, Cloud, and land Elevation Satellite/Geoscience Laser Altimeter System (ICESat/GLAS) estimates of canopy height and its relationship with forest type, MODIS percent tree cover product (MOD44B), elevation and climatology variables (annual mean and seasonality of precipitation and temperature). Only GLAS and MODIS data from 2005 were used. The canopy height product was validated with globally distributed field measurements. Canopy height ranges from 0 to 40 m, and uncertainty is of the order of 6 m (root mean squared error). There are no estimates of the uncertainty for individual grid cells.

### 2.2.6 Burnt fraction

Burnt fraction data (Table 1) were obtained for each month from 1997–2006 from the third version of the Global Fire Emissions Database (GFED3; Giglio et al., 2010). Burnt fraction was calculated from high-resolution, remotely sensed daily fire activity and vegetation production using statistical modelling. Quantitative uncertainties in the estimates of burnt fraction, provided for each grid cell, are a combination of errors in the higher resolution fire activity data and errors associated with the conversion of these maps to low-resolution burnt area.

### 2.2.7 River discharge

River discharge (Table 1) was obtained from monthly measurements at station gauges between 1950 and 2005 (Dai et al., 2009). Dai et al. (2009) use a model-based infilling procedure in their analyses, but the dataset used here is based only on the gauge measurements. The basin associated with gauges close to a river mouth was defined using information from the Global Runoff Data Centre (GRDC: <http://www.bafg.de/GRDC>). Average runoff for the basin was obtained by dividing discharge by total basin area. Although individual gauge measurements may have measurement errors of the order of 10–20 %, the use of spatially integrated discharge values means that the uncertainties are considerably less than this (Dai et al., 2009). Annual average and inter-annual variability comparisons for runoff were made only for years in which there were 12 months of data, to avoid seasonal biases.

### 2.2.8 CO<sub>2</sub> concentration

CO<sub>2</sub> concentration (Table 1) data were taken from 26 Carbon Dioxide Information Analysis Center (CDIAC: [cdiac.ornl.gov](http://cdiac.ornl.gov)) stations (Fig. 3) for seasonal cycle comparisons. For inter-annual comparisons, we used several inversion products (Bousquet et al., 2000; Rödenbeck et al., 2003; Baker et al., 2006; Keeling, 2008; Chevalier et al., 2010), processed as in Prentice et al. (2011). The inversions are designed to isolate

the component of variability in the CO<sub>2</sub> growth rate due to land–atmosphere exchanges. The differences between these inversions (maximum difference 3.8 ppm) give a measure of the associated uncertainty.

## 2.3 Metrics

Many measures with different properties are used in the geosciences literature to compare modelled and observed quantities. These typically fall into three categories: non-normalised metrics; metrics normalised by observational uncertainty; and metrics normalised by observational variance. Non-normalised metrics, which include RMSE (used e.g. by Blyth et al., 2009, 2011) and mean squared error (MSE), cannot be compared directly between different variables as they are in different units. Metrics normalised by observational uncertainty require uncertainty estimates to be given for each site/grid cell in a dataset. Most of the datasets used in this study do not have such estimates, ruling out the use of metrics normalised by observational uncertainty. We therefore use metrics normalised by observational variance, allowing metrics based on both mean deviations (modulus-based) and mean squared deviations as alternative “families”.

The mean, variance and standard deviation provide a basic measure of global agreement between model and observation. Our basic normalised metrics for taking the geographic patterning into account in data–model comparisons of annual averages or totals were the normalised mean error (NME) and the normalised mean squared error (NMSE) (for definitions, limits and applications, see Table 2):

$$\text{NME} = \sum_i |y_i - x_i| / \sum_i |x_i - \bar{x}|, \quad (1)$$

$$\text{NMSE} = \sum_i (y_i - x_i)^2 / \sum_i (x_i - \bar{x})^2, \quad (2)$$

where  $y_i$  is the modelled value of variable  $x$  in grid cell (or at site)  $i$ ,  $x_i$  the corresponding observed value, and  $\bar{x}$  the mean observed value across all grid cells or sites. NMSE is equal to the one-complement of the Nash–Sutcliffe model efficiency metric (Nash and Sutcliffe, 1970). NMSE thus conveys the same information as the Nash–Sutcliffe metric. As NME and NMSE are normalised by the spatial variability of the observations, these scores provide a description of the spatial error of the model. NME differs from NMSE only in the use of mean deviations, which are less sensitive to extreme values than standard deviations. We prefer NME, but retain NMSE because of its direct relation to a metric established in the literature. Both metrics take the value zero when agreement is perfect, unity when agreement is equal to that expected when the mean value of all observations is substituted for the model, and values  $> 1$  when the model's performance is worse than the null model.

**Table 2.** Summary description of the benchmark metrics.  $y_i$  is the modelled and  $x_i$  is the corresponding observed value in cell or site  $i$ , and  $\bar{x}$  is the mean observed value across all grid cells or sites.  $\omega_i$  is the modelled phase, and  $\phi_i$  is the observed phase.  $q_{ij}$  is the modelled and  $p_i$  observed proportion of item  $j$  in cell or site  $i$ .

Metric	Equation	Limits	Use in this study
Normalised mean error (NME)	$NME = \sum_i  y_i - x_i  / \sum_i  x_i - \bar{x} $	0 – Perfect agreement 1 – Model performs as well as observational mean	For burnt fraction and fAPAR: annual averages, phase concentration, inter-annual variability.
Normalised mean squared error (NMSE)	$NMSE = \sum_i (y_i - x_i)^2 / \sum_i (x_i - \bar{x})^2$	2 – complete disagreement for step 3 Infinity – complete disagreement for step 1 and 2	For runoff: annual averages, inter-annual variability For CO <sub>2</sub> : phase concentration For NPP, GPP and height: annual averages
Mean phase difference (MPD)	$MPD = (1/\pi) \arccos [\cos(\omega_i - \phi_i) / n]$	0 – in phase 1 – 6 months out (out of phase)	Assessing difference in seasonality for fAPAR, burnt fraction and CO <sub>2</sub>
Manhattan metric (MM)	$MM = \sum_{ij}  q_{ij} - p_{ij}  / n$	0 – Perfect agreement 2 – Perfect disagreement	Vegetation cover comparisons for life forms, tree, grassland, bare ground, evergreen vs. deciduous tree and broadleaf vs. needleleaf tree.
Squared chord distance (SCD)	$SCD = \sum_{ij} (\sqrt{q_{ij}} - \sqrt{p_{ij}})^2 / n$		

**Table 3.** Mean, absolute variance (as defined in Eq. 3) and standard deviation (SD) of the annual average values of observations. The variance for most variables is from the long-term mean of the gridded or site data, whereas CO<sub>2</sub> is the variance of the inter-annual differences.

Variable	Measure	Mean	Variance	SD
Fraction of photosynthetically active radiation (fAPAR)	Annual average fAPAR	0.18	0.18	0.20
Vegetation cover	Tree cover	0.22	0.22	0.26
	Herb cover	0.52	0.25	0.29
	Bare ground	0.20	0.24	0.30
	Evergreen	0.44	0.33	0.37
	Needleleaf	0.59	0.41	0.43
Net primary production (NPP)	Annual average NPP	688	242	325
Gross primary production (GPP)	Annual average GPP	1540	642	820
Canopy height	Annual average canopy height	18.3	11.8	13.7
Burnt fraction runoff	Annual average burnt fraction	0.028	0.043	0.094
	Annual average 1950–2005	307	12	15
	Annual average 1998–2005	331	8.4	10.6
Atmospheric CO <sub>2</sub> concentration	Bousquet	N/A	0.93	1.10
	Rödenbeck	N/A	0.89	1.13
	Baker	N/A	0.86	1.09
	Chevalier	N/A	0.86	1.06
	Average (all inversions)	N/A	0.919	1.11

3320

D. I. Kelley et al.: Benchmarking system for evaluating global vegetation models

### 2.3.1 Annual average

Annual average comparisons were made using the mean, mean deviation (Eq. 3) and standard deviation of simulated and observed values (Table 3). NME and NMSE comparisons were conducted in three stages: (1)  $x_i$  and  $y_i$  take modelled and observed values; (2)  $x_i$  and  $y_i$  become the difference between observed or modelled values and their respective means ( $x_i \rightarrow x_i - \bar{x}$ ); and (3)  $x_i$  and  $y_i$  from step 2 are divided by either the mean deviation or standard deviation ( $x_i \rightarrow x_i/d(x)$ ):

$$\text{for NME, } d_{\text{NME}}(x) = \sum_i |x_i - \bar{x}|/n; \quad (3)$$

$$\text{for NMSE, } d_{\text{NMSE}}(x) = \sqrt{\sum_i (x_i - \bar{x})^2/n}. \quad (4)$$

Stage 2 removes the influence of the mean, and stage 3 removes the influence of the variability, on the measure. The NMSE at stage 3 is related to the correlation coefficient (Barnston et al., 1992). Van Oijen et al. (2011) showed that MSE can be decomposed into three elements similar to stage 1, 2 and 3 here, but as MSE is not normalised the decomposition is not directly applicable for this study.

### 2.3.2 Inter-annual variability

Inter-annual variability comparisons were made by calculating global values for each year of the model output and observations, and comparing them using Eqs. (1) and (2), but with  $y_i$  now being the global sum of modelled values for year  $i$ , and  $x_i$  the corresponding observed value. Only stage 2 and 3 comparisons were made, as the stage 1 provides no extra information from the annual-average comparisons. Stage 3 comparison measures whether a model has the correct timing or phasing of inter-annual peaks and troughs. For inter-annual CO<sub>2</sub> concentration, the observational data were detrended to remove the effect of anthropogenic emissions.

### 2.3.3 Seasonality

The seasonal expression of change can be characterised in terms of the length and timing of the season, as well as the magnitude of differentiation between seasons. For example, in simulating the fire regime at a particular place, the length of the fire season and the time that fires occur are as important as correctly predicting the area burnt. Seasonality comparisons were conducted in two parts: seasonal concentration (which is inversely related to season length) and phase (expressing the timing of the season). Each simulated or observed month was represented by a vector in the complex plane, the length of the vector corresponding to the magnitude of the variable for each month and the directions of the vector corresponding to the time of year:

$$\theta_t = 2\pi(t-1)/12, \quad (5)$$

where  $\theta_t$  is the direction corresponding to month  $t$ , with month 1 (January) arbitrarily set to an angle of zero. A mean vector  $L$  was calculated by averaging the real and imaginary parts of the 12 vectors,  $x_t$ .

$$L_x = \sum_t x_t \cos(\theta_t) \text{ and } L_y = \sum_t x_t \sin(\theta_t) \quad (6)$$

The length of the mean vector divided by the annual value stands for seasonal concentration,  $C$ ; its direction stands for phase,  $P$ :

$$C = \frac{\sqrt{L_x^2 + L_y^2}}{\sum_t x_t}; \quad (7)$$

$$P = \arctan(L_x/L_y). \quad (8)$$

Thus, if the variable is concentrated all in one month, seasonal concentration is equal to 1 and the phase corresponds to that month. If the variable is evenly spread over all months, then concentration is equal to zero and phase is undefined. If either modelled or observed values have zero values for all months in a given cell or site, then that cell/site is not included in the comparisons. Concentration comparisons use Eqs. (1) and (2) and steps 1, 2 and 3. Modelled and observed phase are compared using mean phase difference (MPD):

$$\text{MPD} = (1/\pi) \arccos[\cos(\omega_i - \phi_i)/n], \quad (9)$$

where  $\omega_i$  is the modelled phase, and  $\phi_i$  is the observed phase. The measure can be interpreted as the average timing error, as a proportion of the maximum error (6 months). For seasonal CO<sub>2</sub> concentrations, where the data are monthly deviations from the mean CO<sub>2</sub>, we compared the seasonal amplitude instead of seasonal concentration by comparing the simulated and observational sum of the absolute CO<sub>2</sub> deviation for each month using Eqs. (1) and (2).

### 2.3.4 Relative abundance

Relative abundance was compared using the Manhattan metric (MM) and squared chord distance (SCD) (Gavin et al., 2003; Cha, 2007):

$$\text{MM} = \sum_{ij} |q_{ij} - p_{ij}|/n; \quad (10)$$

$$\text{SCD} = \sum_{ij} (\sqrt{q_{ij}} - \sqrt{p_{ij}})^2/n \quad (11)$$

where  $q_{ij}$  is the modelled abundance (proportion) of item  $j$  in grid cell  $i$ ,  $p_i$  the observed abundance of item  $j$  in grid cell  $i$ , and  $n$  the number of grid cells or sites. So in the case of comparing life forms, items  $j$  would be trees; herbaceous; and bare ground. The sum of items in each cell must be equal to one for these metrics to be meaningful. They both take the value of 0 for perfect agreement, and 2 for complete disagreement.

### 2.3.5 Null models

To facilitate interpretation of the scores, we compared each benchmark dataset to a dataset of the same size, filled with the mean of the observations (Table 4). We also compared each benchmark dataset with “randomized” datasets (Table 4). This was done using a bootstrapping procedure (Efron, 1979; Efron and Tibshirani, 1993), whereby we constructed a dataset of the same dimensions as the benchmark set, filled by randomly resampling the cells or sites in the original dataset with replacement. We created 1000 randomized datasets to estimate a probability density function of their scores (Fig. 2). Models are described as better/worse than randomized resampling if they were less/more than two standard deviations from the mean randomized score.

As NME and MM are the sum of the absolute spatial variation between the model and observations, the comparison of scores obtained by two different models shows the relative magnitude of their biases with respect to the observations, or how much “better” one model is than another. If a model has an NME score of 0.5, for example, its match to the observations is 50 % better than the mean of the data score of 1.0. Similarly, when this model is compared to a model with an NME score of 0.75, it can be described as 33 % better than the second model as its average spatial error is  $0.5/0.75 = 67\%$  the size. Conversely, the second model would need to reduce its errors/improve by 33 % in order to provide as good a match to observations as the first.

## 2.4 Models

### 2.4.1 SDBM

The SDBM simulates NPP and heterotrophic respiration ( $R_h$ ) as described in Knorr and Heimann (1995) while the embedded water-balance calculation models evapotranspiration and therefore implicitly runoff. NPP is obtained from a simple relationship:

$$NPP = \varepsilon \cdot Ipar \cdot \alpha, \quad (12)$$

where  $\varepsilon$  is light-use efficiency, set at  $1 \text{ g C MJ}^{-1}$ ;  $Ipar$  is incident PAR; and  $\alpha$  is the ratio of actual to equilibrium evapotranspiration, calculated as in Prentice et al. (1993) and Gallego-Sala et al. (2010).  $R_h$  was calculated as a function of temperature and water availability and for each cell is assumed to be equal to NPP each year (i.e. assuming the respiring pool of soil carbon is in equilibrium):

$$R_h = \beta \cdot Q_{10}^{T/10} \cdot \alpha, \quad (13)$$

where  $Q_{10}$  is the slope of the relationship between  $\ln(R_h)$  and temperature (expressed in units of proportional increase per  $10 \text{ K warming}$ ) and takes the value of 1.5; and  $T$  is temperature ( $^{\circ}\text{C}$ ).  $\beta$  is calculated by equating annual  $R_h$  and annual NPP:

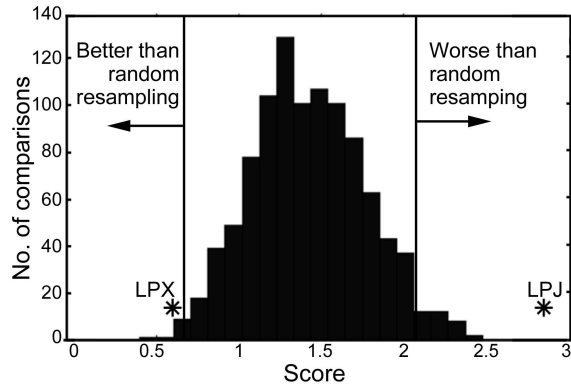


**Fig. 2.** Results of bootstrap resampling of inter-annual variability in global burnt fraction (1997–2005) from the GFED3 dataset. The asterisks labelled LPX and LPJ show the scores achieved by the LPX and LPJ models respectively. The limits for better than and worse than random resampling are set at two standard deviations away from the mean bootstrapping value (vertical lines).

$$\beta = \frac{\sum_t NPP_t}{\sum_t Q_{10}^{T_t/10} \cdot \alpha_t}. \quad (14)$$

GPP was assumed to be twice simulated NPP (Poorter et al., 1990). Runoff was assumed to be the difference between observed precipitation and evapotranspiration. Groundwater exchanges are disregarded. The free parameters  $\varepsilon$  and  $Q_{10}$  were assigned values of 1.0 and 1.5 respectively, following Knorr and Heimann (1995) who obtained these values by tuning to observed seasonal cycles of  $\text{CO}_2$ .

### 2.4.2 LPJ

LPJ (version 2.1: Gerten et al., 2004) simulates the dynamics of terrestrial vegetation via a representation of biogeochemical processes, with different properties prescribed for a small set of plant function types (PFTs). Each PFT is described by its life form (trees or herbaceous), leaf type (needleleaf or broadleaf) and phenology (evergreen or deciduous). A minimal set of bioclimatic limits constrain the global distribution of the PFTs. Nested time steps allow different processes to be simulated at different temporal resolution: photosynthesis, respiration and water balance are calculated on a daily time step while carbon allocation and PFT composition are updated on an annual time step. A weather generator converts monthly data of precipitation and fractional rain days to a daily time series of precipitation amounts. Fire is calculated annually and is based upon a simple empirical model which calculates the probability of fire based on daily moisture content of the uppermost soil layer as a proxy for fuel moisture (Thonicke et al., 2001). Assuming ignitions are always available, burnt fraction and its associated carbon fluxes

3322

D. I. Kelley et al.: Benchmarking system for evaluating global vegetation models

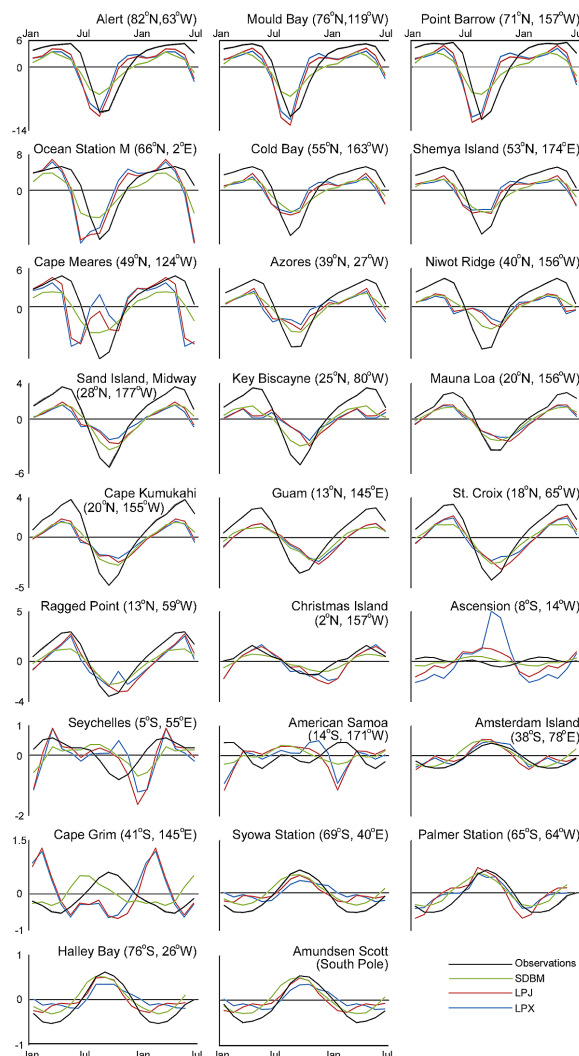


**Fig. 3.** Observed seasonal cycle of atmospheric CO<sub>2</sub> concentrations at 26 CO<sub>2</sub> stations over the period 1998–2005 (black line), taken from the CDIAC website ([cdiac.ornl.gov](http://cdiac.ornl.gov)) compared to the simulated seasonal cycle from the Simple Diagnostic Biosphere Model (SDBM) (green line); LPJ (red); and LPX (blue). The y-axis indicates variation in atmospheric CO<sub>2</sub> concentration about the mean. The x-axis is months from January through 18 months to June.

are calculated from the summed annual probability of fire, using a simple relationship.

#### 2.4.3 LPX

LPX (Prentice et al., 2011), which is a development of LPJ-SPITFIRE (Thonnicke et al., 2010), incorporates a process-based fire scheme, with ignition rates based on the seasonal distribution of lightning strikes and fuel moisture content and

fire spread, intensity and residence time based on climate data and modelling the drying of different fuel types between rain days. Fire intensity influences fire mortality and carbon fluxes. The fire model runs on a daily time step.

#### 2.5 Model protocol

All models were run on a 0.5° global grid using the CRU TS3.0 land mask as in Prentice et al. (2011). Soil texture was prescribed using the FAO soil data (FAO, 1991). The spin-up and historical drivers for the DGVM simulations were exactly as used for LPX by Prentice et al. (2011). For comparability, the same climate data were used to drive the SDBM. In addition SDBM was driven by fAPAR values from SeaWiFS observations. For cells lacking fAPAR values, values were constructed for the missing months by fitting the following equation to available data for each year:

$$\text{fAPAR}(m) = \frac{1}{2} \{ (U - L) \cos[2\pi(m - m_{\max})/12] + U + L, \} \quad (15)$$

where fAPAR( $m$ ) is the fAPAR for months  $m$  with data;  $U$  is the maximum fAPAR value in month  $m_{\max}$ ; and  $L$  is the minimum fAPAR value. As the maximum fAPAR value typically occurs in spring or summer (Prince, 1991) when SeaWiFS data are generally available, and the minimum occurs in the winter when data may be unavailable,  $U$  is set to the highest fAPAR value, whilst  $L$  is tuned to fit the function to the data.

The SDBM was only run for 1998–2005, a limitation imposed by the availability of fAPAR data, and comparisons were confined to this period. For LPX and LPJ, outputs and therefore comparisons were possible from 1950–2006. Comparisons with NPP, GPP, annual average basin runoff, global inter-annual variability in runoff, and the seasonal cycle of CO<sub>2</sub> concentration were made for all three models. LPX and LPJ are compared across a wider range of benchmarks.

Comparisons of the seasonal CO<sub>2</sub> cycle were based on simulated monthly net ecosystem production (NEP: NPP –  $R_h$  – fire carbon flux). NEP for the SDBM was taken as the difference between monthly NPP and  $R_h$ . For LPJ, which simulates fire on an annual basis, monthly fire carbon flux was set to 1/12 the annual value. With LPX, it was possible to use monthly fire carbon flux. For each model, detrended monthly values of NEP for each grid cell were input into the atmospheric transport matrices derived from the TM2 transport model (Kaminski et al., 1996), which allowed us to derive the CO<sub>2</sub> seasonal cycle (Heimann, 1995; Knorr and Heimann, 1995) at the locations of the observation sites.

Average basin runoff was calculated by summing the runoff from all model grid cells within a GRDC-defined basin and dividing by the basin area. If a grid cell fell into more than one GRDC basin, the runoff was divided between basins in proportion to the fraction of the cell within each basin. Inter-annual changes in runoff were calculated by summing runoff over all cells in basins for which there were data for a given year. Seasonal cycles of runoff are dependent

on the dynamics of water transport in the river, which was not modelled.

### 3 Results

#### 3.1 Benchmark results

##### 3.1.1 fAPAR

LPJ scores 0.82 and LPX scores 0.86 using NME for annual average fAPAR (Table 5). This difference in score is equivalent to a negligible (i.e. < 5 %) change in the match to the observations. Both values are considerably better than values for the mean of the data (1.00) and random resampling ( $1.19 \pm 0.004$ ), with the match to observations being 15 % closer and 30 % closer respectively. The models also perform well for seasonal timing (Fig. 4), with scores of 0.19 (LPJ) and 0.18 (LPX) or the equivalent of an average of 34 days different from observations. For comparison, the seasonal timing of the mean of the data and random resampling is ca. 3 months different from observations. The models also perform well for inter-annual variability: LPJ scores 0.60 and LPX scores 0.50 using NME for inter-annual variability, compared to a mean score of 1.00 and a score of  $1.21 \pm 0.34$  from random resampling. The DGVM scores represent, respectively, a 40 % and 50 % better match to observations than the mean of the data. LPJ scores 1.07 and LPX scores 1.14 using NME for seasonal concentration, compared to 1.00 for the mean and  $1.41 \pm 0.006$  for random resampling. This means that the seasonal concentration of fAPAR in the DGVMs is, respectively, 7 % and 14 % worse than the mean of the data compared to observations.

##### 3.1.2 Vegetation cover

LPJ scores 0.78 and LPX scores 0.76 using the MM for the prediction of life forms (Table 5), again a negligible difference in performance (< 3 %) compared to observations. Both values are better than obtained for the mean of the data (0.93) or by randomly resampling ( $0.88 \pm 0.002$ ). Both models were also better than mean and randomly resampling for bare ground. However, both models overestimate tree cover and underestimate herb cover by around a factor of 2 (Table 5). The scores for tree cover (LPJ: 0.62, LPX: 0.56) show, respectively, a 38 % and 24 % poorer match to observations than the mean of the data (0.45), and a 15 % and 4 % poorer match to observations than randomly resampling ( $0.54 \pm 0.002$ ). In the same way, the two DGVMs show a 40 % poorer match to observed grass cover than the mean of the data and a 6 % poorer match than randomly resampling. Both models are worse than mean and random resampling for phenology (Table 5).

##### 3.1.3 NPP/GPP

The models have NME scores for NPP of 0.58 (SDBM), 0.83 (LPJ) and 0.81 (LPX) (Table 5) – better than values obtained for the mean of the data (1.00) and random resampling ( $1.35 \pm 0.09$ ). Removing the biases in mean and variance (Table 5) improves the performance of all three models. The SDBM simulates 1.13 times higher NPP than observed, but correctly predicts the spatial variability shown by the observations, whereas the two DGVMs overestimate NPP but underestimate the spatial variance in NPP. As a result, removing the biases in the mean produces a much larger improvement in the DGVMs. In LPJ, for example, the score goes from 0.83 to 0.69, equivalent to a 29 % better match to the observations. The improvement in the SDBM is equivalent to only a 9 % better match to observations. The two DGVMs perform worse for GPP than NPP. LPX has an NME score of 0.81 for NPP but 0.98 for GPP – this is equivalent to a 17 % better match to NPP observations than to GPP observations. The SDBM performs better for GPP than the DGVMs, obtaining an NME score of 0.71, which is better than the mean of the data (1.00) and randomly resampling ( $1.36 \pm 0.22$ ).

##### 3.1.4 Canopy height

LPJ scores 1.00 and LPX scores 1.04 using NME for the prediction of height (Table 5). These values lie between the mean (1.00) and random resampling ( $1.33 \pm 0.004$ ) scores. This poor performance is due to modelled mean heights ca. 60–65 % lower than observed and muted variance (Table 5, Fig. 6). Removing the mean bias improves the score for both DGVMs to 0.71 for LPJ and 0.73 for LPX, equivalent to a 29 % and 30 % improvement in the match to observations. Model performance is further improved by removing bias in the variance, to 0.64 for LPJ (ca. 11 %) and 0.68 for LPX (ca. 6 %).

##### 3.1.5 Burnt fraction

There is a major difference between the two DGVMs for annual fractional burnt area (Fig. 7): LPJ scores 1.58, while LPX scores 0.85 for NME (Table 5). Thus, LPX produces a 46 % better match to the observations than LPJ. The LPJ score is worse than the mean (1.00) and random resampling ( $1.02 \pm 0.008$ ). The same is true for NME comparisons of inter-annual variability, with LPJ scoring 2.86, worse than the mean (1.00) and random resampling ( $1.35 \pm 0.34$ ), whereas the LPX score of 0.63 is better than both. LPX could also be benchmarked against the seasonality of burnt fraction. It scores 0.10 for MPD comparison of phase, much better than the mean (0.74) and random resampling ( $0.47 \pm 0.001$ ). However, it did not perform well for seasonal concentration, scoring 1.38 compared to the mean (1.00) and random resampling ( $1.33 \pm 0.006$ ).

**Table 4.** Scores obtained using the mean of the data (Data mean), and the mean and standard deviation of the scores obtained from bootstrapping experiments (Bootstrap mean, Bootstrap SD). NME/NMSE denotes the normalised mean error/normalised mean squared error, MPD the mean phase difference and MM/SCD the Manhattan metric/squared chord distance metrics.

Variable	Metric used	Measure	Absolute			Square	
			Data mean	Bootstrap mean	Bootstrap SD	Data mean	Bootstrap mean
fAPAR	NME/ NMSE	Annual average	1.00	1.19	0.004	1.00	1.95
		– with mean removed	1.00	1.21	0.003	1.00	1.93
		– with mean and variance removed	1.00	1.23	0.004	1.00	2.08
		Inter-annual variability	1.00	1.21	0.34	1.00	1.92
		– with variance removed	1.00	1.30	0.36	1.00	2.15
	MPD MM	Seasonal concentration	1.00	1.41	0.006	1.00	2.02
		– with mean removed	1.00	1.41	0.006	1.00	2.02
		– with mean and variance removed	1.00	1.40	0.005	1.00	2.00
		Phase	0.54	0.49	0.001	N/A	N/A
		Life forms	0.93	0.88	0.002	0.37	0.47
Vegetation cover	MPD MM	Tree vs. non-tree	0.45	0.54	0.002	0.14	0.27
		Herb vs. non-herb	0.50	0.66	0.002	0.17	0.33
		Bare ground vs. covered ground	0.48	0.56	0.002	0.18	0.35
		Evergreen vs. deciduous	0.68	0.87	0.003	0.30	0.580
		Broadleaf vs. needleleaf	0.77	0.94	0.004	0.36	0.75
	NME/ NMSE	Annual average	1.00	1.35	0.09	1.00	2.00
		– with mean removed	1.00	1.35	0.09	1.00	2.00
		– with mean and variance removed	1.00	1.35	0.08	1.00	2.01
		Inter-annual variability	1.00	1.36	0.22	1.00	2.01
		– with variance removed	1.00	1.36	0.22	1.00	2.00
Net primary production	NME/ NMSE	Annual average	1.00	1.36	0.22	1.00	2.01
		– with mean removed	1.00	1.36	0.22	1.00	2.00
		– with mean and variance removed	1.00	1.36	0.17	1.00	2.00
		Seasonal concentration	1.00	1.33	0.004	1.00	1.98
		– with mean removed	1.00	1.33	0.004	1.00	1.98
	NME/ NMSE	Canopy height	1.00	1.33	0.004	1.00	1.98
		– with mean removed	1.00	1.33	0.004	1.00	1.98
		– with mean and variance removed	1.00	1.33	0.004	1.00	2.00
		Inter-annual variability	1.00	1.33	0.004	1.00	1.98
		– with variance removed	1.00	1.33	0.004	1.00	1.98
Burnt fraction	NME/ NMSE	Annual average	1.00	1.02	0.008	1.00	1.98
		– with mean removed	1.00	1.09	0.005	1.00	1.99
		– with mean and variance removed	1.00	1.14	0.004	1.00	2.36
		Inter-annual variability	1.00	1.35	0.34	1.00	1.93
		– with variance removed	1.00	1.39	0.32	1.00	2.15
	MPD NME/ NMSE	Seasonal concentration	1.00	1.33	0.006	1.00	1.99
		– with mean removed	1.00	1.33	0.006	1.00	1.99
		– with mean and variance removed	1.00	1.33	0.005	1.00	2.00
		Inter-annual variability	1.00	1.40	0.14	1.00	2.00
		– with variance removed	1.00	1.45	0.172	1.00	2.01
Runoff	NME/ NMSE	Inter-annual variability 1950–2005	1.00	1.35	0.52	1.00	1.89
		– with mean removed	1.00	1.76	0.71	1.00	2.02
		– with mean and variance removed	1.00	1.17	0.28	1.00	1.97
		Annual average 1998–2005	1.00	1.27	0.33	1.00	1.96
		– with mean removed	1.00	1.18	0.05	1.00	2.00
	MPD NME/ NMSE	– with mean and variance removed	1.00	1.33	0.34	1.00	1.87
		Inter-annual variability 1950–2005	1.00	1.40	0.14	1.00	2.00
		– with variance removed	1.00	1.33	0.34	1.00	1.83
		Inter-annual variability 1998–2005	1.00	1.34	0.34	1.00	0.82
		– with variance removed	1.00	1.34	0.34	1.00	0.82

**Table 4.** Continued.

Variable	Metric used	Measure	Absolute			Square	
			Data mean	Bootstrap mean	Bootstrap SD	Data mean	Bootstrap mean
Atmospheric CO <sub>2</sub> concentration	NME/ NMSE	Inter-annual variability – Bousquet (Jan 1980–June 1998)	1.00	1.36	0.058	1.00	2.00
		– with variance removed	1.00	1.36	0.058	1.00	2.00
		Inter-annual variability – Rödenbeck (Jan 1982–Dec 2001)	1.00	1.38	0.081	1.00	1.99
		– with variance removed	1.00	1.38	0.082	1.00	1.99
		Inter-annual variability – Baker (Jan 1988–Dec 2004)	1.00	1.39	0.07	1.00	1.99
		– with variance removed	1.00	1.40	0.07	1.00	1.99
		Inter-annual variability – Chevalier (Jul 1988–Jun 2005)	1.00	1.38	0.07	1.00	2.00
		– with variance removed	1.00	1.39	0.07	1.00	2.00
		Inter-annual variability – Average (Jan 1980–Jun 2005)	1.00	1.37	0.05	1.00	2.00
		– with variance removed	1.00	1.37	0.05	1.00	2.00
Amplitude	NME	Amplitude	1.00	1.38	0.28	1.00	2.04
		– with mean removed	1.00	1.40	0.39	1.00	2.00
		– with mean and variance removed	1.00	1.39	0.14	1.00	2.02
	Phase	Phase	0.33	0.42	0.051	N/A	N/A

### 3.1.6 River discharge

Comparing average runoff for 1950–2005, both DGVMs score 0.28 for NME, better than the mean (1.00) and random resampling ( $1.18 \pm 0.48$ ). The models perform much less well for inter-annual comparisons, with NME scores of 1.33 (LPJ) and 1.32 (LPX), worse than 1.00 for the mean and  $1.45 \pm 0.17$  for random resampling. Agreement is slightly improved by removing variance bias (LPJ: 1.07, LPX: 1.11). Neither of the DGVMs examined here treat water-routing explicitly. Introducing a one-year lag for inter-annual comparisons (Fig. 8) produces a 21 % (LPJ) and 19 % (LPX) improvement in the match to observations, confirming that taking account of delays in water transport is important when assessing the inter-annual variation in runoff. All three models were compared for 1998–2005. For annual average comparisons, they all performed better than the mean and random resampling (Table 5). However, all models performed poorly for inter-annual variability, obtaining similar scores (1.64 to 2.38) compared to the mean (1.00) and random resampling ( $1.34 \pm 0.34$ ). Removing variability bias and introducing a one-year lag improved performance, with the SDBM scoring 1.37, LPJ 1.36 and LPX 1.35.

### 3.1.7 CO<sub>2</sub> concentration

The generalised form of the seasonal cycle in CO<sub>2</sub> concentrations at different sites can be compared for all three models. The SDBM scores 0.21 whereas LPJ scores 0.34 and LPX 0.34 in the MPD comparisons of seasonal timing, compared to the mean of the data (0.33) and random resampling ( $0.42 \pm 0.05$ ). Thus, the SDBM produces an estimate of peak timing that is 22 days closer to observations than the mean of the data, while the DGVMs produce estimates that are 6 days further away from the observations than the mean of the data (Fig. 3). The scores for NME comparison of seasonal concentration for the SDBM (0.68), LPJ (0.46) and LPX (0.58) are all better than the mean (1.00) and random resampling ( $1.38 \pm 0.28$ ). Thus, although the difference between the models is non-trivial (ca. 30 %), all three models are ca. 30–50 % closer to observations than the mean of the data. Only the DGVMs can be evaluated with respect to inter-annual variability in global CO<sub>2</sub> concentrations. Both models capture the inter-annual variability relatively well (Table 5). LPJ scores 0.89 and LPX scores 0.83 for the average of all inversion datasets, compared to the mean of the data (1.00) and random resampling ( $1.37 \pm 0.05$ ).

3326

D. I. Kelley et al.: Benchmarking system for evaluating global vegetation models

**Table 5.** Comparison metric scores for model simulations against observations. Mean and variance rows show mean and variance of simulation for annual average values, followed in brackets by the ratio of the mean/variance with observed mean or variance in Table 3. Numbers in bold indicate the model with the best performance for that variable. Italic indicates model scores better than the mean of the data score listed in Table 4. Asterisks indicate model scores that are significantly better than randomly resampling listed in Table 4. NME/NMSE denotes the normalised mean error/normalised mean squared error, MPD the mean phase difference and MM/SCD the Manhattan metric/squared chord distance metrics. fAPAR is the fraction of absorbed photosynthetically active radiation, NPP net primary productivity, and GPP gross primary productivity.

Variable	Metric used	Measure	SDBM		LPJ		LPX	
			Absolute	Squared	Absolute	Squared	Absolute	Squared
fAPAR	Mean (ratio)	Annual average	N/A	N/A	0.30 (1.63)	N/A	0.26	N/A
	Variance (ratio)		N/A	N/A	0.15 (0.85)	0.17 (0.86)	0.16 (0.91)	0.18 (0.90)
	NME/ NMSE	Annual average	N/A	N/A	<b>0.82*</b> <i>0.75*</i>	<b>1.04*</b> <i>0.76*</i>	0.86* 0.76*	1.09* 0.78*
		– with mean removed			<b>0.80*</b>	<b>0.83*</b>	0.82*	0.90*
		– with mean and variance removed						
		Inter-annual variability	N/A	N/A	<b>0.60*</b>	<b>0.36*</b>	<b>0.50*</b>	<b>0.27*</b>
		– with variance removed			0.73*	0.36*	<b>0.44*</b>	<b>0.23*</b>
	MPD	Seasonal concentration	N/A	N/A	<b>1.07*</b>	<b>1.28*</b>	1.14*	1.37*
		– with mean removed			<b>1.02*</b>	<b>1.20*</b>	1.05*	1.25*
		– with mean and variance removed			<b>1.03*</b>	<b>1.26*</b>	1.06*	1.31*
		Phase	N/A	N/A	0.19*	N/A	<b>0.18*</b>	N/A
		Tree vs. non-tree	N/A	N/A	0.49 (2.23)	N/A	0.42 (1.91)	N/A
Vegetation cover	Mean (ratio)	Herb vs. non-herb	N/A	N/A	0.28 (0.54)	N/A	0.31 (0.60)	N/A
		Bare ground vs. covered ground	N/A	N/A	0.23 (1.14)	N/A	0.27 (1.33)	N/A
		Evergreen vs. deciduous	N/A	N/A	0.34 (0.79)	N/A	0.28 (0.73)	N/A
		Broadleaf vs. needleleaf	N/A	N/A	0.67 (1.08)	N/A	0.65 (1.10)	N/A
		Tree vs. non-tree	N/A	N/A	0.45 (2.03)	0.45 (1.73)	0.46 (2.06)	0.46 (1.75)
	Variance (ratio)	Herb vs. non-herb	N/A	N/A	0.30 (1.18)	0.35 (1.21)	0.32 (1.27)	0.36 (1.24)
		Bare ground vs. covered ground	N/A	N/A	0.30 (1.26)	0.36 (1.20)	0.32 (1.33)	0.37 (1.23)
		Evergreen vs. deciduous	N/A	N/A	0.35 (1.06)	0.39 (1.07)	0.36 (1.18)	0.41 (1.18)
		Broadleaf vs. needleleaf	N/A	N/A	0.40 (1.02)	0.43 (1.02)	0.43 (1.07)	0.46 (1.07)
		Life forms	N/A	N/A	0.78*	0.44*	<b>0.76*</b>	<b>0.42*</b>
NPP	MM	Tree vs. non-tree	N/A	N/A	0.62	0.39	<b>0.56</b>	<b>0.33</b>
		Herb vs. non-herb	N/A	N/A	0.71	0.39	<b>0.67</b>	<b>0.36</b>
		Bare ground vs. covered ground	N/A	N/A	<b>0.23*</b>	<b>0.10*</b>	0.30*	0.156*
		Evergreen vs. deciduous	N/A	N/A	<b>0.93</b>	<b>0.47*</b>	0.94	0.48*
		Broadleaf vs. needleleaf	N/A	N/A	<b>0.89*</b>	<b>0.47*</b>	0.92*	0.55*
	NPP	Mean (ratio)	Annual average	612 (1.13)	N/A	688 (1.28)	N/A	685 (1.27)
		Variance (ratio)		297 (1.00)	351 (0.96)	242 (0.81)	325 (0.887)	283 (0.95)
		NME/ NMSE	Annual average	<b>0.58*</b>	<b>0.35*</b>	<b>0.83*</b>	<b>0.68*</b>	<b>0.81*</b>
			– with mean removed	<b>0.53*</b>	<b>0.32*</b>	<b>0.69*</b>	<b>0.52*</b>	<b>0.68*</b>
		– with mean and variance removed		<b>0.53*</b>	<b>0.33*</b>	0.75*	0.57*	0.69*
								0.53*

**Table 5.** Continued.

Variable	Metric used	Measure	SDBM		LPJ		LPX	
			Absolute	Squared	Absolute	Squared	Absolute	Squared
GPP	Mean (ratio)	Annual average	1231 (0.80)	N/A	1354 (0.88)	N/A	1127 (0.73)	N/A
		Variance (ratio)	316 (0.49)	492 (0.60)	288 (0.45)	388 (0.47)	240 (0.37)	304 (0.37)
	NME/ NMSE	Annual average	<b>0.71*</b>	<b>0.57*</b>	<b>0.80*</b>	<b>0.63*</b>	<b>0.98*</b>	<b>1.19*</b>
		– with mean removed	<b>0.63*</b>	<b>0.40*</b>	<b>0.82*</b>	<b>0.58*</b>	<b>1.02*</b>	<b>0.93*</b>
		– with mean and variance removed	<b>0.59*</b>	<b>0.37*</b>	<b>0.90*</b>	<b>0.63*</b>	<b>1.33*</b>	<b>1.45*</b>
	Canopy height	Annual average	N/A	N/A	6.92 (0.38)	N/A	6.36 (0.35)	N/A
		Variance (ratio)	N/A	N/A	6.17 (0.52)	6.70 (0.49)	6.69 (0.57)	7.18 (0.52)
	NME/ NMSE	Annual average	N/A	N/A	<b>1.00*</b>	<b>1.22*</b>	<b>1.04*</b>	<b>1.29*</b>
		– with mean removed			<b>0.71*</b>	<b>0.53*</b>	<b>0.73*</b>	<b>0.55*</b>
		– with mean and variance removed			<b>0.64*</b>	<b>0.50*</b>	<b>0.68*</b>	<b>0.58*</b>
Burnt fraction	Mean (ratio)	Annual average	N/A	N/A	0.014 (0.50)	N/A	0.022 (0.81)	N/A
		Variance (ratio)	N/A	N/A	0.016 (0.37)	0.027 (0.29)	0.032 (0.75)	0.46 (0.49)
	NME/ NMSE	Annual average	N/A	N/A	1.58	1.18	<b>0.85*</b>	<b>1.01*</b>
		– with mean removed			1.55	1.17	<b>0.91*</b>	<b>1.01*</b>
		– with mean and variance removed			1.72	1.29	<b>0.99*</b>	<b>1.60*</b>
	Inter-annual variability	Annual average	N/A	N/A	2.86	8.10	<b>0.63*</b>	<b>0.49</b>
		– with variance removed			1.90	3.08	<b>0.77</b>	<b>0.56</b>
		Seasonal concentration	N/A	N/A	N/A	N/A	<b>1.38</b>	<b>2.00</b>
	MPD	– with mean removed					<b>1.37</b>	<b>1.99</b>
		– with mean and variance removed					<b>1.26*</b>	<b>1.77*</b>
Runoff	Mean (ratio)	Phase	N/A	N/A	N/A	N/A	<b>0.10*</b>	N/A
		Annual average 1950–2005	N/A	N/A	388 (1.26)	N/A	396 (1.29)	N/A
	Variance (ratio)	Annual average 1998–2005	466 (1.41)	N/A	426 (1.29)	N/A	429 (1.30)	N/A
		Annual average 1950–2005	N/A	N/A	17.8 (1.44)	22.7 (1.50)	16.6 (1.35)	21.0 (1.38)
	NME/ NMSE	Annual average 1998–2005	11.9 (1.42)	15.6 (1.48)	15.9 (1.90)	18.9 (1.79)	14.3 (1.70)	17.1 (1.62)
		– with mean removed			<b>0.28*</b>	<b>0.067*</b>	<b>0.28*</b>	<b>0.054*</b>
		– with mean and variance removed			<b>0.34*</b>	<b>0.065*</b>	<b>0.35*</b>	<b>0.052*</b>
	Annual average 1998–2005	– with mean removed			<b>0.20*</b>	<b>0.021*</b>	<b>0.24*</b>	<b>0.031*</b>
		– with mean removed	0.42*	0.28*	<b>0.23*</b>	<b>0.039*</b>	<b>0.23*</b>	<b>0.026*</b>
		– with mean and variance removed	0.55*	0.26*	<b>0.26*</b>	<b>0.039*</b>	<b>0.26*</b>	<b>0.025*</b>
	Inter-annual variability	– with mean removed	0.22*	0.033*	<b>0.18*</b>	<b>0.013*</b>	<b>0.20*</b>	<b>0.018*</b>
		1950–2005	N/A	N/A	1.33*	1.91*	<b>1.32*</b>	<b>1.88*</b>
		– with variance removed			<b>1.07*</b>	<b>1.11*</b>	1.11*	1.25*
	Inter-annual variability 1950–2005 with 1yr lag				<b>1.03*</b>	<b>1.21*</b>	1.06*	1.19*
	– with variance removed				<b>0.84*</b>	<b>0.70*</b>	0.90*	0.79*

3328

D. I. Kelley et al.: Benchmarking system for evaluating global vegetation models

**Table 5.** Continued.

Variable	Metric used	Measure	SDBM		LPJ		LPX	
			Absolute	Squared	Absolute	Squared	Absolute	Squared
CO <sub>2</sub>	Variance (ratio)	Inter-annual variability 1998–2005 – with variance removed	<b>1.64</b>	<b>2.91</b>	2.38	4.59	2.27	4.09
		Inter-annual variability 1950–2005 with 1yr lag – with variance removed	<b>1.49</b>	<b>2.00</b>	2.10	4.23	1.94	3.64
		Inter-annual variability – Bousquet (Jan 1980–June 1998)	N/A	N/A	1.12 (1.21)	1.35 (1.22)	1.09 (1.18)	1.37 (1.24)
		Inter-annual variability – Rödenbeck (Jan 1982–Dec 2001)	N/A	N/A	1.15 (1.30)	1.32 (1.16)	1.02 (1.15)	1.24 (1.09)
		Inter-annual variability – Baker (Jan 1988–Dec 2004)	N/A	N/A	1.11 (1.28)	1.30 (1.19)	0.94 (1.09)	1.16 (1.07)
		Inter-annual variability – Chevalier (Jul 1988–Jun 2005)	N/A	N/A	1.08 (1.26)	1.28 (1.20)	0.96 (1.11)	1.19 (1.12)
		Inter-annual variability – Bousquet (Jan 1980–June 1998) – with variance removed	N/A	N/A	0.98* <b>0.86*</b>	<b>1.1*</b> 0.82*	<b>0.95*</b> 0.87*	1.1* <b>0.81*</b>
		Inter-annual variability – Rödenbeck (Jan 1982–Dec 2001) – with variance removed	N/A	N/A	0.82* 0.67*	0.59* 0.48*	<b>0.70*</b> <b>0.64*</b>	<b>0.41*</b> <b>0.37*</b>
		Inter-annual variability – Baker (Jan 1988–Dec 2004) – with variance removed	N/A	N/A	0.85* <b>0.66*</b>	0.78* 0.62*	<b>0.78*</b> 0.72*	<b>0.64*</b> <b>0.60*</b>
		Inter-annual variability – Chevalier (Jul 1988–Jun 2005) – with variance removed	N/A	N/A	0.93* 0.79*	0.72* 0.56*	<b>0.73*</b> <b>0.68*</b>	<b>0.51*</b> <b>0.44*</b>
NME/ NMSE		Inter-annual variability – Average (Jan 1980–Jun 2005) – with variance removed	N/A	N/A	0.89* <b>0.73*</b>	0.82* <b>0.62*</b>	<b>0.83*</b> 0.74*	<b>0.82*</b> 0.64*
		Amplitude – with mean removed – with mean and variance removed	0.68* 0.50* <b>0.10*</b>	0.60* 0.26* <b>0.02*</b>	<b>0.46*</b> <b>0.40*</b> 0.50*	<b>0.27*</b> <b>0.17*</b> 0.23*	0.58* 0.48* 0.59*	0.40* 0.25* 0.34*
		Phase	<b>0.21*</b>	N/A	0.34	N/A	0.34	N/A

### 3.2 Sensitivity tests

#### 3.2.1 Incorporating data uncertainties

In calculating the performance metrics, we have disregarded observational uncertainty. Few land-based datasets provide quantitative information on the uncertainties associated with

site or gridded values. However, the GFED burnt fraction (Giglio et al., 2010) and the Luyssaert et al. (2007) NPP datasets do provide quantitative estimates of uncertainty. We use these datasets to evaluate the impact of taking account observational uncertainty in the evaluation of model performance by calculating NME scores for annual averages of each variable using the maximum and minimum uncertainty

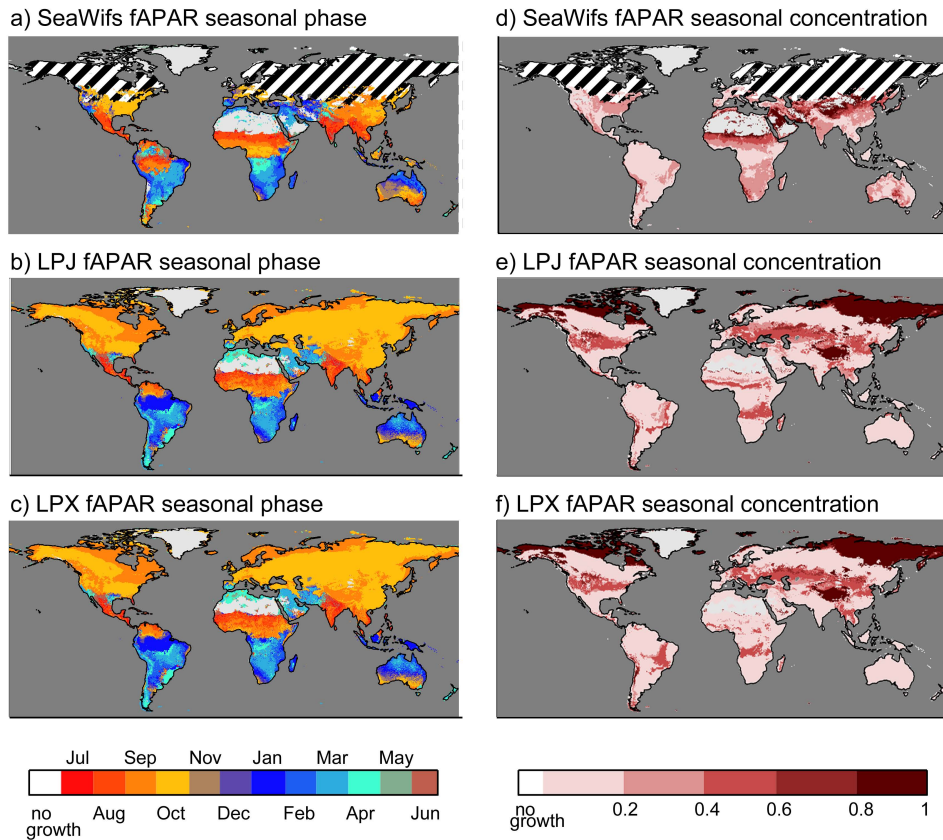


**Fig. 4.** Comparison of observed and simulated seasonal phase and seasonal concentration of fraction of absorbed photosynthetically active radiation (fAPAR) averaged over the period 1998–2005 from (a) seasonal phase from SeaWiFS (Gobron et al., 2006) and as simulated by (b) LPJ and (c) LPX; seasonal concentration from (d) SeaWiFS, (e) LPJ and (f) LPX. Hashed area in (a) and (d) shows areas where comparison is possible.

values at each site or grid cell to calculate the maximum and minimum potential distance between models and observations.

In the standard NME comparison for annual fractional burnt area, LPJ scores 1.58 while LPX scores 0.85. Taking into account the uncertainties produces minimum and maximum scores of 1.27 and 1.85 for LPJ, and 0.35 and 1.17 for LPX. Since these ranges are non-overlapping, the improvement in the match to observations shown by LPX compared to LPJ is demonstrably larger than observational uncertainty. This is not the case for the Luyssaert et al. (2007) only site-based annual average NPP comparisons, where the ranges are 0.26–1.36 (SDBM), 0.37–1.43 (LPJ) and 0.39–1.50 (LPX). Similarly, the apparent biases in mean annual NPP shown by all three models are within the observational uncertainty. Removing the slight high bias in mean annual NPP produced an improvement in the performance of the SDBM, with a change in the Luyssaert et al. (2007) only score from 0.72 to 0.59, equivalent to a 18 % better match to the observations.

However, the range of scores obtained for the SDBM taking into account the observational uncertainties after removing the high bias is 0.21–1.25. As this overlaps with the scores obtained prior to removing these biases (0.26–1.36), the improvement gained from removing the influence of the mean in NPP in the SDBM is less than the observational uncertainty.

Another approach to estimating the influence of uncertainty is to use alternative realizations of the observations. This approach has been used by the climate-modelling community to evaluate performance against modern climate observations (e.g. Gleckler et al., 2008) and is used here for CO<sub>2</sub> inter-annual comparisons. The scores obtained in comparisons with individual inversion products range from 0.82 to 0.98 for LPJ, and from 0.70 to 0.95 for LPX. Thus, the conclusion that the two DGVMs capture the inter-annual variability equally well, based on the average scores of all inversion datasets, is supported when taking into account uncertainty expressed in the differences between the inversions.

3330

D. I. Kelley et al.: Benchmarking system for evaluating global vegetation models

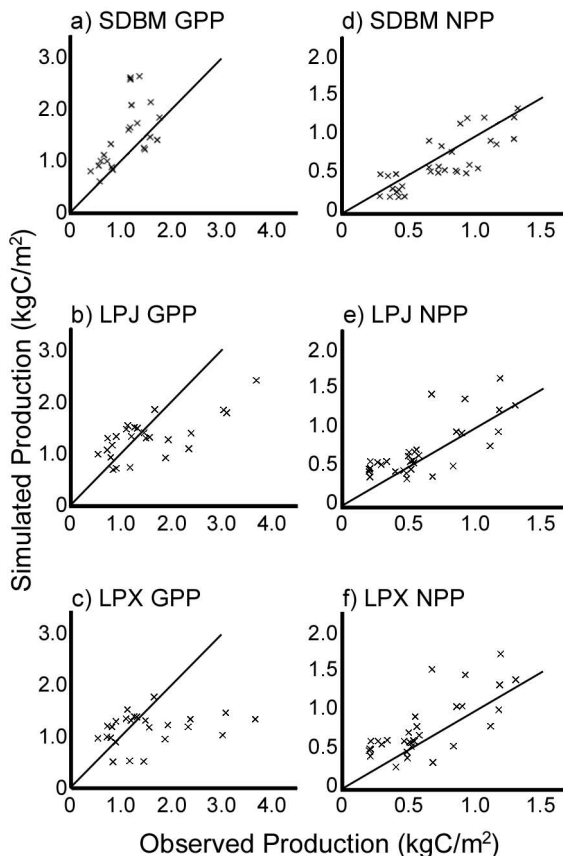


**Fig. 5.** Comparisons of observed and simulated NPP and GPP in  $\text{kg C m}^{-2}$ . The NPP observations (x-axis) are from the dataset made by combining sites from the Luyssaert et al. (2007) dataset and the Ecosystem/Model Data Intercomparison dataset (Olson et al., 2001). The GPP observations are derived from the Luyssaert et al. (2007) dataset. The simulated values (y-axis) are annual averages for the period 1998–2005. The observations are compared with NPP (a) and GPP (b) from the Simple Diagnostic Biosphere Model (SDBM), NPP (c) and GPP (d) from LPJ and NPP (e) and GPP (f) from LPX. The solid line shows the 1 : 1 relationship.

### 3.2.2 The influence of choice of dataset

The use of alternative datasets for a given variable implies that there are no grounds for distinguishing which is more reliable. It also highlights the fact that there is an element of subjectivity in the choice of datasets and that this introduces another source of uncertainty into the process of benchmarking. We have explicitly excluded from the benchmarking procedure any datasets that involve manipulations of original measurements based on statistical or physical models that are driven by the same inputs as the vegetation models being tested (e.g. MODIS NPP, remotely sensed evapotranspiration, upscaled GPP). However, such products often provide

**Table 6.** Mean annual gross primary production (GPP) normalised mean error (NME) comparison metrics using Luyssaert et al. (2007) and Beer et al. (2010) as alternative benchmarks. In the case of Beer et al. (2010), the comparisons are made for all grid cells (global) and also from the grid cells which contain sites in the Luyssaert et al. (2007) dataset (at sites).

Variable	Measure	SDBM	LPJ	LPX
GPP from Luyssaert et al. (2007)	global	N/A	N/A	N/A
GPP from Beer et al. (2010)	at sites	0.71	0.80	0.98
GPP from Beer et al. (2010)	global	0.56	0.60	0.51
GPP from Beer et al. (2010)	at sites	0.34	0.84	0.74

global coverage of variables that may not be as well represented in other datasets and thus could provide a useful alternative realization of the observations.

Here, we test the use of the Beer et al. (2010) dataset as an alternative to the Luyssaert et al. (2007) GPP dataset. The Beer et al. (2010) GPP dataset is based on a much larger number of flux-tower measurements than are included in the Luyssaert et al. (2007) dataset, but uses both diagnostic models and statistical relationships with climate to scale up these measurements to provide global coverage. We compare the annual average GPP scores using Beer et al. (2010), calculated using all grid cells and considering only those grid cells which correspond to locations with site data in the Luyssaert et al. (2007) dataset. These comparisons (Table 6) show that LPX and SDBM perform better against the Beer et al. (2010) dataset than against the Luyssaert et al. (2007) at the site locations, while the results obtained for LPJ against the two datasets are roughly similar. There is a further improvement in performance when the models are compared against all the grid cells. The improvement in performance at the site locations presumably reflects the fact that the Beer et al. (2010) dataset smooths out idiosyncratic site characteristics; the additional improvement in performance in the global comparison reflects both the smoothing and the much larger number of flux sites included in the Beer et al. (2010) dataset. Nevertheless, the conclusion that the SDBM performs better than the DGVMs is not influenced by the choice of dataset. LPJ performs marginally better than LPX when the Luyssaert et al. (2007) dataset is used as the benchmark (0.8 versus 0.98), but worse than LPX when the Beer et al. (2010) dataset is used as a benchmark (0.6 versus 0.51). This indicates that the difference between the two DGVMs is less than the observational uncertainty.

The release of new, updated datasets poses problems for the implementation of a benchmarking system, but could be regarded as a special case of the use of alternative realizations of the observations. The GFED3 burnt fraction dataset, used here, is a comparatively recent update of an earlier burnt fraction dataset (GFED2: van der Werf et al., 2006). When LPJ and LPX are evaluated against GFED2, the NME score for

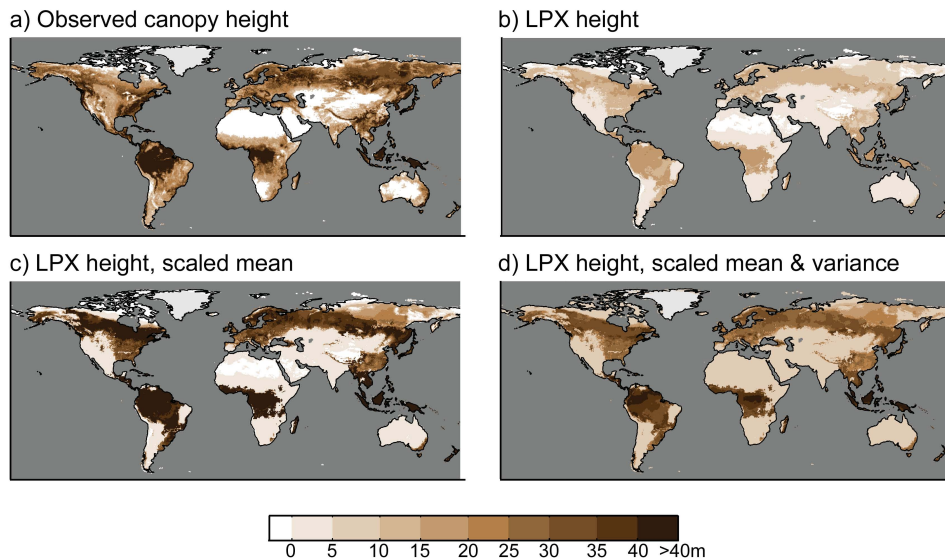


**Fig. 6.** Comparisons of observed and simulated height. **(a)** Observed canopy height (in 2005) from the Simard et al. (2011) dataset compared to **(b)** simulated height in the same year from LPX; **(c)** LPX-simulated height, multiplied by a factor of 2.67 so that the simulated global mean height is the same as the observations; **(d)** height from **(c)** with values reduced by a factor of 1.40 about the mean so that the simulations have the same global mean and variance as the observations.

the annual average burnt fraction changes from 1.58 (against GFED3) to 1.91 (against GFED2) for LPJ and from 0.85 (GFED3) to 0.92 (GFED2) for LPX (i.e. both models produce a better match to GFED3 than to GFED2), but the difference between the two models is preserved (i.e. LPX, with its more explicitly process-based fire model, is more realistic than LPJ).

### 3.2.3 Benchmarking the sensitivity to parameter tuning

Benchmarking can be used to evaluate how much tuning of individual parameters improves model performance and to ensure that the simulations capture specific processes correctly. We examine how well the current system serves in this respect by running sensitivity experiments using the SDBM. The SDBM underestimates the amplitude of CO<sub>2</sub> seasonal cycle (Fig. 3). A better match to CO<sub>2</sub> observations can be achieved by tuning the light-use efficiency parameter ( $\varepsilon$  in Eq. 12). The best possible match to CO<sub>2</sub> seasonal amplitude (0.18) is obtained when  $\varepsilon$  is equal to 1.73 g C MJ<sup>-1</sup>, but this increases both the mean and the variance of NPP compared to observations: the overall performance of the SDBM is therefore worse (Table 7). The seasonal amplitude of CO<sub>2</sub> depends on simulating the correct balance between NPP and  $R_h$ . Thus, given that the model produces a reasonable simulation of annual average NPP, improvement in CO<sub>2</sub> seasonality should come from changes in the simulation of  $R_h$ . Removing the requirement that NPP and  $R_h$  are in equilibrium, by setting total NPP to be 1.2 times  $R_h$ , improves the CO<sub>2</sub> sea-

sonal amplitude score to 0.51. In the baseline simulation, the  $Q_{10}$  for  $R_h$  is 1.5 (Eq. 13). Changing this response by increasing  $Q_{10}$  to 2 degrades the simulation of the seasonal amplitude and phase of CO<sub>2</sub>, while decreasing  $Q_{10}$  to 1.3 improves the simulation of the seasonal amplitude and phase of CO<sub>2</sub> (Table 7). Removing the seasonal response of  $R_h$  to moisture (i.e. removing  $\alpha$  from Eq. 13) improves the score for seasonal amplitude (0.39) but does not change the score for the phase. However, this degrades its performance against annual average NPP from 0.58 to 0.82. We expect that  $R_h$  should be sensitive to soil moisture changes, but this analysis suggests that the treatment of this dependency in the SDBM is unrealistic.

## 4 Discussion and conclusion

Model benchmarking serves multiple functions, including (a) showing whether processes are represented correctly in a model, (b) discriminating between models and determining which performs better for a specific process, and (c) comparing between the model scores and those obtained by comparing mean and random resampling of observations, thus helping to identify processes that need improvement.

As found by Heimann et al. (1998), the SDBM produces a good simulation of the seasonal cycle of atmospheric CO<sub>2</sub> concentration. However, we show that the simulated amplitude of the seasonal cycle is too low (Table 5; Fig. 3). The SDBM's performance depends on getting the right balance

3332

## D. I. Kelley et al.: Benchmarking system for evaluating global vegetation models

**Table 7.** Comparison metric scores for simulations with the Simple Diagnostic Biosphere Model (SDBM) against observations of the seasonal cycle of atmospheric CO<sub>2</sub> concentration and annual average NPP. Numbers in bold indicate the model with the best performance for that variable. Italic indicates model scores better than the SDBM simulation tuned using CO<sub>2</sub> seasonal observations. NME/NMSE denotes the normalised mean error/normalised mean squared error and MPD the mean phase difference. The details of each experiment are explained in the text.

Measure	SDBM standard run		SDBM tuned to CO <sub>2</sub> seasonal amplitude		SDBM NPP = 1.2 × R <sub>h</sub>		SDBM Q <sub>10</sub> = 1.3		SDBM Q <sub>10</sub> = 2		SDBM constant $\alpha$	
	NME	NMSE	NME	NMSE	NME	NMSE	NME	NMSE	NME	NMSE	NME	NMSE
CO <sub>2</sub> Amplitude	0.68	0.60	0.18	0.04	0.51	0.34	<i>0.15</i>	<i>0.02</i>	1.04	1.34	0.39	0.19
– mean removed	0.50	0.26	0.18	0.04	0.39	0.16	<i>0.11</i>	<i>0.01</i>	0.74	0.54	0.30	0.09
– mean and variance removed	<b>0.10</b>	0.02	<b>0.10</b>	0.02	<b>0.10</b>	0.02	<b>0.10</b>	<b>0.01</b>	0.18	0.07	0.12	0.02
MPD	0.21	N/A	0.21	N/A	<b>0.20</b>	N/A	<b>0.20</b>	N/A	0.26	N/A	0.21	N/A
NPP Annual Average	<b>0.58</b>	<i>0.36</i>	1.76	3.00	<b>0.58</b>	<i>0.36</i>	<b>0.58</b>	<i>0.36</i>	<b>0.58</b>	<i>0.36</i>	0.82	0.70
– mean removed	<b>0.53</b>	<i>0.32</i>	0.96	0.99	<b>0.53</b>	<i>0.32</i>	<b>0.53</b>	<i>0.32</i>	<b>0.53</b>	<i>0.32</i>	0.63	0.42
– mean and variance	<b>0.53</b>	<i>0.33</i>	<b>0.53</b>	<b>0.33</b>	<b>0.53</b>	<i>0.33</i>	<b>0.53</b>	<i>0.33</i>	<b>0.53</b>	<i>0.33</i>	0.63	0.44

of NPP and R<sub>h</sub>. Improved simulation of CO<sub>2</sub> seasonal amplitude can be achieved through tuning the light-use efficiency using CO<sub>2</sub> station data, but this degrades the simulated NPP. The seasonal variation of R<sub>h</sub> can be altered by changing the response of R<sub>h</sub> to temperature (Q<sub>10</sub>). Although many models (e.g. Potter et al., 1993; Cox et al., 2000) use Q<sub>10</sub> values of 2, benchmarking shows that the value of 1.5 used in the SDBM provides a better match to seasonal CO<sub>2</sub> observations. However, reducing the Q<sub>10</sub> to 1.3 improves the simulation still further. Mehecha et al. (2010), based on an analysis of FLUXNET data, have shown that Q<sub>10</sub> values are 1.4 ± 0.1 independent of temperature or vegetation type. Thus, both the initial and “improved” Q<sub>10</sub> values used here are consistent with observations, whereas values of 2 are not. Sensitivity analyses show that the SDBM can produce a seasonal cycle comparable to observations with respect to both amplitude and phase by removing the assumption that NPP and R<sub>h</sub> are in equilibrium, and the dependence of R<sub>h</sub> on seasonal changes in moisture availability. The idea that NPP and R<sub>h</sub> are not in equilibrium is realistic; the idea that moisture availability has no impact on R<sub>h</sub> is not. Thus, these analyses illustrate how benchmarking can be used to identify whether processes are represented correctly in a model, and pinpoint specific areas that should be targeted for investigation in further developments of the SDBM.

The benchmarking system can discriminate between models. LPJ and LPX are closely related models, differing primarily in the complexity of their treatment of fire and the feedbacks from fire disturbance to vegetation. The two DGVMs perform equally well against the benchmarks, e.g. for NPP (Fig. 9), inter-annual CO<sub>2</sub> concentrations (Fig. 10) and inter-annual and annual average runoff (Fig. 8). However, LPX performs better than LPJ with respect to all measures associated with fire (Fig. 7).

We were able to show several areas where both DGVMs perform poorly against the benchmarks, and use the comparisons to evaluate possible reasons. Deficiencies common to

both models include a low bias in canopy height (Table 5; Fig. 6), poor simulation of the seasonal concentration of fAPAR and of the balance of tree and grass cover (Table 5), and poor simulation of the inter-annual variability in runoff (Fig. 8).

Both DGVMs score poorly against the canopy height benchmark (Fig. 6), averaging around 1/3 of observed heights (Table 5). However, they capture the spatial pattern of the differences in height reasonably well. A good match to canopy height was not expected, because LPJ and LPX do not simulate a size- or age-structured tree population but rather represent the properties of an “average individual”. In contrast, the canopy height dataset represents the mean top height of forests within the grid cell. However, the models should, and do, capture broad geographic patterns of variation in height. The canopy height benchmark could provide a rigorous test for models that explicitly simulate cohorts of different ages of trees, such as the Ecosystem Demography (ED) model (Moorecroft et al., 2001). For models adopting a similar strategy to the LPJ/LPX family, the key test is whether the spatial patterns are correctly simulated. In either case, the use of remotely sensed canopy height data represents a valuable addition to the benchmarking toolkit.

Poor performance in the simulation of seasonal concentration of fAPAR (Table 5) demonstrates that both DGVMs predict the length of the growing season inaccurately: the growing season is too long at low latitudes and too short at mid-latitudes. This poor performance indicates that the phenology of both evergreen and deciduous vegetation requires improvement. Both models overestimate the amount of tree cover and underestimate grass cover (Table 5). The oversharp boundaries between forests and grasslands suggest that the models have problems in simulating the coexistence of these life forms. This probably also affects, and is exacerbated by, the simulation of fire in the models (Fig. 7).

The DGVMs simulate annual average runoff reasonably well, but inter-annual variability in runoff is poorly

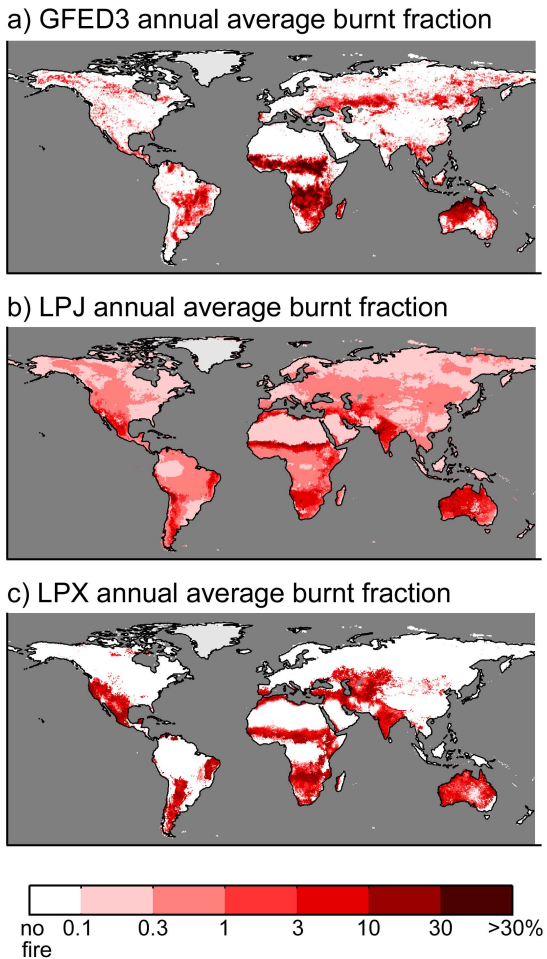


**Fig. 7.** Annual average burnt fraction between 1997–2005 from (a) GFED3 observations (Giglio et al., 2010) and as simulated by (b) LPJ and (c) LPX.

simulated. In large basins, water can take many months to reach the river mouth (Ducharne et al., 2003) and this delay has a major impact on the timing of peaks in river discharge. Neither LPX nor the version of LPJ evaluated here includes river routing; runoff is simulated as the instantaneous difference in the water balance. Thus, it is unsurprising that neither model produces a good match to observations of inter-annual variability. Murray et al. (2011) have pointed out that inclusion of a river routing scheme should improve the simulation of runoff in LPX, and this is supported by the fact that introducing a one-year lag improved model performance against the runoff benchmark (Fig. 8). There is already a version of LPJ (LPJmL v3.2: Rost et al., 2008) that incorporates a water storage and transport model (and also includes human extraction), and produces a more realistic simulation of

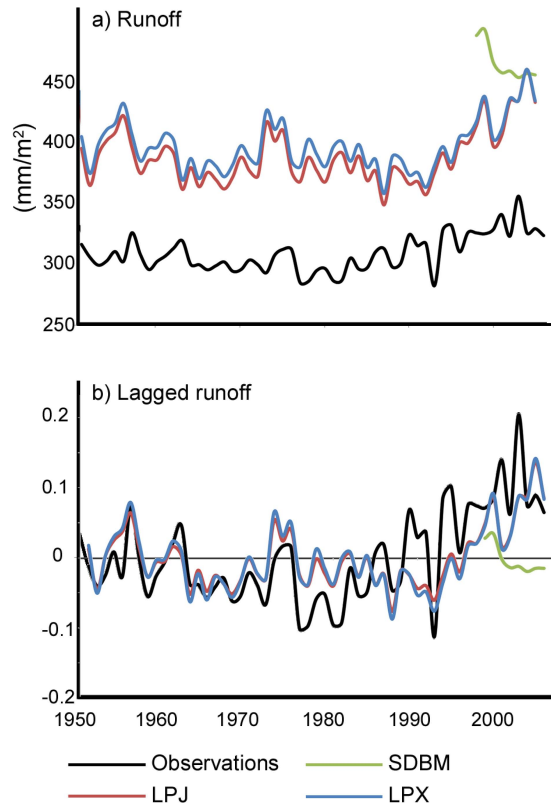


**Fig. 8.** Observed inter-annual runoff for 1950–2005 averaged over basins from the Dai et al. (2009) dataset (black line) compared to average simulated runoff over the same basins from LPJ (red line) and LPX (blue line). (a) shows inter-annual runoff, and (b) shows inter-annual variability in runoff where the simulated values are lagged by a year.

inter-annual variability in runoff than the version examined here.

In this paper, we have emphasised the use of global metrics for benchmarking, although both the NME and MM metrics provide a measure of the impact of the correct simulation of geographical patterning on global performance. However, the metrics could also be used to evaluate model performance at smaller geographic scales (e.g. for specific latitudinal bands, or individual continents or biomes). For example, comparison of the mean annual burnt fraction scores for specific latitudinal bands shows that the two DGVMs simulate fire in tropical regions better than in extratropical regions or overall, with NME scores for the tropics of 1.27 (LPJ) and 0.82 (LPX) compared to the global scores of 1.58 (LPJ) and 0.85 (LPX).

Some variables, such as runoff and burnt fraction, display considerable inter-annual variability linked to climate (e.g. changes in ENSO: van der Werf et al., 2004;

3334

D. I. Kelley et al.: Benchmarking system for evaluating global vegetation models

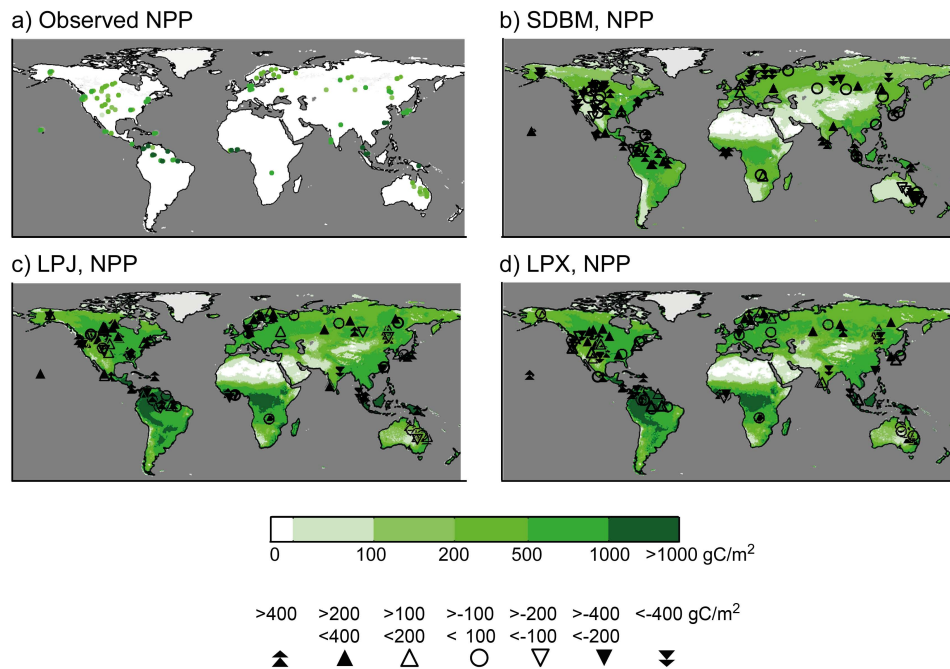


**Fig. 9.** Comparison of observed and simulated annual average net primary production (NPP). Observed values are from the Luyssaert et al. (2007) and Ecosystem/Model Data Intercomparison datasets (Olson et al., 2001), and the simulated values are from (**b**) Simple Diagnostic Biosphere Model (SDBM), (**c**) LPJ and (**d**) LPX. The symbols in (**b**), (**c**) and (**d**) indicate the magnitude and direction of disagreement between simulation and observed values, where the upward and downward facing triangles represent over- and undersimulation respectively. Double triangles indicate a difference in NPP of  $> 400 \text{ g C m}^{-2}$ , single filled triangles a difference between  $200$  and  $400 \text{ g C m}^{-2}$ , single empty triangles a difference  $100$  and  $200 \text{ g C m}^{-2}$ , and empty circles a difference of  $< 100 \text{ g C m}^{-2}$

post-volcanic cooling events: Riaño et al., 2007), and valuable information is obtained by considering this variability. The vegetation cover and canopy height datasets used for benchmarking here are single-year “snapshots”: this is entirely appropriate for variables that change only slowly. Nevertheless, given that vegetation is already responding to changes in climate (Parmesan, 2006; Hickling et al., 2006; Fischlin et al., 2007), additional “snapshots” of these variables would be useful adjuncts to a benchmarking system allowing evaluation of models’ ability to reproduce decadal-scale variability in vegetation properties.

In general, remote sensing data are most likely to provide the global coverage necessary for a benchmark dataset. Nevertheless, we have found considerable value in using site-based datasets for river discharge, CO<sub>2</sub>, GPP and NPP. River discharge data are spatially integrated over basins that together cover much of the global land surface, while CO<sub>2</sub> station measurements intrinsically integrate land–atmosphere CO<sub>2</sub> fluxes over moderately large areas through atmospheric transport. The coverage of the site-based GPP and NPP datasets is more limited and currently does not represent the full range of biomes. We have shown that model performance against the Beer et al. (2010) gridded GPP dataset is better

than performance against the site-specific estimates of GPP in the Luyssaert et al. (2007) dataset – a function of the much higher number of flux-tower measurements included in the newer dataset and the smoothing of individual measurements inherent in the interpolation of these measurements to produce a gridded dataset. We do not use the Beer et al. (2010) dataset as a standard benchmark, because it was derived, in part, using the same climate variables that are used for the simulation of GPP in the vegetation models. However, the apparent improvement in model performance against the Beer et al. (2010) dataset at the Luyssaert et al. (2007) sites indicates the importance of making quality-controlled summaries of the primary flux-tower data available to the modelling community for benchmarking purposes.

GPP and NPP have also been derived from remotely sensed products (e.g. Running et al., 2004; Turner et al., 2006). This is not an optimal approach because the results are heavily influenced by the model used to translate the spectral vegetation indices, and the reliability of the product varies with spatial scale and for a given ecosystem type (Lu and Ji, 2006).

A more general issue with the development of benchmarking systems is the fact that target datasets are constantly

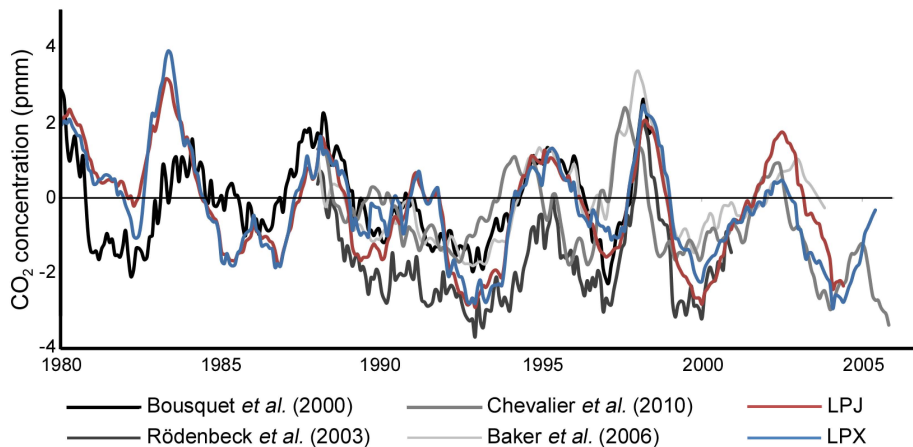


**Fig. 10.** Twelve-month running mean of inter-annual variability in global atmospheric CO<sub>2</sub> concentration between 1998–2005 from Bousquet et al. (2000), Rödenbeck et al. (2003), Baker et al. (2006) and Chevalier et al. (2010) compared to simulated inter-annual variability from LPJ and LPX.

being extended in time and upgraded in quality. This is potentially problematic if the benchmark system is to be used to evaluate improvements in model performance through time, since this requires the use of a fixed target against which to compare successive model versions, but this target may have been superseded in the interim. In the current system, for example, we use the Dai et al. (2009) dataset for runoff, which supersedes an earlier product (Dai and Trenberth, 2002) and improves upon this earlier product by including more and longer records. The use of an updated version of the same target dataset may change the numeric scores obtained for a given simulation, but our comparison of the GFED2 and GFED3 datasets suggests this is unlikely to change the interpretation of how well a model performs. Any benchmarking system will need to evolve as new data products become available. In practical terms, this may mean that data–model comparisons will have to be performed against both the old and new versions of the products in order to establish how different these products are from one another and to establish a new baseline comparison value for any given model. As with the datasets used in this study, any new datasets should be freely available to the scientific community, to allow different modelling groups to undertake comparable benchmarking exercises.

A major limitation of the benchmarking approach presented here is that it does not take into account observational uncertainties, because very few datasets provide a quantitative estimate of such uncertainties. We have shown that observational uncertainty is larger than differences in model performance with respect to site-based annual average NPP measurements, and these observational uncertainties are also greater than model biases in NPP. However, differences in the performance of LPJ and LPX with respect to annual average burnt fraction are considerably larger than observational un-

certainties. Approaches such as the use of multiple datasets (e.g. our use of multiple CO<sub>2</sub> inversions) may be one way of assessing uncertainty where there are no grounds for selecting a particular dataset as being more accurate or realistic. However, the only comprehensive solution to the problem is for measurement uncertainties to be routinely assessed for each site/grid cell and included with all datasets.

We have not attempted to provide an overall assessment of model performance by combining the metric scores obtained from each of the benchmarks into a composite skill score, although this has been done in some previous analyses (e.g. Randerson et al., 2009), because this requires subjective decisions about how to weight the importance of each metric. Composite skill scores have been used in data-assimilation studies to obtain better estimates of model parameters (e.g. Trudinger et al., 2007). The choice of weights used in these multi-variable composite metrics alters the outcome of parameter optimization (Trudinger et al., 2007; Weng and Luo, 2011; Xu et al., 2006). Decisions about how to weight individual vegetation-model benchmarks may heavily influence model performance scores (Luo et al., 2012).

The community-wide adoption of a standard system of benchmarking, as first proposed by C-LAMP (Randerson et al., 2009) and by ILAMB (Luo et al., 2012), would help users to evaluate the uncertainties associated with specific vegetation-model simulations and help to determine which projections of the response of vegetation to future climate changes are likely to be more reliable. As such, it will help to enhance confidence in these tools. At the same time, as we have shown here, systematic benchmarking provides a good way to identify ways of improving the current models and should lead to better models in the future.

**Acknowledgements.** S. P. Harrison and I. C. Prentice were responsible for the design of the benchmarking system; I. C. Prentice, K. O. Willis and D. I. Kelley designed the metrics; D. I. Kelley ran the LPJ and LPX simulations, coded metrics and made the statistical analyses; H. Wang and D. I. Kelley collated and regridded datasets and coded and ran the SDBM. J. B. Fisher and M. Simard provided remote-sensed datasets. D. I. Kelley, S. P. Harrison and I. C. Prentice wrote the first draft of the paper; all authors contributed to the final version of the manuscript. D. I. Kelley is supported by a Macquarie University International Research Scholarship (iMQRES). We thank Gab Abramowitz and the ILAMB project (<http://www.ilamb.org>) for discussions of benchmarking strategy and Stephen Sitch for supplying the atmospheric transport matrices. Metrics were scripted using R (R Development Core Team, 2012). The benchmarking system, datasets and scripts for data–model comparison metrics are available at <http://bio.mq.edu.au/bcd/benchmarks/>.

Edited by: E. Falge

## References

- Arora, V. K. and Boer, G. J.: Fire as an interactive component of dynamic vegetation models, *J. Geophys. Res.*, 110, G02008, doi:10.1029/2005JG000042, 2005.
- Baker, D. F., Doney, S. C., and Schimel, D. S.: Variational data assimilation for atmospheric CO<sub>2</sub>, *Tellus B*, 58, 359–365, 2006.
- Barnston, G. A.: Correspondence among the correlation, RMSE, and Heidke forecast verification measures; refinement of the Heidke score, Boston, MA, USA, American Meteorological Society, 1992.
- Beer, C., Reichstein, M., Tomelleri, E., Ciais, P., Jung, M., Carvalhais, N., Rödenbeck, C., Arain, M. A., Baldocchi, D., Bonan, G. B., Bondeau, A., Cescatti, A., Lasslop, G., Lindroth, A., Lomas, M., Luyssaert, S., Margolis, H., Oleson, K. W., Roupsard, O., Veenendaal, E., Viovy, N., Williams, C., Woodward, F. I., and Pampale, D.: Terrestrial Gross Carbon Dioxide Uptake: Global Distribution and Covariation with Climate, *Science*, 329, 834–838, 2010.
- Blyth, E., Gash, J., Lloyd, A., Pryor, M., Weedon, G. P., and Shuttleworth, J.: Evaluating the JULES land surface model energy fluxes using FLUXNET data, *J. Hydrometeorol.*, 11, 509–519, 2009.
- Blyth, E., Clark, D. B., Ellis, R., Huntingford, C., Los, S., Pryor, M., Best, M., and Sitch, S.: A comprehensive set of benchmark tests for a land surface model of simultaneous fluxes of water and carbon at both the global and seasonal scale, *Geosci. Model Dev.*, 4, 255–269, doi:10.5194/gmd-4-255-2011, 2011.
- Bonan, G. B., Lawrence, P. J., Oleson, K. W., Levis, S., Jung, M., Reichstein, M., Lawrence, D. M. and Swenson, S. C.: Improving canopy processes in the Community Land Model version 4 (CLM4) using global flux fields empirically inferred from FLUXNET data, *J. Geophys. Res.*, 116, G02014, doi:10.1029/2010JG001593, 2011.
- Bousquet, P., Peylin, P., Ciais, P., Le Quéré, C., Friedlingstein, P., and Tans, P. P.: Regional changes in carbon dioxide fluxes of land and oceans since 1980, *Science*, 290, 1342–1346, 2000.
- Cadule, P., Friedlingstein, P., Bopp, L., Sitch, S., Jones, C. D., Ciais, P., Piao, S. L., and Peylin, P.: Benchmarking coupled climate-carbon models against long-term atmospheric CO<sub>2</sub> measurements, *Glob. Biogeochem. Cy.*, 24, GB2016, doi:10.1029/2009GB003556, 2010.
- Carmona-Moreno, C., Belward, A., Malingreau, J.-P., Hartley, A., Garcia-Alegre, M., Antonovskiy, M., Buchshtaber, V., and Povarov, V.: Characterizing interannual variations in global fire calendar using data from Earth observing satellites, *Glob. Change Biol.*, 11, 1537–1555, 2005.
- Cha, S.: Comprehensive survey on distance / similarity measures between probability density functions, *Int. J. Math. Models Methods Appl. Sci.*, 1, 301–307, 2007.
- Chevallier, F., Ciais, P., Conway, T. J., Aalto, T., Anderson, B. E., Bousquet, P., Brunke, E. G., Ciattaglia, L., Esaki, Y., Fröhlich, M., Gomez, A., Gomez-Pelaez, A. J., Haszpra, L., Krummel, P. B., Langenfelds, R. L., Leuenberger, M., Machida, T., Maignan, F., Matsueda, H., Morguí, J. A., Mukai, H., Nakazawa, T., Peylin, P., Ramonet, M., Rivier, L., Sawa, Y., Schmidt, M., Steele, L. P., Vay, S. A., Vermeulen, A. T., Wofsy, S. and Worthy, D.: CO<sub>2</sub> surface fluxes at grid point scale estimated from a global 21 year reanalysis of atmospheric measurements, *J. Geophys. Res.*, 115, D21307, doi:10.1029/2010JD013887, 2010.
- Cox, P. M., Betts, R. A., Jones, C. D., Spall, S. A., and Totterdell, I. J.: Acceleration of global warming due to carbon-cycle feedbacks in a coupled climate model, *Nature*, 408, 184–187, 2000.
- Cramer, W., Kicklighter, D. W., Bondeau, A., Moore, B., Churkina, G., Nemry, B., Ruimy, A., and Schloss, A. L.: Comparing global models of terrestrial net primary productivity (NPP): overview and key results, *Global Change Biol.*, 5, 1–15, 1999.
- Dai, A. and Trenberth, K. E.: Estimates of freshwater discharge from continents: latitudinal and seasonal variations, *J. Hydrometeorol.*, 3, 660–687, 2002.
- Dai, A., Qian, T., Trenberth, K. E., and Milliman, J. D.: Changes in continental freshwater discharge from 1948 to 2004, *J. Climate*, 22, 2773–2792, 2009.
- DeFries, R. and Hansen, M. C.: ISLSCP II Continuous Fields of Vegetation Cover, 1992–1993, in: ISLSCP Initiative II Collection, Data set, edited by: Hall, F. G., Collatz, G., Meeson, B., Los, S., Brown De Colstoun, E., and Landis, D., Oak Ridge, Tennessee, USA, available at:<http://daac.ornl.gov/> from Oak Ridge National Laboratory Distributed Active Archive Center, last access: 13 January 2011, 2009.
- DeFries, R. S., Townshend, J. R. G., and Hansen, M. C.: Continuous fields of vegetation characteristics at the global scale at 1-km resolution, *J. Geophys. Res.*, 104, 16911–16923, 1999.
- DeFries, R. S., Hansen, M. C., Townshend, J. R. G., Janetos, A. C., and Loveland, T. R.: A new global 1-km dataset of percentage tree cover derived from remote sensing, *Glob. Change Biol.*, 6, 247–254, 2000.
- Denman, K. L., Brasseur, G., Chidthaisong, A., Ciais, P., Cox, P. M., Dickinson, R. E., Hauglustaine, D., Heinze, C., Holland, E., Jacob, D., Lohmann, U., Ramachandran, S., da Silva Dias, P. L., Wofsy, S. C., and Zhang, X.: Couplings between changes in the climate system and biogeochemistry, in: Climate Change 2007: The Physical Science Basis, Contribution of Working Group I to the Fourth Assessment Report of the Intergovernmental Panel on Climate Change, edited by: Solomon, S., Qin, D., Manning, M., Chen, Z., Marquis, M., Averyt, K. B., Tignor, M., and Miller, H. L., Cambridge and New York, Cambridge University Press, 499–587, 2007.

- Ducharne, A., Golaz, C., Leblois, E., Laval, K., Polcher, J., Ledoux, E., and De Marsily, G.: Development of a high resolution runoff routing model, calibration and application to assess runoff from the LMD GCM, *J. Hydrol.*, 280, 207–228, 2003.
- Efron, B.: Bootstrap methods: another look at the Jackknife, *Ann. Stat.*, 7, 1–26, 1979.
- Efron, B. and Tibshirani, R. J.: An Introduction to the Bootstrap, New York, Chapman & Hall, 1993.
- FAO: The Digitized Soil Map of the World (Release 1.0), edited by: Food and Agriculture Organization of the United Nations, Rome, Italy, World Soil Resources Report 67/1, 1991.
- Fischlin, A., Midgley, G. F., Price, J., Leemans, R., Gopal, B., Turley, C., Rounsevell, M., Dube, P., Tarazona, J., Velichko, A., Atlaphopheng, J., Beniston, M., Bond, W. J., Brander, K., Bugmann, H., Callaghan, T. V., de Chazal, J., Dikinya, O., Guisan, A., Gyalistras, D., Hughes, L., Kgope, B. S., Körner, C., Lucht, W., Lunn, N. J., Neilson, R. P., Pêcheux, M., Thuiller, W., and Warren, R.: Ecosystems, their properties, goods, and services, in: Climate Change 2007: impacts, adaptation and vulnerability, Contribution of Working Group II to the Fourth Assessment Report of the Intergovernmental Panel on Climate Change, edited by: Parry, M. L., Canziani, O. F., Palutikof, J. P., Van Der Linden, P. J., and Hanson, C. E., Cambridge, United Kingdom, Cambridge University Press, 211–272, 2007.
- Fisher, J. B., Tu, K. P., and Baldocchi, D. D.: Global estimates of the land–atmosphere water flux based on monthly AVHRR and ISLSCP-II data, validated at 16 FLUXNET sites, *Remote Sens. Environ.*, 112, 901–919, 2008.
- Fisher, J. B., Whittaker, R. J., and Malhi, Y.: ET come home: potential evapotranspiration in geographical ecology, *Glob. Ecol. Biogeogr.*, 20, 1–18, 2011.
- Friedlingstein, P., Cox, P., Betts, R., Bopp, L., von Bloh, W., Brovkin, V., Cadule, P., Doney, S., Eby, M., Fung, I., Bala, G., John, J., Jones, C., Joos, F., Kato, T., Kawamiya, M., Knorr, W., Lindsay, K., Matthews, H. D., Raddatz, T., Rayner, P., Reick, C., Roeckner, E., Schnitzler, K.-G., Schnur, R., Strassmann, K., Weaver, A. J., Yoshikawa, C., and Zeng, N.: Climate–carbon cycle feedback analysis: Results from the C4MIP model intercomparison, *J. Climate*, 19, 3337–3353, 2006.
- Gallego-Sala, A. V., Clark, J. M., House, J. I., Orr, H. G., Prentice, I. C., Smith, P., Farewell, T., and Chapman, S. J.: Bioclimatic envelope model of climate change impacts on blanket peatland distribution in Great Britain, *Clim. Res.*, 45, 151–162, 2010.
- Gavin, D. G., Oswald, W. W., Wahl, E. R., and William, J. W.: A statistical approach to evaluating distance metrics and analog assignments for pollen records, *Quat. Res.*, 60, 356–367, 2003.
- Gerten, D., Schaphoff, S., Haberlandt, U., Lucht, W., and Sitch, S.: Terrestrial vegetation and water balance – hydrological evaluation of a dynamic global vegetation model, *J. Hydrol.*, 286, 249–270, 2004.
- Giglio, L., Csiszar, I., and Justice, C. O.: Global distribution and seasonality of active fires as observed with the Terra and Aqua Moderate Resolution Imaging Spectroradiometer (MODIS) sensors, *J. Geophys. Res.*, 111, G02016, doi:10.1029/2005JG000142, 2006.
- Giglio, L., Randerson, J. T., van der Werf, G. R., Kasibhatla, P. S., Collatz, G. J., Morton, D. C., and DeFries, R. S.: Assessing variability and long-term trends in burned area by merging multiple satellite fire products, *Biogeosciences*, 7, 1171–1186, doi:10.5194/bg-7-1171-2010, 2010.
- Gleckler, P. J., Taylor, K. E., and Doutriaux, C.: Performance metrics for climate models, *J. Geophys. Res.*, 113, D06104, doi:10.1029/2007JD008972, 2008.
- Gobron, N., Pinty, B., Taberner, M., Mélin, F., Verstraete, M. and Widlowski, J.: Monitoring the photosynthetic activity of vegetation from remote sensing data, *Adv. Space Res.*, 38, 2196–2202, 2006.
- Hall, A. and Qu, X.: Using the current seasonal cycle to constrain snow albedo feedback in future climate change, *Geophys. Res. Lett.*, 33, L03502, doi:10.1029/2005GL025127, 2006.
- Hall, F. G., Brown De Colstoun, E., Collatz, G. J., Landis, D., Dirmeyer, P., Betts, A., Huffman, G. J., Bounoua, L., and Meeson, B.: ISLSCP Initiative II global data sets: Surface boundary conditions and atmospheric forcings for land-atmosphere studies, *J. Geophys. Res.*, 111, D22S01, doi:10.1029/2006JD007366, 2006.
- Heimann, M.: The global atmospheric tracer model TM2: model description and user manual, in: The Global Atmospheric Tracer Model TM2, edited by: Deutsches Klimarechenzentrum, Max-Planck-Institut für Meteorologie, <http://mms.dkrz.de/pdf/klimadaten/servicesupport/documents/reports/ReportNo.10.pdf> (last access: 7 September 2011), Hamburg, Germany, 1995.
- Heimann, M., Esser, G., Haxeltine, A., Kaduk, J., Kicklighter, D. W., Knorr, W., Kohlmaier, G. H., McGuire, A. D., Melillo, J., Moore III, B., Otto, R. D., Prentice, I. C., Sauf, W., Schloss, A., Sitch, S., Wittenberg, U., and Würth, G.: Evaluation of terrestrial carbon cycle models through simulations of the seasonal cycle of atmospheric CO<sub>2</sub>: First results of a model intercomparison study, *Global Biogeochem. Cy.*, 12, 1–24, 1998.
- Hickling, R., Roy, D. B., Hill, J. K., Fox, R., and Thomas, C. D.: The distributions of a wide range of taxonomic groups are expanding polewards, *Glob. Change Biol.*, 12, 450–455, 2006.
- Jackson, C. S., Sen, M. K., Huerta, G., Deng, Y., and Bowman, K. P.: Error reduction and convergence in climate prediction, *J. Climate*, 21, 6698–6709, 2008.
- Jones, P. and Harris, I.: CRU Time Series (TS) high resolution gridded datasets, edited by: Climate Research Unit, available at: [http://badc.nerc.ac.uk/view/badc.nerc.ac.uk\\_ATOM\\_dataent\\_1256223773328276](http://badc.nerc.ac.uk/view/badc.nerc.ac.uk_ATOM_dataent_1256223773328276), BAD C, last access: 26 September 2012.
- Jung, M., Reichstein, M., and Bondeau, A.: Towards global empirical upscaling of FLUXNET eddy covariance observations: validation of a model tree ensemble approach using a biosphere model, *Biogeosciences*, 6, 2001–2013, doi:10.5194/bg-6-2001-2009, 2009.
- Jung, M., Reichstein, M., Ciais, P., Seneviratne, S. I., Sheffield, J., Goulden, M. L., Bonan, G. B., Cescatti, A., Chen, J., de Jeu, R., Dolman, A. J., Eugster, W., Gerten, D., Gianelle, D., Gobron, N., Heinke, J., Kimball, J. S., Law, B. E., Montagnani, L., Mu, Q., Mueller, B., Oleson, K. W., Papale, D., Richardson, A. D., Roupsard, O., Running, S. W., Tomelleri, E., Viovy, N., Weber, U., Williams, C., Wood, E., Zaehle, S., and Zhang, K.: Recent decline in the global land evapotranspiration trend due to limited moisture supply, *Nature*, 467, 951–954, 2010.
- Kaminski, T., Giering, R., and Heimann, M.: Sensitivity of the seasonal cycle of CO<sub>2</sub> at remote monitoring stations with respect to seasonal surface exchange fluxes determined with the adjoint of an atmospheric transport model, *Phys. Chem. Earth*, 21, 457–462, 1996.

- Keeling, R.: Atmospheric science – Recording Earth's vital signs, *Science*, 319, 1771–1772, 2008.
- Knorr, W. and Heimann, M.: Impact of drought stress and other factors on seasonal land biosphere CO<sub>2</sub> exchange studied through an atmospheric tracer transport model, *Tellus B*, 47, 471–489, 1995.
- Le Quéré, C., Aumont, O., Bopp, L., Bousquet, P., Ciais, P., Francey, R., Heimann, M., Keeling, C. D., Keeling, R. F., Kheshgi, H., Peylin, P., Piper, S. C., Prentice, I. C., and Rayner, P. J.: Two decades of ocean CO<sub>2</sub> sink and variability, *Tellus B*, 55, 649–656, 2003.
- Lenderink, G.: Exploring metrics of extreme daily precipitation in a large ensemble of regional climate model simulations, *Clim. Res.*, 44, 151–166, 2010.
- Lu, J. and Ji, J.: A simulation and mechanism analysis of long-term variations at land surface over arid/semi-arid area in north China, *J. Geophys. Res.*, 111, doi:10.1029/2005JD006252, 2006.
- Luo, Y. Q., Randerson, J. T., Abramowitz, G., Bacour, C., Blyth, E., Carvalhais, N., Ciais, P., Dalmonech, D., Fisher, J. B., Fisher, R., Friedlingstein, P., Hibbard, K., Hoffman, F., Huntzinger, D., Jones, C. D., Koven, C., Lawrence, D., Li, D. J., Mahecha, M., Niu, S. L., Norby, R., Piao, S. L., Qi, X., Peylin, P., Prentice, I. C., Riley, W., Reichstein, M., Schwalm, C., Wang, Y. P., Xia, J. Y., Zaehle, S., and Zhou, X. H.: A framework for benchmarking land models, *Biogeosciences*, 9, 3857–3874, doi:10.5194/bg-9-3857-2012, 2012.
- Luyssaert, S., Inglima, I., Jung, M., Richardson, A. D., Reichstein, M., Papale, D., Piao, S. L., Schulze, E. -D., Wingate, L., Matteucci, G., Aragao, L., Aubinet, M., Beer, C., Bernhofer, C., Black, K. G., Bonal, D., Bonnefond, J. -M., Chambers, J., Ciais, P., Cook, B., Davis, K. J., Dolman, A. J., Gielen, B., Goulden, M., Grace, J., Granier, A., Grelle, A., Griffis, T., Grünwald, T., Guidolotti, G., Hanson, P. J., Harding, R., Hollinger, D. Y., Hutyra, L. R., Kolari, P., Kruijt, B., Kutsch, W., Lagergren, F., Laurila, T., Law, B. E., Le Maire, G., Lindroth, A., Loustau, D., Malhi, Y., Mateus, J., Migliavacca, M., Misson, L., Montagnani, L., Moncrieff, J., Moors, E., Munger, J. W., Nikinmaa, E., Ollinger, S. V., Pita, G., Rebmann, C., Roupsard, O., Saigusa, N., Sanz, M. J., Seufert, G., Sierra, C., Smith, M. -L., Tang, J., Valentini, R., Vesala, T. and Janssens, I. A.: CO<sub>2</sub> balance of boreal, temperate, and tropical forests derived from a global database, *Glob. Change Biol.*, 13, 2509–2537, 2007.
- Mahecha, M. D., Reichstein, M., Carvalhais, N., Lasslop, G., Lange, H., Seneviratne, S. I., Vargas, R., Ammann, C., Arain, A. M., Cescatti, A., Janssens, I. A., Migliavacca, M., Montagnani, L., and Richardson, A. D.: Global Convergence in the Temperature Sensitivity of Respiration at Ecosystem Level, *Science*, 329, 838–840, 2010.
- Moise, A. F. and Delage, F. P.: New climate model metrics based on object-orientated pattern matching of rainfall, *J. Geophys. Res.*, 116, D12108, doi:10.1029/2010JD015318, 2011.
- Monteith, J. L.: Solar radiation and productivity in tropical ecosystems, *J. Appl. Ecol.*, 9, 747–766, 1972.
- Moorcroft, P. R., Hurtt, G. C., and Pacala, S. W.: A method for scaling vegetation dynamics: the Ecosystem Demography model (ED), *Ecol. Monogr.*, 71, 557–586, 2001.
- Mu, Q., Zhao, M., and Running, S. W.: Improvements to a MODIS global terrestrial evapotranspiration algorithm, *Remote Sens. Environ.*, 115, 1781–1800, 2011.
- Murphy, J. M., Sexton, D. M. H., Barnett, D. N., Jones, G. S., Webb, M. J., Collin, M., and Stainforth, D. A.: Quantification of modelling uncertainties in a large ensemble of climate change simulations, *Nature*, 430, 768–772, 2004.
- Murray, S. J., Foster, P. N., and Prentice, I. C.: Evaluation of global continental hydrology as simulated by the Land-surface Processes and eXchanges Dynamic Global Vegetation Model, *Hydrolog. Earth Syst. Sci.*, 15, 91–105, doi:10.5194/hess-15-91-2011, 2011.
- Nash, J. E. and Sutcliffe, J. V.: River flow forecasting through conceptual models part I – A discussion of principles, *J. Hydrol.*, 10, 282–290, 1970.
- Nevison, C. D., Mahowald, N. M., Doney, S. C., Lima, I. D., van der Werf, G. R., Randerson, J. T., Baker, D. F., Kasibhatla, P., and McKinley, G. A.: Contribution of ocean, fossil fuel, land biosphere, and biomass burning carbon fluxes to seasonal and interannual variability in atmospheric CO<sub>2</sub>, *J. Geophys. Res.*, 113, G01010, doi:10.1029/2007JG000408, 2008.
- Olson, R. J., Scurlock, J. M. O., Prince, S. D., Zheng, D. L., and Johnson, K. R.: NPP Multi-Biome: NPP and Driver Data for Ecosystem Model-Data Intercomparison, Oak Ridge National Laboratory Distributed Active Archive Center, Oak Ridge, Tennessee, USA, 2001.
- Parmesan, C.: Ecological and Evolutionary Responses to Recent Climate Change, *Annu. Rev. Ecol. Evol. Syst.*, 37, 637–669, 2006.
- Piani, C., Frame, D. J., Stainforth, D. A., and Allen, M. R.: Constraints on climate change from a multi-thousand member ensemble of simulations, *Geophys. Res. Lett.*, 32, L23825, doi:10.1029/2005GL024452, 2005.
- Poorter, H., Remkes, C., and Lambers, H.: Carbon and nitrogen economy of 24 wild species differing in relative growth rate, *Plant Physiol.*, 94, 621–627, 1990.
- Potter, C. S., Randerson, J. T., Field, C. B., Matson, P. A., Vitousek, P. M., Mooney, H. A., and Klooster, S. A.: Terrestrial ecosystem production: A process model based on global satellite and surface data, *Global Biogeochem. Cy.*, 7, 9144–9224, 1993.
- Prentice, I. C., Sykes, M. T., and Cramer, W.: A simulation model for the transient effects of climate change on forest landscapes, *Ecol. Model.*, 65, 51–70, 1993.
- Prentice, I. C., Bondeau, A., Cramer, W., Harrison, S. P., Hickler, T., Lucht, W., Sitch, S., Smith, B., and Sykes, M. T.: Dynamic Global Vegetation Modelling: quantifying terrestrial ecosystem responses to large-scale environmental change Terrestrial Ecosystems in a Changing World, Springer Berlin Heidelberg, 2007.
- Prentice, I. C., Kelley, D. I., Foster, P. N., Friedlingstein, P., Harrison, S. P., and Bartlein, P. J.: Modeling fire and the terrestrial carbon balance, *Global Biogeochem. Cy.*, 25, GB3005, doi:10.1029/2010GB003906, 2011.
- Prince, S. D.: A model of regional primary production for use with coarse resolution satellite data, *Int. J. Remote Sens.*, 12, 1313–1330, 1991.
- R Development Core Team: R: A Language and Environment for Statistical Computing, R Foundation for Statistical Computing, Vienna, Austria, available at: <http://www.R-project.org/>, last access: 11 July 2012.
- Randall, D. A., Wood, R. A., Bony, S., Colman, R., Fichefet, T., Fyfe, J., Kattsov, V., Pitman, A., Shukla, J., Srinivasan, J., Stouf-

- fer, R. J., Sumi A., and Taylor K. E.: Climate models and their evaluation, in: Climate change 2007: the physical science basis, Contribution of working group 1 to the fourth assessment report of the intergovernmental panel on climate change edited by: Solomon, S., Qin, D., Manning, M., Chen, Z., Marquis, M., Averyt, K. B., Tignor M., and Miller H. L., Cambridge University Press, Cambridge, United Kingdom and New York, NY, USA, 2007.
- Randerson, J. T., Hoffman, F. M., Thornton, P. E., Mahowald, N. M., Lindsay, K., Lee, Y. H., Nevison, C. D., Doney, S. C., Bonan, G., Stockli, R., Covey, C., Running, S. W., and Fung, I. Y.: Systematic assessment of terrestrial biogeochemistry in coupled climate–carbon models, *Glob. Change Biol.*, 15, 2462–2484, 2009.
- Raupach, M. R., Briggs, P. R., Haverd, V., King, E. A., Paget, M. and Trudinger, C. M.: Australian Water Availability Project (AWAP): CSIRO Marine and Atmospheric Research Component: Final Report for Phase 3, in: CAWCR Technical Report, Melbourne, Australia, The Centre for Australian Weather and Climate Research, 2009.
- Riaño, D., Moreno Ruiz, J. A., Barón Martínez, J., and Ustin, S. L.: Burned area forecasting using past burned area records and Southern Oscillation Index for tropical Africa (1981–1999), *Remote Sens. Environ.*, 107, 571–581, 2007.
- Reichler, T. and Kim, J.: How well do coupled models simulate today's climate?, *B. Am. Meteorol. Soc.*, 89, 303–311, doi:10.1175/BAMS-89-3-303, 2008.
- Rödenbeck, C., Houweling, S., Gloor, M., and Heimann, M.: CO<sub>2</sub> flux history 1982–2001 inferred from atmospheric data using a global inversion of atmospheric transport, *Atmos. Chem. Phys.*, 3, 1919–1964, doi:10.5194/acp-3-1919-2003, 2003.
- Rost, S., Gerten, D., Bondeau, A., Lucht, W., Rohwer, J., and Schaphoff, S.: Agricultural green and blue water consumption and its influence on the global water system, *Water Resour. Res.*, 44, 1–17, 2008.
- Running, S. W., Nemani, R. R., Heinrichs, F. A., Zhao, M., Reeves, M., and Hashimoto, H.: A continuous satellite-derived measure of global terrestrial primary production, *Bioscience*, 54, 547–560, 2004.
- Scheiter, S. and Higgins, S. I.: Impacts of climate change on the vegetation of Africa: an adaptive dynamic vegetation modelling approach, *Globm Change Biol.*, 15, 2224–2246, 2009.
- Scholze, M., Knorr, W., Arnell, N. W., and Prentice, I. C.: A climate-change risk analysis for world ecosystems, *P. Natl. Acad. Sci.*, 103, 13116–13120, 2006.
- Shukla, J., DelSole, T., Fennessy, M., Kinter, J., and Paolino, D.: Climate model fidelity and projections of climate change. *Geophys. Res. Lett.*, 33, L07702, doi:10.1029/2005GL025579, 2006.
- Simard, M., Pinto, N., Fisher, J. B., and Baccini, A.: Mapping forest canopy height globally with spaceborne lidar, *J. Geophys. Res.*, 116, G04021, doi:10.1029/2011JG001708, 2011.
- Sitch, S., Smith, B., Prentice, I. C., Arneth, A., Bondeau, A., Cramer, W., Kaplan, J. O., Levis, S., Lucht, W., Sykes, M. T., Thonicke, K., and Venevsky, S.: Evaluation of ecosystem dynamics, plant geography and terrestrial carbon cycling in the LPJ dynamic global vegetation model, *Glob. Change Biol.*, 9, 161–185, 2003.
- Sitch, S., Huntingford, C., Gedney, N., Levy, P. E., Lomas, M., Piao, S. L., Betts, R., Ciais, P., Cox, P., Friedlingstein, P., Jones, C., Prentice, I. C., and Woodward, F. I.: Evaluation of the terrestrial carbon cycle, future plant geography and climate–carbon cycle feedbacks using five Dynamic Global Vegetation Models (DGVMs), *Glob. Change Biol.*, 14, 2015–2039, 2008.
- Taylor, K. E.: Summarizing multiple aspects of model performance in a single diagram, *J. Geophys. Res.*, 106, 7183–7192, doi:10.1029/2000JD900719, 2001.
- Thonicke, K., Venevsky, S., Sitch, S., and Cramer, W.: The role of fire disturbance for global vegetation dynamics: coupling fire into a Dynamic Global Vegetation Model, *Global Ecol. Biogeogr.*, 10, 661–677, 2001.
- Thonicke, K., Spessa, A., Prentice, I. C., Harrison, S. P., Dong, L., and Carmona-Moreno, C.: The influence of vegetation, fire spread and fire behaviour on biomass burning and trace gas emissions: results from a process-based model, *Biogeosciences*, 7, 1991–2011, doi:10.5194/bg-7-1991-2010, 2010.
- Trudinger , C. M., Raupach, M. R., Rayner, P. J., Kattge, J., Liu, Q., Pak, B., Reichstein, M., Renzullo, L., Richardson, A. D., Roxburgh, S. H., Styles, J., Wang, Y. P., Briggs, P., Barrett, D., and Nikolova, S.: OptIC project: An intercomparison of optimization techniques for parameter estimation in terrestrial biogeochemical models, *J. Geophys. Res.*, 112, G02027, doi:10.1029/2006JG000367, 2007.
- Turner, D. P., Ritts, W. D., Maosheng, Z., Kurc, S. A., Dunn, A. L., Wofsy, S. C., Small, E. E., and Running, S. W.: Assessing inter-annual variation in MODIS-based estimates of gross primary production, *Geosci. Remote Sens., IEEE T.*, 44, 1899–1907, 2006.
- van der Werf, G. R., Randerson, J. T., Collatz, G. J., Giglio, L., Kasibhatla, P. S., Arellano Jr, A. F., Olsen, S. C., and Kasischke, E. S.: Continental-scale partitioning of fire emissions during the 1997 to 2001 El Niño/La Niña period, *Science*, 303, 73–76, 2004.
- van der Werf, G. R., Randerson, J. T., Giglio, L., Collatz, G. J., Kasibhatla, P. S., and Arellano Jr, A. F.: Interannual variability in global biomass burning emissions from 1997 to 2004, *Atmos. Chem. Phys.*, 6, 3423–3441, doi:10.5194/acp-6-3423-2006, 2006.
- van der Werf, G. R., Randerson, J. T., Giglio, L., Collatz, G. J., Mu, M., Kasibhatla, P. S., Morton, D. C., DeFries, R. S., Jin, Y., and van Leeuwen, T. T.: Global fire emissions and the contribution of deforestation, savanna, forest, agricultural, and peat fires (1997–2009), *Atmos. Chem. Phys.*, 10, 11707–11735, doi:10.5194/acp-10-11707-2010, 2010.
- van Oijen, M., Cameron, D. R., Butterbach-Bahl, K., Farahbakhs-hazard, N., Jansson, P. E., Kiese, R., Rahn, K. H., Werner, C., and Yeluripati J. B.: A Bayesian framework for model calibration, comparison and analysis: Application to four models for the biogeochemistry of a Norway spruce forest, *Agr. Forest Meteorol.*, 151, 1609–1621, 2011.
- Weng, E. and Luo, Y.: Relative information contributions of model vs. data to short- and long-term forecasts of forest carbon dynamics, *Ecol. Appl.*, 21, 1490–1505, 2011.
- Woodward, F. I. and Lomas, M. R.: Vegetation dynamics – simulating responses to climatic change, *Biol. Rev.*, 79, 643–670, 2004.
- Xu, T., White, L., Hui, D., and Luo, Y.: Probabilistic inversion of a terrestrial ecosystem model: Analysis of uncertainty in parameter estimation and model prediction, *Global Biogeochem. Cy.*, 20, GB2007, doi:10.1029/2005GB002468, 2006.

3340

**D. I. Kelley et al.: Benchmarking system for evaluating global vegetation models**

- Yokoi, S., Takayabu, Y. N., Nishii, K., Nakamura, H., Endo, H., Ichikawa, H., Inoue, T., Kimoto, M., Kosaka, Y., Miyasaka, T., Oshima, K., Sato, N., Tsushima, Y., and Watanabe, M.: Application of cluster analysis to climate model performance metrics. *J. Appl. Meteor. Climatol.*, 50, 1666–1675, 2011.
- Zeng, X., Zeng, X., and Barlage, M.: Growing temperate shrubs over arid and semiarid regions in the Community Land Model; Dynamic Global Vegetation Model, *Global Biogeochem. Cy.*, 22, GB3003, doi:10.1029/2007GB003014, 2008.





*Epicormic shoot*

# 3

## Patterns in the abundance of post-fire resprouting in Australia based on plot-level measurements.

---

Harrison, S.P.<sup>1,2</sup>, Kelley, D.I.<sup>1</sup>, Wang, H.<sup>1</sup>, Herbert, A.<sup>1</sup>, Li, G.<sup>1</sup>, Bradstock,  
R.<sup>3</sup>, Fontaine, J.<sup>4</sup>, Enright, N.<sup>4</sup>, Murphy, B.P.<sup>5</sup>, Pekin, B.K.<sup>6</sup>, Penman, T.<sup>3</sup>,  
Russell-Smith, J.<sup>7</sup>, Wittkuhn, R.S<sup>8</sup>

<sup>1</sup>Department of Biological Sciences, Macquarie University, North Ryde, NSW 2109, Australia; sandy.harrison@mq.edu.au

<sup>2</sup>Geography & Environmental Sciences, School of Archaeology, Geography and Environmental Sciences (SAGES), University of Reading, Whiteknights, Reading, RG6 6AB, UK. s.p.harrison@reading.ac.uk

<sup>3</sup>Centre for Environmental Risk Management of Bushfires, University of Wollongong, Wollongong, NSW 2522, Australia; rossb@uow.edu.au; mailto:tpenman@uow.edu.au

<sup>4</sup>School of Veterinary and Life Sciences, Murdoch University, Murdoch, WA 6150, Australia; j.fontaine@murdoch.edu.au; n.enright@murdoch.edu.au

<sup>5</sup>NERP Environmental Decisions Hub, School of Botany, The University of Melbourne, Parkville, VIC 3010, Australia; brett.murphy@unimelb.edu.au

<sup>6</sup>Institute for Conservation Research, San Diego Zoo Global, Escondido, CA 92027, USA; bpekin@sandiegozoo.org

<sup>7</sup>Darwin Centre for Bushfire Research, Charles Darwin University, Darwin, NT

0909, Australia; jeremy.russell-smith@cdu.edu.au

<sup>8</sup>Tranen Revegetation Systems, 1/110 Jersey Street, Jolimont, WA, 6014, Australia;  
roy.wittkuhn@tranen.com.au

---

### Biosketch

The authors of this paper are members of the Australian Centre for Ecological Analysis and Synthesis (ACEAS) Working group ‘Using plant functional traits to predict ecosystem vulnerability to changing fire regimes’. The goal of the Working Group is to synthesis data on plant traits, including fire-resistance and post-fire response traits, in order to understand how plants respond to fire disturbance and to develop predictive models of ecosystem-level response to potential future changes in fire regimes. The Working Group includes field ecologists specializing in the observation of ecosystem responses to fire, statisticians and data analysts, and modellers developing of fire-enabled dynamic global vegetation models. The lead author, Sandy Harrison, focuses on the use of data analysis and vegetation modeling to address land-atmosphere interactions and biogeochemical cycling in the context of past and future climate changes.

---

### This chapter has been submitted for publication:

Harrison, S., Kelley, D., Wang, H., Herbert, A., Li, G., Bradstock, R., Fontaine, J. B., Enright, N. J., Murphy, B. P., Pekin, B. K., Penman, T., Russell-Smith, J. & Wittkuhn, R. S.: Patterns in the abundance of post-fire resprouting in Australia based on plot-level measurements., Glob. Ecol. Biogeogr., submitted

---

## 3.1 Abstract.

*Aim.* To determine if there are differences in the abundance of resprouting, and types of resprouting, between plant functional types (PFTs) and along environmental gradients within fire-prone temperate and tropical ecosystems.

*Location.* Australia

*Methods.* We constructed a database of plot-based information on species abundance and species attributions of fire-response traits (species, subspecies and varieties are treated as distinct taxa). Every taxon is characterized by life form, leaf type, plant phenology and climatic range to allow classification into PFTs. The significance of PFT-related differences in resprouting abundance, and of apical, epicormic, basal/collar, underground resprouting, was established using a G-test. The significance of variation in the abundance of resprouting (and categories of resprouting) along productivity and climate gradients was tested using a generalized linear model.

*Results.* There are significant differences in post-fire resprouting ability between PFTs: shrubs are less likely to resprout than trees, and temperate trees are less likely to resprout than tropical trees. The number of taxa in particular resprouting categories also varies significantly between PFTs. Although basal/collar resprouting occurs in >90% of woody taxa, epicormic resprouting is more common in tropical trees than temperate trees or shrubs, while underground resprouting is more common in shrubs than trees. The abundance of post-fire resprouting (and resprouting categories) varies along climate and productivity gradients. In non-seasonal climates, resprouters are most abundant at intermediate levels of precipitation and productivity. In highly seasonal climates, resprouting abundance increases monotonically with precipitation but, for any mean annual precipitation, resprouters are more common in climates with winter than with summer drought. These climate relationships translate into geographic gradients in the abundance of post-fire resprouters.

*Main Conclusions.* The prevalence of resprouting as a response to fire varies between PFTs, and along productivity and climate gradients.

## 3.2 Introduction

Fire is a natural, recurring but episodic disturbance in almost all types of vegetation, although most prominent in tropical and temperate savannas, Mediterranean woodlands and shrublands, and boreal forests (Bowman *et al.*, 2009). Fire is important in regulating ecosystem dynamics and diversity (Bond & van Wilgen, 1996), and in carbon cycling (Arneth *et al.*, 2010). The importance of fire as an ecological and biogeochemical agent has motivated the development of dynamic global vegetation models (DGVMs) which explicitly simulate fire behavior (e.g. Kloster *et al.*, 2010; Prentice *et al.*, 2011a), a development that has gained impetus because of recent climate-related increases in the number and impact of fires (Riao *et al.*, 2007) and the probability that fire will increase in the future in response to global warming (e.g. Moritz *et al.*, 2012).

Plants in ecosystems that undergo regular burning typically display adaptations that confer either resistance to fire damage or allow rapid population recovery after fire (Bond & van Wilgen, 1996). There are many traits that promote rapid recovery after fire, including resprouting, fire-induced seed release (serotiny), and fire-induced (i.e. heat- or smoke-induced) germination. Studies have shown that the abundance of plants displaying these response traits varies between ecosystems (Vesk & Westoby, 2004), along climate gradients (Lloret *et al.*, 2005; Russell-Smith *et al.*, 2012; Clark *et al.*, 2013) and in different types of fire regime (Lloret *et al.*, 2005; Enright *et al.*, 2011; Buma *et al.*, 2013).

Despite a growing understanding of the ways that plant populations survive fire, global models generally treat vegetation responses to fire in a relatively simplistic fashion. While most models incorporate fire resistance, by allowing bark thickness (a key persistence trait) to vary amongst plant functional types (PFTs) and modelling death at a given fire intensity as a function of bark thickness (see e.g. Prentice *et al.*, 2011a), no model explicitly simulates fire-response traits. One reason for this is the lack of large-scale data sets providing quantitative information about the relationship

between these traits and climate or vegetation types, data sets that could be used to parameterize and/or validate fire-enabled models.

Here, as part of an effort to incorporate fire-response traits within the Land Processes and eXchanges (LPX: Prentice *et al.*, 2011a; Kelley *et al.*, 2014) fire-enabled DGVM, we synthesise and standardize a large number of plot-based observations of the abundance of specific fire-response traits from across Australia. We focus on a sample of temperate and tropical ecosystems of intermediate productivity, where the frequency of fire varies and there are strong contrasts in fire seasonality. The resulting database provides information on the abundance of several fire-response traits (resprouting, obligate seeding, location of seed storage). Here, we use the database to document and analyse patterns in the abundance of resprouters (and specific categories of resprouters). This allows us to address two questions which are important in determining how to incorporate resprouting in process-based models: (a) does the abundance of resprouting vary between PFTs and (b) does the abundance of resprouting vary along environmental and/or climatic gradients?

### 3.3 Methods

#### 3.3.1 Structure of the database

The database contains records of species and their abundance at individual plots from around Australia, and the fire-response traits of each of these species. Species, subspecies and varieties are treated as distinct taxa. Information on the life form, leaf form, phenology and climatic range of each taxon is also given, to allow classification into PFTs. Metadata for each plot (latitude, longitude, elevation) is included, as is data on key climatic, bioclimatic and environmental variables for each site. The fire-response database is constructed in Microsoft Access.

#### 3.3.2 Plot data

The database currently contains plot data from four regions: northern Australia, southwestern Australia, the Sydney Basin and southern New South Wales (Fig. 3.1). The regions differ from one another in terms of rainfall seasonality, with northern Australia being characterized by seasonal summer-wet climates, southwestern Australia by seasonal winter-wet climates and the Sydney Basin and southern New South Wales by non-seasonal climates. However, there are gradients in climate and vegetation productivity within each region.

The northern Australian plot data come from Eucalyptus savanna woodlands and sandstone heaths of three large national parks (Kakadu, Litchfield and Nitmiluk) in the high rainfall zone ( $>1000$  mm per year) of the Northern Territory. Lowland areas are dominated by shallow, infertile lateritic soils, while soils on the sandstone plateau uplands are sandy and skeletal. We used 137 monitoring plots from savanna woodlands and 20 plots from heaths, described by Edwards *et al.* (2003). The basal area of live adult trees (DBH 5 cm) was assessed in 20 40 m plots. The densities of small woody

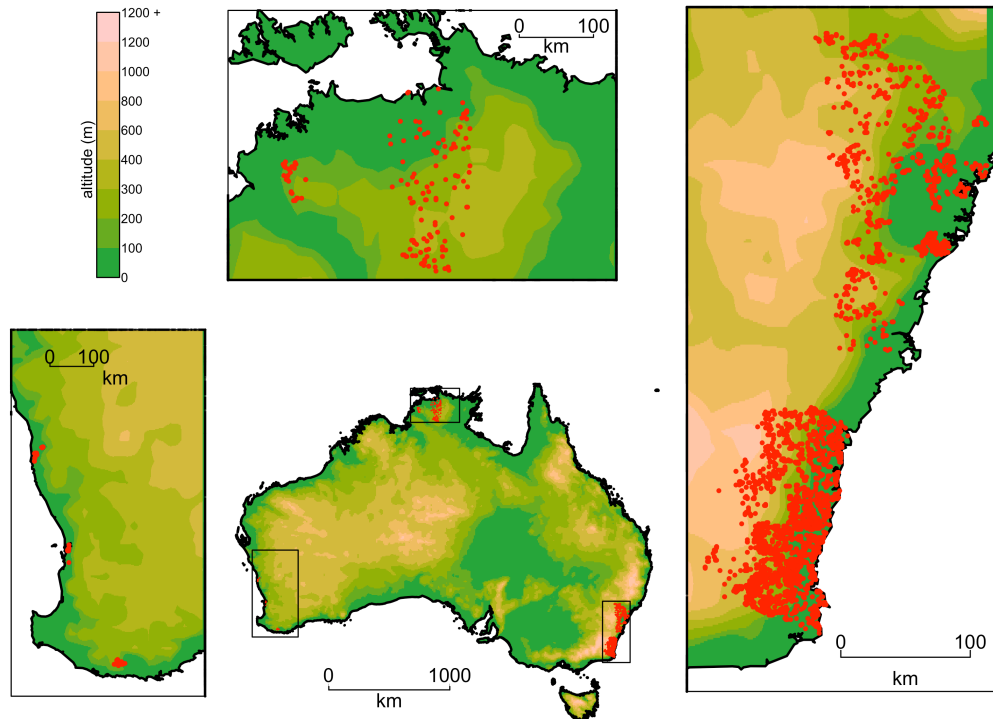


FIGURE 3.1: Distribution of the sites used in this study and included in the database. The underlying base map shows topography (altitude, m above sea level). The insets show each of the sampling regions in more detail.

understorey plants (<50 cm height) were assessed in two 40 × 1 m transects within each tree plot. The densities of medium (0.52 m height) and large (>2 m height) woody understorey plants were assessed in one 40 × 10 m sub-plot within each tree plot. The understorey woody plant assessments included both juvenile trees and true shrubs. No information was collected on other understory plants.

The data from southwestern Australia span a precipitation gradient from 1200 to 450 mm annual rainfall across a 600 km transect extending from the Southern Ocean (near Walpole) northwards to the Eneabba sandplain. Soils are sandy and nutrient poor, but range from somewhat more fertile calcareous sands over limestone to deep, leached acid sands overlaying a clay/lateritic layer. The southernmost, wetter part of this transect is characterized by forest (*Eucalyptus marginata*, *Corymbia calophylla*), Banksia woodland dominates the intermediate sites and the northern part of the gradient is dominated by shrubs (see Enright *et al.*, 2011 for a description of the shrubland sites, and Pekin *et al.*, 2011 for a description of the southern forests). The abundance of all vascular plants was measured within 10 × 10 m plots at the northern sites, and 30 × 30 m plots in the case of the southern forests, during spring in the period 2007–2009, using Braun-Blanquet cover abundance scores.

There are two data sets from the coastal and hinterland mountain regions of southeastern Australia: the Sydney Basin and southern New South Wales. Rainfall in these regions ranges from > 1000 mm near the coast and at high elevations to < 800 mm

in the interior. The soils are developed on a variety of parent materials including sandstone, quartzite, and granite but are generally nutrient poor. The predominant vegetation is open forest and woodland, often with a shrubby understorey, but heaths, shrublands, and small patches of rainforest occur within this forest matrix. We collated data on cover abundance scores of all vascular plant taxa from small plots (e.g. 0.1 ha, Keith & Benson, 1988) sampled in vegetation surveys.

### 3.3.3 Derivation of abundance scores

Different methods were used to estimate the plot-level abundance of taxa in the different regions, including the Braun-Blanquet scheme, modifications of this scheme, counts of numbers of individuals, and measurements of basal area. The original measurements are preserved in the database, but to compare results from different plots we (a) made estimates of the percent cover for each species, and (b) calculated abundance scores. For those plots with Braun-Blanquet values, the percentage cover was taken to be the mid-point of each of the Braun-Blanquet percentage ranges with the cover values for the lowest Braun-Blanquet category being derived following Wikum & Shanholtzer (1978). For the northern Australian plots, the percentage cover was calculated from the basal area of each taxon and the plot area, using a simple linear relationship between basal area and cover (Lehmann *et al.*, 2009). These percentages were then converted to Braun-Blanquet values so the abundance scores could be calculated in the same way as for sites with only Braun-Blanquet values. For those plots where the number of individuals in different size classes was counted, we estimated the total cover using allometric relationships between individual height and cover. The total percent cover for each taxon was then converted to Braun-Blanquet values to calculate abundance scores. Abundance and cover information were calculated using R (R Core Team, 2013).

### 3.3.4 Plant functional type attribution

DGVMs simulate the behavior of a suite of PFTs, where each PFT is characterized in terms of a limited number of functional traits such as life form (e.g. tree, shrub, grass), leaf form (e.g. broad, needle or scale leaved), phenology (e.g. deciduous or evergreen) and climatic range (e.g. tropical, temperate, boreal). Definitions of these functional traits are given in Table 3.S1. Combining these traits gives rise to multiple PFTs, although the number of PFTs simulated varies from model to model. Here we classify the taxa into the PFTs used in the Land Processes and eXchanges (LPX) model (Prentice *et al.*, 2011a) but also including a number of other PFTs that are important in Australian ecosystems and likely to have distinctive responses to fire, specifically tuft trees, scale-leaved woody plants, shrubs, dwarf shrubs and perennial forbs.

### 3.3.5 Fire-response attribution

The fire-response of each taxon in response to moderate to full canopy scorch (following Gill, 1981) was assessed on the basis of field observation and general knowledge or

through querying existing databases (Bradstock & Kenny, 2003; Russell-Smith *et al.*, 2012). We recognize four categories of resprouting: apical, epicormic, basal/collar (including lignotubers) and underground (root suckers and rhizomes) following Clarke *et al.* (2013) (see Table 3.S1 for definitions). A taxon may exhibit more than one category of resprouting. In cases where the type of resprouting was not known or uncertain, the taxon was classed simply as a resprouter. Taxa that can resprout, even if they only do so rarely, were classified as resprouters. Thus, the category non-resprouter only contains taxa that definitively do not resprout after fire.

### 3.3.6 Derivation of climate and environmental data

We constructed a 30-year gridded climatology of monthly precipitation, temperature and fractional sunshine-hours using ANUCLIM (Xu & Hutchinson, 2011) outputs for the interval from January 1970 through December 1999. This climatology was used to derive climatic and bioclimatic variables for each site, calculated following Prentice *et al.* (1993) and Wang *et al.* (2013). These variables include: mean annual temperature (MAT), mean temperature of the coldest month (MTCO), mean temperature of the warmest month (MTWA), the accumulated temperature sum during the growing season ( $GDD_0$ ), mean annual precipitation (MAP), precipitation during the month of maximum ( $P_{\text{wet}}$ ) and minimum ( $P_{\text{dry}}$ ) rainfall, temperature during the month of maximum ( $T_{\text{wet}}$ ) and minimum ( $T_{\text{dry}}$ ) rainfall, the seasonal concentration of precipitation ( $Pr_\Theta$ ), the timing or phase of precipitation, expressed in terms of when the wet season occurs ( $Pr_\phi$ ), and inter-annual variability of precipitation ( $Pr_{IAV}$ ), the Cramer–Prentice  $\alpha$  index of plant-available moisture (Prentice *et al.*, 1993) and a moisture index (MI) calculated as the ratio of MAP to total annual equilibrium evapotranspiration (Wang *et al.*, 2013).  $Pr_\Theta$  and  $Pr_\phi$  are calculated from the precipitation climatology as in Kelley *et al.* (2013). Seasonal concentration varies between 0 and 1, where 0 indicates that rain is evenly distributed through the year and 1 that all the rain is concentrated in a single month.  $Pr_\phi$  is the timing of the middle of the wet season.  $Pr_{IAV}$  is calculated as the standard deviation of MAP divided by MAP. The bioclimatic limits (MTCO, MTWA,  $GDD_0$ ,  $\alpha$ , MI) correspond to physiological limits on plant growth (Harrison *et al.*, 2010). Climate variables were added to the database using RNetCDF (Michna, 2012).

We also provide two types of information about the vegetation cover, specifically photosynthetically-active radiation (PAR) accumulated during the growing season, as defined by temperatures above 0°C ( $PAR_0$ ), and a measure based on the Enhanced Vegetation Index (EVI: [https://lpdaac.usgs.gov/products/modis\\_products\\_table/mod13q1](https://lpdaac.usgs.gov/products/modis_products_table/mod13q1)).  $PAR_0$  is a measure of fractional sunshine hours and hence available energy for growth. Monthly PAR values were calculated using monthly fractional sunshine hours as described in Gallego-Sala *et al.* (2010). The EVI is an index of vegetation cover that is influenced by canopy structure variations including leaf area index, canopy type, plant physiognomy and canopy architecture. We also include an estimate of net primary productivity (NPP) for each site, based on climate-driven calculations using a modified version of the Simple Diagnostic Biosphere Model (SDBM: Heimann *et al.*, 1998;

Kelley *et al.*, 2013). In addition to these variables, we estimated the seasonal phase and concentration of EVI using the same approach as for precipitation.

### 3.3.7 Statistical analyses

We compare the relative abundance of different fire-response traits amongst PFTs, using the tree and grass PFTs simulated by LPX but also considering tuft trees, scale-leaved woody plants, shrubs and forbs. These comparisons are based on the number of taxa with a given trait and confined to PFTs where the number of taxa in the whole data set is  $>10$  (there are insufficient numbers of temperate broadleaved deciduous trees or temperate needle-leaved trees in the database to be included in the analysis). We only consider the responses of perennial C<sub>3</sub> and C<sub>4</sub> grasses, and perennial forbs, because the concept of resprouting is not meaningful for annual taxa. We have information on the category of resprouting (apical, epicormic, basal or collar, underground) for a subset of the woody taxa, and use these data to compare the relative importance of different categories of the resprouting trait within PFTs. The comparisons of trait categories are also only made for PFTs where the number of taxa with information is  $>10$ . We assessed whether differences in trait (and trait category) abundance between PFTs were significant using a G-test. The significance of patterns in geographic and climate space was assessed using a generalized linear model (GLM), using climate and productivity variables as the predictors and resprouting abundance at each site as the predictand. We assume that the underlying relationships are Gaussian. Partial residual plots were used to examine the fitted underlying relationship between each variable and the predicted probabilities. The statistical analyses were performed using R packages by Lees (2013) and Lemon (2006).

## 3.4 Results

The database contains records for 4385 sites and 3466 unique taxa (Fig. 3.1). There is information allowing a classification into resprouter and non-resprouter for 2308 taxa, and complete information about the PFT and resprouting trait categories for 1251 of these taxa.

The sites provide a reasonable sampling of the climate space of Australia (Fig. 3.2, Fig. 3.S1), with about 30% of all observed climates in Australia sampled. Our focus on fire-prone regions of intermediate productivity means that hot wet, cold wet and arid parts of the continent were deliberately not sampled. The highly seasonal nature of precipitation in northern and southwestern Australia (Fig. 3.2b) means that  $\alpha$  can be quite low, and the sampled range in these two regions is between 0.4 and 0.7 (Fig. 3.S1). Higher  $\alpha$  values are found in non-seasonal climates. The temperature variables (MAT, MTCO, MTWA, GDD<sub>0</sub>) are all highly correlated with one another (Table 3.S2), and therefore convey no independent information in terms of the variability of controls on trait distribution. However, there is variability in the moisture variables that is independent of variability in temperature, and similarly the correlations between temperature (or moisture) variables and productivity are only moderate

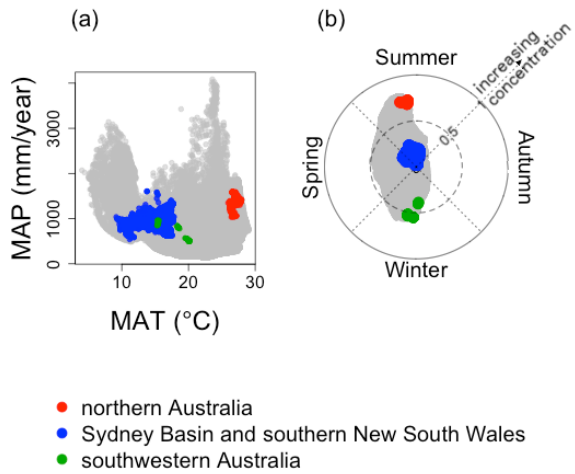


FIGURE 3.2: The distribution of the sites used in this study in climate space, as represented by **a**) mean annual temperature (MAT) and mean annual precipitation (MAP) and **b**) the seasonal concentration ( $Pr_\Theta$ ) and phase ( $Pr_\phi$ ) of precipitation. The grey dots represent all of the  $0.05^\circ$  grid cells covering Australia, while the coloured dots are the location of the sampled sites in climate space (red: sites from the northern Australia, blue: sites from the Sydney Basin and southern New South Wales; green: sites from southwestern Australia).

(Table 3.S2). In analyses of the abundance of resprouting in environmental space, we therefore focus on a subset of the variables to describe these three independent gradients (NPP,  $PAR_0$ ,  $\alpha$ ,  $T_{dry}$ ,  $P_{dry}$ ). These variables were selected because they reflect potentially independent influences on the fundamental controls of fire: availability of fuel and fuel dryness (Bistinas *et al.*, 2014).

### 3.4.1 Fire responses and PFTs

There are marked differences in the relative importance of resprouting between PFTs (Fig. 3.3a). Shrubs have a much higher proportion of non-resprouting taxa (ca 40%) than trees (<20%), and temperate trees have a higher number of non-resprouting taxa (20%) than tropical trees (<10%). All of the tuft tree taxa are resprouters. Scale-leaved woody plants have a relatively high number of non-resprouting taxa (62%). Differences between trees and shrubs, and between tropical and temperate trees, are significant at the 95% confidence level (Table 3.1). Differences in the proportion of evergreen and deciduous tropical trees that resprout are non-significant. Differences in the proportion of resprouting shrubs and dwarf shrubs are also non-significant. Amongst non-woody groups, perennial forbs have the highest number of non-resprouters (30%), followed by perennial C<sub>4</sub> grasses (10%) and perennial C<sub>3</sub> grasses (6%). The difference in resprouting

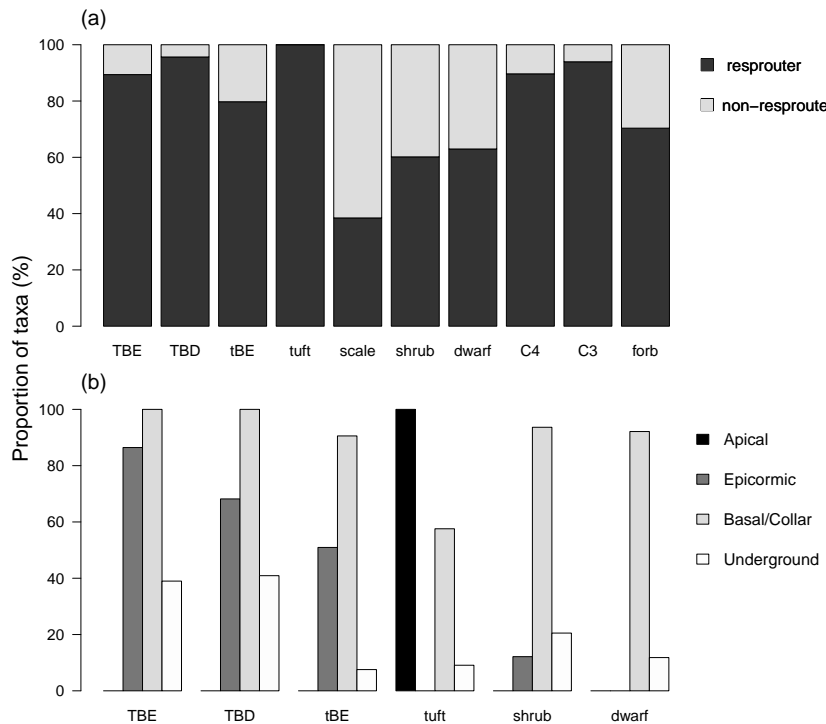


FIGURE 3.3: Abundance of resprouting, and resprouting trait categories by plant functional types (PFTs). The PFTs are tropical broadleaf evergreen tree (TBE), tropical broadleaf deciduous tree (TBD), temperate broadleaf evergreen tree (tBE), tuft tree (tuft), scale-leaved woody plant (scale), shrub, dwarf shrub (dwarf), perennial C<sub>4</sub> grass (C<sub>4</sub>), perennial C<sub>3</sub> grass (C<sub>3</sub>), and perennial forb (forb) (see Table 3.S1 for definitions). The upper panel **a**) shows the relative abundance of resprouters and non-resprouters for each PFT with >10 taxa in the database. The lower panel **b**) shows the percentage of woody taxa displaying apical, epicormic, basal/collar, underground resprouting (see Table 3.S1 for definitions). Taxa may display more than one kind of resprouting.

between the two types of grasses is not significant, although the difference between forbs and grasses (and particularly forbs and C<sub>3</sub> grasses) is significant (Table 3.1).

There are differences in the abundance of different resprouting categories within the woody PFTs (Fig. 3.3b). Apical resprouting is confined to tuft trees. Basal or collar resprouting is the most common category (>90%) in all the other woody PFTs. Epicormic resprouting is more common than underground resprouting in tree PFTs (excluding tuft trees), but the reverse is true for shrub PFTs. There is variation in the expression of epicormic resprouting among the tree PFTs: tropical evergreen trees are more likely to display epicormic resprouting (86%) than tropical deciduous trees (68%) which in turn are more likely to display epicormic resprouting than temperate evergreen trees (51%). However, these differences are not statistically significant (Table 3.2).

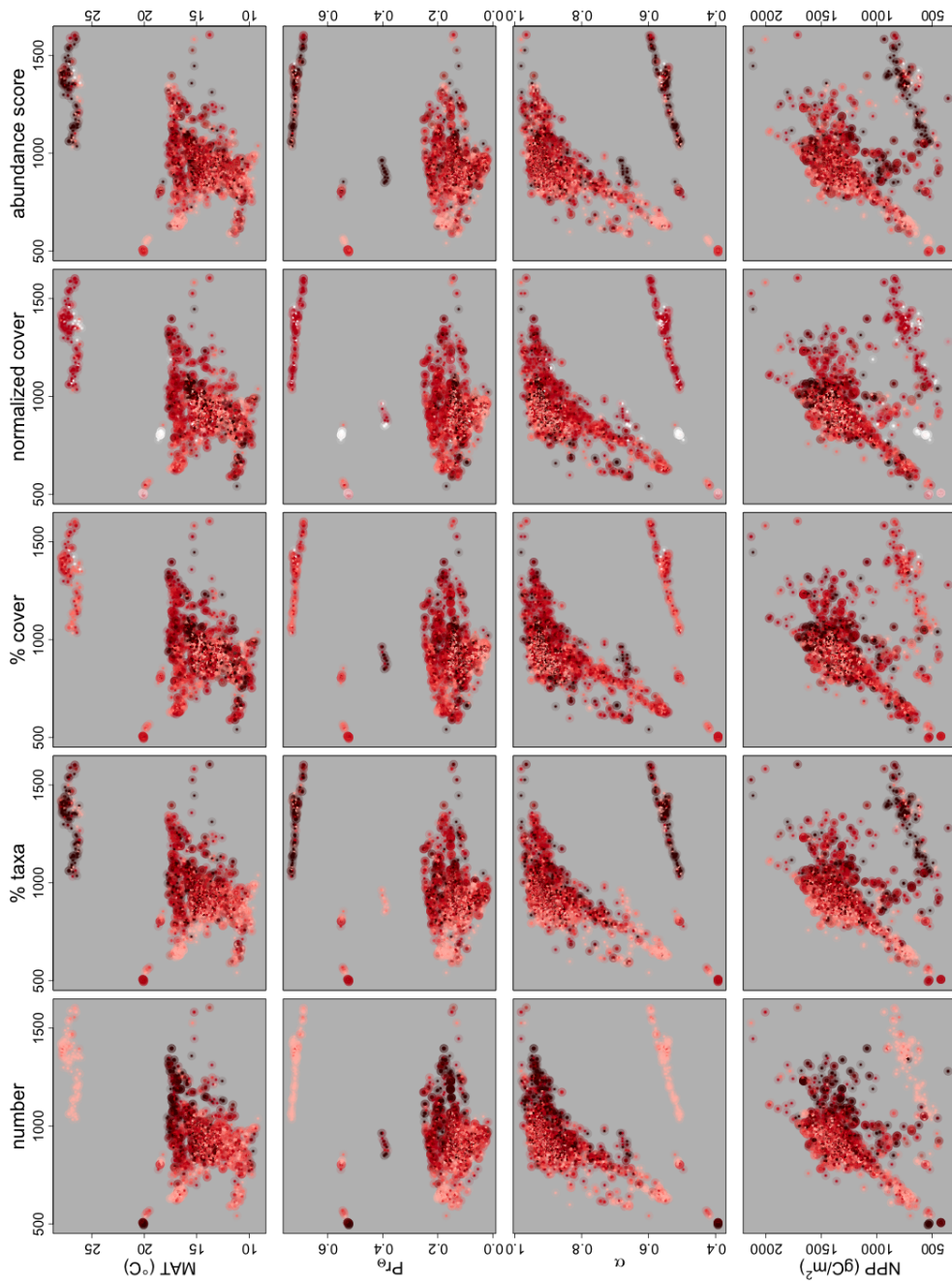
TABLE 3.1: Probability matrix comparing the abundance of resprouting and non-resprouting taxa in each plant functional type.

	TBE	TBD	tBE	Scale	Tuft	Shrub	Dwarf	C <sub>3</sub>	C <sub>4</sub>	Forb
TBE		0.43	<b>0.03</b>	0.00	<b>0.02</b>	0.00	0.00	<b>0.03</b>	0.36	0.00
TBD	0.43		<b>0.03</b>	0.00	0.18	0.00	0.00	<b>0.03</b>	0.16	0.00
tBE	<b>0.03</b>	<b>0.03</b>		0.00	0.00	0.00	0.00	0.72	0.53	0.00
Scale	0.00	0.00	0.00		0.00	0.12	0.08	<b>0.01</b>	0.00	0.02
Tuft	<b>0.02</b>	0.18	0.00	<b>0.00</b>		<b>0.00</b>	<b>0.00</b>	0.00	0.01	0.00
Shrub	0.00	0.00	0.00	0.12	0.00		0.43	0.00	0.00	0.00
Dwarf	0.00	0.00	0.00	0.08	0.00	0.43		<b>0.01</b>	<b>0.01</b>	0.05
C <sub>3</sub>	<b>0.03</b>	<b>0.03</b>	0.72	<b>0.01</b>	0.00	0.00	<b>0.01</b>		0.43	0.13
C <sub>4</sub>	0.36	0.16	0.53	<b>0.00</b>	<b>0.01</b>	0.00	<b>0.01</b>	0.43		0.07
Forb	0.00	0.00	0.00	0.02	0.00	0.00	<b>0.05</b>	0.13	0.07	

TABLE 3.2: Probability matrix comparing the abundance of resprouting syndromes in each woody plant functional type.

PFT	Type	TBE	TBD	tBE	Tuft	Shrub	Dwarf
TBE	Apical		1.00	1.00	<b>0.00</b>	1.00	1.00
TBD	Epicormic		0.71	0.68	<b>0.00</b>	<b>0.00</b>	<b>0.00</b>
tBE	Basal/Collar		0.86	0.24	0.54	<b>0.04</b>	<b>0.02</b>
tBE	Underground		0.81	<b>0.00</b>	0.06	0.84	0.29
TBD	Apical	1.00		1.00	<b>0.00</b>	1.00	1.00
TBD	Epicormic	0.71		0.91	<b>0.00</b>	<b>0.00</b>	<b>0.00</b>
tBE	Basal/Collar	0.86		0.55	0.51	0.27	0.16
tBE	Underground	0.81		<b>0.01</b>	0.08	0.68	0.30
Tuft	Apical	1.00	1.00		<b>0.00</b>	1.00	1.00
Tuft	Epicormic	0.68	0.91		<b>0.00</b>	<b>0.00</b>	<b>0.00</b>
Tuft	Basal/Collar	0.24	0.55		0.15	0.31	0.14
Tuft	Underground	<b>0.00</b>	<b>0.01</b>		0.92	<b>0.00</b>	0.06
Shrub	Apical	1.00	1.00	1.00	<b>0.00</b>		1.00
Shrub	Epicormic	<b>0.00</b>	<b>0.00</b>	<b>0.00</b>	<b>0.00</b>		<b>0.00</b>
Shrub	Basal/Collar	<b>0.04</b>	0.27	0.31	<b>0.05</b>		0.45
Shrub	Underground	0.84	0.68	<b>0.00</b>	0.06		0.28
Dwarf	Apical	1.00	1.00	1.00	<b>0.00</b>	1.00	
Dwarf	Epicormic	<b>0.00</b>	<b>0.00</b>	<b>0.00</b>	1.00	<b>0.00</b>	
Dwarf	Basal/Collar	<b>0.02</b>	0.16	0.14	<b>0.03</b>	0.45	
Dwarf	Underground	0.29	0.30	0.06	0.27	0.28	

PATTERNS IN THE ABUNDANCE OF POST-FIRE RESPROUTING IN AUSTRALIA BASED  
106 ON PLOT-LEVEL MEASUREMENTS.



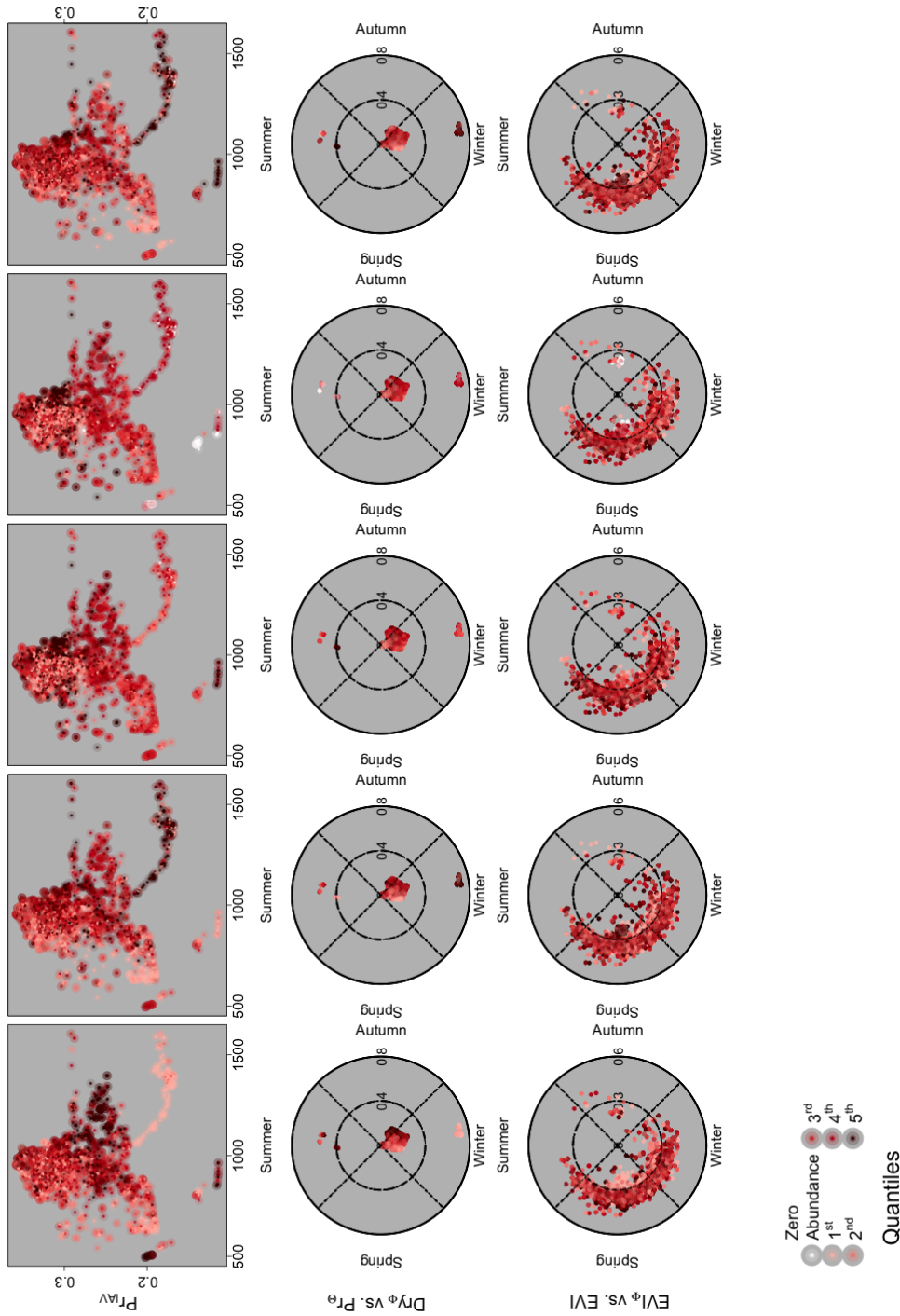


FIGURE 3.4: Distribution of resprouting expressed in quantiles plotted in climate and environmental space, described in terms of a) mean annual precipitation (MAP) versus mean annual temperature (MAT), b) MAP versus precipitation seasonality ( $P_\Theta$ ), c) MAP versus the Cramer–Prentice index of plant-available moisture ( $\alpha$ ), d) MAP versus net primary productivity (NPP), e) MAP versus interannual variability in MAP ( $P_{RIAV}$ ), f) phase of the wet season ( $Pr_\phi$ ) versus precipitation seasonality ( $P_\Theta$ ), and g) fraction of absorbed photosynthetically active radiation (EVI) versus phase of EVI (EVI $\Theta$ ). The plots show different measures of the abundance of resprouters, including number of taxa (number), percentage of total taxa (% taxa), cover (% cover), normalised percentage cover (normalised cover) and the normalised abundance score (abundance score, see text for description of how this score was calculated).

In contrast, the differences in underground resprouting amongst the tree PFTs are significant, with tropical trees having much higher abundances (ca 40%) than temperate evergreen trees (<10%). Differences in the abundance of resprouting categories between trees and shrubs are generally significant (Table 3.2), but differences between shrubs and dwarf shrubs (with the exception of epicormic resprouting which is not displayed by dwarf shrubs) are not significant.

### 3.4.2 Fire responses and climate

The number of resprouting taxa is maximal at intermediate temperature (15-20°C) and precipitation (800-1400 mm/year) levels (Fig. 3.4), which also translates into intermediate levels of  $\alpha$  (0.7-0.9) and NPP (900-1700 gC/m<sup>2</sup>). The decrease in number of resprouters with high precipitation is only apparent in temperate regions, and there appears to be an increase in number of resprouters with precipitation in the tropical sites. The marked decrease in the number of resprouters at high temperatures largely reflects differences in biodiversity across this climate gradient. Gradients in abundance, whether measured as percentage of the taxa present, percentage cover, normalized percentage cover, or the abundance score, show maxima at the hot, wetter end of the sampled climate gradient and decreasing abundance towards both drier and cooler conditions (Fig. 3.4). In temperate non-seasonal climates, there is a decrease in the abundance of resprouters in very wet conditions (>1300 mm/year) but this effect is not seen in the highly seasonal high rainfall areas. However, the seasonality of precipitation does have an impact on the abundance of resprouters, with resprouters being more abundant for any given level of MAP in regions of winter rather than summer drought (Fig. 3.4). The timing of the drought is reflected in the seasonal cycle of EVI, with the greening-up of the landscape after drought corresponding to maximum EVI. Thus, the differences in abundance of resprouters between regions of winter rather than summer drought explains why resprouters are more abundant in regions with higher EVI in spring than autumn.

These patterns can be explained in terms of the climatic controls on the availability of fuel and fuel dryness (Table 3.3). The abundance of resprouters is independently and positively correlated with factors controlling overall productivity and hence availability of fuel, specifically PAR<sub>0</sub> and  $\alpha$ . The positive relationship with both PAR<sub>0</sub> and  $\alpha$  is consistent with the fact that overall productivity can be increased by an increase in either factor. (The partial relationship with NPP is non-significant when PAR<sub>0</sub> is included in the GLM, but significant and positive if PAR<sub>0</sub> is omitted.) The abundance of resprouters is also significantly positively correlated with the temperature of the driest month (T<sub>dry</sub>), although precipitation during the dry season has no additional explanatory power. (As might be expected, precipitation during the dry season is negatively correlated with the abundance of resprouters if T<sub>dry</sub> is omitted from the GLM). Overall, the highest abundances of resprouters occur under climate conditions that maximize the amount and/or frequency of fire.

These analyses help to explain why the seasonality of precipitation has such a marked effect on resprouter abundance. Thus, given that increasing precipitation will generally increase fuel abundance, the contrast between the continued increase in the

abundance of resprouters with increasing MAP in seasonally-dry climates and the decline in the abundance of resprouters at high MAP in non-seasonal climates arises because high precipitation leads to fuel that is too wet to burn. Similarly, the higher abundance of resprouters in winter-droughted than summer-droughted climates emerges because fuel production (and hence fuel load) is maximal in seasonal climates with wet summer.

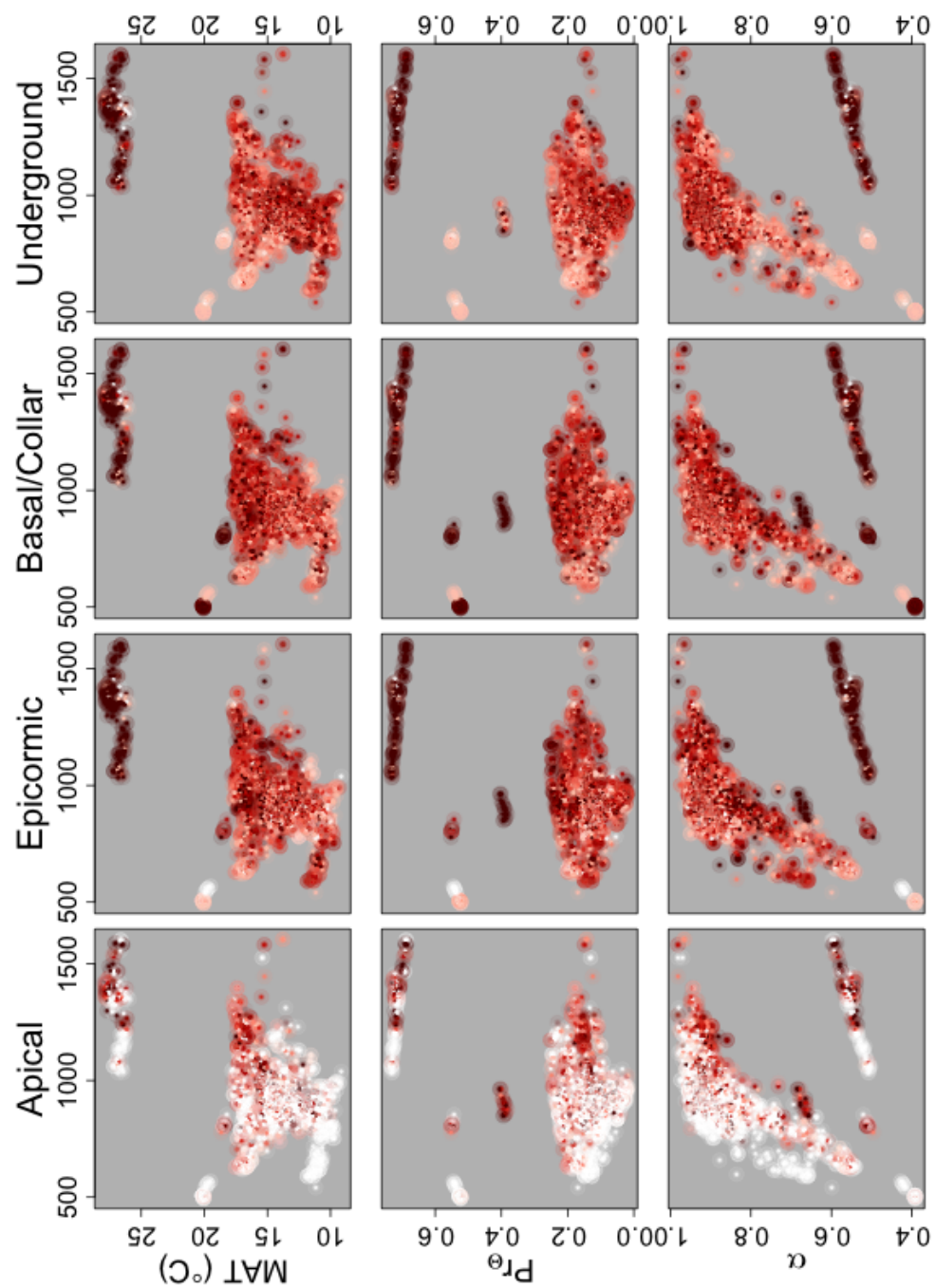
TABLE 3.3: Regression coefficients from the generalized linear model for abundance of resprouting (and types of resprouter) with controls on productivity and fuel dryness. Significant values ( $P < 0.05$ ) are shown in bold.

	<b>Resprouter</b>	<b>Apical</b>	<b>Epicormic</b>	<b>Basal or Collar</b>	<b>Underground</b>
$\text{PAR}_0$	<b>0.36</b>	0.041	<b>0.61</b>	<b>0.31</b>	<b>0.4</b>
NPP	-0.04		<b>0.085</b>	-0.046	0.0028
$\alpha$	<b>0.41</b>	0.052	<b>0.49</b>	<b>0.21</b>	0.53
$T_{\text{dry}}$	<b>0.15</b>	<b>0.14</b>	<b>0.1</b>	<b>0.2</b>	-0.056
$P_{\text{dry}}$	0.065		-0.055	-0.19	<b>-0.3</b>

The abundance of different categories of resprouting changes along climate gradients (Fig. 3.5). Apical resprouting is concentrated at the warmest and wettest end of the sampled gradient, as measured by MAT and MAP. High abundances of apical resprouters also occur at relatively low values of  $\alpha$  (ca 0.5) in the highly seasonal climates of northern Australia. Epicormic resprouting is abundant throughout the sampled climate range, though tending to be lowest at cooler temperature (MAT) and in drier (as measured by MAP or  $\alpha$ ) conditions. Similar patterns are shown for basal/collar and underground resprouting. All three categories are maximally abundant in seasonal climates characterized by summer drought and higher EVI in spring than autumn. The interannual variability of precipitation ( $\text{Pr}_{\text{IAV}}$ ) appears to have little impact on the abundance of epicormic and basal/collar resprouters, but the abundance of underground resprouters decreases as  $\text{Pr}_{\text{IAV}}$  decreases in regions with non-seasonal precipitation climates (Fig. 3.5). Results from the GLM analysis (Table 3.3) show that the abundance of different types of resprouting behavior is broadly controlled by productivity and fuel dryness.  $\text{PAR}_0$  and  $\alpha$  are positively correlated with the abundance of epicormic, basal/collar and underground resprouters.  $T_{\text{dry}}$  is also positively correlated with the abundance of these three types of resprouting, although  $P_{\text{dry}}$  also exerts an independent and significant negative effect on abundance in the case of epicormic and underground resprouters. In the case of apical resprouters, here largely confined to palms, NPP replaces  $\text{PAR}_0$  as a measure of productivity and  $\alpha$  appears to have no significant effect presumably because palms are confined to relatively wet locations.

### 3.4.3 Geographical patterns in fire responses

The decrease in abundance of resprouting, and of the different resprouting categories, with decreasing moisture is responsible for the geographic patterns in abundance seen within each region of Australia (Fig. 3.6). The abundance of resprouters is highest



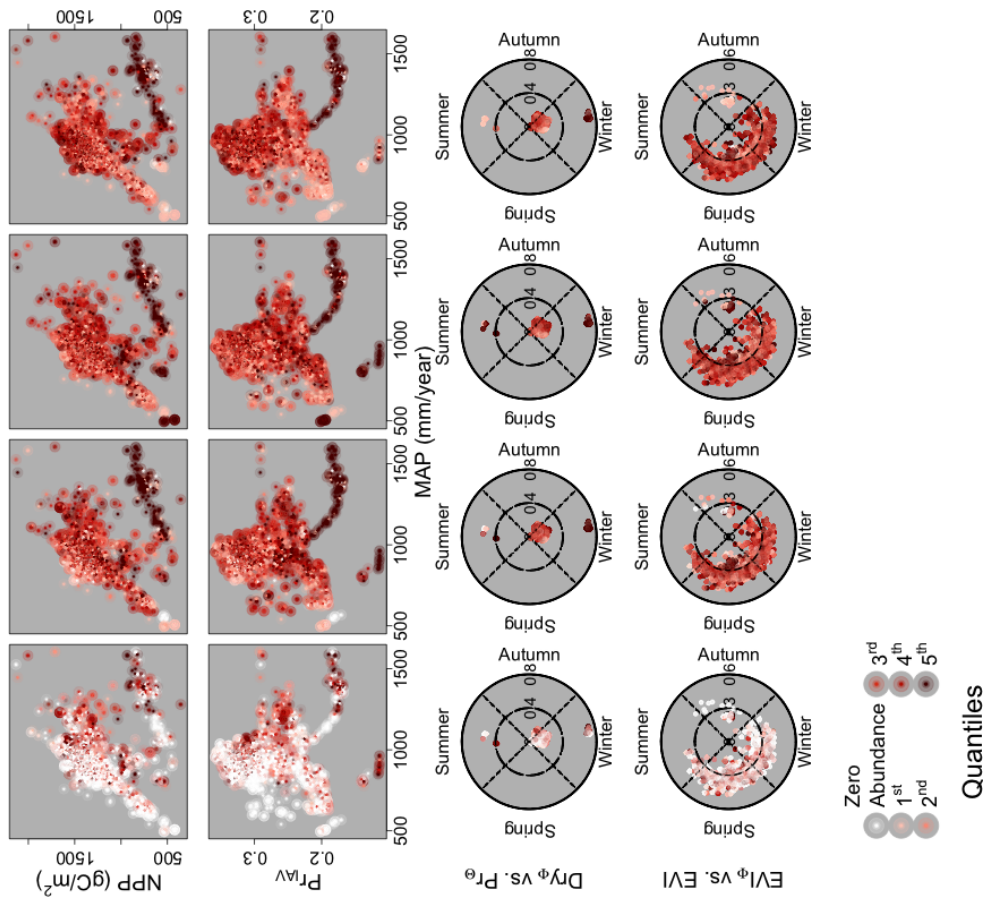


FIGURE 3.5: Abundance score for resprouting trait categories expressed in quantiles plotted in climate and environmental space, as described in terms of **a)** mean annual precipitation (MAP) versus mean annual temperature (MAT), **b)** MAP versus precipitation seasonality ( $P_\Theta$ ), **c)** MAP versus the Cramer–Prentice index of plant-available moisture ( $\alpha$ ), **d)** MAP versus net primary productivity (NPP), **e)** MAP versus interannual variability in MAP ( $P_{\text{IAV}}$ ), **f)** phase of the precipitation season ( $P_\phi$ ) versus precipitation seasonality ( $P_\Theta$ ), and **g)** fraction of absorbed photosynthetically active radiation (EVI) versus phase of EVI ( $EVI_\Theta$ ).

in the coastal plains of southeastern Australia, for example, and lowest in sites in the interior. In southwestern Australia, the lowest abundance of resprouters occurs at the northernmost sites, again reflecting the fact that both MAP and  $\alpha$  are lower than at the sites further south. The east-west gradient in the abundance of resprouters in northern Australia also reflects the moisture gradient. Patterns in the abundance of resprouting categories (Fig. 3.6) in general show the same patterns, except that apical resprouters are relatively uncommon in the sites from the Sydney Basin and southern New South Wales and there is a significant difference in the abundance of underground resprouters between the Sydney Basin and southern New South Wales. The difference appears to reflect differences in  $Pr_{IAV}$  between these two regions.

### 3.5 Discussion and Conclusions

We have shown that there are significant differences in resprouting ability between life forms: shrubs are less likely to resprout than trees, and temperate trees less likely to resprout than tropical trees. The difference between shrubs and trees makes intuitive sense: longer-lived plants have a greater investment in vegetative structure and the adoption of resprouting is a useful regeneration tactic to preserve this investment in fire-prone regions. The difference in the abundance of resprouters between tropical and temperate trees may be influenced by the fact that our sampling of tropical ecosystems is confined to regions with highly seasonal climates, where high productivity coupled with a significant period of drought leads to high fire risk. This may also explain why epicormic and basal/collar resprouting is more common in tropical than temperate trees. However, the difference between tropical and temperate trees may also reflect the prevalence of other forms of disturbance that could trigger resprouting e.g. cyclones. Previous studies of resprouting ability have tended to focus on differences between ecosystems, ontogeny, or with respect to climate rather than differences between PFTs which are more important in a modeling context. Nevertheless, our results appear to be consistent with the limited amount of information available. For example, Clarke *et al.* (2009) showed that shrubs were less likely to be resprouters than trees in a range of temperate ecosystems on the New England tablelands of Australia.

Our data set targeted sites from moderately warm, wet climates with intermediate levels of NPP. Nevertheless, even within this limited climate range, there are differences in the abundance of resprouters along moisture gradients with resprouting, and the expression of individual resprouting categories, declining towards more arid climates. This is also apparent in individual geographic regions, where the abundance of resprouting (and individual resprouting categories) is always highest in the wetter end of the climate gradient. Our analyses suggest that resprouting is less common in environments where MAP is <800 mm/year. A number of regional studies have shown that the number of resprouters increases with MAP in Australia. Pausas & Bradstock (2007), for example, showed that the number of taxa exhibiting resprouting increased along a rainfall gradient from 200-600 mm/year in southern Australia, while Russell-Smith *et al.* (2012) showed a similar increase in number of resprouters

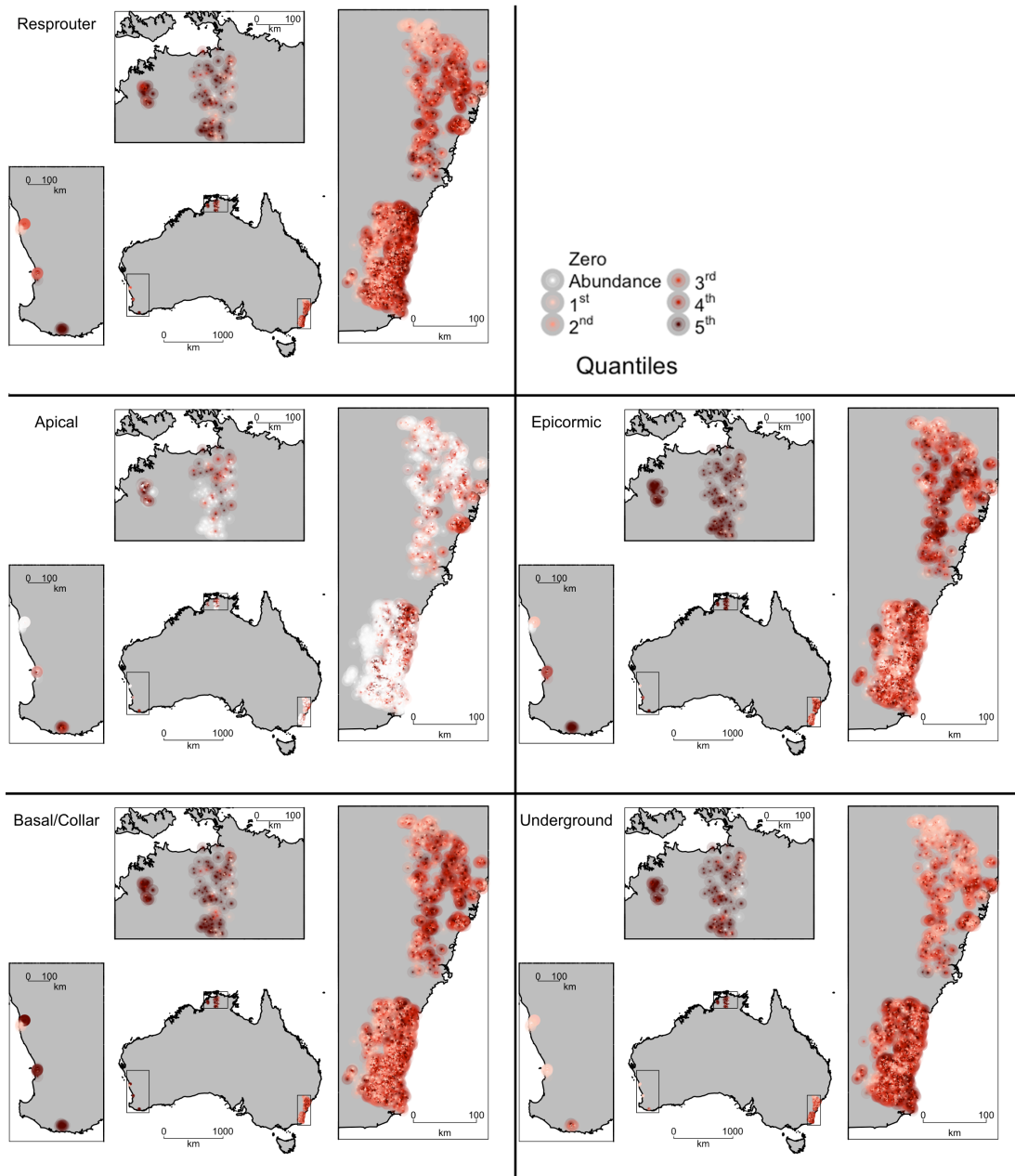


FIGURE 3.6: Abundance of resprouting trait categories, based on the abundance scores, in geographic space. The colour scale distinguishes the quintiles of the total range of each syndrome. The insets show each of the sampling regions in more detail.

along a rainfall gradient from 200-2000 mm/year in northern Australia. Our results are consistent with increases in taxon number with rainfall. However, the situation with respect to abundance is more complicated. Our data indicate that the abundance of resprouters declines when MAP > 1400 mm/year in non-seasonal climates, but there is no indication that this is the case in the seasonal climates of northern Australia where resprouters remain abundant at MAP > 1600 mm/year. Our analyses suggest that these differences emerge because the abundance of resprouters is ultimately controlled by the incidence of fire. Variation in climate space therefore reflects the influence of climate on the primary controls of fire, specifically fuel availability and fuel dryness (see e.g. Bistinas *et al.*, 2014). Other things being equal, increasing precipitation leads to increased productivity (and hence increased fuel availability) but also increases the wetness of the fuel and thus prevents fires from spreading. However, this is not the case in highly seasonal precipitation regimes, where increasing precipitation affects fuel production and availability but has limited or no impact on fuel drying. Thus, the abundance of resprouters continues to increase as precipitation increases in seasonal climates. The timing of seasonal precipitation also influences fuel production, with summer rainfall areas producing more grass (and hence fine fuel) than winter rainfall areas. Our analyses show that the abundance of resprouters is indeed higher in regions with summer rainfall (winter drought), consistent with the idea that abundance reflects the incidence of fire as determined by fuel production.

Clarke *et al.* (2013) have discussed a conceptual model of the distribution of different categories of resprouting with aridity, which suggests that epicormic and apical resprouting is confined to sub-humid to humid climates while basal/collar and underground resprouting occur more widely and persist even in arid climates. However, this analysis focuses on occurrence rather than changing abundance, and thus is not strictly comparable to the present study. The co-occurrence of the different categories of resprouting in humid climates is supported by our analysis. However, we find no evidence that the decline in abundance of basal/collar and underground resprouting with increasing aridity is different from the decline in the abundance of epicormic resprouting. It is possible that differences in the climate regimes of epicormic and basal/collar and underground resprouters would be more apparent if we had included data from more arid environments in the database.

Our attributions were made assuming that the ability to resprout is a taxon characteristic, and that this ability exists even when the taxon occurs in different parts of environmental or climatic space. The implication is that the expression of the trait is an emergent ecosystem property, and that variations in abundance therefore reflect successional stage (e.g. Bellingham & Sparrow, 2000) or environmental conditions (e.g. Wright *et al.*, 2004; Hollingsworth *et al.*, 2013). This assumption underpins the creation of trait-attribution tables and has been used in both morphological-trait (e.g. Meng *et al.*, 2009) and fire-trait analyses (e.g. Pausas *et al.*, 2004; Paula & Pausas, 2006). However, the fire-response trait assessments were based on field observations and/or anecdotal information, and thus may reflect the history of the site. Some taxa may have been classified as non-resprouters, for example, because they were observed in sites that have not experienced the environmental conditions that would give rise

to the expression of the resprouting trait. In general, the sites were chosen to be representative of mature ecosystems and the field assessments were made after the sites have been subjected to burns with close to 100% leaf scorch (following Gill, 1981; Gill & Bradstock, 1992). Thus, we think it unlikely that the trait is present in mature plants and is not captured in our allocations. However, the attribution of fire-response categories to all occurrences of the taxon means that the observed differences in abundance discussed here are a function of species replacement. The data cannot be used to investigate the degree of plasticity in species responses along environmental gradients (see e.g. Prentice *et al.*, 2011b; Kichenin *et al.*, 2013). Given that the degree to which resprouting is expressed within an ecosystem is likely to be affected by the severity and frequency of fire, it would be useful to compile site-based information on the expression of specific trait categories. This would require post-fire and/or experimental sampling as well as a standardized approach for recording fire severity.

The current version of the database allocates taxa to only a limited number of plant functional types. These PFTs were chosen to be congruent with PFTs used in global vegetation modeling, mostly the types used in the LPX model but including shrubs, dwarf shrubs and perennial forbs because these have been used in other models. This suite of PFTs is not ideal in terms of adequately characterizing fire relations. Woody or semi-woody climbing plants (i.e. lianas and climbers) are an important fuel source in particular ecosystems (e.g. Berry *et al.*, 2011). Fire behavior in northern and interior Australia is strongly influenced by the presence of tussock or hummock grasses and frequent fires increase the cover of such grasses (e.g. Prober *et al.*, 2007). The classification of grasses into C<sub>3</sub> and C<sub>4</sub> types does not map onto the tussock versus non-tussock classification: tussock grasses include both C<sub>3</sub> and C<sub>4</sub> grasses, and occur in both temperate and tropical climates (Moore, 1970). Future expansion of the set of PFTs included in the database will allow a more comprehensive investigation of the controls on fire responses across functional groups.

The existence of large, supra-regional trait databases permits a more rigorous investigation of trait-climate or trait-environment relationships than is possible from individual studies. The creation and exploitation of such databases for fire-related traits is comparatively recent (although see e.g. Pausas *et al.*, 2004; Vesk & Westoby, 2004). In addition to providing fundamental insights into the mechanisms allowing plants to survive in fire-prone habitats, such databases have a unique role in the parameterization and validation of process-based fire models. The database presented here already provides numerous targets for the evaluation of simulated abundances of fire-response syndromes in fire-enabled DGVMs (see e.g. Kelley *et al.*, 2014). Continued expansion of the current database would provide a valuable tool for the ecological and modeling communities.

**Acknowledgements.** This synthesis is a contribution to the ACEAS Working Group on Ecosystem vulnerability to changing fire regimes. Funding for the data compilation was provided by Macquarie University. DIK, GL and AH are supported by International Postgraduate Research Scholarships at Macquarie University. BM is supported by a fellowship from the Australian Research Council (DE130100434). The database is available from <http://bio.mq.edu.au/bcd/benchmarks/>. Some data from

the far southwest of Western Australia was collected as part of the Bushfire Cooperative Research Centre project while RSW was working for the Western Australian Department of Environment and Conservation.

### 3.6 References

- Arneth, A., Harrison, S.P., Zaehle, S., Tsigaridis, K., Menon, S., Bartlein, P.J., Feichter, H., Korhola, A., Kulmala, M., O'Donnell, D., Schurgers, S., Sorvari, S. & Vesala, T. (2010) Terrestrial biogeochemical feedbacks in the climate system. *Nature Geoscience*, 3, 525-532.
- Bellingham, P.J. & Sparrow, A.D. (2000) Resprouting as a life history strategy in woody plant communities, *Oikos*, 89, 409416.
- Berry, Z. C., Wevill, K., & Curran, T. J. (2011) The invasive weed Lantana camara increases fire risk in dry rainforest by altering fuel beds. *Weed Research*, 51, 525-533.
- Bistinas, I., Harrison, S.P., Prentice, I.C., & Pereira, J.M.C., 2014. Causal relationships vs. emergent patterns in the global controls of fire frequency. *Biogeosciences Discussions* 11: 3865-3892.
- Bond, W.J. & van Wilgen, B.W. (1996) Fire and Plants, pp. 263, Chapman & Hall, London, UK.
- Bowman, D.M.J.S., Balch, J.K., Artaxo, P., Bond, W.J., Cochrane, M.A., DAntonia, C.M., DeFries, R.S., Doyle, J.C., Harrison, S.P., Johnston, F.H., Keeley, J.E., Krawchuk, M.A., Kull, C.A., Marston, J.B., Moritz, M.A., Prentice, I.C., Roos, C.I., Scott, A.C., Swetnam, T.W., van der Werf, G.R. & Pyne, S.J. (2009) Fire in the earth system. *Science*, 324, 481-484.
- Bradstock, R.A. & Kenny, B.J. (2003) An application of plant functional types to fire management in a conservation reserve in southeastern Australia. *Journal of Vegetation Science*, 14, 345354.
- Buma, B., Brown, C.D., Donato, D.C., Fontaine, J.B. & Johnstone, J.F. (2013) The impacts of changing disturbance regimes on serotinous plant populations and communities. *Bioscience*. 63 doi:10.1525/bio.2013.63.11.5
- Clarke, P.J., Knox, K.J.E., Campbell, M.C., Copeland, L. (2009). Post-fire recovery of woody plants in the New England Tableland Bioregion. *Cunninghamia*, 11, 221239.
- Clarke, P.J., Lawes, M.J., Midgley, J.J., Lamont, B.B., Ojeda, F., Burrows, G.E., Enright, N.J. & Knox, K.J.E. (2013) Resprouting as a key functional trait: how buds,

- protection and resources drive persistence after fire. *New Phytologist*, 197, 1935.
- Dickinson, M.B., Jolliff, J. & Bova, A.S. (2004) Vascular cambium necrosis in forest fires: using hyperbolic temperature regimes to estimate parameters of a tissue response model. *Australian Journal of Botany*, 52, 757763.
- Edwards, A., Kennett, R., Price, O., Russell-Smith, J., Spiers, G. & Woinarski, J.C.Z. (2003) Monitoring the impacts of fire regimes on vegetation in northern Australia: an example from Kakadu National Park. *International Journal of Wildland Fire*, 12, 427-440.
- Enright, N.J., Fontaine, J.B., Lade, J.C., Miller, B.P., Westcott, V.C. (2011) Fire interval effects on persistence of resprouter species in Mediterranean-type shrublands. *Plant Ecology*, 212, 20712083.
- Gallego-Sala, A.V., Clark, J.M., House, J.I., Orr, H.G., Prentice, I.C., Smith, P., Farewell, T. & Chapman, S.J. (2010) Bioclimatic envelope model of climate change impacts on blanket peatland distribution in Great Britain. *Climate Research*, 45, 151-162.
- Gill, A.M. (1981) Adaptive responses of Australian vascular plant species to fires. *Fire and the Australian biota* (eds. Gill, A.M., Groves, R.H. & Noble, I.R.), pp. 243271. Australian Academy of Science, Canberra.
- Gill, A.M. & Bradstock, R.A. (1992) A national register for the fire responses of plant species. *Cunninghamia*, 2, 653660.
- Harrison, S.P., Prentice, I.C., Sutra, J-P., Barboni, D., Kohfeld, K.E. & Ni. J. (2010) Ecophysiological and bioclimatic foundations for a global plant functional classification. *Journal of Vegetation Science*, 21, 300-317.
- Heimann, M., Esser, G., Haxeltine, A., Kaduk, J., Kicklighter, D.W., Knorr, W., Kohlmaier, G.H., McGuire, A.D., Melillo, J., Moore III, B., Otto, R.D., Prentice, I.C., Sauf, W., Schloss, A., Sitch, S., Wittenberg, U. & Wrth, G. (1998) Evaluation of terrestrial carbon cycle models through simulations of the seasonal cycle of atmospheric CO<sub>2</sub>: First results of a model intercomparison study. *Global Biogeochemical Cycles*, 12, 1-24.
- Hollingsworth, T.N., Johnstone, J.F., Bernhardt, E.L. & Chapin, F.S. III (2013) Fire severity filters regeneration traits to shape community assembly in Alaskas boreal forest. *PLoS ONE*, 8, e56033, doi:10.1371/journal.pone.0056033.
- Keith, D. A. & Benson, D. H. (1988) The natural vegetation of the Katoomba 1:100 000 map sheet. *Cunninghamia*, 2, 107-143.

Kelley, D.I., Prentice, I.C., Harrison, S.P., Wang, H. & Willis, K. (2013) A comprehensive benchmarking system for evaluating dynamic global vegetation models. *Biogeosciences*, 10, 3313-3340.

Kelley, D.I., Harrison, S.P. & Prentice, I.C. (2014) Improved simulation of fire-vegetation interactions in the Land surface Processes and eXchanges Dynamic Global Vegetation Model (LPX-Mv1). *Geoscientific Model Development Discussions* 7: 1-70.

Kichenin, E., Wardle, D.A., Peltzer, D.A., Morse, C.W., Freschet, G.T. (2013) Contrasting effects of plant inter- and intraspecific variation on community-level trait measures along an environmental gradient. *Functional Ecology*, doi: 10.1111/1365-2435.12116.

Kloster, S., Mahowald, N.M., Randerson, J.T., Thornton, P.E., Hoffman, F.M., Levis, S., Lawrence, P.J., Feddema, J.J., Oleson, K.W. & Lawrence, D.M. (2010) Fire dynamics during the 20th century simulated by the Community Land Model. *Biogeosciences*, 7, 18771902.

Lawes, M.J., Richards, A., Dathe, J. & Midgley, J.J. (2011) Bark thickness determines fire resistance of selected tree species from fire-prone tropical savanna in north Australia. *Plant Ecology*, 212, 20572059.

Lees, J.M. (2013). GEOmap: Topographic and Geologic Mapping. R package version 2.1. Available at: <http://CRAN.R-project.org/package=GEOmap>

Lehmann, C.E.R., Prior, L.D. & Bowman, D.M.J.S. (2009) Decadal dynamics of tree cover in an Australian tropical savanna. *Austral Ecology*, 34, 601-612.

Lemon, J. (2006) Plotrix: a package in the red light district of R. *R-News*, 6, 8-12.

Lloret, F., Estevan, H., Vayreda, J. & Terradas, J. (2005) Fire regenerative syndromes of forest woody species across re and climate gradients. *Oecologia*, 146, 461468.

Meng, T., Ni, J. & Harrison, S.P. (2009) Plant morphometric traits and climate gradients in northern China: a meta-analysis using quadrat and flora data. *Annals of Botany*, doi: 10.1093/aob/mcp230.

Michaletz, S.T., Johnson, E.A. & Tyree, M.T. (2012) Moving beyond the cambium necrosis hypothesis of post-fire tree mortality: cavitation and deformation of xylem in forest fires. *New Phytologist*, 194, 254263.

Michna, P. (2012) RNetCDF: R Interface to NetCDF Datasets. Available at: <http://cran.r-project.org/package=RNetCDF>

- Moore, R.M. (Ed) (1970) Australian Grasslands, pp. 473. CSIRO Publications, Melbourne.
- Moritz, M.A., Parisien, M.-A., Batllori, E., Krawchuk, M.A., Van Dorn, J., Ganz, D.J. & Hayhoe, K. (2012) Climate change and disruptions to global fire activity. *Ecosphere*, 3, Article 49. Available at: <http://dx.doi.org/10.1890/ES11-00345.1>.
- Paula, S. & Pausas, J.G. (2006) Leaf traits and resprouting ability in the Mediterranean basin. *Functional Ecology*, 20, 941-947.
- Paula, S., Arianoutsou, M., Kazanis, D., Tavsanoglu, C., Lloret, F., Buhk, C., Ojeda, F., Luna, B., Moreno, J.M., Rodrigo, A., Espelta, J.M., Palacio, S., Fernández-Santos, B. & Fernandes, P.M. (2009) Fire-related traits for plant species of the Mediterranean basin. *Ecology*, 90, 14201420.
- Pausas, J.G. & Bradstock R.A. (2007) Fire persistence traits of plants along a productivity and disturbance gradient in Mediterranean shrublands of south-east Australia. *Global Ecology and Biogeography*, 16, 330340.
- Pausas, J.G., Bradstock, R.A., Keith, D.A. & Keeley, J.E. (2004) Plant functional traits in relation to fire in crown-fire ecosystems. *Ecology*, 85, 10851100.
- Pekin, B.K., Wittkuhn, R.S., Boer, M.M., Macfarlane, C. & Grierson, P.F. (2011) Plant functional traits along environmental gradients in seasonally dry and fire-prone ecosystem. *Journal of Vegetation Science*, 22: 10091020.
- Prentice, I.C., Sykes, M.T. & Cramer, W. (1993) A simulation model for the transient effects of climate change on forest landscapes. *Ecological Modelling*, 65, 51-70.
- Prentice, I.C., Kelley, D.I., Foster, P.N., Friedlingstein, P., Harrison, S.P. & Bartlein, P.J. (2011a) Modeling fire and the terrestrial carbon balance. *Global Biogeochemical Cycles*, 25, GB3005, doi:10.1029/2010GB003906.
- Prentice, I.C., Meng, T., Wang, H., Harrison, S.P., Ni, J. & Wang, G. (2011b) Evidence for a universal scaling relationship of leaf CO<sub>2</sub> drawdown along a moisture gradient. *New Phytologist*, 190, 169180.
- Prober, S.M., Thiele, K.R. & Lunt, I.D. (2007) Fire frequency regulates tussock grass composition, structure and resilience in endangered temperate woodlands. *Austral Ecology*, 32, 808824, doi: 10.1111/j.1442-9993.2007.01762.x
- R Core Team (2013) R: A Language and Environment for Statistical Computing, R Foundation for Statistical Computing, Vienna, Austria. Available at: <http://www.R-project.org/>

Riao, D., Ruiz, J., Isidoro, D., Ustin, S. (2007) Global spatial patterns and temporal trends of burned area between 1981 and 2000 using NOAA-NASA Pathfinder. *Global Change Biology*, 13, 4050.

Russell-Smith, J., Gardener, M.R., Brock, C., Brennan, K., Yates, C.P. & Grace, B. (2012) Fire persistence traits can be used to predict vegetation response to changing fire regimes at expansive landscape scales – an Australian example. *Journal of Biogeography*, 39, 1657–1668.

Vesk, P.A. & Westoby, M. (2004) Sprouting ability across diverse disturbances and vegetation types worldwide. *Journal of Ecology*, 92, 310–320.

Wang, H., Prentice, I.C. & Ni, J. (2013) Data-based modelling and environmental sensitivity of vegetation in China. *Biogeosciences*, 10, 5817–5830.

Wikum, D.A. & Shanholtzer, G.F. (1978) Application of the Braun-Blanquet cover-abundance scale for vegetation analysis. *Land Development Studies*, 2, 323–329.

Wright, I.J., Reich, P.B., Westoby, M., Ackerly, D.D., Baruch, Z., Bongers, F., Cavender-Bares, J., Chapin, T., Cornelissen, J.H.C., Diemer, M., Flexas, J., Garnier, E., Groom, P.K., Gulias, J., Hikosaka, K., Lamont, B.B., Lee, T., Lee, W., Lusk, C., Midgley, J.J., Navas, M.-L., Niinemets, U., Oleksyn, J., Osada, N., Poorter, H., Poot, P., Prior, L., Pyankov, V.I., Roumet, C., Thomas, S.C., Tjoelker, M.G., Veneklaas, E.J. & Villar, R. (2004) The worldwide leaf economics spectrum. *Nature*, 428, 821–827.

Xu, T. & Hutchinson, M.F. (2011) ANUCLIM Version 6.1: User Guide. Fenner School of Environment and Society, Australian National University, Australia.

### **3.S1 Supplementary Information**

The SI contains information on (a) the climate space sampled by the sites used in our analyses (Figure 3.S1), (b) definitions of the plant traits used in the database (Table 3.S1) and (c) correlations between climate variables in Australian climate space (Table 3.S2).

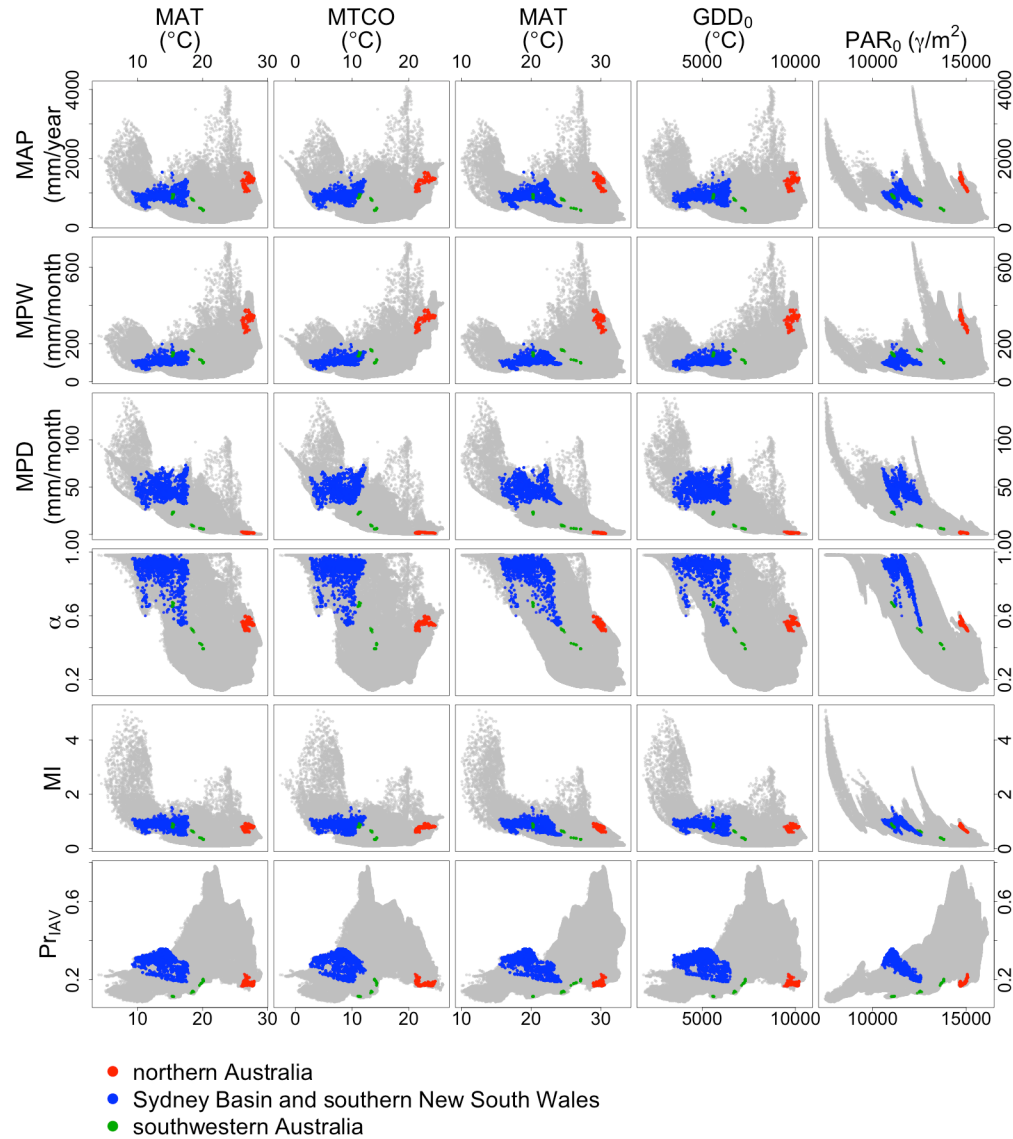


FIGURE 3.S1: The distribution of the sites used in this study in climate space. The grey dots represent all of the  $0.05^{\circ}$  grid cells covering Australia, while the coloured dots are the location of the sampled sites in climate space (red: sites from the Northern Territory, blue: sites from New South Wales; green: sites from Western Australia). The climate variables are arranged such that temperature and radiation-related variables are arranged in rows and the moisture-related variables in columns. The variables are: mean annual temperature (MAT), mean temperature of the coldest month (MTCO), mean temperature of the warmest month (MTWA), the accumulated temperature during the growing season as defined by a temperature threshold of  $0^{\circ}$  C, growing degree days ( $GDD_0$ ), photosynthetically-active radiation accumulated during the growing season, as defined by temperatures above  $0^{\circ}$  C ( $PAR_0$ ), mean annual precipitation (MAP), mean precipitation during the wettest month (MPW), mean precipitation during the driest month (MPD), the Cramer–Prentice index of plant-available moisture ( $\alpha$ ), a moisture index calculated as the ratio of MAP to total annual equilibrium evapotranspiration (MI) and interannual variability of rainfall ( $Pr_{IAV}$ ).

TABLE 3.S1: Definitions of the plant and fire-response traits and trait categories included in the database.

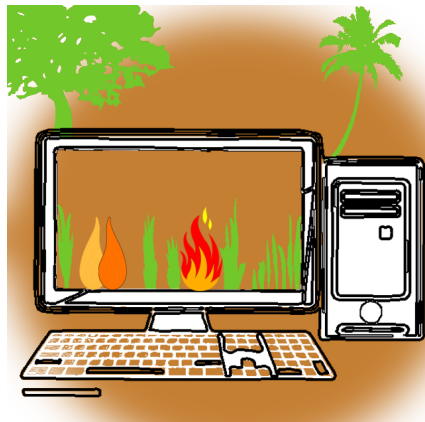
Trait	Definition
Resprouter	Plant that regenerates by sprouting after moderate fire damage
Apical resprouter	Plants that regenerate from an apical meristem, which is protected from fire damage by tightly clustered leaf primordial or leaf bases.
Epicormic resprouter	Plants that regenerate from an epicormic meristem which is protected by bark and/or woody tissue.
Basal/collar resprouter	Woody plants that regenerate from the base of the trunk, close to ground level, including lignotuberous plants
Underground resprouter	Plants that regenerate from roots or rhizomes, with the meristems protected from fire by soil.
Obligate seeder	Plant where regeneration from seed is triggered by fire, i.e. where seed release or seed germination requires heating and or chemical treatment associated with fire
Soil seedbank	Seeds stored in the soil for more than one year
Aerial seedbank	Seeds stored in the plant canopy
Single-stemmed tree	Woody plant, greater than 5m in height, with a single stem
Multi-stemmed tree	Woody plant, greater than 5m in height, with multiple stems
Tuft tree	Woody plant where the leaves grow from the top of a single unbranched stem. Examples include palms and grasstrees ( <i>Xanthorrhoea</i> )
Shrub	Woody plant, less than 5m high, and usually with multiple stems arising from close to the ground
Dwarf shrub (sub-shrub)	Shrub that is less than 50 cm high when fully mature, including those that have a prostrate habit
Perennial forb	Non-graminoid herbs, which are persistent for more than a year
C <sub>3</sub> grass	Member of the Poaceae, with C <sub>3</sub> photosynthesis
C <sub>4</sub> grass	Member of the Poaceae, with C <sub>4</sub> photosynthesis
Broadleaf	Functional leaves that are broad
Needleleaf	Needle-shaped leaves, typical of most gymnosperms
Scaleleaf	True scale leaves, leaves that are reduced highly reduced in size (picophyll) or functional leaves that are scale-like
Cold-deciduous	Plants that lose their leaves at least once a year, as either a temperature or day length response, including leaf exchangers
Drought-deciduous	Plants that lose their leaves in response to drought stress, i.e. are facultatively deciduous
Evergreen	Plants that maintain a full canopy all year round
Climatic range - tropical	Frost-free climates, with mean temperature of the coldest month (MTCO) > 15°C. Although expressed as climate, these correspond to physiological plant traits such as the presence/absence of specific cold tolerance mechanisms.
Climatic range – warm-temperate	Warm-winter climates, with MTCO > 5°C
Climatic range - temperate	Cold winter climates, with MTCO > -15°C

TABLE 3.S2: Regression analysis of climate, bioclimate and environmental variables. Inputs are the gridded values of these variables for all of the  $0.05^{\circ}$  gridcells covering Australia. Variables that are significantly correlated with one another ( $p < 0.005$ ) are shown in bold.

	MAT	MTWA	MTCO	GDD <sub>0</sub>	MAP	P <sub>φ</sub>	P <sub>e</sub>	P <sub>IAV</sub>	Dry <sub>φ</sub>	MPW	MPD	MI	EVI <sub>φ</sub>	EVI <sub>Pφ</sub>	EVI <sub>max</sub>	EVI <sub>min</sub>	PAR <sub>0</sub>	NPP	
MAT	0.83	0.86	1	0	0.69	0.41	0.1	0.12	0.62	0.18	0.14	0.09	0.24	0	0.11	0.09	0.11	0.76	0.16
MTWA	0.83	0.48	0.82	0.09	0.35	0.37	0.34	0.17	0.64	0.01	0.41	0.3	0.14	0.02	0.35	0.32	0.36	0.91	0.4
MTCO	0.86	0.48	0.86	0.09	0.82	0.32	0	0.08	0.46	0.45	0.01	0	0.22	0.02	0.01	0	0	0.43	0.02
GDD <sub>0</sub>	1	0.82	0.86	0	0.7	0.42	0.1	0.12	0.62	0.18	0.14	0.09	0.24	0	0.11	0.09	0.11	0.76	0.15
MAP	0	0.09	0.09	0	0.13	0	0.43	0.03	0.16	0.79	0.72	0.8	0.09	0.04	0.61	0.49	0.61	0.15	0.62
P <sub>φ</sub>	0.69	0.35	0.82	0.7	0.13	0.33	0	0.05	0.34	0.48	0	0.01	0.21	0.05	0	0.01	0	0.34	0
P <sub>e</sub>	0.41	0.37	0.32	0.42	0	0.33	0.12	0.09	0.26	0.07	0.06	0.02	0.17	0	0.04	0.05	0.05	0.35	0.05
P <sub>IAV</sub>	0.1	0.34	0	0.1	0.43	0	0.12	0.02	0.21	0.23	0.56	0.39	0.01	0.16	0.44	0.55	0.54	0.36	0.48
Dry <sub>φ</sub>	0.12	0.17	0.08	0.12	0.03	0.05	0.09	0.02	0.15	0	0.11	0.09	0.04	0.02	0.07	0.1	0.09	0.2	0.09
MPD	0.62	0.64	0.46	0.62	0.16	0.34	0.26	0.21	0.15	0	0.49	0.46	0.03	0	0.38	0.23	0.33	0.71	0.44
MPW	0.18	0.01	0.45	0.18	0.79	0.48	0.07	0.23	0	0	0.35	0.41	0.17	0.06	0.31	0.28	0.32	0	0.28
$\alpha$	0.14	0.41	0.01	0.14	0.72	0	0.06	0.56	0.11	0.49	0.35	0.77	0.01	0.06	0.79	0.68	0.81	0.49	0.89
MI	0.09	0.3	0	0.09	0.8	0.01	0.02	0.39	0.09	0.46	0.41	0.77	0.02	0.02	0.62	0.45	0.59	0.39	0.65
EVI <sub>φ</sub>	0.24	0.14	0.22	0.24	0.09	0.21	0.17	0.01	0.04	0.03	0.17	0.01	0.02	0.03	0.01	0.01	0	0.15	0
EVI <sub>Pφ</sub>	0	0.02	0	0.02	0	0.04	0.05	0	0.16	0.02	0	0.06	0.02	0.03	0	0.35	0.11	0.03	0.04
EVI <sub>min</sub>	0.11	0.35	0.01	0.11	0.61	0	0.04	0.44	0.07	0.38	0.31	0.79	0.62	0.01	0	0.65	0.9	0.4	0.87
EVI <sub>max</sub>	0.09	0.32	0	0.09	0.49	0.01	0.05	0.55	0.1	0.23	0.28	0.68	0.45	0.01	0.35	0.65	0.89	0.38	0.76
EVI	0.11	0.36	0	0.11	0.61	0	0.05	0.54	0.09	0.33	0.32	0.81	0.59	0	0.11	0.9	0.89	0.43	0.92
PAR <sub>0</sub>	0.76	0.91	0.43	0.76	0.15	0.34	0.35	0.36	0.2	0.71	0	0.49	0.39	0.15	0.03	0.4	0.38	0.43	0.46
NPP	0.16	0.4	0.02	0.15	0.62	0	0.05	0.48	0.09	0.44	0.28	0.89	0.65	0	0.04	0.87	0.76	0.92	0.46

PATTERNS IN THE ABUNDANCE OF POST-FIRE RESPROUTING IN AUSTRALIA BASED  
124 ON PLOT-LEVEL MEASUREMENTS.

---



# 4

## Improved simulation of fire-vegetation interactions in the Land surface Processes and eXchanges dynamic global vegetation model (LPX-Mv1)

---

D. I. Kelley<sup>1</sup>, S. P. Harrison<sup>1,2</sup>, I. C. Prentice,<sup>1,3</sup>

<sup>1</sup>Biological Sciences, Macquarie University, North Ryde, NSW 2109, Australia

<sup>2</sup>Geography & Environmental Sciences, School of Archaeology, Geography & Environmental Sciences, University of Reading, Whiteknights, Reading, RG6 6AB, UK.

<sup>3</sup>AXA Chair of Biosphere & Climate Impacts, Grantham Institute for Climate Change & Dept of Life Sciences, Imperial College, Silwood Park, Ascot, SL5 7PY, UK

---

**This chapter is presented as the published journal article:**

Kelley, D. I., Harrison, S. P. and Prentice, I. C.: Improved simulation of fire-vegetation interactions in the Land surface Processes and eXchanges Dynamic Global Vegetation Model (LPX-Mv1), Geoscientific Model Development. 7, 2411-2433, 2014

**Paper and reviewers discussion available at:**

[www.geosci-model-dev.net/7/2411/2014/](http://www.geosci-model-dev.net/7/2411/2014/)

---

Reproduced under Creative Commons Attribution 3.0 License courtesy of Copernicus Publications on behalf of the European Geosciences Union (EGU).

---

Geosci. Model Dev., 7, 2411–2433, 2014  
www.geosci-model-dev.net/7/2411/2014/  
doi:10.5194/gmd-7-2411-2014  
© Author(s) 2014. CC Attribution 3.0 License.



Geoscientific  
Model Development  
Open Access



## Improved simulation of fire–vegetation interactions in the Land surface Processes and eXchanges dynamic global vegetation model (LPX-Mv1)

D. I. Kelley<sup>1</sup>, S. P. Harrison<sup>1,2</sup>, and I. C. Prentice<sup>1,3</sup>

<sup>1</sup>Department of Biological Sciences, Macquarie University, North Ryde, NSW 2109, Australia

<sup>2</sup>Geography & Environmental Sciences, School of Archaeology, Geography and Environmental Sciences (SAGES), University of Reading, Whiteknights, Reading, RG6 6AH, UK

<sup>3</sup>AXA Chair of Biosphere and Climate Impacts, Grantham Institute for Climate Change and Department of Life Sciences, Imperial College, Silwood Park Campus, Ascot SL5 7PY, UK

Correspondence to: D. I. Kelley (douglas.kelley@students.mq.edu.au)

Received: 30 October 2013 – Published in Geosci. Model Dev. Discuss.: 23 January 2014

Revised: 16 July 2014 – Accepted: 25 July 2014 – Published: 16 October 2014

**Abstract.** The Land surface Processes and eXchanges (LPX) model is a fire-enabled dynamic global vegetation model that performs well globally but has problems representing fire regimes and vegetative mix in savannas. Here we focus on improving the fire module. To improve the representation of ignitions, we introduced a treatment of lightning that allows the fraction of ground strikes to vary spatially and seasonally, realistically partitions strike distribution between wet and dry days, and varies the number of dry days with strikes. Fuel availability and moisture content were improved by implementing decomposition rates specific to individual plant functional types and litter classes, and litter drying rates driven by atmospheric water content. To improve water extraction by grasses, we use realistic plant-specific treatments of deep roots. To improve fire responses, we introduced adaptive bark thickness and post-fire resprouting for tropical and temperate broadleaf trees. All improvements are based on extensive analyses of relevant observational data sets. We test model performance for Australia, first evaluating parameterisations separately and then measuring overall behaviour against standard benchmarks. Changes to the lightning parameterisation produce a more realistic simulation of fires in southeastern and central Australia. Implementation of PFT-specific decomposition rates enhances performance in central Australia. Changes in fuel drying improve fire in northern Australia, while changes in rooting depth produce a more realistic simulation of fuel availability and

structure in central and northern Australia. The introduction of adaptive bark thickness and resprouting produces more realistic fire regimes in Australian savannas. We also show that the model simulates biomass recovery rates consistent with observations from several different regions of the world characterised by resprouting vegetation. The new model (LPX-Mv1) produces an improved simulation of observed vegetation composition and mean annual burnt area, by 33 and 18 % respectively compared to LPX.

### 1 Introduction

The Land surface Processes and eXchanges (LPX) dynamic global vegetation model (DGVM) incorporates fire through a coupled fire module (Prentice et al., 2011) as fire is a major agent in vegetation disturbance regimes (Bond and Van Wilgen, 1996) and contributes to changes in interannual atmospheric carbon fluxes (van der Werf et al., 2008; Prentice et al., 2011). In common with several other fire models (e.g. Arora and Boer, 2005; Kloster et al., 2010; Thonicke et al., 2010; Li et al., 2012; Prentice et al., 2011; Pfeiffer et al., 2013), LPX explicitly simulates lightning ignitions, fuel load, susceptibility to burning, fire spread and fire-induced mortality. However, it does not consider anthropogenic ignitions because the dependencies of such ignition on population density, used as a basis for such ignitions in other

models, have been shown to be unrealistic (Prentice et al., 2011; Bistinas et al., 2014). LPX realistically simulates fire and vegetation cover globally but performs relatively poorly in grassland and savanna ecosystems (Kelley et al., 2013) – areas where fire is particularly important for maintaining vegetation diversity and ecosystem structure (e.g. Williams et al., 2002; Lehmann et al., 2008; Biganzoli et al., 2009). Specifically:

- LPX produces sharp boundaries between areas of high burning and no burning in tropical and temperate regions. These sharp fire boundaries produce sharp boundaries between grasslands and closed-canopy forests. The unrealistically high fire-induced tree mortality prevents the development of vegetation characterised by varying mixtures of tree and grass plant functional types (PFTs) that are characteristic of more open forests, savannas and woodlands.
- LPX simulates too little fire in areas of high but seasonal rainfall because fuel takes an unrealistically long time to dry, and because LPX fails to produce open woody vegetation in these areas.
- In arid areas, where fire is limited by fuel availability, LPX simulates too much net primary production (NPP) resulting in unrealistically high fuel loads and generating more fire than observed.

To address these shortcomings in the version of LPX running at Macquarie University (here termed LPX-M), we re-parameterised lightning ignitions, fuel moisture, fuel decomposition, plant adaptations to arid conditions via rooting depth, and woody plant resistance to fire through bark thickness. In each case, the new parameterisation was developed based on extensive data analysis. We tested each parameterisation separately, and then all parameterisations combined, using a comprehensive benchmarking system (Kelley et al., 2013) which assesses model performance against observations of key vegetation and fire processes. We then included a new treatment of woody plant recovery after fire through resprouting – a behavioural trait that increases post-fire competitiveness compared to non-resprouters in fire-prone areas (Clarke et al., 2013) and thus affects the speed of ecosystem recovery with major implications for the carbon cycle – and tested the impact of introducing this new component on model performance. In this paper, we begin by describing the basic fire parameterisations in LPX (Sect. 2) and then go on to explain how these parameterisations were changed in LPX-Mv1 (Sect. 3) before evaluating whether these new data-derived parameterisations improve the simulation of vegetation patterns and fire regimes (Sect. 4).

## 2 LPX model description

LPX is a plant-functional-type (PFT)-based model. Nine PFTs are distinguished by a combination of life form (tree, grass) and leaf type (broad, needle), phenology (evergreen, deciduous) and climate range (tropical, temperate, boreal) for trees and photosynthetic pathway ( $C_3$ ,  $C_4$ ) for grasses. PFTs are represented by a set of parameters. Each PFT that occurs within a grid cell is represented by an “average” plant, and ecosystem-level behaviour is calculated by multiplying the simulated properties of this average plant by the simulated number of individuals in the PFT in that grid cell. PFT-specific properties (e.g. establishment, mortality and growth) are updated annually, but water and carbon-exchange processes are simulated on shorter time steps.

LPX incorporates a process-based fire scheme (Fig. 1) run on a daily time step (Prentice et al., 2011). The LPX fire scheme is modified from the Spread and Ignitions FIRE model (SPITFIRE; Thonicke et al., 2010). In this section, we describe those aspects of the LPX fire model that appear to contribute to poor simulation of fire regimes in Australia (and likely other semiarid regions) and which we have re-examined and re-parameterised on the basis of data analyses (see Sect. 3). Ignition rates are derived from a monthly lightning climatology, interpolated to the daily time step. The number of lightning strikes that reach the ground (cloud to ground; CG) is specified as 20 % of the total number of strikes (Thonicke et al., 2010). The CG lightning is split into dry ( $CG_{dry}$ ) and wet strikes based on the fraction of wet days in the month ( $P_{wet}$ ):

$$CG_{dry} = CG \cdot (1 - P_{wet}^\beta), \quad (1)$$

where  $\beta$  is a parameter tuned to 0.00001. “Wet” lightning is not considered to be an ignition source (Prentice et al., 2011). Lightning is finally scaled down by 85 % to allow for discontinuous current strikes. Numerical precision limits of the compiled code means the function described by Eq. (1) effectively removes all strikes in months with more than two wet days in LPX. Monthly “dry” lightning is distributed evenly across all dry days.

Fuel loads are generated from litter production and decay using the vegetation dynamics algorithms in LPJ (Lund-Potsdam-Jena; Sitch et al., 2003). LPX does not simulate competition between  $C_3$  and  $C_4$  grasses explicitly; in grid cells where  $C_3$  and  $C_4$  grasses co-exist, the total NPP is estimated as the potential NPP of each grass type in the absence of the other type and this produces erroneously high NPP. This problem can be corrected by scaling the foliage projective cover (FPC) and leaf area index (LAI) of each grass PFT by the ratio of total simulated grass leaf mass of both PFTs to the leaf mass expected if only one grass PFT was present (B. Stocker, personal communication, 2012). This was done in LPX-Mv1.

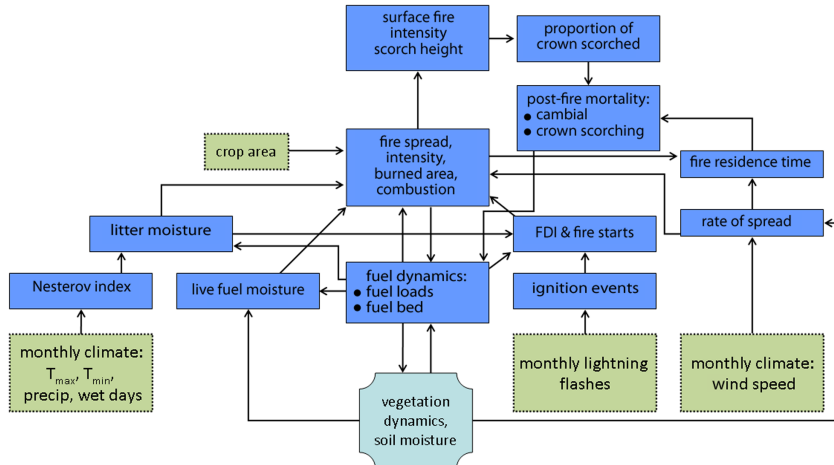


**Figure 1.** Description of the structure of the fire component of LPX, reproduced from Prentice et al. (2011). Inputs to the model are identified by green boxes, outputs from the vegetation dynamics component of the model are identified by light blue boxes, and internal processes and exchanges that are explicitly simulated by the fire component of the model are identified by blue boxes. FDI is the Nesterov Fire Danger Index.

Fuel decomposition rate ( $k$ ) depends on temperature and moisture, and is the same for all PFTs and fuel structure types:

$$k = k_{10} \cdot g(T) \cdot f(w), \quad (2)$$

where  $k_{10}$  is a decomposition rate at a reference temperature of 10 °C, set to 35 % each year;  $g(T)$  describes the response to monthly mean soil temperature ( $T_{\text{soil}, m}$ ) described by Lloyd and Taylor (1994):

$$g(T) = \begin{cases} e^{308.56 \cdot \left( \frac{1}{36.02} - \frac{1}{T_{\text{soil}, m} + 46.02} \right)}, & \text{if } T_{\text{soil}, m} \geq -40 \\ 0, & \text{otherwise,} \end{cases} \quad (3)$$

and  $f(w)$  is the moisture response to the top layer soil water content ( $w$ ) described by Foley (1995):

$$f(w) = 0.25 + 0.75 \cdot w, \quad (4)$$

where  $w$  is in fractional water content.

The litter is allocated to four fuel categories based on litter size as described by Thonicke et al. (2010):

- *1 h fuel* – which represents leaves and small twigs, is the leaf and herb mass plus 4.5 % of the litter that comes from tree heart- and sapwood.
- *10 h fuel* – representing small branches, is 7.5 % of the litter from heart- and sapwood.
- *100 h fuel* – large branches, is 21 % of the litter that comes from heart- and sapwood.
- *1000 h fuel* – boles and trunks, is the remaining 67 % of the litter that comes from heart- and sapwood.

The hour designation represents the decay rate of fuel moisture, and is equal to the amount of time for the moisture of the fuel to become  $(1 - 1/\exp) = 63\%$  closer to the moisture of its surroundings (Albini, 1976; Anderson et al., 1982).

In LPX, litter drying rate is described by the cumulative Nesterov fire danger index (NI; Nesterov, 1949) as described by Running (1987), and a fuel-specific drying rate parameter ( $\alpha_{\text{xhr}}$ ; Venevsky et al., 2002) which was tuned to provide the best results against fire observations (Thonicke et al., 2010). NI is cumulated for each consecutive day with rainfall  $\leq 3$  mm, and is calculated using maximum daily temperature ( $T_{\text{max}}$ ) and an approximation of dew point temperature:

$$T_{\text{dew}} = T_{\text{min}} - 4, \quad (5)$$

where  $T_{\text{min}}$  is the daily minimum temperature and both  $T_{\text{min}}$  and  $T_{\text{max}}$  are in degrees Celcius.

Daily precipitation is simulated based on monthly precipitation and fractional wet days using a simple weather generator (Gerten et al., 2004), and the diurnal temperature range is calculated from daily maximum and minimum temperature interpolated from monthly data.

Fire spread, intensity and residence time are based on weather conditions and fuel moisture, and calculated using the Rothermel equations (Rothermel, 1972). Fire intensity and residence time influence fire mortality via crown scorching and cambial damage.

The amount of cambial damage is determined by fire intensity and residence time in relation to bark thickness, with thicker bark offering protection for longer fire residence times. Bark thickness (BT) is calculated as a linear function of tree diameter at breast height (DBH), with specific slope

and intercept values for each PFT:

$$BT = a + b \cdot DBH. \quad (6)$$

The values of  $a$  and  $b$  can be found in Thonicke et al. (2010).

The probability of mortality from cambial damage ( $P_m$ ) is calculated from the fire residence time ( $\tau_l$ ) and a critical time till cambial damage ( $\tau_c$ ) based on bark thickness:

$$P_m(\tau) = \begin{cases} 0, & \text{if } \frac{\tau_l}{\tau_c} \leq 0.22 \\ 0.563 \cdot \frac{\tau_l}{\tau_c} - 0.125, & \text{if } 0.22 \leq \frac{\tau_l}{\tau_c} \leq 2 \\ 1, & \text{if } \frac{\tau_l}{\tau_c} \geq 2 \end{cases} \quad (7)$$

and

$$\tau_c = 2.9 \cdot BT^2, \quad (8)$$

where  $\tau$  is the ratio  $\tau_l / \tau_c$ . Both  $\tau_l$  and  $\tau_c$  are in minutes and BT is in centimetres.

LPX uses a two-layer soil model. The water content of the upper (50 cm) layer is the difference between throughfall (precipitation – interception) and evapotranspiration (ET), and runoff and percolation to the lower soil layer. Water content in the lower 1 m layer is the difference between percolation from the upper layer, transpiration from deep roots and runoff (Gerten et al., 2004). The upper soil layer responds more rapidly to changes in inputs, whereas the water content of the lower soil layer is generally more stable. The fraction of roots in each soil layer is a PFT-specific parameter.

### 3 Changes to the LPX-M fire module

Improvements to the LPX-M fire module focussed on re-parameterisation of lightning ignitions, fuel drying rate, fuel decomposition rate, rooting depth, and the introduction of adaptive bark thickness and of resprouting. The improvements are based on analyses of large-scale regional and/or global data sets, and are therefore generic. Although we focus on Australia for model evaluation, we have made no attempt to tune the new parameterisations using Australian observations.

#### 3.1 Lightning ignitions

Regional studies have shown that the CG proportion of total lightning strikes varies between 0.1 and 50 % of total strikes. This variability has been related to latitude (Price and Rind, 1993; Pierce, 1970; Prentice and Mackerras, 1977), storm size (Kuleshov and Jayaratne, 2004), total flash count (Boccippio et al., 2001), and topography (Boccippio et al., 2001; de Souza et al., 2009). We compared remotely sensed data on total flash counts (i.e. intercloud, or IC, plus CG) from the Lightning Imaging Sensor (LIS – Christian et al., 1999; Christian, 1999, <http://grip.nsstc.nasa.gov/>) with the

National Lightning Detection Network Database (NLDN) records of lightning ground-strikes (CG) for the contiguous United States (see <http://thunderstorm.vaisala.com/> for information; Cummins and Murphy, 2009), for each month in 2005 at the 0.5° resolution of LPX. These analyses were confined to south of 35° N, a limitation imposed by satellite coverage of the total strikes (Christian et al., 1999).

The LIS observed each cell for roughly 90 s during each overpass, with 11–21 overpasses each month depending on latitude (Christian et al., 1999), and therefore only represents a sample of the total lightning. Overpasses for each 0.5° cell have a time stamp for the start and end of each overpass, along with detection efficiency and total observation time, which allows for observational blackouts. We scaled the flash count from each overpass for detection efficiency and the ratio of observed to total overpass time. These scaled flash counts were summed for each month, to give monthly recorded total lightning (RL), which includes both cloud to cloud and cloud to ground strikes (i.e. IC + CG).

NLDN registered each ground lightning strike separately with a time stamp accurate to 1/1000th of a second, which allowed us to calculate the number of ground-registered NLDN strikes for each LIS overpass. This number of ground strikes was then scaled for a universal detection efficiency of 90 % (Boccippio et al., 2001; Cummins and Murphy, 2009), and summed up for the month, to give monthly recorded CG strikes (RG). The CG fraction was taken as RG/RL. Total flash count ( $L$ ) was calculated by scaling the total ground registered lightning for each month by the CG fraction. The relationship between fractional CG and total lightning was determined using non-linear least squares regression, testing for both power and exponential functions. The best (Fig. 2a) was given by

$$CG = L \cdot \min(1, 0.0408 \cdot L^{-0.4180}), \quad (9)$$

where  $L$  is in flash km<sup>-2</sup> day<sup>-1</sup>. We also tested topography and topographic complexity, calculated from topographic data from WORLDCLIM (Hijmans et al., 2005). These variables were not significantly related to the observed CG fraction, and so we have not included them as predictors in the new parameterisation.

We examined the relationship between CG strikes and the daily distribution of precipitation using the Climate Prediction Center (CPC) US Unified Precipitation data (Higgins and Centre, 2000; Higgins et al., 1996) provided by the NOAA/OAR/ESRL PSD (Physical Sciences Division), Boulder, Colorado, USA (<http://www.esrl.noaa.gov/psd/>). Days are classified as dry if there was zero precipitation. We used data for every month of 2005, this time covering the whole of the contiguous United States. We used generalised linear modelling (GLM; Hastie and Pregibon, 1992) to compare CG<sub>dry</sub> to  $P_{wet}$  and monthly precipitation from CPC and the Climate Research Unit (CRU) TS3.1 data set (Harris et al., 2013), as well as temperature from CRU TS3.1

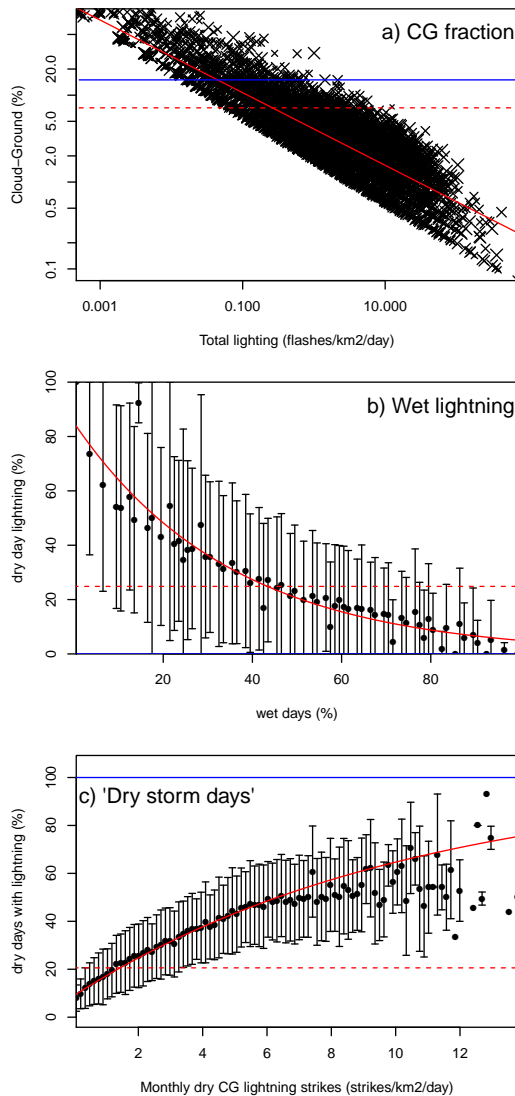


**Figure 2.** Observed relationships between (a) total and cloud-to-ground lightning flashes, (b) the percentage of dry lightning with respect to the number of wet days per month, and (c) percentage of dry days with lightning with respect to monthly dry lightning strikes. These analyses are based on the LIS remotely sensed data set (Christian et al., 1999; Christian, 1999) and NLDN ground observation of lightning strikes (Cummins and Murphy, 2009) for North America. The red line shows the best fit used by LPX-Mv1, the red dotted line shows the mean of the observations, and the blue line shows the relationship used in LPX. To aid visualisation, observations were binned every 1% (b) or 0.1 strikes (c) along the x axis, with the dots showing the mean of each bin and the error bars showing the standard deviations.

(Harris et al., 2013).  $P_{\text{wet}}$  from both CPC and CRU were the best and only significant predictors. Using CPC for consistency, the best relationship for  $\text{CG}_{\text{dry}}$  (Fig. 2b) was

$$\text{CG}_{\text{dry}} = 0.85033 \cdot \text{CG} \cdot e^{-2.835 \cdot P_{\text{wet}}}, \quad (10)$$

where  $\text{CG}_{\text{dry}}$  is the number of strikes on days with zero precipitation, and  $P_{\text{wet}}$  is the amount of precipitation on days with rain. We determined a new parameter for the fraction of dry days with lightning strikes (“dry storm days”) by comparing the fraction of dry days in CPC when lightning occurred ( $P_{\text{dry, lightn}}$ ) with  $\text{CG}_{\text{dry}}$  calculated in Eq. (10) (Fig. 2c). The analysis was performed using the same spatial domain as the analysis of  $\text{CG}_{\text{dry}}$ . The best relationship with the least squared residuals (Fig. 2c) was

$$P_{\text{dry lightn}} = 1 - \frac{1}{1.099 \cdot (\text{CG}_{\text{dry}} + 1)^{94.678.69}}. \quad (11)$$

The results of these analyses were used in the new parameterisation of lightning in LPX-Mv1. IC lightning was removed by applying Eq. (9), where  $L$  is taken from the monthly lightning climatology inputs. Wet lightning was removed from the remaining CG strikes by applying Eq. (10). A sensitivity test including lightning on wet days shows that such ignitions have little impact or degrade the simulation of burnt area (see Supplement). The remaining  $\text{CG}_{\text{dry}}$  was distributed evenly onto the number of dry days defined by Eq. (11). The dry lightning days were selected randomly from the days without precipitation as determined by the weather generator (Gerten et al., 2004). Polarity affects the duration of lightning pulses, with negative polarity more likely to produce discontinuous pulses that are insufficient to raise the temperature to ignition point. This discontinuous current lightning was removed at the same constant rate as in LPX because there are no data sets that would allow analyses on which to base a re-parameterisation.

Pfeiffer et al. (2013) have argued that interannual variability in lightning is important, especially in high-latitude regions with relatively few fires, and have introduced this in a version of LPJ (LPJ-LMfire v1.0) based on a scaling with convective available potential energy (CAPE). This idea was adopted from Peterson et al. (2010), who demonstrated that the probability of lightning occurring on a dry day varies interannually with CAPE. However, LPJ-LMfire (v1.0) does not contain a treatment of dry lightning nor “storm days”, so the approach taken there is parallel to ours. Murray et al. (2012) have shown that interannual variability in total flash count (i.e. standard deviation of IC + CG) is < 10 % in tropical and temperate regions. This, and the fact that the LIS data set only covers a period of 10 yr and that it is not obvious how to extrapolate lightning under a changing climate, means that we have retained the use of a lightning climatology for total lightning in LPX-Mv1, but with seasonally and interannually varying treatments of dry lightning and dry storm days.

### 3.2 Fuel drying

The formulation of fuel drying in LPX results in drying times that are too slow in most tropical and temperate regions. Under stable and dry weather conditions with a  $T_{\max}$  of 30 °C and  $T_{\text{dew}}$  of 0 °C, for example, 1 h fuel in LPX would take 25 h to lose 63 % of its moisture, 10 h fuel would take roughly 20 days, 100 h fuel would take 2 months, and 1000 h fuel would take 3 yr. The approximation of  $T_{\text{dew}}$  used in LPX has been shown to be too high in arid and semiarid areas, and during dry periods in seasonal climates (Friend, 1998; Running, 1987), which also contributes to slower-than-expected drying. Additionally, given that the moisture content is calculated cumulatively, a sequence of days with < 3 mm of rain could result in complete drying of fuel, no matter what the moisture content of the air.

In order to improve this formulation, we replace the description of fuel moisture content in LPX with one based on the moisture content of the air. As fuel types are distinguished by the time it takes for fuel to come into equilibrium with the surroundings, this new formulation is consistent with the definition of fuel types. Fuel moisture decays towards an “equilibrium moisture content” ( $m_{\text{eq}}$ ) at a rate that matches the definition of the fuel class (i.e. 1 h fuel takes 1/24th of a day to become 63 % closer to  $m_{\text{eq}}$ ):

$$m_{x,d} = \frac{m_{\text{eq}}}{100} + \left( m_{x,d-1} - \frac{m_{\text{eq}}}{100} \right) \cdot e^{-24/x}, \quad (12)$$

where  $m_{x,d}$  is the daily moisture content of fuel size in each drying-time class ( $x$ ) with a moisture decay rate of  $24/x$ ; and  $m_{x,d-1}$  is the moisture content on the previous day.

There are several choices of fuel equilibrium models that could be used for  $m_{\text{eq}}$ , with variation in the magnitude of the  $m_{\text{eq}}$  response to relative humidity ( $H_R$ ), particularly at extremes (i.e.  $H_R \rightarrow 0, 100\%$ ), and the potential for opposite responses to temperature depending on weather conditions (Sharples et al., 2009; Viney, 1991). Viney (1991) attributed this variation to the choice of fuel type for which each model was calibrated. We chose the model described by Van Wagner and Pickett (1985) for  $m_{\text{eq}}$  as it has been calibrated against multiple fuel types (Van Wagner, 1972) and is designed to be more accurate at both high and low  $H_R$  (Sharples et al., 2009; Viney, 1991):

$$m_{\text{eq}} = \begin{cases} m_{\text{eq},1} + m_{\text{eq},2} + m_{\text{eq},3}, & \text{if } Pr_d \leq 3 \text{ mm} \\ 100, & \text{otherwise,} \end{cases} \quad (13)$$

where

$$m_{\text{eq},1} = 0.942 \cdot (H_R^{0.679}), \quad (14)$$

$$m_{\text{eq},2} = 0.000499 \cdot e^{0.1 \cdot H_R}, \quad (15)$$

$$m_{\text{eq},3} = 0.18 \cdot (21.1 - T_{\max}) \cdot (1 - e^{-0.115 \cdot H_R}). \quad (16)$$

$H_R$  is calculated using the August–Roche–Magnus approximation (Lawrence, 2005), which has been shown to be

accurate for  $T_{\text{dew}}$  of between 0 and 50 °C and for  $T_{\max}$  between 0 and 60 °C (Lawrence, 2005):

$$H_R = 100 \cdot \frac{e^{17.271 \cdot T_{\text{dew}} / (237.7 + T_{\text{dew}})}}{e^{17.271 \cdot T_{\max} / (237.7 + T_{\max})}}. \quad (17)$$

We use a new formulation for  $T_{\text{dew}}$  derived from information from 20 weather stations across the United States (Kimball et al., 1997):

$$T_{\text{dew},k} = T_{\min,k} \cdot (-0.127 + 1.121 \cdot W_{\text{EF}} + 0.0006 \cdot \Delta T), \quad (18)$$

where  $T_{\text{dew},k}$  is the daily dew point temperature in Kelvin;  $\Delta T$  is the difference between daily  $T_{\max}$  and  $T_{\min}$ , and  $W_{\text{EF}}$  is given by

$$W_{\text{EF}} = (1.003 - 1.444 \cdot EF + 12.312 \cdot EF^2 - 32.766 \cdot EF^3), \quad (19)$$

where EF is the ratio of daily potential evapotranspiration ( $PET_d$ ) – calculated as described in Gerten et al. (2004) – and annual precipitation ( $Pr_a$ ):

$$EF = PET_d / Pr_a. \quad (20)$$

Kimball et al. (1997) showed that this approximation of  $T_{\text{dew}}$  improved the correlation with  $T_{\text{dew}}$  measurements by 20 % when tested against 32 independent weather stations, with  $T_{\text{dew}}$  showing differences of up to 20 °C in semiarid and arid climates. The more conventional assumption that  $T_{\text{dew}} = T_{\min} - 4$  would thus result in higher dew-point temperatures and slower fuel-drying rates. Although we have replaced the formulation of fuel-drying rate, including the formulation of  $T_{\text{dew}}$ , we continue to use the NI to describe the likelihood of an ignition starting a fire in LPX-Mv1.

### 3.3 Fuel decomposition

Fuel decomposition rates vary with the size and type of material (Cornwell et al., 2008, 2009; Weedon et al., 2009; Chave et al., 2009). Brokvkin et al. (2012) analysed decomposition rates derived from the TRY plant trait database (Kattge et al., 2011, <http://www.try-db.org/TryWeb/About.php>) and showed that there was an order of magnitude difference in the decomposition rates of wood and leaf/grass litter. Thus, grass decomposes at an average rate of 94 % per year, while wood decomposes at a rate of 5.7 % per year. The rate of both leaf and wood decomposition varies between PFTs to a lesser extent than between wood and grass, although the variation is still significant (Brokvkin et al., 2012), with leaf decomposition ranging between 76 and 120 %, and wood between 3.9 and 10.4 % per year (Table 1). Brokvkin et al. (2012) also showed that the decomposition rates of woody material are not moisture dependent.

We have implemented the PFT-specific relationships found by Brokvkin et al. (2012), for woody ( $k_{10,\text{wood}}$  for 10–1000 h fuel – see Table 1) and leaf ( $k_{10,\text{leaf}}$  for 1 h fuel – see

**Table 1.** PFT-specific values used in LPX-Mv1. TBE denotes tropical broadleaf evergreen tree, TBD denotes tropical broadleaf deciduous tree, tBE denotes temperate broadleaf evergreen tree, and tBD temperate broadleaf deciduous tree. Values for RS variants of each of these PFTs are given in brackets. If no resprouting value is given then the resprouting PFT takes the normal PFT value. tNE denotes temperate needleleaf evergreen; BNE denotes boreal needleleaf evergreen; BBD denotes boreal broadleaf deciduous; C<sub>3</sub> denotes grasses using the C<sub>3</sub> photosynthetic pathway; and C<sub>4</sub> denotes grasses using the C<sub>4</sub> photosynthetic pathway. BT par<sub>i</sub> is the bark thickness parameter used in Eqs. (25) and (26); k<sub>10,leaf</sub> and k<sub>10,wood</sub> are the reference litter decomposition rates of leaf and grass used in Eq. (2); and Q<sub>10</sub> is the parameter describing woody litter decomposition rate changes with temperature in Eq. (21).

	TBE	TBD	tNE	tBE	tBD	BNE	BBD	C <sub>3</sub>	C <sub>4</sub>	Source
Fraction of roots in upper soil layer	0.80	0.70	0.85	0.80	0.80	0.85	0.80	0.90	0.85	Sect. 3.4; Table 2; Fig. 3
BT par <sub>lower</sub>	0.00395 (0.0292)	0.00463 (0.0109)	0.00609 (0.0286)	0.0125 (0.0106)	0.00617 (0.0106)	0.0158	0.00875	N/A	N/A	Sect. 3.5;
BT par <sub>mid0</sub>	0.0167 (0.0629)	0.0194 (0.0568)	0.0257 (0.0586)	0.0302 (0.0343)	0.0230 (0.0343)	0.0261	0.0316	N/A	N/A	Table S1; Fig. 4
BT par <sub>upper</sub>	0.0399 (0.183)	0.0571 (0.188)	0.0576 (0.156)	0.0909 (0.106)	0.0559 (0.106)	0.0529	0.112	N/A	N/A	
k <sub>10,leaf</sub>	0.93	1.17	0.70	0.86	0.95	0.78	0.94	1.20	0.97	Sect. 3.3;
k <sub>10,wood</sub>	0.039	0.039	0.041	0.104	0.104	0.041	0.104	N/A	N/A	Brovkin et al. (2012)
Q <sub>10</sub>	2.75	2.75	1.97	1.37	1.37	1.97	1.37	N/A	N/A	

Table 1) litters. We use a relationship between decomposition and temperature for woody fuel that removes the soil moisture dependence in LPX:

$$k_{\text{wood}} = k_{10,\text{wood}} \cdot Q_{10}^{(T_{m,\text{soil}} - 10)/10}. \quad (21)$$

Q<sub>10</sub> is the PFT-specific temperature response of wood decomposition described in Table 1 and k<sub>10,wood</sub> is the decomposition rate at a reference temperature of 10 °C. Leaf decomposition still follows Eq. (2).

### 3.4 Rooting depth

There are inconsistencies in the values used in LPX for the fraction of deep roots specified for each PFT. For example, the fraction of deep roots specified for C<sub>4</sub> grasses (20 %) is greater than the fraction specified for tropical broadleaf evergreen trees (15 %), even though trees have deeper roots than grasses (Schenk and Jackson, 2005). Additionally, benchmarking against arid grassland and desert litter production shows that simulated fine-litter production is roughly 250 % greater than observations. Having a high proportion of deep roots allows plants to survive more arid conditions, thanks to a more stable water supply in deep soil.

We re-examined the PFT-specific values assigned to rooting fraction using site-based data for the cumulative rooting fraction depth from Schenk and Jackson (2002a, b, 2005). In the original publications, life form, leaf type, leaf phenology and the cause of leaf fall (i.e. cold or drought) were recorded for each site. This allowed us to classify sites into LPX PFTs as shown in Table 2. The original data source does not distinguish different types of grassland. We therefore separated these sites into warm (C<sub>4</sub> dominated) and cool (C<sub>3</sub> dominated) grasslands depending on their location and climate. Sites were classified as warm grasslands if they occurred in

locations where the mean temperature of the coldest month (MTCO) was > 15.5 °C and to cool grasslands where MTCO was ≤ 15.5 °C as in Harrison et al. (2010). MTCO for each site was based on average conditions for 1970–2000 derived from the CRU TS3.1 data set (Harris et al., 2013).

The rooting-depth data set gives the cumulative fraction depth of 50 (D<sub>50</sub>) and 95 % (D<sub>95</sub>) of the roots at a site. These were used to calculate the cumulative root fraction at 50 cm (i.e. the fraction in the upper soil layer):

$$R_{50\text{cm}} = 1/(1 + (0.5/D_{50}^c)), \quad (22)$$

where

$$c = \frac{\log 0.5/0.95}{\log D_{95}/D_{50}}. \quad (23)$$

We derived Eqs. (22) and (23) by re-arranging Eq. (1) in Schenk and Jackson (2002b).

The PFT-specific (Fig. 3) fraction of deep roots (DR<sub>pft</sub>) is then implemented as

$$\text{DR}_{\text{pft}} = 1 - \text{mean}(R_{50\text{cm},\text{pft}}). \quad (24)$$

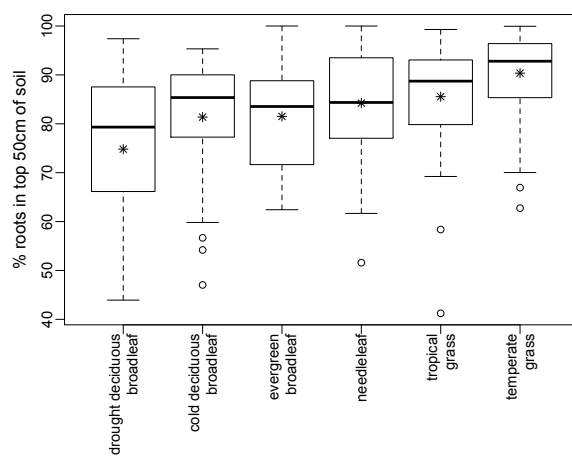
See Table 1 for new parameter values.

### 3.5 Bark thickness

There is considerable variability in bark thickness between different tree species (Halliwell and Apps, 1997; Fyllas and Patino, 2009; Paine et al., 2010), such that it is unrealistic to prescribe a single constant value for the relationship between bark thickness and stem diameter within a PFT. Furthermore, bark thickness within related species appears to vary as a function of environmental conditions, and most particularly with fire frequency (Brando et al., 2012; Climent

**Table 2.** Translation between LPX PFTs and the vegetation trait information available for sites which were used to provide rooting depths.

LPX PFT	Rooting depth vegetation type from Fig. 3	Site leaf type	Site phenology	Site climate	Site life form
TBE tBE	Evergreen broadleaf	Broad only	Evergreen	Any	Tree only
TBD	Drought deciduous broadleaf	Broad only	Drought deciduous	Any	Tree only
tBD BBB	Cold deciduous broadleaf	Broad only	Cold/winter deciduous	Any	Tree only
tNE BNE	Needle leaf	Needle only	Any	Any	Tree only
C <sub>3</sub> Grass	Cold grassland	Any	Any	MTCO $\leq$ 15.5 °C	Grass or herb
C <sub>4</sub> Grass	Warm grassland	Any	Any	MTCO > 15.5 °C	Grass or herb

**Figure 3.** Proportion of roots in the upper 50 cm of the soil by PFT. The data were derived from Schenk and Jackson (2002a, 2005) and reclassified into the PFT recognised by LPX as shown in Table 2.

et al., 2004; Cochrane, 2003; Lawes et al., 2011a). Thus, at an ecosystem level, bark thickness is an adaptive trait.

We assess the relationship between bark thickness and stem diameter based on 13 297 measurements from 1364 species (see Supplement for information on the studies these were obtained from). The species were classified into PFTs based on their leaf type, phenology and climate range (Table S1 in the Supplement); in cases where this was not provided by the original data contributors, we used information from trait databases, floras and the literature (e.g. Kauffman, 1991; Greene et al., 1999; Bellingham and Sparrow, 2000; Williams, 2000; Bond and Midgley, 2001; Del Tredici, 2001; Pausas et al., 2004; Paula et al., 2009; Lunt et al., 2011). The climate range was based on the overall range of the species, not derived from the climate of the sites.

For each PFT, we calculated the best fit and the 5–95 % range (Koenker, 2013, Fig. 4) using the simple linear relationship:

$$BT_i = \text{par}_i \cdot DBH, \quad (25)$$

where  $i$  is either the best fit (mid) or in the 5–95 % (lower–upper) range. Values for  $\text{par}_i$  are given in Table 1.

We define a probability distribution of bark thicknesses for each PFT using a triangular relationship defined by the 5 and 95 % limits of the observations (Fig. 4):

$$T(BT) = \begin{cases} 0, & \text{if } BT \leq BT_{\text{lower}} \\ T_1(BT), & \text{if } BT_{\text{lower}} \leq BT \leq BT_{\text{mid}}, \\ T_2(BT), & \text{if } BT_{\text{mid}} \leq BT \leq BT_{\text{upper}}, \\ 0, & \text{if } BT \geq BT_{\text{upper}} \end{cases}, \quad (26)$$

where  $BT_{\text{lower}}/BT_{\text{upper}}/BT_{\text{mid}}$  are the upper/lower/mid range of BT for a given DBH, calculated using Eq. (25), with  $\text{par}_i$  values in Table 1; and

$$T_1(BT) = \frac{2 \cdot (BT - BT_{\text{lower}})}{(BT_{\text{upper}} - BT_{\text{lower}}) \cdot (BT_{\text{mid}} - BT_{\text{lower}})}, \quad (27)$$

$$T_2(BT) = \frac{2 \cdot (BT_{\text{upper}} - BT)}{(BT_{\text{upper}} - BT_{\text{lower}}) \cdot (BT_{\text{upper}} - BT_{\text{mid}})}. \quad (28)$$

The distribution is initialised using  $\text{par}_i$  values in Table 1.  $\text{par}_{\text{lower}}$  and  $\text{par}_{\text{upper}}$  remain unchanged from the initial value (Table 1).  $\text{par}_{\text{mid}}$  changes after a fire event, based on the bark thickness of surviving plants. It will also change with establishment, when the post-establishment value represents the weighted average of the bark thickness of new and existing plants (Fig. 5).

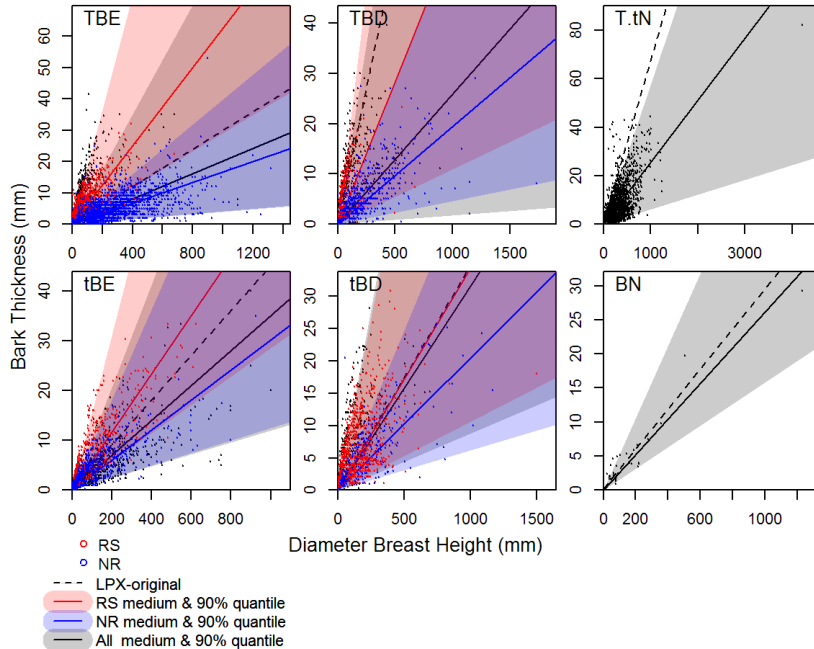


**Figure 4.** BT vs. DBH for each LPX PFT. Red dots show data used to constrain BT parameters in Table 1 for RS PFTs in LPX-Mv1-rs; blue dots show data from NR PFTs in LPX-Mv1-rs. Red, blue and grey dots are used to distinguish the PFTs in LPX-Mv1-nr. Red and blue lines show best fit lines. Red/blue shaded areas show 90 % quantile ranges. Black line/shaded area shows the best fit and 90 % range for all points. The black dotted line is the relationship used in LPX-M.

The average bark thickness of trees surviving fire is dependent on the current state of  $T(BT)$  and  $P_m$  given in Eq. (7), and is calculated by solving the following integrals:

$$BT_{\text{mean}} = \frac{N_* \cdot \int_{BT_{\text{lower}}}^{BT_{\text{upper}}} BT \cdot (1 - P_m(\tau)) \cdot T(BT) dB\tau}{N}, \quad (29)$$

where  $N_*$  is the number of individuals before the fire event and  $N$  the number of individuals that survive the fire, given by

$$N = N_* \cdot \int_{BT_{\text{lower}}}^{BT_{\text{upper}}} (1 - P_m(\tau)) \cdot T(BT) dB\tau, \quad (30)$$

where  $\tau$  is the ratio  $\tau_1/\tau_c$ .

A new midpoint of the distribution,  $BT_{\text{mid}}$ , is calculated from  $BT_{\text{mean}}$ :

$$BT_{\text{mid}} = 3 \cdot BT_{\text{mean}} - BT_{\text{lower}} - BT_{\text{upper}}. \quad (31)$$

The updated  $par_{\text{mid}}$  value is calculated from the fractional distance between  $BT_{\text{mid}}$  before the fire event ( $BT_{\text{mid}}^*$ ), and  $BT_{\text{upper}}$ :

$$par_{\text{mid}} = par_{\text{mid}}^* + BT_{\text{mid,frac}} \cdot (p_{\text{upper}} - p_{\text{mid}}^*), \quad (32)$$

where  $p_{\text{mid}}^*$  was  $p_{\text{mid}}$  before the fire event and

$$BT_{\text{mid,frac}} = \frac{BT_{\text{mid}} - BT_{\text{mid}}^*}{BT_{\text{upper}} - BT_{\text{mid},0}^*}. \quad (33)$$

Newly established plants have a bark thickness distribution ( $E(BT)$ ) described by Eq. (26) based on the initial  $p_{\text{mid},0}$  given in Table 1. Post-establishment  $BT_{\text{mean}}$  is calculated as the average of pre-establishment  $T(BT)$  and  $E(BT)$ , weighted by the number of newly established ( $m$ ) and old individuals ( $n$ ):

$$BT_{\text{mean}} = \frac{\int_{BT_{\text{lower}}}^{BT_{\text{upper}}} BT \cdot (n \cdot T(BT) + m \cdot E(BT)) dB\tau}{n + m}. \quad (34)$$

The new  $par_{\text{mid}}$  is calculated again using Eqs. (31) and (32). In cases where no trees survive fire,  $T(BT)$  is set to its initial value when the PFT re-establishes.

### 3.6 Resprouting

Many species have the ability to resprout from below-ground or above-ground meristems after fire (Clarke et al., 2013). Resprouting ensures rapid recovery of leaf mass, and thus conveys a competitive advantage over non-resprouting species which have to regenerate from seed. Post-fire recovery in ecosystems that include resprouting trees is fast, with

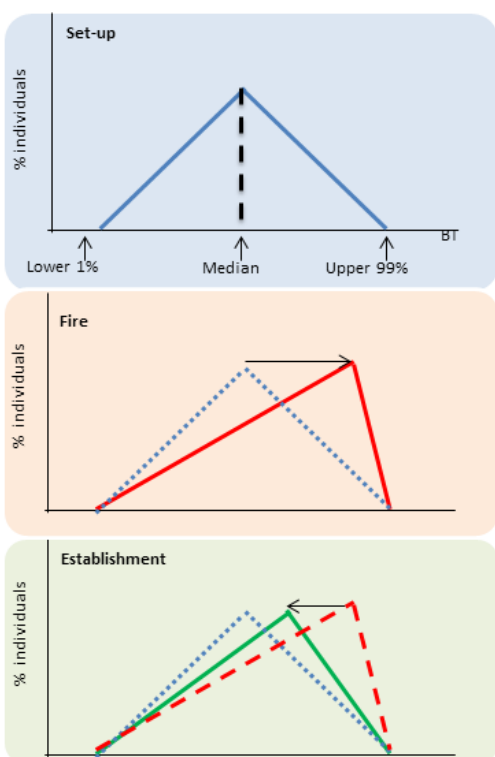


**Figure 5.** Illustration of the variable bark thickness scheme. The initial set-up is based on parameter values (Table 1) obtained from Fig. 4. Fire preferentially kills individual plants with thin bark, changing the distribution towards individuals with thicker bark. Establishment shifts the distribution back towards the initial set-up.

ca. 50 % of leaf mass being recovered within a year and full recovery within ca. 5–7 yr (Viedma et al., 1997; Calvo et al., 2003; Casady, 2008; Casady et al., 2009; Gouveia et al., 2010; van Leeuwen et al., 2010; Gharun et al., 2013, see Fig. 7 and Table S3 in the Supplement).

However, species that resprout from aerial tissue (apical or epicormic resprouters in the terminology of Clarke et al., 2013) either need to have thick bark (see e.g. Midgley et al., 2011) or some other morphological adaptation to protect the meristem (e.g. see Lawes et al., 2011a, b). Investment in resprouting appears to be at the cost of seed production: in general, resprouting trees produce much less seed and therefore have a lower rate of post-disturbance establishment than non-resprouters (Midgley et al., 2010).

Aerial resprouting is found in both tropical and temperate trees, regardless of phenology (Kaufmann and Hartmann, 1991; Bellingham and Sparrow, 2000; Williams, 2000; Bond and Midgley, 2001; Del Tredici, 2001; Paula et al., 2009). It is very uncommon in gymnosperms (Del Tredici, 2001; Paula et al., 2009; Lunt et al., 2011) and does not seem to be promoted by fire in deciduous broadleaf trees in boreal

climates (Greene et al., 1999). We therefore introduced resprouting variants of four PFTs in LPX-Mv1: tropical broadleaf evergreen tree (TBE), tropical broadleaf deciduous tree (TBD), temperate broadleaf evergreen tree (tBE), and temperate broadleaf deciduous tree (tBD). Parameter values were assigned to be the same as for the non-resprouting variant of each PFT, except for BT and establishment rate.

The species used in the bark thickness analysis were categorised into aerial resprouters, other resprouters and non-resprouters (see Table S1 in the Supplement) based on field observations by the original data contributors, trait databases (e.g. <http://www.landmanager.org.au>; Kattge et al., 2011; Paula et al., 2009) or information in the literature (e.g. Harrison et al., 2014; Malanson and Westman, 1985; Pausas, 1997; Dagit, 2002; Tapias et al., 2004; Keeley, 2006).

Resprouting is facultative, and whether it is observed in a given species at a given site may depend on the fire regime and fire history of that site. Any species that was observed to resprout in one location was assumed to be capable of resprouting, even if it was classified as a non-resprouter in some studies. The range of BT for each resprouting (RS) PFT was calculated as in Sect. 3.5 (see Fig. 4 and Table 1). The range of BT was also re-assigned for their non-resprouting (NR) counterparts using species classified as having no resprouting ability.

The BT and post-fire mortality of RS PFTs is calculated in the same way as for NR PFTs. The allocation of fire-killed material in RS PFTs to fuel classes is also the same as for NR PFTs. However, after fire events, the RS PFTs are not killed, as described in Eq. (7), but allowed to resprout. The new average plant for RS PFTs is calculated as the average of trees not affected by fire and fire-affected trees RS trees.

Seeding recruitment after disturbance is contingent on many environmental factors. Few studies have compared post-disturbance seedling recruitment by resprouters and non-resprouters, and there is no standardised reporting of environmental conditions or responses in those studies that do exist. However, most studies show that post-disturbance (and particularly post-fire) recruitment by resprouters is lower than by non-resprouters (see e.g. Table S2 in the Supplement). Some studies show no differences in initial recruitment (e.g. Knox and Clarke, 2006), although non-resprouters may show strategies that ensure more recruitment over a number of years (e.g. Zammit and Westoby, 1987). More systematic studies are required to characterise quantitatively the difference between resprouters and non-resprouters, but it would appear that reducing the recruitment of resprouters to ca. 10 % of that of non-resprouters is conservative. We therefore set the establishment rate of all resprouting PFTs to 10 % of that of the equivalent non-resprouting PFTs.

#### 4 Model configuration and test

Each change in parameterisation was implemented and evaluated separately. For each change, the model was spun-up using detrended climate data from the period 1950–2000 and the standard lightning climatology (following the protocol outlined in Prentice et al., 2011) until the carbon pools were in equilibrium. The length of the spin-up varies but is always more than 5000 yr. After spin-up, the model was run using a monthly lightning climatology from the Lightning Imaging Sensor–Optical Transient Detector high-resolution flash count ([http://gcmd.nasa.gov/records/GCMD\\_lohrmc.html](http://gcmd.nasa.gov/records/GCMD_lohrmc.html)), time-varying climate data derived from the CRU (Mitchell and Jones, 2005) and National Centers for Environmental Prediction (NCEP) reanalysis wind (NOAA Climate Diagnostics Center, Boulder, Colorado; <http://www.cdc.noaa.gov/>) data sets as described in Prentice et al. (2011). We took the opportunity to correct an error in the NCEP wind inputs used by Kelley et al. (2013) but, given that this correction was made for all of LPX-Mv1 runs, this change has no impact on the differences caused by the new parameterisations.

We used the benchmarking system of Kelley et al. (2013) to evaluate the impacts of each change on the simulation of fire and vegetation processes. This benchmarking system quantifies differences between model outputs and observations using remotely sensed and ground observations of a suite of vegetation and fire variables and specifically designed metrics to provide a “performance score”. We make the comparison only for the continent of Australia, since this is a highly fire-prone region (van der Werf et al., 2008; Giglio et al., 2010; Bradstock et al., 2012) and was the worst simulated in the original model (see Kelley et al., 2013). We used the benchmark observational data sets described in Kelley et al. (2013), with the exception of CO<sub>2</sub> concentrations, runoff, GPP (gross primary production) and NPP. There are too few data points (< 10) from Australia in the runoff, GPP and NPP data sets to make comparisons statistically meaningful. We did not use the CO<sub>2</sub> concentrations because this requires global fluxes to be calculated.

We have expanded the Kelley et al. (2013) benchmarking system to include Australia-specific data sets for production and fire (Table 3). To benchmark production, we compared modelled 1 h fuel production to the Vegetation and Soil-carbon Transfer (VAST) fine-litter production data set for Australian grassland ecosystems (Barrett, 2001). Kelley et al. (2013) provide a burnt area benchmark based on the third version of the Global Fire Database (GFED3; Giglio et al., 2010). This has recently been updated (GFED4; Giglio et al., 2013). We re-gridded the data for the period (i.e. the period for which we have climate data to drive the LPX-Mv1 simulations) to 0.5° resolution to serve as a benchmark for the model simulations, although we continue to use GFED3 for comparison with results from Kelley et al. (2013). We also use a burnt area product for southeastern Australia based on

ground observations of the extent of individual fires during the fire year (July–June) for the period from July 1970 to June 2009 on a 0.001° grid (Bradstock et al., 2014). These data were re-gridded to 0.5° resolution for annual average and interannual comparisons with simulated burnt area for July 1996–June 2005.

The difference between simulation and observation was assessed using the metrics described in Kelley et al. (2013). Annual average and interannual comparisons were conducted using the normalised mean error metric (NME). Seasonal length was benchmarked by calculating the concentration of the variable in one part of the year for both model and observations, and comparing these concentrations with NME. Possible scores for NME run from 0 to  $\infty$ , with 0 being a perfect match. Changes in NME are directly proportional to the change in model agreement to observations, therefore a percentage of improvement or degradation in model performance is obtained from the ratio of the original model to the new model score. NME takes a value of 1 when agreement is equal to that expected when the mean value of all observations is used as the model. Following Kelley et al. (2013), we describe model scores greater/less than 1 as better/worse than the “mean null model” and we also use random resampling of the observations to develop a second “randomly resampled” null model. Models are described as better/worse than randomly resampled if they were less/more than two standard deviations from the mean randomised score. The values for the randomly resampling null model for each variable are listed in Table 4.

For comparisons using NME, removing the influence of first the mean, and then the mean and variance, of both simulated and observed values allowed us to assess the performance of the mapped range and spatial (for annual average and season length comparisons) or temporal (for interannual) patterns for each variable using NME.

We used the mean phase difference (MPD) metric to compare the timing of the season and the Manhattan metric (MM; Gavin et al., 2003; Cha, 2007) to compare vegetation type cover (Kelley et al., 2013). Both these metrics take the value 0 when the model agrees perfectly with the data. MPD has a maximum value of 1 when the modelled seasonal timing is completely out of phase with observations; whereas MM scores 2 when there is a perfect disagreement. Scores for the mean and random resampling null models for MM and MPD comparisons are given in Table 4.

The metric scores for each simulation were compared with the scores obtained with the original LPX (Table 5). Because many of the fire parameterisations in LPX were tuned to provide a reasonable simulation of fire, implementing individual improvements to these parameterisations can lead to a degradation of the simulation – we therefore use the performance scores for individual parameterisation changes only to help interpret the overall model performance. We only introduced resprouting after the other re-parameterisations had been made. The run that includes all the new parameterisations

**Table 3.** Summary description of the benchmark data sets.

Data set	Variable	Type	Period	Comparison	Reference
GFED4	Fractional burnt area	Gridded	1996–2005	Annual average, seasonal phase and concentration, interannual variability	Giglio et al. (2013)
GFED3	Fractional burnt area	Gridded	1996–2005	Annual average, seasonal phase and concentration, interannual variability	Giglio et al. (2010)
SE ground observations	Fractional burnt area	Gridded	1996–2005	Annual average	Bradstock et al. (2014)
VAST	Above-ground fine-litter production	Site	1996–2005	Annual average, interannual variability	Barrett (2001)
ISLSCP II vegetation continuous fields	Vegetation fractional cover	Gridded	Snapshot 1992/1993	Fractional cover of bare ground, herbaceous and tree; tree cover split into evergreen or deciduous, and broadleaf or needleleaf	DeFries and Hansen (2009)
SeaWiFS	Fraction of absorbed photosynthetically active radiation (fAPAR)	Gridded	1998–2005	Annual average, seasonal phase and concentration, interannual variability	Gobron et al. (2006)
Canopy height	Annual average	Gridded	2005	Direct comparison	Simard et al. (2011)

except resprouting is termed LPX-Mv1-nr and the run including resprouting is termed LPX-Mv1-rs.

#### 4.1 Testing the formulation of resprouting

To assess the response of vegetation to the presence/absence of resprouting, we ran both LPX-Mv1-rs and LPX as described above for southeastern Australia woodland and forest ecosystems with  $\geq 20\%$  wood cover as determined by the International Satellite Land-Surface Climatology Project (ISLSCP) II vegetation continuous field (VCF) remotely sensed data set (Hall et al., 2006; DeFries and Hansen, 2009) (Fig. 8). Normal fire regimes were simulated until 1990, when a fire was forced burning 100% of the grid cells, and killing (or causing to resprout, in the case of RS PFTs) 60% of the plants. Fire was stopped for the rest of the simulation to assess recovery from this fire. As the proportion of individuals killed was fixed, this experiment only tested the RS scheme and not factors affecting mortality. The LPX simulation therefore serves as a test for NR PFTs in LPX-Mv1 as well. The simulated total FPC in the post-fire years was compared against site-based remotely sensed observations of interannual post-fire greening following fire in fire-prone sites with Mediterranean or humid subtropical vegetation from several different regions of the world (Table S3), split into sites dominated by either RS and other fire adapted vegetation (normally obligate seeders – OS) as defined in Sect. 3.6 based on the dominant species listed in each study (Table S3 in the Supplement). (The use of observations from other

regions of the world reflects the lack of observations of post-fire recovery in Australia.) We also used studies from boreal areas with low fire frequency to examine the response in ecosystems where fire-response traits are uncommon (Table S3 in the Supplement). The comparison between simulated and observed regeneration was performed using a simple regeneration index (RI) that describes the percentage of recovery of lost normalised difference vegetation index (NDVI) at a given time,  $t$ , after an observed fire:

$$RI_t = 100 \cdot \frac{QVI_t - \min(QVI_{\text{postfire}})}{\overline{QVI}_{\text{prefire}}}, \quad (35)$$

where  $QVI_t$  is the ratio of the vegetation index (VI) of the burnt areas at time  $t$  after a fire compared to that of either an unburnt control site or, in studies where a control site was not used, the average VI of the years immediately preceding the fire;  $\min(QVI_{\text{postfire}})$  is the minimum QVI in the years immediately following the fire; and  $\overline{QVI}_{\text{prefire}}$  is the average QVI in the years immediately preceding the fire. NDVI was the most commonly used remotely sensed VI in the studies used for comparison. FPC has a linear relationship against NDVI (Purevdorj et al., 1998). However, this relationship differs between grass and woody plants (Xiao and Moody, 2005). As NDVI is normalised when used in Eq. (35), a direct conversion from FPC to NDVI is not necessary. Instead, we scaled for the different contributions from tree and grass, defining  $NDVI_{\text{sim}}$  based on the statistical model described in Sellers et al. (1996) and Lu and Shuttleworth (2002) (see

## D. I. Kelley et al.: Parameterisation of fire in LPX1 vegetation model

2423

**Table 4.** Scores obtained using the mean of the data (data mean), and the mean and standard deviation (SD) of the scores obtained from randomly resampled null model experiments (Bootstrap mean, Bootstrap SD). Step 1 is a straight comparison; 2 is a comparison with the influence of the mean removed; and 3 is with mean and variance removed. The scores given for fire represent the range of scores over all fire data sets for that comparison. Scores for individual data sets can be found in Table S4 in the Supplement.

Variable	Step	Measure	Time period	Mean	Bootstrap mean	Bootstrap SD
Fire: All Aus.	1	Annual average	1997–2006	1.00	1.14–1.25	0.0028–0.015
	2			1.00	1.24–1.26	0.0037–0.015
	3			1.00	1.28–1.30	0.0053–0.016
	2	IAV		1.00	1.31–1.50	0.34–0.36
	1	Seasonal concentration		1.00	1.33–1.36	0.02–0.043
	N/A	Phase		0.39–0.45	0.44–0.47	0.0015–0.0046
	1	Annual average		1.00	1.18–1.19	0.024–0.026
	2			1.00	1.10–1.19	0.024–0.027
	3			1.00	1.20–1.21	0.024–0.025
	2	IAV		1.00	1.24–1.32	0.33–0.37
Fire: SE Aus.	1	Seasonal concentration		1.00	1.31–1.33	0.043–0.053
	N/A	Phase		0.44–0.47	0.47	0.010–0.011
Veg. cover	N/A	Life forms	1992–1993	0.71	0.89	0.0018
	N/A	Tree cover		0.43	0.54	0.0015
	N/A	Herb cover		0.49	0.66	0.0017
	N/A	Bare ground		0.46	0.56	0.0017
	N/A	Broadleaf		0.83	0.96	0.0041
	N/A	Evergreen		0.70	0.87	0.0032
Fine-litter NPP	1	Annual average	1997–2005	1.00	1.44	0.21
	2			1.00	1.44	0.22
	3			1.00	1.43	0.095
	1	Annual average	1997–2005	1.00	1.33	0.015
	2			1.00	1.33	0.015
fAPAR	3			1.00	1.32	0.014
	2	IAV		1.00	1.23	0.32
	3			1.00	1.35	0.36
	1	Seasonal Conc		1.00	1.46	0.014
	2			1.00	1.46	0.014
	3			1.00	1.45	0.014
	N/A	Phase		0.30	0.38	0.0033
	1	Annual average	2005	1.00	1.32	0.016
	2			1.00	1.32	0.016
	3			1.00	1.31	0.016
Height						

Supplement, Eqs. S1–S4):

$$\text{NDVI}_{\text{sim}} = \text{FPC}_{\text{tree}} + 0.32 \cdot \text{FPC}_{\text{grass}}, \quad (36)$$

where  $\text{FPC}_{\text{tree}}$  is the fractional cover of trees and  $\text{FPC}_{\text{grass}}$  of grasses.

A site or model simulation was considered to have recovered when vegetation cover reached 90 % of the pre-fire cover (i.e. when  $\text{RI} = 90\%$ ). Recovery times for each site are listed in Table S3. Note that RI is a measure of the recovery of vegetation cover, not recovery in productivity or biomass. If a site or model simulation failed to recover before the end of the study, the recovery point was calculated by extending RI forward by fitting the post-fire data from the

site to

$$\text{RI} = 100 \cdot \left( 1 - \frac{1}{1 + p \cdot t} \right), \quad (37)$$

where  $p$  is the fitted parameter. The contribution of each site to the estimated mean and standard deviation of recovery time for a range of fire-adapted ecosystems was weighted based on the time since the last observation (Table S3 in the Supplement). Sites that have observations during that time were given full weight, with weight decreasing exponentially with increasing time since the last observation.

**Table 5.** Scores obtained for the individual parameterisation experiments, and for the LPX-Mv1-nr and LPX-Mv1-rs experiments compared to the scores obtained for the LPX experiment. The metrics used are NME, MPD and the MM. S1 are step 1 comparisons, S2 are step 2, and S3 are step 3. The individual parameterisation experiments are Lightn: lightning re-parameterisation, Drying: fuel drying-time re-parameterisation, Roots: rooting depth re-parameterisation, Litter: litter decomposition re-parameterisation, and Bark: inclusion of adaptive bark thickness. LPX-M-v1-nr incorporates all of these parameterisations and LPX-M-v1-rs incorporates resprouting into LPX-Mv1-nr. Numbers in bold are better than the original LPX model; numbers in italics are better than the mean null model; and \* means better than the randomly resampled null model. The scores given for fire represent the range of scores over all fire data sets for that comparison. Scores for comparisons against individual data sets can be found in Table S5 in the Supplement.

Variable	Metric	Measure	LPX	Lightn	Drying	Roots	Litter	Bark	LPX-M v1-nr	LPX-M v1-rs
Burnt area	Mean	Annual Average	0.082	0.12	0.084	0.086	0.02	0.003	0.049	0.050
	Mean ratio		1.13–1.21	1.64–1.77	1.15–1.24	1.18–1.27	0.28–0.29	0.039–0.043	0.67–0.72	0.69–0.74
NME S1	Annual Average		1.00*–1.01*	1.24*–1.29	1.00*–1.02*	1.00*–1.02*	<b>0.90*–0.93*</b>	<b>0.88*–0.90*</b>	<b>0.88*–0.89*</b>	<b>0.85*–0.88*</b>
NME S2			<b>0.97*–0.97*</b>	<b>1.06*–1.09*</b>	<b>0.97*–0.98*</b>	<b>0.97*–0.97*</b>	1.03*–1.04*	1.02*–1.02*	<b>0.90*–0.94*</b>	<b>0.89*–0.93*</b>
NME S3			1.20*–1.22*	1.32–1.32	1.21*–1.23*	1.20*–1.23*	1.22–1.23*	1.38–1.39	<b>1.10*–1.12*</b>	<b>1.09*–1.09*</b>
NME S2	Interannual variability		0.94–1.05*	1.05*–1.06	0.97*–1.08*	0.97*–1.17*	<b>0.89*–1.03*</b>	1.00*–1.03*	<b>0.66*–0.91</b>	<b>0.68*–0.90*</b>
NME S1	Seasonal Conc.		1.39–1.43	<b>1.30*–1.33</b>	1.35*–1.43	1.36*–1.44	<b>1.31*–1.44*</b>	<b>1.31*–1.44*</b>	<b>1.31*–1.32*</b>	<b>1.31*–1.32*</b>
MPD	Phase		<b>0.44*–0.50</b>	<b>0.38*–0.46*</b>	<b>0.44*–0.50</b>	<b>0.44*–0.49*</b>	0.57–0.57	0.53–0.59	0.49*–0.52	0.49*–0.52
Burnt area: SE Aus.	Mean	Annual Average	0.048	0.099	0.053	0.051	0.012	0.002	0.024	0.024
	Mean ratio		6.00–10.9	12.4–22.6	6.68–12.2	6.37–11.6	1.55–2.83	0.25–0.49	3.07–6.61	3.12–5.68
NME S1	Annual Average		4.03–7.19	7.97–14	4.35–7.67	4.23–7.59	<b>1.59*–2.40</b>	0.81*–0.92*	<b>2.29*–4.27</b>	<b>2.33*–3.67</b>
NME S2			3.58–6.13	5.07–7.91	<b>3.6*–6.06</b>	3.61–6.21	<b>1.78*–2.99</b>	<b>1.05*–1.08*</b>	<b>2.50*–4.75</b>	<b>2.53*–4.20</b>
NME S3			1.41–2.07	<b>1.23*–1.35</b>	<b>1.35*–1.37</b>	<b>1.38*–1.40</b>	1.22–1.25	<b>1.18*–1.22</b>	1.29–1.29	<b>1.28*–1.30</b>
NME S2	Interannual variability		8.59–16.6	10.1–19.3	9.05–17.5	10.1–19.4	<b>3.83*–7.65</b>	<b>1.27*–2.33</b>	<b>5.56*–11.5</b>	5.71–11.2
Veg. cover	Mean	Trees	0.034	0.011	0.022	0.034	0.059	0.075	0.042	0.049
	Mean ratio		0.4	0.13	0.26	0.4	0.69	0.88	0.49	0.58
Mean	Herb		0.44	0.34	0.45	0.44	0.55	0.57	0.55	0.55
Mean	Mean ratio		0.65	0.5	0.65	0.65	0.81	0.84	0.80	0.81
Mean	Bare ground		0.52	0.65	0.53	0.52	0.39	0.35	0.41	0.4
Mean	Mean ratio		2.79	3.45	2.83	2.77	2.08	1.88	2.18	2.12
Mean	Phenology		0.066	0.014	0.042	0.063	0.12	0.15	0.10	0.12
Mean	Mean ratio		0.13	0.026	0.081	0.12	0.23	0.28	0.20	0.22
Mean	Leaf type		0.055	0.01	0.035	0.056	0.1	0.14	0.096	0.11
Mean	Mean ratio		0.094	0.018	0.059	0.096	0.18	0.24	0.17	0.18
Veg. Cover	MM	Life form	<b>0.77*</b>	0.96	0.79*	<b>0.76*</b>	<b>0.59*</b>	<b>0.56*</b>	<b>0.59*</b>	<b>0.58*</b>
	Trees		<b>0.16*</b>	<b>0.17*</b>	<b>0.17*</b>	<b>0.17*</b>	<b>0.17*</b>	<b>0.19*</b>	<b>0.17*</b>	<b>0.16*</b>
	Herb		0.66	0.77	0.67	<b>0.65*</b>	<b>0.53*</b>	<b>0.52*</b>	<b>0.51*</b>	<b>0.51*</b>
	Bare ground		0.72	0.95	0.73	<b>0.71</b>	<b>0.49*</b>	<b>0.42*</b>	<b>0.51*</b>	<b>0.49*</b>
	Phenology		0.29*	0.33*	<b>0.24*</b>	0.29*	<b>0.61*</b>	0.81*	0.72	0.46
	Leaf type		0.51*	1.01	0.62*	<b>0.46*</b>	<b>0.34*</b>	<b>0.27*</b>	<b>0.15*</b>	<b>0.19*</b>
Fine NPP	Mean	Annual average	628	112	192	180	177	176	181	202
	Mean ratio		2.67	0.5	0.85	0.8	0.78	0.80	0.82	0.90
NME S1			2.62	<b>0.96*</b>	<b>0.79*</b>	<b>0.78*</b>	<b>0.82*</b>	<b>1.13*</b>	<b>0.80*</b>	<b>0.73*</b>
NME S2			1.47	<b>0.83*</b>	<b>0.79*</b>	<b>0.78*</b>	<b>0.83*</b>	<b>1.22*</b>	<b>0.79*</b>	<b>0.74*</b>
NME S3			0.97*	<b>0.91*</b>	1.01*	<b>0.89*</b>	1.01*	2.00	0.99*	<b>0.87*</b>
fAPAR	Mean	Annual average	0.19	0.12	0.19	0.18	0.24	0.26	0.22	0.22
	Mean ratio		1.59	1.02	1.56	1.55	2.02	2.18	1.83	1.87
NME S1	Annual average		1.11*	<b>0.98*</b>	1.11*	<b>1.07*</b>	1.61	1.8	1.31	1.35
NME S2			0.69*	0.97*	0.72*	<b>0.68*</b>	0.7*	<b>0.69*</b>	<b>0.61*</b>	<b>0.61*</b>
NME S3			0.71*	1.21*	0.76*	0.71*	<b>0.57*</b>	<b>0.51*</b>	<b>0.57*</b>	<b>0.54*</b>
NME S2	Interannual variability		1.01	1.11	1.01	<b>0.97</b>	2.44	2.86	1.83	1.85
NME S3	Seasonal concentration		1.34*	1.44	1.35*	1.36*	<b>1.31*</b>	<b>1.31*</b>	<b>1.32*</b>	<b>1.33*</b>
MPD	Phase		0.25*	0.25*	0.25*	<b>0.24*</b>	0.25*	0.25*	<b>0.24*</b>	<b>0.24*</b>
Height	Mean	Annual Average	0.5	0.2	0.29	0.5	0.84	1.03	0.39	0.63
	Mean ratio		0.056	0.022	0.033	0.057	0.096	0.12	0.045	0.072
NME S1			1.07*	1.1*	1.09*	1.07*	<b>1.02*</b>	<b>1.01*</b>	1.08*	<b>1.05*</b>
NME S2			0.94*	0.98*	0.97*	0.94*	<b>0.91*</b>	0.9*	<b>0.96*</b>	<b>0.94*</b>
NME S3			1.25*	1.39	1.31*	1.26*	<b>1.11*</b>	<b>1.08*</b>	<b>1.18*</b>	<b>1.13*</b>

## 5 Model performance

Evaluation of the model simulations focuses on changes in vegetation distribution (expressed through changes in the relative abundance of PFTs) and changes in burnt area (both total area burnt each year in each grid cell, i.e. fractional burnt

area, and the seasonal distribution and timing of burning). We show the simulated change in tree cover (Fig. 8) and in mean annual burnt area (Fig. 9) for the original model compared to the simulations with LPX-M-v1 in both the resprouting (LPX-M-v1-rs) and non-resprouting (LPX-Mv1-nr) variants, as well as the differences between the two LPX-M-v1

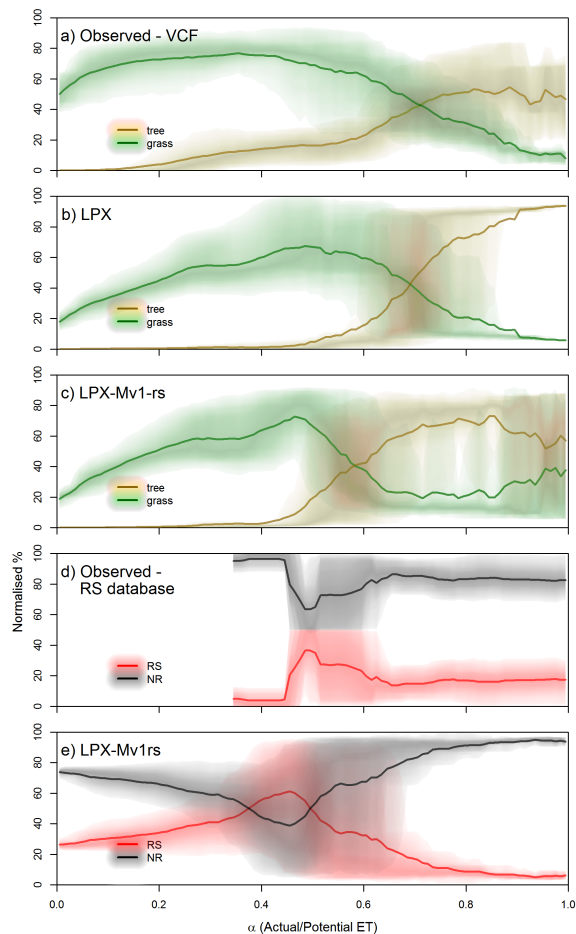


**Figure 6.** Comparison of the simulated abundance of grass, trees and resprouting trees along the climatic gradient in moisture, as measured by  $\alpha$  (actual potential evapotranspiration). Remotely sensed observations (**a**) of tree and grass cover from DeFries and Hansen (2009) compared to distribution of grass and trees simulated (**b**) by LPX and (**c**) LPX-Mv1-rs. (**d**) Observations of the abundance of aerial resprouters (RS – red) and other species (NR – black) from Harrison et al. (2014) compared to (**e**) RS (red) and non-resprouting (NR) PFTs (black) simulated by LPX-M-v1-rs. Note that some of the species included in the observed NR category may exhibit post-fire recovery behaviours such as underground (clonal) regrowth.  $\alpha$  was calculated as described by Gallego-Sala et al. (2010) in (**a**) and (**d**), and simulated by the relevant model in (**b**), (**c**) and (**e**). Abundance in (**d**) and (**e**) is normalised to show the percentage of the total vegetative cover of each category. Solid lines denote the 0.1 running mean and shading denotes the density of sites based on quantiles for each 0.1 running interval of  $\alpha$ .

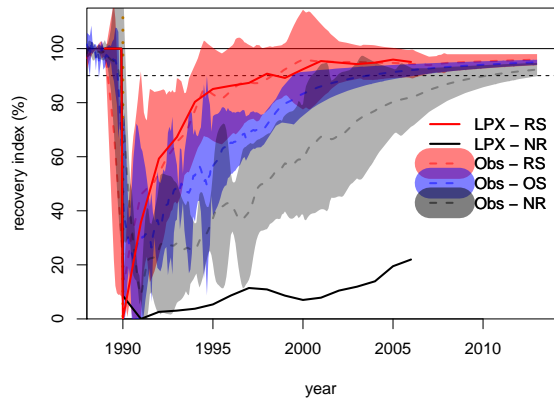


**Figure 7.** Comparison of the time taken for leaf area (as indexed by total foliage projective cover, FPC), to recover after fire in different ecosystems, as shown in the LPX-Mv1-rs simulations and from observations listed in Table S3. For comparison with the observations, which were all made after a significant loss of above-ground biomass through fire, the LPX simulations show recovery after a loss of 60 % of the leaf area. Red denotes ecosystems dominated by above-ground RS species; blue denotes ecosystems dominated by other fire-adapted species, mostly OS; black denotes vegetation which does not display specific fire adaptations (NR). The solid lines show LPX simulations; dotted lines show the mean of the relevant observations; the shaded areas show interquartile ranges of the relevant observations. The plots show that LPX-M-v1 reproduces the observed recovery rate in ecosystems dominated by resprouting species; recovery in ecosystems lacking resprouting trees is slower than observed, which could either reflect issues with simulated growth rates or the absence of other forms of fire adaptation.

simulations. We use benchmarking metrics to quantify the differences between the simulations (Table 5, Table S5 in the Supplement). Following (Kelley et al., 2013), we calculate the metrics in three steps in order to take account of biases: Step 1 is a straight comparison; 2 is a comparison with the influence of the mean removed; and 3 is with mean and variance removed.

As the NME and MM metrics are the sum of the absolute spatial variation between the model and observations, the comparison of scores obtained by two different models shows the relative magnitude of their biases with respect to the observations, and the improvement can be expressed in percentage terms. Although we focus on vegetation distribution and fire, we have also evaluated model performance in terms of other vegetation characteristics, including fAPAR, net primary production, and height (Table S5 in the Supplement), to ensure that changes in the model do not degrade the simulation of these characteristics.

### 5.1 LPX-Mv1-nr

The simulation of annual average burnt area for Australia in LPX-Mv1-nr is more realistic than in LPX: the NME score is

2426

D. I. Kelley et al.: Parameterisation of fire in LPX1 vegetation model

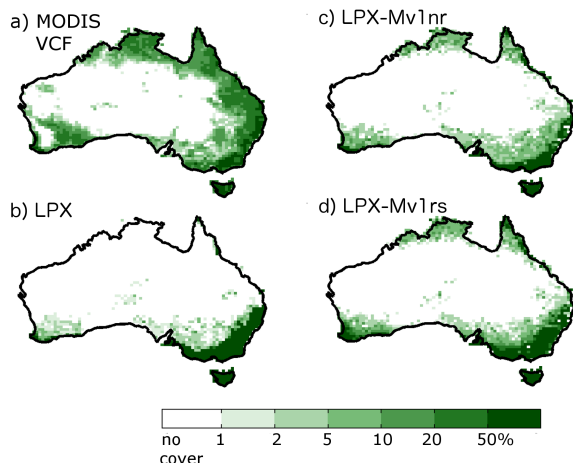


**Figure 8.** Comparison of percentage of tree cover from (a) observations (DeFries and Hansen, 2009) and as simulated by LPX-M, LPX-Mv1-nr and LPX-Mv1-rs (b–d, respectively).

0.88–0.89 (better than the mean model) compared to scores for LPX of 1.00–1.01 (performance equal to or worse than the mean model). The change in NME (Table 5) is equivalent to a 13–14 % improvement in model performance. The improvement in annual burnt area can be attributed to an improved match to the observed spatial pattern of fire and a better description of spatial variance. The improved NME scores obtained after removing the influence of the mean and variance of both model outputs and observations (step 3 in Table 5) is due to the introduction of fire into climates without a pronounced dry season, such as southeastern Australia (Fig. 9) which results from the lightning re-parameterisation (Fig. S1 in the Supplement). The improvement in spatial variability (step 2 in Table 5) is a result of a decrease in fire in the arid interior of the continent and an increase in fire in seasonally dry areas of northern Australia (Fig. 9). The decrease in fire in fuel-limited regions of the interior is a result of a decrease in fuel load from faster fuel decomposition, resulting from the re-parameterisation of decomposition, and a decrease in grassland production resulting from the rooting depth re-parameterisation which leads to a decrease in the proportion of grass roots in the lower soil layer and increased water stress. Comparison of the simulated fine-fuel production with VAST observations shows that the re-parameterisation of rooting depth improves simulation of fine-tissue production by 228 %. The improvement in the amount of fire in seasonally dry regions is a result of the re-parameterisation of fuel drying rates (Fig. S1 in the Supplement).

LPX-Mv1-nr produces an improved simulation of the interannual variability (IAV) of fire by 15–42 % from an NME of 0.94–1.05 to 0.66–0.91 (Table 5) – now better than the mean null model score of 1.00 (Table 4). This improvement

was due to the combination of the re-parameterisation of fuel drying time, which describes the impact of drier-than-normal conditions in certain years on fire incidence in northern and southeastern Australia, and a better description of litter decomposition in fine-fuel-dominated grassland, which allows for a more realistic description of fuel limitation in dry years where last year's fuel has decomposed and no new fuel is being produced.

The simulation of the length of the fire season also improved by 6–8 %. The improved NME score of 1.31–1.32 is better than the randomly resampled null model ( $1.332 \pm 0.02$ –0.043), but not the mean model 1.00 (Table 4). Improvements come from the parameterisation of lightning, drying times and fuel decomposition. The new lightning parameterisation leads to an increase in the length of the fire season, because fire starts occur over a longer period in coastal regions. The changes in drying time produce an earlier start to the fire season in all regions of Australia. The change to the decomposition parameterisation leads to a decrease in fire in the arid interior of Australia towards the end of the dry season by reducing fuel loads.

Despite an improvement of 68–76 %, LPX-Mv1-nr still performs poorly for southeastern Australia when compared against ground observations. The score is better when satellite observations are used for comparison but NME scores are still worse than the randomly resampled null model (Tables S4 and S5 in the Supplement). The model simulates too much fire in the Southern Tablelands (Fig. 9) but simulation of fire in more heavily wooded regions is more accurate, with burnt areas of ca. 1–5 %, in agreement with observations.

The improvement in vegetation distribution is largely due to simulating more realistic transitions between forest and grassland, chiefly through the parameterisation of adaptive bark thickness (which by itself yields a 37 % improvement in performance) but also through improved competition between trees and grasses for water, which results from the re-parameterisation of rooting depth. The degradation of the MM score for tree cover only (0.17 or LPX-Mv1-nr compared to 0.16 for LPX) is because the new model simulates slightly too much tree cover in southeastern Australia. The boundaries between closed forests and savanna in this region are still too sharp (Fig. 8).

Performance is degraded in LPX-Mv1-nr relative to LPX for annual average and interannual fAPAR (from 1.11 and 1.01 to 1.31 and 1.83, respectively) and cover of evergreen/deciduous types (from 0.29 to 0.72). fAPAR was already on average 59 % higher in LPX compared to observations (Table 5), mostly due to simulating too much tree cover in southeastern Australia (Fig. 8b). The introduction of adaptive bark thickness has caused an even higher average fAPAR value (Table 5) from the spread of woody vegetation into fire-prone areas (Fig. 8c). However, the inclusion of adaptive bark thickness helped improve the spatial pattern and variability (Table 5) from 0.71 to 0.57 by increasing tree cover in the north and by allowing a smoother transition between dense,

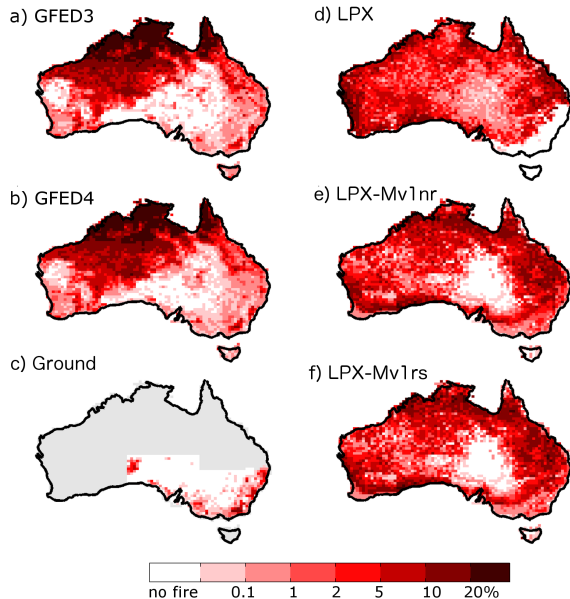


**Figure 9.** Annual average burnt area between 1997 and 2005 based on observations from (a) GFED3 (Giglio et al., 2010) and (b) GFED4 (Giglio et al., 2013), (c) southeastern Australia ground observations (Bradstock et al., 2014), and as simulated by (d) LPX, (e) LPX-Mv1-nr, and (f) LPX-Mv1-rs.

high fAPAR forest near the coast and lower fAPAR grassland and desert in the interior. An MM comparison for phenology in areas where both LPX and LPX-Mv1-nr have woody cover shows little change in simulated phenology, with both scoring 0.29.

## 5.2 LPX-Mv1-rs

Including resprouting in LPX-Mv1 (LPX-Mv1-rs) produces a more accurate representation of the transition from forest through woodland/savanna to grassland (Fig. 8) and improves the simulations of vegetation cover by 2 % compared to LPX-Mv1-nr and tree cover by 6 %. There is also a significant improvement in phenology compared to LPX-Mv1-nr, with NME scores changing from 0.72 in LPX-Mv1-nr to 0.46 in LPX-Mv1-rs (Table 5). The simulation of burnt area also improves: the NME for LPX-Mv1-rs is 0.85–0.88 compared to 0.88–0.89 for LPX-Mv1-nr, representing an overall improvement of 1–4 %. This improvement is equally due to the decrease in burnt area resulting from increased tree cover in southwestern Queensland (QL) and southeastern Australia (Fig. 10).

The simulated distribution of trees in climate space is improved in LPX-Mv1-rs compared to LPX. Trees are slightly more abundant at values of  $\alpha$  (the ratio of actual to equilibrium evapotranspiration) between 0.2 and 0.4 in LPX-Mv1-rs than in LPX; while in humid climates, where  $\alpha > 0.8$ , trees

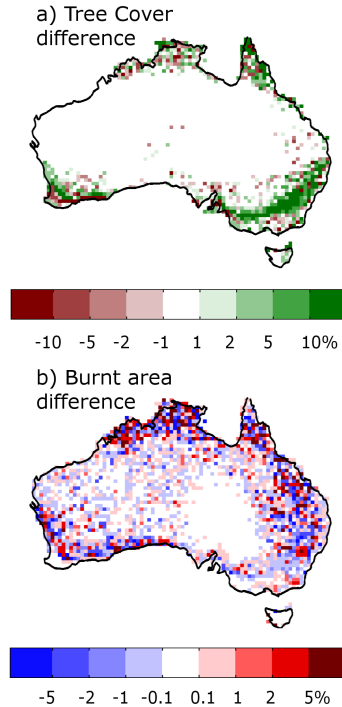


**Figure 10.** The difference in (a) tree cover and (b) burnt area between the non-resprouting (LPX-MV1-nr) and resprouting (LPX-MV1-rs) versions of LPX.

are less abundant than in LPX. The simulated abundance of trees in LPX-Mv1-rs is in reasonable agreement with observations (Fig. 6)

The simulated distribution of RS dominance over NR PFTs is plausible. The observations indicate that aerial (apical and epicormic) resprouters are most abundant at intermediate moisture levels ( $\alpha$  values between 0.4 and 0.6) but occur at higher moisture levels; the simulated abundance of RS is maximal at  $\alpha$  values between 0.4 and 0.5 and, although it declines more rapidly at higher moisture levels than shown by the observations, resprouting still occurs in moist environments. RS has a competitive advantage over NR when  $\alpha$  is between 0.5 and 0.8 (Fig. S2 in the Supplement).

The simulated regeneration after fire in RS-dominated communities in southeastern Australia is fast: NDVI<sub>sim</sub> reaches 90 % of pre-fire values within 7 yr; whereas post-fire regrowth takes 30 yr in the simulations that do not include RS (Fig. 7). Observations show that post-fire recovery in RS-dominated vegetation takes between 4 and 14 yr with a mean recovery time of 7 yr; whereas the recovery takes 8–16 yr (with a mean of 13 yr) in OS-dominated communities; and 7–22 yr (mean of 19) in boreal ecosystems.

## 6 Discussion

The introduction of new parameterisations in the LPX-DGVM improves the simulation of vegetation composition and fire regimes across the fire-prone continent of Australia. The overall improvements in performance in LPX-Mv1-rs compared to LPX are 15–18 % for burnt area, 17–38 % for interannual variability of fire, and 33 % for vegetation composition. These improvements result from the combination of all the new parameterisations. The introduction of individual parameterisations frequently led to a degradation of performance because LPX, in common with many other fire-enabled DGVMs, was tuned to produce a reasonably realistic simulation of burnt area. Our approach here has been to develop realistic parameterisations based on analysis of large data sets; the model was not tuned against fire observations. Post-fire aerial resprouting behaviour has not been included in DGVMs until now, although resprouting has been included in forest succession models (e.g. Loehle, 2000) and the BORFIRE (Boreal Fire Effects) stand-level fire-response model (Groot et al., 2003). Adaptive bark thickness has not been included in any vegetation model before, despite considerable within- and between-ecosystem variation in this trait and the fact that the average thickness within an ecosystem shifts with changes in fire regime. The incorporation of both processes is responsible for a significant part of the overall model improvement in LPX-Mv1-rs vs. LPX; it produces more realistic vegetation transitions from forests to woodland/savanna and, as shown by the regrowth comparisons, a more dynamically responsive DGVM.

The ability to resprout is a fundamental characteristic of many woody plants in fire-prone regions and means that these ecosystems recover biomass much more quickly after fire than if regeneration occurs from seed. Thus, in addition to improving the modern simulations, the incorporation of resprouting in LPX-Mv1 should lead to a more accurate prediction of vegetation changes and carbon sequestration in response to future climate-induced changes in fire regimes. The rapid post-fire regeneration in RS-dominated ecosystems is well reproduced using the modelling framework adopted here. However, simulated NR ecosystem recovery is slower than observations (Fig. 7). This might, at least in part, be because the model does not yet include fire-recovery strategies found in other ecosystems. There are other post-fire recovery mechanisms including resprouting from basal or underground parts of trees and obligate seeding (Clarke et al., 2013). We focused on aerial resprouting because this has the fastest impact on ecosystem recovery (Crisp et al., 2011; Clarke et al., 2013) and thus the greatest potential to influence carbon stocks and vegetation patterns. However, basal/collar resprouting is important in shrubs (Harrison et al., 2014), and thus should be included in models that simulate shrub PFTs explicitly. The “obligate seeder” strategy (i.e. the release of seeds from canopy stores by fire or the triggering of germination of seeds stored in

the soil by smoke or fire-produced chemicals) also leads to a more rapid recovery than non-stimulated regeneration from seed. Obligate seeders are found in a wider range of ecosystems than resprouters, including boreal ecosystems.

The ability to include a wider range of post-fire responses is currently limited by the availability of large data sets which could be used to develop appropriate parameterisations. Synthesis of the quantitative information available from the vast number of field studies on these traits would be useful for the modelling community. A similar argument could be made for information on rooting depth: although this is a trait that varies considerably within PFTs and depending on environmental conditions (Schenk and Jackson, 2002b, 2005), lack of species-level data has prevented us from implementing an adaptive deep root fraction within LPX-Mv1.

Despite the improvement in the simulation of fire in southeastern Australia, LPX-Mv1-rs simulates ca. 5 times more fire than observed in some parts of Queensland, New South Wales and Victoria, where, although the natural vegetation is woodland/savanna, the proportion of the land used for agriculture (crops, pasture) is high, i.e. > 80 % (Klein Goldewijk et al., 2011). The overall impact of agriculture is to reduce burnt area dramatically (Archibald et al., 2009; Bowman et al., 2009), through increasing landscape fragmentation (Archibald et al., 2012) and preventing fires from spreading. Incorporating land fragmentation into LPX-Mv1 could provide a more realistic simulation of fire in agricultural areas, such as in southeastern Australia.

We have used the benchmarking system described in Kelley et al. (2013) to assess the performance of the two new versions of LPX-Mv1 and to determine which new parameterisations contributed to improvements in performance. However, we needed to modify the existing system to take into account the recent update of the global burnt area product (GFED4) and to improve comparisons for Australia by using alternative burnt area products and the VAST data set for the assessment of fine-fuel production. As pointed out by Kelley et al. (2013), the incorporation of new processes into DGVMs will require the creation of new benchmarks. We have used the conceptual model of Clarke et al. (2013), which is based on extensive field observations, to evaluate our simulations of RS dominance in a qualitative way. Spatially explicit data on the distribution and abundance of resprouting species are required to test our simulations quantitatively. An Australian data set of RS abundance in fire-prone ecosystems is currently under development (Harrison et al., 2014); it would be useful if such a data set were available for a wider range of ecosystems and climates. Similarly, we have shown that an adaptive bark thickness parameterisation produces qualitatively plausible changes in average bark thickness in different regions and under different fire regimes, using field-based studies. A spatially explicit database of bark thickness would enable us to test the simulated patterns in bark thickness across ecosystems and fire regimes in a quantitative way.

## 7 Conclusions

Fire–vegetation interactions involve many processes and feedbacks. It is possible to tune a model to provide the best fit to an emergent property of the fire–vegetation system, such as observed burnt area, in multiple ways. Good simulations of burnt area can be obtained through many different combinations of parameter values. Such tuning can also lead to the assignment of parameter values that are wrong. Our approach in developing new fire parameterisations for LPX-Mv1 has been to rely on the analysis of data directly relevant to each individual process. This approach is possible because of the steadily increasing amount of data available through satellite observations and geographically explicit syntheses of ground observations.

The new model incorporates a more realistic description of fire processes, and has been shown to produce a better simulation of vegetation properties and fire regimes across Australia. The new changes are generic and have not been tuned for Australian conditions; thus, the new parameterisations should produce an improvement in the simulation of fire regimes and transitions between vegetation types in other fire-prone regions of the world. Further tests are underway to establish that this is indeed the case. Our work has been motivated by the fact that fire has a major impact on the carbon cycle, with non-negligible feedbacks to climate. The improvements introduced in LPX, resulting as they have from extensive data analysis and avoiding explicit tuning, give us greater confidence that this version of the model will provide more realistic predictions of the responses of vegetation, fire regimes and the terrestrial carbon cycle to potential future changes in climate. In this context, the incorporation of more realistic treatments of ecosystem-level fire resistance (through adaptive bark thickness) and post-fire recovery rates (through resprouting) is key for the accurate simulation of fire-induced changes in the carbon cycle.

**The Supplement related to this article is available online at doi:10.5194/gmd-7-2411-2014-supplement.**

**Acknowledgements.** We thank Belinda Medlyn and Peter M. van Bodegom for discussion of the treatment of variable bark thickness, and Joe Fontaine, Mike Lawes, Jeremy Midgley, Peter Clarke, Zhixin Fang, Bill Hoffman, Marin Pompa-Garcia, Daniel Laughlin, Peter M. van Bodegom, Timothy Paine, Christopher Baraloto, Paulo Brando, Emily Swaine, William Bond and Jon Lloyd for provision of bark thickness data. We also thank Victor Brokin and Thomas Kleinen for providing their litter decomposition code. D. I. Kelley is supported by an iMQRES at Macquarie University.

Benchmarking data sets and scripts for data–model comparison metrics from both Kelley et al. (2013) and the updates described here are available at <http://bio.mq.edu.au/bcd/benchmarks/>.

Information and code used for data analysis are available at [https://bitbucket.org/teambcd/lpx2013\\_data\\_analysis](https://bitbucket.org/teambcd/lpx2013_data_analysis). Benchmarking and data analysis were scripted using R (R Development Core Team) and the quantreg (Koenker, 2013), raster (van Etten and Hijmans, 2013), glm (R Core Team, 2013), RNetCDF (Michna, 2012) and Hmisc (Harrell Jr., 2012) packages.

Edited by: M.-H. Lo

## References

- Albini, F. A.: Estimating wildfire behavior and effects, Intermountain Forest and Range Experiment Station, Forest Service, US Department of Agriculture, 1976.
- Anderson, D. H., Catchpole, E. A., De Mestre, N. J., and Parkes, T.: Modelling the spread of grass fires, *J. Aust. Math. Soc.*, 23, 451–466, 1982.
- Archibald, S., Roy, D. P., van Wilgen, B. W., and Scholze, R. J.: What limits fire?, an examination of drivers of burnt area in southern Africa, *Glob. Change Biol.*, 15, 613–630, doi:10.1111/j.1365-2486.2008.01754.x, 2009.
- Archibald, S., Staver, A. C., and Levin, S. A.: Evolution of human-driven fire regimes in Africa, *P. Natl. Acad. Sci. USA*, 109, 847–852, doi:10.1073/pnas.1118648109, 2012.
- Arora, V. K., and Boer, G. J.: Fire as an interactive component of dynamic vegetation models, *J. Geophys. Res.*, 110, G02008, doi:10.1029/2005JG000042, 2005.
- Barrett, D. J.: NPP multi-biome: VAST calibration data, 1965–1998, available at: <http://www.daac.ornl.gov> (last access: 13 January 2011), 2001.
- Bellingham, P. J. and Sparrow, A. D.: Resprouting as a life history strategy in woody plant communities, *Oikos*, 89, 409–416, 2000.
- Biganzoli, F., Wiegand, T., and Batista, W. B.: Fire-mediated interactions between shrubs in a South American temperate savannah, *Oikos*, 118, 1383–1395, doi:10.1111/j.1600-0706.2009.17349.x, 2009.
- Bistinas, I., Harrison, S. P., Prentice, I. C., and Pereira, J. M. C.: Causal relationships vs. emergent patterns in the global controls of fire frequency, *Biogeosciences Discuss.*, 11, 3865–3892, doi:10.5194/bg-11-3865-2014, 2014.
- Baldocchi, D., Cummins, K. L., Christian, H. J., and Goodman, S. J.: Combined satellite- and surface-based estimation of the intracloud – cloud-to-ground lightning ratio over the continental United States, *Mon. Weather Rev.*, 129, 108–122, 2001.
- Bond, W. J. and Midgley, J. J.: Ecology of sprouting in woody plants: the persistence niche, *Trends Ecol. Evol.*, 16, 45–51, 2001.
- Bond, W. J. and Van Wilgen, B. W.: Fire and Plants, Population and Community Biology Series, 14, 1–15, 1996.
- Bowman, D. M. J. S., Balch, J. K., Artaxo, P., Bond, W. J., Carlson, J. M., Cochrane, M. a., D'Antonio, C. M., Defries, R. S., Doyle, J. C., Harrison, S. P., Johnston, F. H., Keeley, J. E., Krawchuk, M. A., Kull, C. A., Marston, J. B., Moritz, M. A., Prentice, I. C., Roos, C. I., Scott, A. C., Swetnam, T. W., van der Werf, G. R., and Pyne, S. J.: Fire in the earth system, *Science*, 324, 481–484, doi:10.1126/science.1163886, 2009.
- Bradstock, R., Williams, R., and Gill, A.: Flammable Australia: Fire Regimes, Biodiversity and Ecosystems in a Changing World, CSIRO Publishing, 2012.

- Bradstock, R., Penman, T., Boer, M., Price, O., and Clarke, H.: Divergent responses of fire to recent warming and drying across south-eastern Australia, *Glob. Change Biol.*, 20, 1412–1428, doi:10.1111/gcb.12449, 2014.
- Brando, P. M., Nepstad, D. C., Balch, J. K., Bolker, B., Christman, M. C., Coe, M., and Putz, F. E.: Fire-induced tree mortality in a neotropical forest: the roles of bark traits, tree size, wood density and fire behavior, *Glob. Change Biol.*, 18, 630–641, doi:10.1111/j.1365-2486.2011.02533.x, 2012.
- Brovkin, V., van Bodegom, P. M., Kleinhenz, T., Wirth, C., Cornwell, W. K., Cornelissen, J. H. C., and Kattge, J.: Plant-driven variation in decomposition rates improves projections of global litter stock distribution, *Biogeosciences*, 9, 565–576, doi:10.5194/bg-9-565-2012, 2012.
- Calvo, L., Santalla, S., Marcos, E., Valbuena, L., Tárrega, R., and Luis, E.: Regeneration after wildfire in communities dominated by *Pinus pinaster*, an obligate seeder, and in others dominated by *Quercus pyrenaica*, a typical resprouter, *Forest Ecol. Manag.*, 184, 209–223, doi:10.1016/S0378-1127(03)00207-X, 2003.
- Casady, G.: Examining Drivers of Post-Wildfire Vegetation Dynamics Across Multiple Scales Using Time-Series Remote Sensing, ProQuest, 2008.
- Casady, G. M., van Leeuwen, W. J. D., and Marsh, S. E.: Evaluating post-wildfire vegetation regeneration as a response to multiple environmental determinants, *Environ. Model. Assess.*, 15, 295–307, doi:10.1007/s10666-009-9210-x, 2009.
- Cha, S.-H.: Comprehensive survey on distance/similarity measures between probability density functions, *Int. J. Math. Model. Met. Appl. Sci.*, 4, 300–307, 2007.
- Chave, J., Coomes, D., Jansen, S., Lewis, S. L., Swenson, N. G., and Zanne, A. E.: Towards a worldwide wood economics spectrum, *Ecol. Lett.*, 12, 351–366, doi:10.1111/j.1461-0248.2009.01285.x, 2009.
- Christian, H. J.: Optical detection of lightning from space, in: Proceedings of the 11th International Conference on Atmospheric Electricity, Guntersville, Alabama, 715–718, 1999.
- Christian, H. J., Blakeslee, R. J., Goodman, S. J., Mach, D. A., Stewart, M. F., Buechler, D. E., Koshak, W. J., Hall, J. M., Boeck, W. L., Driscoll, K. T., and Bocippio, D. J.: The lightning imaging sensor, in: Proceedings of the 11th International Conference On Atmospheric Electricity, Guntersville, Alabama, 746–749, 1999.
- Clarke, P. J., Lawes, M. J., Midgley, J. J., Lamont, B. B., Ojeda, F., Burrows, G. E., Enright, N. J., and Knox, K. J. E.: Resprouting as a key functional trait: how buds, protection and resources drive persistence after fire, *New Phytol.*, 197, 19–35, doi:10.1111/nph.12001, 2013.
- Clement, J., Tapias, R., Pardos, J. A., and Gil, L.: Fire adaptations in the Canary Islands pine (*Pinus canariensis*), *Plant Ecol.*, 171, 185–196, 2004.
- Cochrane, M. A.: Fire science for rainforests, *Nature*, 421, 913–919, doi:10.1038/nature01437, 2003.
- Cornwell, W. K., Cornelissen, J. H. C., Amatangelo, K., Dorrepael, E., Eviner, V. T., Godoy, O., Hobbie, S. E., Hoorens, B., Kurokawa, H., Pérez-Harguindeguy, N., Quested, H. M., Santiago, L. S., Wardle, D. A., Wright, I. J., Aerts, R., Allison, S. D., van Bodegom, P., Brovkin, V., Chatain, A., Callaghan, T. V., Diaz, S., Garnier, E., Gurvich, D. E., Kazakou, E., Klein, J. A., Read, J., Reich, P. B., Soudzilovskaia, N. A., Vaieretti, M. V., and Westoby, M.: Plant species traits are the predominant control on litter decomposition rates within biomes worldwide, *Ecol. Lett.*, 11, 1065–71, doi:10.1111/j.1461-0248.2008.01219.x, 2008.
- Cornwell, W. K., Cornelissen, J. H. C., Allison, S. D., Bauhus, J., Eggleton, P., Preston, C. M., Scarff, F., Weedon, J. T., Wirth, C., and Zanne, A. E.: Plant traits and wood fates across the globe: rotted, burned, or consumed?, *Glob. Change Biol.*, 15, 2431–2449, doi:10.1111/j.1365-2486.2009.01916.x, 2009.
- Crisp, M. D., Burrows, G. E., Cook, L. G., Thornhill, A. H., and Bowman, D. M. J. S.: Flammable biomes dominated by eucalypts originated at the Cretaceous-Palaeogene boundary, *Nature Com.*, 2, 193, doi:10.1038/ncomms1191, 2011.
- Cummins, K. and Murphy, M.: An overview of lightning locating systems: history, techniques, and data uses, with an in-depth look at the US NLDN, electromagnetic compatibility, *IEEE*, 51, 499–518, 2009.
- Dagit, R.: Post-fire monitoring of coast live Oaks (*Quercus agrifolia*) burned in the 1993 Old Topanga fire, *Proceedings of the Fifth Natural Resources*, 90290, 243–249, 2002.
- DeFries, R. and Hansen, M.: ISLSCP II Continuous fields of vegetation cover, 1992–1993, in: ISLSCP Initiative II Collection, edited by: Hall, F., Collatz, G., Brown de Colstoun, E., Lands, D., Los, S., and Meeson, B., Oak Ridge National Laboratory Distributed Active Archive Center, Oak Ridge, Tennessee, USA, doi:10.3334/ORNLDAAC/931, 2009.
- de Souza, P. E., Pinto, O., Pinto, I. R. C. A., Ferreira, N. J., and Dos Santos, A. F.: The intracloud/cloud-to-ground lightning ratio in southeastern Brazil, *Atmos. Res.*, 91, 491–499, 2009.
- Del Tredici, P.: Sprouting in temperate trees: a morphological and ecological review, *Bot. Rev.*, 67, 121–140, 2001.
- Foley, J.: An equilibrium model of the terrestrial carbon budget, *Tellus B*, 47, 310–319, 1995.
- Friend, A. D.: Parameterisation of a global daily weather generator for terrestrial ecosystem modelling, *Ecol. Model.*, 109, 121–140, doi:10.1016/S0304-3800(98)00036-2, 1998.
- Fyllas, N. M., Patiño, S., Baker, T. R., Bielefeld Nardoto, G., Martinelli, L. A., Quesada, C. A., Paiva, R., Schwarz, M., Horna, V., Mercado, L. M., Santos, A., Arroyo, L., Jiménez, E. M., Luizão, F. J., Neill, D. A., Silva, N., Prieto, A., Rudas, A., Silviera, M., Vieira, I. C. G., Lopez-Gonzalez, G., Malhi, Y., Phillips, O. L., and Lloyd, J.: Basin-wide variations in foliar properties of Amazonian forest: phylogeny, soils and climate, *Biogeosciences*, 6, 2677–2708, doi:10.5194/bg-6-2677-2009, 2009.
- Gallego-Sala, A. V., Clark, J. M., House, J. I., Orr, H. G., Prentice, I. C., Smith, P., Farewell, T., and Chapman, S. J.: Bioclimatic envelope model of climate change impacts on blanket peatland distribution in Great Britain, *Clim. Res.*, 45, 151–162, 2010.
- Gavin, D. G., Oswald, W. W., Wahl, E. R., and Williams, J. W.: A statistical approach to evaluating distance metrics and analog assignments for pollen records, *Quaternary Res.*, 60, 356–367, 2003.
- Gerten, D., Schaphoff, S., Haberlandt, U., Lucht, W., and Sitch, S.: Terrestrial vegetation and water balance – hydrological evaluation of a dynamic global vegetation model, *J. Hydrol.*, 286, 249–270, doi:10.1016/j.jhydrol.2003.09.029, 2004.
- Gharun, M., Turnbull, T. L., and Adams, M. A.: Stand water use status in relation to fire in a mixed species eucalypt forest, *Forest Ecol. Manag.*, 304, 162–170, 2013.

- Giglio, L., Randerson, J. T., van der Werf, G. R., Kasibhatla, P. S., Collatz, G. J., Morton, D. C., and DeFries, R. S.: Assessing variability and long-term trends in burned area by merging multiple satellite fire products, *Biogeosciences*, 7, 1171–1186, doi:10.5194/bg-7-1171-2010, 2010.
- Giglio, L., Randerson, J. T., and Werf, G. R.: Analysis of daily, monthly, and annual burned area using the fourth-generation Global Fire Emissions Database (GFED4), *J. Geophys. Res.-Biogeosci.*, 118, 317–328, doi:10.1002/jgrg.20042, 2013.
- Gobron, N., Pinty, B., Taberner, M., Mélin, F., Verstraete, M. M., and Widlowski, J.-L.: Monitoring the photosynthetic activity of vegetation from remote sensing data, *Adv. Space Res.*, 38, 2196–2202, 2006.
- Gouveia, C., DaCamara, C. C., and Trigo, R. M.: Post-fire vegetation recovery in Portugal based on spot/vegetation data, *Nat. Hazards Earth Syst. Sci.*, 10, 673–684, doi:10.5194/nhess-10-673-2010, 2010.
- Greene, D. F., Zasada, J. C., Sirois, L., Kneeshaw, D., Morin, H., Charron, I., and Simard, M.-J.: A review of the regeneration dynamics of north American boreal forest tree species, *Can. J. Forest Res.*, 29, 824–839, 1999.
- Groot, W. J., Bothwell, P. M., Carlsson, D. H., and Logan, K. A.: Simulating the effects of future fire regimes on western Canadian boreal forests, *J. Veg. Sci.*, 14, 355–364, 2003.
- Hall, F. G., de Colstoun, E., Collatz, G. J., Landis, D., Dirmeyer, P., Betts, A., Huffman, G. J., Bounoua, L., and Meeson, B.: ISLSCP Initiative II global data sets: surface boundary conditions and atmospheric forcings for land-atmosphere studies, *J. Geophys. Res.-Atmos.*, 111, D22S01, doi:10.1029/2006JD007366, 2006.
- Halliwell, D. H. and Apps, M. J.: BOREAL Ecosystem-Atmosphere Study (BOREAS) biometry and auxiliary sites: overstory and understory data, Northern Forestry Centre Edmonton, Canada, 1997.
- Harrell Jr., F. E.: Hmisc: Harrell miscellaneous, available at: <http://cran.r-project.org/package=Hmisc> (last access: 16 December 2013), 2012.
- Harris, I., Jones, P. D., Osborn, T. J., and Lister, D. H.: Updated high-resolution grids of monthly climatic observations – the CRU TS3.10 Dataset, *Int. J. Climatol.*, doi:10.1002/joc.3711, 2013.
- Harrison, S. P., Prentice, I. C., Barboni, D., Kohfeld, K. E., Ni, J., and Sutra, J.-P.: Ecophysiological and bioclimatic foundations for a global plant functional classification, *J. Veg. Sci.*, 21, 300–317, doi:10.1111/j.1654-1103.2009.01144.x, 2010.
- Harrison, S., Kelley, D., Wang, H., Herbert, A., Li, G., Bradstock, R., Fontaine, J., Enright, N., Murphy, B., Penman, T., and Russell-Smith, J.: Patterns in fire-response trait abundances in Australia using a new database of plot-level measurements for fire model evaluation, *Global Ecology and Biogeography*, submitted, 2014.
- Hastie, T. J. and Pregibon, D.: Generalized linear models, Chapter 6 of Statistical Models in S, edited by: Chambers, J. M. and Hastie, T. J., Wadsworth & Brooks/Cole, 1992.
- Higgins, R. W. and Centre, U. C. P.: Improved United States precipitation quality control system and analysis, in: NCEP/Climate Prediction Center ATLAS No. 6, NOAA, National Weather Service, National Centers for Environmental Prediction, Climate Prediction Center, Camp Springs, MD, 2000.
- Higgins, R. W., Janowiak, J. E., and Yao, Y.-P.: A gridded hourly precipitation data base for the United States (1963–1993), in: NCEP/Climate prediction center atlas 1, p. 46, NOAA, National Weather Service, National Centers for Environmental Prediction, Climate Prediction Center, Camp Springs, MD, 1996.
- Hijmans, R. J., Cameron, S. E., Parra, J. L., Jones, P. G., and Jarvis, A.: Very high resolution interpolated climate surfaces for global land areas, *Int. J. Climatol.*, 25, 1965–1978, 2005.
- Kattge, J., Diaz, S., Lavelle, S., Prentice, I. C., Leadley, P., Bonisch, G., Garnier, E., Westoby, M., Reich, P. B., Wright, I. J., Cornelissen, J. H. C., Viole, C., Harrison, S. P., Van Bodegom, P. M., Reichstein, M., Enquist, B. J., Soudzilovskaya, N. A., Ackerly, D. D., Anand, M., Atkin, O., Bahn, M., Baker, T. R., Baldocchi, D., Bekker, R., Blanco, C. C., Blonder, B., Bond, W. J., Bradstock, R., Bunker, D. E., Casanoves, F., Cavender-Bares, J., Chambers, J. Q., Chapin III, F. S., Chave, J., Coomes, D., Cornwell, W. K., Craine, J. M., Dobrin, B. H., Duarte, L., Durka, W., Elser, J., Esser, G., Estiarte, M., Fagan, W. F., Fang, J., Fernandez-Mendez, F., Fidelis, A., Finegan, B., Flores, O., Ford, H., Frank, D., Freschet, G. T., Fyllas, N. M., Gallagher, R. V., Green, W. A., Gutierrez, A. G., Hickler, T., Higgins, S. I., Hodgson, J. G., Jalili, A., Jansen, S., Joly, C. A., Kerkhoff, A. J., Kirkup, D., Kitajima, K., Kleyer, M., Klotz, S., Knops, J. M. H., Kramer, K., Kuhn, I., Kurokawa, H., Laughlin, D., Lee, T. D., Leishman, M., Lens, F., Lenz, T., Lewis, S. L., Lloyd, J., Llusia, J., Louault, F., Ma, S., Machecha, M. D., Manning, P., Massad, T., Medlyn, B. E., Messier, J., Moles, A. T., Muller, S. C., Nadrowski, K., Naeem, S., Niinemets, U., Nollert, S., Nuske, A., Ogaya, R., Oleksyn, J., Onipchenko, V. G., Onoda, Y., Ordonez, J., Overbeck, G., Ozinga, W. A., Patino, S., Paula, S., Pausas, J. G., Penuelas, J., Phillips, O. L., Pillar, V., Poorter, H., Poorter, L., Poschlod, P., Prinzing, A., Proulx, R., Rammig, A., Reinsch, S., Reu, B., Sack, L., Salgado-Negret, B., Sardans, J., Shiodera, S., Shipley, B., Siefert, A., Sosinski, E., Soussana, J.-F., Swaine, E., Swenson, N., Thompson, K., Thornton, P., Waldram, M., Weher, E., White, M., White, S., Wright, S. J., Yguel, B., Zaehle, S., Zanne, A. E., and Wirth, C.: TRY – a global database of plant traits, *Glob. Change Biol.*, 17, 2905–2935, doi:10.1111/j.1365-2486.2011.02451.x, 2011.
- Kauffman, J. B.: Survival by sprouting following fire in tropical forests of the eastern Amazon, *Biotropica*, 23, 219–224, 1991.
- Kaufmann, W. F. and Hartmann, K. M.: Earth-based spectroradiometric monitoring of forest decline, *J. Plant Physiol.*, 138, 270–273, 1991.
- Keeley, J. E.: Fire severity and plant age in postfire resprouting of woody plants in sage scrub and chaparral, *Madrono*, 53, 373–379, 2006.
- Kelley, D. I., Prentice, I. C., Harrison, S. P., Wang, H., Simard, M., Fisher, J. B., and Willis, K. O.: A comprehensive benchmarking system for evaluating global vegetation models, *Biogeosciences*, 10, 3313–3340, doi:10.5194/bg-10-3313-2013, 2013.
- Kimball, J. S., Running, S. W., and Nemani, R.: An improved method for estimating surface humidity from daily minimum temperature, *Agr. Forest Meteorol.*, 85, 87–98, 1997.
- Klein Goldewijk, K., Beusen, A., Van Drecht, G., and De Vos, M.: The HYDE 3.1 spatially explicit database of human-induced global land-use change over the past 12,000 years, *Global Ecol. Biogeogr.*, 20, 73–86, 2011.

- Kloster, S., Mahowald, N. M., Randerson, J. T., Thornton, P. E., Hoffman, F. M., Levis, S., Lawrence, P. J., Feddema, J. J., Oleson, K. W., and Lawrence, D. M.: Fire dynamics during the 20th century simulated by the Community Land Model, *Biogeosciences*, 7, 1877–1902, doi:10.5194/bg-7-1877-2010, 2010.
- Knox, K. J. E. and Clarke, P. J.: Fire season and intensity affect shrub recruitment in temperate sclerophyllous woodlands, *Oecologia*, 149, 730–739, doi:10.1007/s00442-006-0480-6, 2006.
- Koenker, R.: Package “quantreg”: quantile regression, available at: <http://cran.r-project.org/package=quantreg> (last access: 6 December 2013), 2013.
- Kuleshov, Y. and Jayaratne, R.: Estimates of lightning ground flash density in Australia and its relationship to thunder-days, *Aust. Meteorol. Mag.*, 53, 189–196, 2004.
- Lawes, M. J., Adie, H., Russell-Smith, J., Murphy, B., and Midgley, J. J.: How do small savanna trees avoid stem mortality by fire? The roles of stem diameter, height and bark thickness, *Ecosphere*, 2, 42, doi:10.1890/ES10-00204.1, 2011a.
- Lawes, M. J., Richards, A., Dathe, J., and Midgley, J. J.: Bark thickness determines fire resistance of selected tree species from fire-prone tropical savanna in north Australia, *Plant Ecol.*, 212, 2057–2069, doi:10.1007/s11258-011-9954-7, 2011b.
- Lawrence, M. G.: The relationship between relative humidity and the dewpoint temperature in moist air: a simple conversion and applications, *B. Am. Meteorol. Soc.*, 86, 225–233, doi:10.1175/BAMS-86-2-225, 2005.
- Lehmann, C. E. R., Prior, L. D., Williams, R. J., and Bowman, D. M. J. S.: Spatio-temporal trends in tree cover of a tropical mesic savanna are driven by landscape disturbance, *J. Appl. Ecol.*, 45, 1304–1311, doi:10.1111/j.1365-2664.2008.01496.x, 2008.
- Li, F., Zeng, X. D., and Levis, S.: A process-based fire parameterization of intermediate complexity in a Dynamic Global Vegetation Model, *Biogeosciences*, 9, 2761–2780, doi:10.5194/bg-9-2761-2012, 2012.
- Lloyd, J. and Taylor, J.: On the temperature dependence of soil respiration, *Funct. Ecol.*, 8, 315–323, 1994.
- Loehle, C.: Strategy space and the disturbance spectrum: a life-history model for tree species coexistence, *Am. Nat.*, 156, 14–33, 2000.
- Lu, L. and Shuttleworth, J. W.: Incorporating NDVI-Derived LAI into the climate version of RAMS and its impact on regional climate, *J. Hydrometeorol.*, 3, 347–362, 2002.
- Lunt, I. D., Zimmer, H. C., and Cheal, D. C.: The tortoise and the hare? Post-fire regeneration in mixed Eucalyptus–Callitris forest, *Aust. J. Bot.*, 59, 575–581, 2011.
- Malanson, G. P. and Westman, W. E.: Postfire succession in Californian coastal Sage scrub: the role of continual Basal sprouting, *Am. Midl. Nat.*, 113, 309–318, doi:10.2307/2425576, 1985.
- Michna, P.: RNetCDF: R Interface to NetCDF Datasets, available at: <http://cran.r-project.org/package=RNetCDF> (last access: 6 December 2013), 2012.
- Midgley, J. J., Lawes, M. J., and Chamaillé-Jammes, S.: Turner Review No. 19. Savanna woody plant dynamics: the role of fire and herbivory, separately and synergistically, *Austr. J. Bot.*, 58, 1–11, doi:10.1071/BT09034, 2010.
- Midgley, J., Kruger, L., and Skelton, R.: How do fires kill plants? The hydraulic death hypothesis and Cape Proteaceae “fire-resisters”, *S. Afr. J. Bot.*, 77, 381–386, doi:10.1016/j.sajb.2010.10.001, 2011.
- Mitchell, T. D. and Jones, P. D.: An improved method of constructing a database of monthly climate observations and associated high-resolution grids, *Int. J. Climatol.*, 25, 693–712, doi:10.1002/joc.1181, 2005.
- Murray, L. T., Jacob, D. J., Logan, J. A., Hudman, R. C., and Koshak, W. J.: Optimized regional and interannual variability of lightning in a global chemical transport model constrained by LIS/OTD satellite data, *J. Geophys. Res.-Atmos.*, 117, D20307, doi:10.1029/2012JD017934, 2012.
- Nesterov, V. G.: Combustibility of the forest and methods for its determination, Goslesbumaga, Moscow, 1949.
- Paine, C. E. T., Stahl, C., Courtois, E. A., Patiño, S., Sarmiento, C., and Baraloto, C.: Functional explanations for variation in bark thickness in tropical rain forest trees, *Funct. Ecol.*, 24, 1202–1210, doi:10.1111/j.1365-2435.2010.01736.x, 2010.
- Paula, S., Arianoutsou, M., Kazanis, D., Tavsanoglu, C., Lloret, F., Buhk, C., Ojeda, F., Luna, B., Moreno, J. M., Rodrigo, A., Espelta, J. M., Pausas, J. G., Fernández-Santos, B., Fernandes, P. M., and Pausas, J. G.: Fire-related traits for plant species of the Mediterranean Basin, *Ecol.*, 90, 1420 pp., 2009.
- Pausas, J. G.: Resprouting of *Quercus suber* in NE Spain after fire, *J. Veg. Sci.*, 8, 703–706, 1997.
- Pausas, J. G., Bradstock, Ross A., and Keith, D. A., and Keeley, J. E.: Plant functional traits in relation to fire in crown-fire ecosystems, *Ecol.*, 85, 1085–1100, 2004.
- Peterson, D., Wang, J., Ichoku, C., and Remer, L. A.: Effects of lightning and other meteorological factors on fire activity in the North American boreal forest: implications for fire weather forecasting, *Atmos. Chem. Phys.*, 10, 6873–6888, doi:10.5194/acp-10-6873-2010, 2010.
- Pfeiffer, M., Spessa, A., and Kaplan, J. O.: A model for global biomass burning in preindustrial time: LPJ-LMfire (v1.0), *Geosci. Model Dev.*, 6, 643–685, doi:10.5194/gmd-6-643-2013, 2013.
- Pierce, E. T.: Latitudinal variation of lightning parameters, *J. Appl. Meteorol.*, 9, 194–195, doi:10.1175/1520-0450(1970)009<0194:LVOLP>2.0.CO;2, 1970.
- Prentice, I. C., Kelley, D. I., Foster, P. N., Friedlingstein, P., Harrison, S. P., and Bartlein, P. J.: Modeling fire and the terrestrial carbon balance, *Global Biogeochem. Cy.*, 25, 1–13, doi:10.1029/2010GB003906, 2011.
- Prentice, S. and Mackerras, D.: The ratio of cloud to cloud-ground lightning flashes in thunderstorms, *J. Appl. Meteorol.*, 16, 545–550, 1977.
- Price, C. and Rind, D.: What determines the cloud-to-ground lightning fraction, 20, 463–466, doi:10.1029/93gl00226, 1993.
- Purevdorj, T., Tateishi, R., Ishiyama, T., and Honda, Y.: Relationships between percent vegetation cover and vegetation indices, *Int. J. Remote Sens.*, 19, 3519–3535, doi:10.1080/014311698213795, 1998.
- R Core Team: R: A language and environment for statistical computing, R Foundation for Statistical Computing, Vienna, Austria, available at: <http://www.r-project.org/>, last access: 6 December 2013.
- R Development Core Team: R: A language and environment for statistical computing, available at: <http://www.r-project.org/>, last access: 6 December 2013.

- Rothermel, R. C.: A mathematical model for predicting fire spread in wildland fuels, USFS, 1972.
- Running, S.: Extrapolation of synoptic meteorological data in mountainous terrain and its use for simulating forest evapotranspiration and photosynthesis, *Can. J. Forest Res.*, 17, 472–483, 1987.
- Schenk, H. J. and Jackson, R. B.: Rooting depths, lateral root spreads and belowground aboveground allometries of plants in water limited ecosystems, *J. Ecol.*, 90, 480–494, 2002a.
- Schenk, H. J. and Jackson, R. B.: The global biogeography of roots, *Ecol. Monogr.*, 72, 311–328, 2002b.
- Schenk, H. J. and Jackson, R. B.: Mapping the global distribution of deep roots in relation to climate and soil characteristics, *Geoderma*, 126, 129–140, doi:10.1016/j.geoderma.2004.11.018, 2005.
- Sellers, P. J., Tucker, C. J., Collatz, G. J., Los, S. O., Justice, C. O., Dazlich, D. A., and Randall, D. A.: A revised land surface parameterization (SiB2) for atmospheric GCMs, Part II: The generation of global fields of terrestrial biophysical parameters from satellite data, *J. Climate*, 4, 706–737, 1996.
- Sharples, J. J., McRae, R. H. D., Weber, R. O., and Gill, A. M.: A simple index for assessing fuel moisture content, *Environ. Modell. Softw.*, 24, 637–646, doi:10.1016/j.envsoft.2008.10.012, 2009.
- Simard, M., Baccini, A., Fisher, J. B., and Pinto, N.: Mapping forest canopy height globally with spaceborne lidar, *J. Geophys. Res.*, 116, G04021, doi:10.1029/2011JG001708, 2011.
- Sitch, S., Smith, B., Prentice, I. C., Arneth, A., Bondeau, A., Cramer, W., Kaplan, J. O., Levis, S., Lucht, W., Sykes, M. T., Thonicke, K., and Venevsky, S.: Evaluation of ecosystem dynamics, plant geography and terrestrial carbon cycling in the LPJ dynamic global vegetation model, *Glob. Change Biol.*, 9, 161–185, 2003.
- Tapias, R., Climent, J., Pardos, J. A., and Gil, L.: Life histories of Mediterranean pines, *Plant Ecol.*, 171, 53–68, 2004.
- Thonicke, K., Spessa, A., Prentice, I. C., Harrison, S. P., Dong, L., and Carmona-Moreno, C.: The influence of vegetation, fire spread and fire behaviour on biomass burning and trace gas emissions: results from a process-based model, *Biogeosciences*, 7, 1991–2011, doi:10.5194/bg-7-1991-2010, 2010.
- van der Werf, G. R., Randerson, J. T., Giglio, L., Gobron, N., and Dolman, A. J.: Climate controls on the variability of fires in the tropics and subtropics, *Global Biogeochem. Cy.*, 22, GB3028, doi:10.1029/2007GB003122, 2008.
- van Etten, J. and Hijmans, R. J.: raster: Geographic data analysis and modeling, available at: <http://cran.r-project.org/package=raster> (last access: 16 December 2013), 2013.
- van Leeuwen, W. J. D., Casady, G. M., Neary, D. G., Bautista, S., Alloza, J. A., Carmel, Y., Wittenberg, L., Malkinson, D., and Orr, B. J.: Monitoring post-wildfire vegetation response with remotely sensed time-series data in Spain, USA and Israel, *Int. J. Wildland Fire*, 19, 75–93, doi:10.1071/WF08078, 2010.
- Van Wagner, C. E.: Equilibrium moisture contents of some fine forest fuels in eastern Canada, Information Report, Petawawa Forest Experiment Station, 1972.
- Van Wagner, C. E. and Pickett, T. L.: Equations and FORTRAN program for the Canadian forest fire weather index system, in: Canadian Forestry Service, Petawawa national forestry institute, Chalk River, Ontario, Vol. 33, 1985.
- Venevsky, S., Thonicke, K., Sitch, S., and Cramer, W.: Simulating fire regimes in human-dominated ecosystems: Iberian Peninsula case study, *Glob. Change Biol.*, 8, 984–998, doi:10.1046/j.1365-2486.2002.00528.x, 2002.
- Viedma, O., Meliá, J., Segarra, D., and García-Haro, J.: Modeling rates of ecosystem recovery after fires by using landsat TM data, *Remote Sens.*, 61, 383–398, 1997.
- Viney, N.: A review of fine fuel moisture modelling, *Int. J. Wildland Fire*, 1, 215–234, doi:10.1071/WF9910215, 1991.
- Weedon, J. T., Cornwell, W. K., Cornelissen, J. H. C., Zanne, A. E., Wirth, C., and Coomes, D. A.: Global meta-analysis of wood decomposition rates: a role for trait variation among tree species?, *Ecol. Lett.*, 12, 45–56, doi:10.1111/j.1461-0248.2008.01259.x, 2009.
- Williams, P. R.: Fire-stimulated rainforest seedling recruitment and vegetative regeneration in a densely grassed wet sclerophyll forest of north-eastern Australia, *Aust. J. Bot.*, 48, 651–658, 2000.
- Williams, R. J., Griffiths, A. D., and Allan, G.: Fire regimes and biodiversity in the wet-dry tropical savanna landscapes of northern Australia, in: Flammable Australia: Fire Regimes and Biodiversity of a Continent, edited by: Bradstock, R., Williams, J. A., and Gill, A., 281–304, Cambridge University Press, Cambridge, 2002.
- Xiao, J. and Moody, A.: A comparison of methods for estimating fractional green vegetation cover within a desert-to-upland transition zone in central New Mexico, USA, *Remote Sens. Environ.*, 98, 237–250, doi:10.1016/j.rse.2005.07.011, 2005.
- Zammit, C. and Westoby, M.: Seedling recruitment strategies in obligate-seeding and resprouting Banksia shrubs, *Ecology*, 1984–1992, 1987.

Supplement of Geosci. Model Dev., 7, 2411–2433, 2014  
<http://www.geosci-model-dev.net/7/2411/2014/>  
doi:10.5194/gmd-7-2411-2014-supplement  
© Author(s) 2014. CC Attribution 3.0 License.



Geoscientific  
Model Development  
Open Access



*Supplement of*

**Improved simulation of fire–vegetation interactions in the Land surface  
Processes and eXchanges dynamic global vegetation model (LPX-Mv1)**

**D. I. Kelley et al.**

*Correspondence to:* D. I. Kelley (douglas.kelley@students.mq.edu.au)

**Supplementary Information**

Table S1 provides information on the allocation of species to plant functional types and to resprouting and non-resprouting classes, as used in the bark thickness analyses. Table S2 provides a summary of the studies about post-fire recruitment rates and Table S3 provides information used to calculate recovery rates. Benchmarking scores in the main text are a summary of skill scores obtained using the Kelley et al. (2013) benchmarking system. Tables S4 and S5 give the full set of scores for comparisons against all datasets, split into individual parameterisations and the combination of all parameterisations with and without resprouting (LPX-Mv1-nr and LPX-Mv1-rs respectively). Fig. S1 shows simulated burnt area for each individual parameterisation, and Fig. S2 shows where resprouting (RS) has a competitive advantage over non-resprouting (NR) PFTs in climate space. Fig S3 shows the results of the sensitivity test to including ignitions on wet days. Table S6 provides the benchmarking metrics for this sensitivity test. Eq. S1-S4 describes the derivation of the ratio of NDVI from tree and grass used in Eq. 36 in the main text. We also provide a complete list of references for the data used to parameterize adaptive bark thickness.

**Table S1.** Allocation of species to plant functional type (PFT) and to aerial resprouting (RS) and non-resprouting (NR) and other resprouting/unknown resprouting type (other) categories for the bark thickness analyses. All species listed (RS, NR and other) for each PFT were used for the parametrisation of bark thickness (BT) in LPX-Mv1-nr; RS species were used to parameterise BT for LPX-Mv1-rs PFTs; and NR for LPX-Mv1-rs NR PFTs. The taxon names are given as in the original source, and have not been changed for taxonomic correctness.

PFT	Type	Species
TBE	RS	<i>Acacia lamprocarpa, Alstonia actinophylla, Banksia sp., B. dentata, Corymbia bella, Eucalyptus miniata, E. phoenicea, E. tectifica, E. tetrodonta, Gardenia megasperma, Lophostemon lactifluus, Melaleuca sp., M. nervosa, M. viridiflora, Persoonia falcata, Syzygium eucalyptoides subsp. bleeseri, S. suborbiculare, Xanthostemon paradoxus</i>
NR		<i>Abarema jupunba, A. mataybifolia, Acacia auriculiformis, Agonandra silvatica, Aiouea longipetiolata, Alexa wachenheimii, Amaioua corymbosa, A. guianensis, Ambelania acida, Amblygonocarpus obtusangulus, Amburana cearensis, Amherstia nobilis, Amphirrhox longifolia, Anacardium spruceanum, Anartia meyeri, Aniba guianensis, A. hostmanniana, A. panurensis, A. terminalis, A. williamsii, Annona prevostiae, Antonia ovata, Arachidendron kunstleri, Aspidosperma album, A. cruentum, A. marcgravianum, A. oblongum, A. spruceanum, Astronium lecointei, A. ulei, Bagassa guianensis, Baikiaea insignis subsp. minor, Balizia pedicellaris, Bauhinia aculeata, B. blakeana, B. monandra, B. tomentosa, Bocoa alterna, B. prouacensis, Bonafousia undulata, Brosimum guianense, B. rubescens, B. utile, Brownea ariza, B. latifolia, Buchenavia sp., B. grandis, B. guianensis, B. tetraphylla, Bunchosia sp., Caesalpinia calycina, C. echinata, C. ferrea, C. nicaraguensis, C. pluviosa, C. pulcherrima, C. sappan, C. vesicaria, Calliandra sancti-pauli, Calyptranthes speciosa, Capirona decorticans, Carapa procera, Casearia sp., C. decandra, C. javitensis, C. sylvestris, Cassipourea guianensis, Castanospermum australe, Cathedra acuminata, Catostemma fragrans, Cecropia obtusa, Chaetocarpus sp., C. schomburgkianus, Chaunochiton kappleri, Cheiloclinium cognatum, Chimarrhis turbinata, Chloroleucon mangense, Coccobola mollis, Cojoba filicifolia, Conceveiba guianensis, Couratari calycina, C. gloriae, C. guianensis, C. multiflora, C. oblongifolia, Crepidospermum goudotianum, Cupania diphylla, C. rubiginosa, C. scrobiculata, C. scrobiculata var. guianensis, Cupaniopsis anacordioides, Cyrillopsis paraensis, Dacryodes cuspidata, D. nitens, Dalbergia ferruginea, D. frutescens, D. glandulosa, D. monetaria, D. nigra, D. polyphylla, D. riparia, D. villosa, Dendrobaena boliviensis, Dicorynia guianensis, Diospyros calycantha, D. caprifolia, D. carbonaria, D. cavalcantei, D. dichroa, Diplopan cuspidatum, Diplotropis purpurea, D. brachypetala, Dipteryx odorata, D. punctata, Discophora guianensis, Drypetes deplanchei, Duguetia calycina, D. surinamensis, Dulacia guianensis, Duroia aquatica, D. eriopila, D. longiflora, Ecclinusa lanceolata, E. ramiflora, Ecuadendron acosta-solisianum, Elaeoluma sp., E. nuda, Emmotum sagifolium, Endlicheria melinonii, Enterolobium schomburgkii, Eperua falcata, E. grandiflora, Erisma floribundum, E. uncinatum, Eschweilera apiculata, E. chartaceifolia, E. congestiflora, E. coriacea, E. decolorans, E. grandiflora, E. micrantha, E. parviflora, E. pedicellata, E. praeclera, E. sagotiana, E. simiorum, E. squamata, Eugenia sp., E. coffeeifolia, E. cucullata, E. cupulata, E. macrocalyx, E. patrisii, E. pseudopsidium, E. tapacumensis, E. tetraptera, Euterpe oleracea, Exelloendron barbatum, Exocarpus latifolius, Faramea pedunculata, Ferdinandusa paraensis, Fusaea longifolia, Geissospermum laeve, Grevillea sp., G. pteridifolia, G. costata, G. grandifolia, G. guidonia, G. scabra, G. silvatica, Guatteria anthracina, G. guianensis, G. wachenheimii, Guibourtia copallifera, Gustavia hexapetala, Haematoxylum campechianum, H. campeshianum, Hebepepalum humiriifolium, Heisteria densifrons, Helicostylis pedunculata, H. tomentosa, Henrietella flavescentia, Hevea guianensis, Holocalyx glaziovii, Hortia excelsa, Humiriastrum subcrenatum, Hyeronima alchorneoides, Ilex arnhemensis, Inga sp.,</i>

PFT	Type	Species
TBE	NR	<i>I. acreana</i> , <i>I. acrocephala</i> , <i>I. alba</i> , <i>I. albicoria</i> , <i>I. brachystachys</i> , <i>I. calderonii</i> , <i>I. densiflora</i> , <i>I. edulis</i> , <i>I. fanchoniana</i> , <i>I. gracilifolia</i> , <i>I. huberi</i> , <i>I. leiocalycina</i> , <i>I. longipedunculata</i> , <i>I. loubryana</i> , <i>I. marginata</i> , <i>I. melinonis</i> , <i>I. nobilis</i> , <i>I. nouraguensis</i> , <i>I. nuda</i> , <i>I. oerstediana</i> , <i>I. paraensis</i> , <i>I. pezizifera</i> , <i>I. punctata</i> , <i>I. rubiginosa</i> , <i>I. sarmentosa</i> , <i>I. sessilis</i> , <i>I. spectabilis</i> , <i>I. stipularis</i> , <i>I. subnuda</i> , <i>I. tenuistipula</i> , <i>Iryanthera hostmannii</i> , <i>I. sagotiana</i> , <i>Jessenia bataua</i> , <i>Lacistema grandifolium</i> , <i>Lacistema aculeata</i> , <i>Lacunaria crenata</i> , <i>L. jenmanii</i> , <i>Lecythis chartacea</i> , <i>L. corrugata</i> , <i>L. holcogyne</i> , <i>L. idatimon</i> , <i>L. persistens</i> , <i>L. poiteaui</i> , <i>L. zabucajo</i> , <i>Leonia glycycarpa</i> , <i>Licania</i> sp., <i>L. alba</i> , <i>L. canescens</i> , <i>L. glabriflora</i> , <i>L. heteromorpha</i> , <i>L. kunthiana</i> , <i>L. laevigata</i> , <i>L. latistipula</i> , <i>L. laxiflora</i> , <i>L. licaniiiflora</i> , <i>L. majuscula</i> , <i>L. membranacea</i> , <i>L. micrantha</i> , <i>L. minutiflora</i> , <i>L. octandra</i> , <i>L. ovalifolia</i> , <i>L. sprucei</i> , <i>Licaria cannella</i> , <i>L. chrysophylla</i> , <i>L. guianensis</i> , <i>Loreya arborea</i> , <i>Lueheopsis rugosa</i> , <i>Mabea</i> sp., <i>M. piriri</i> , <i>M. speciosa</i> , <i>Machaerium acaciaefolium</i> , <i>M. inundatum</i> , <i>M. stipitatum</i> , <i>Macoubea guianensis</i> , <i>Mallotus philippensis</i> , <i>Malouetia guianensis</i> , <i>Manilkara bidentata</i> , <i>M. huberi</i> , <i>Maprounea guianensis</i> , <i>Maquira calophylla</i> , <i>M. guianensis</i> , <i>Maytenus guyanensis</i> , <i>M. myrsinoides</i> , <i>M. oblongata</i> , <i>Melicoccus pedicellaris</i> , <i>Mezoneuron hildebrandtii</i> , <i>Miconia</i> sp., <i>M. acuminata</i> , <i>M. chartacea</i> , <i>M. cuspidata</i> , <i>M. fragilis</i> , <i>M. punctata</i> , <i>M. tschudyoides</i> , <i>Micropholis</i> sp., <i>M. cayennensis</i> , <i>M. egensis</i> , <i>M. guyanensis</i> , <i>M. longipedicellata</i> , <i>M. melinoniana</i> , <i>M. mensalis</i> , <i>M. obscura</i> , <i>M. porphyrocarpa</i> , <i>M. sanctae-rosae</i> , <i>M. venulosa</i> , <i>Minquartia guianensis</i> , <i>Moronobea coccinea</i> , <i>Mouriri crassifolia</i> , <i>M. huberi</i> , <i>M. sagotiana</i> , <i>Moutabea guianensis</i> , <i>Myrcia</i> sp., <i>M. decorticans</i> , <i>M. fallax</i> , <i>Myrciaria floribunda</i> , <i>Myroxylon balsamum</i> , <i>Neea floribunda</i> , <i>Ocotea</i> sp., <i>O. amazonica</i> , <i>O. argyrophylla</i> , <i>O. cinerea</i> , <i>O. indirectinervia</i> , <i>O. percurrentis</i> , <i>O. schomburgkiana</i> , <i>O. subterminalis</i> , <i>O. tomentella</i> , <i>Oenocarpus bacaba</i> , <i>Ormosia coccinea</i> , <i>O. flava</i> , <i>O. pachycarpa</i> , <i>O. stipularis</i> , <i>Osteophloeum platyspermum</i> , <i>Oxandra asbeckii</i> , <i>Pachira dolichocalyx</i> , <i>Palicourea guianensis</i> , <i>Parahancornia fasciculata</i> , <i>Parkia decussata</i> , <i>P. nitida</i> , <i>P. ulei</i> , <i>Parkinsonia aculeata</i> , <i>Perebea guianensis</i> , <i>P. rubra</i> , <i>Pithecellobium pruinatum</i> , <i>P. unguis-cati</i> , <i>Platonia insignis</i> , <i>Poecilanthe effusa</i> , <i>P. parviflora</i> , <i>Pogonophora schomburgkiana</i> , <i>Polyalthia australis</i> , <i>Poraqueiba guianensis</i> , <i>Posoqueria latifolia</i> , <i>Pourouma bicolor</i> , <i>P. minor</i> , <i>P. tomentosa</i> , <i>Pouteria</i> sp., <i>P. ambelaniifolia</i> , <i>P. bangii</i> , <i>P. benai</i> , <i>P. bilocularis</i> , <i>P. cladantha</i> , <i>P. cuspidata</i> , <i>P. decorticans</i> , <i>P. durlandii</i> , <i>P. egregia</i> , <i>P. engleri</i> , <i>P. eugeniiifolia</i> , <i>P. filipes</i> , <i>P. simbriata</i> , <i>P. flavilate</i> , <i>P. glomerata</i> , <i>P. gonggrijpii</i> , <i>P. grandis</i> , <i>P. guianensis</i> , <i>P. hispida</i> , <i>P. jariensis</i> , <i>P. laevigata</i> , <i>P. macrocarpa</i> , <i>P. macrophylla</i> , <i>P. maxima</i> , <i>P. melanopoda</i> , <i>P. petiolata</i> , <i>P. putamen-ovi</i> , <i>P. reticulata</i> , <i>P. retinervis</i> , <i>P. rodriquesiana</i> , <i>P. singularis</i> , <i>P. torta</i> , <i>Pradosia</i> sp., <i>P. cochlearia</i> , <i>P. ptychandra</i> , <i>Prosopis articulata</i> , <i>P. juliflora</i> , <i>P. palmeri</i> , <i>Protium</i> sp., <i>P. apiculatum</i> , <i>P. cuneatum</i> , <i>P. decandrum</i> , <i>P. demerarensis</i> , <i>P. gallicum</i> , <i>P. giganteum</i> , <i>P. guianense</i> , <i>P. morii</i> , <i>P. opacum</i> , <i>P. pallidum</i> , <i>P. plagiocarpum</i> , <i>P. sagotianum</i> , <i>P. subserratum</i> , <i>P. tenuifolium</i> , <i>P. trifoliolatum</i> , <i>Pseudopiptadenia psilospatha</i> , <i>P. suaveolens</i> , <i>Pseudoxandra cuspidata</i> , <i>Psychotria ficiifolia</i> , <i>P. mapourioides</i> , <i>Pterolobium lacerans</i> , <i>P. stellatum</i> , <i>Ptychopetalum olacoides</i> , <i>Qualea</i> sp., <i>Q. rosea</i> , <i>Quarariblea duckei</i> , <i>Q. spatulata</i> , <i>Quiina</i> sp., <i>Q. guianensis</i> , <i>Q. obovata</i> , <i>Recordoxylon speciosum</i> , <i>Rhabdodendron amazonicum</i> , <i>Rheedia madruno</i> , <i>Rhodostemonodaphne grandis</i> , <i>R. kunthiana</i> , <i>R. praeclera</i> , <i>R. rufovirgata</i> , <i>Rinorea</i> sp., <i>Rollinia elliptica</i> , <i>Ruizterania albiflora</i> , <i>Sacoglottis</i> sp., <i>S. cydonioides</i> , <i>S. guianensis</i> , <i>Salacia elliptica</i> , <i>Sandwithia guianensis</i> , <i>Saraca indica</i> , <i>Schefflera decaphylla</i> , <i>S. morototoni</i> , <i>Schotia humboldtioides</i> , <i>Sextonia rubra</i> , <i>Simaba cedron</i> , <i>S. morettii</i> , <i>S. polyphylla</i> , <i>Simarouba amara</i> , <i>Siparuna cristata</i> , <i>S. decipiens</i> , <i>S. pachyantha</i> , <i>Sloanea</i> sp., <i>S. brevipes</i> , <i>S. echinocarpa</i> , <i>S. eichleri</i> , <i>S. garckeana</i> , <i>S. guianensis</i> , <i>S. latifolia</i> , <i>Stachyarrhena acuminata</i> , <i>Sterculia frondosa</i> , <i>S. lisae</i> , <i>S. multiovula</i> , <i>S. parviflora</i> , <i>Sympodia</i> sp., <i>S. globulifera</i> , <i>Symplocos martinicensis</i> , <i>Tachigali bracteolata</i> , <i>T. guianensis</i> , <i>T. melinonii</i> , <i>T. paniculata</i> , <i>T. paraensis</i> , <i>Talisia</i> sp., <i>T. clathrata</i> , <i>T. hexaphylla</i> , <i>T. microphylla</i> , <i>T. praeculta</i> , <i>T. simaboides</i> , <i>Tamarindus indica</i> , <i>Tapirira bethanniana</i> , <i>T. guianensis</i> , <i>T. obtusa</i> , <i>Tapura amazonica</i> , <i>T. capitulifera</i> , <i>T.</i>

PFT	Type	Species
TBE	NR	<i>gianensis</i> , <i>Tetragastris altissima</i> , <i>T. panamensis</i> , <i>Theobroma subincanum</i> , <i>T. velutinum</i> , <i>Thyrsodium guianense</i> , <i>T. puberulum</i> , <i>Torresea cearensis</i> , <i>Touroulia guianensis</i> , <i>Tovomita</i> sp., <i>Trachylobium hornemannianum</i> , <i>Trattinnickia</i> sp., <i>Trichilia cipo</i> , <i>T. euneura</i> , <i>T. micrantha</i> , <i>T. pallida</i> , <i>T. schomburgkii</i> , <i>T. surinamensis</i> , <i>Trymatococcus amazonicus</i> , <i>T. oligandrus</i> , <i>Unonopsis perrottetii</i> , <i>U. rufescens</i> , <i>Vatarea erythrocarpa</i> , <i>Vataireopsis surinamensis</i> , <i>Virola kwatae</i> , <i>V. michelii</i> , <i>V. multicostata</i> , <i>Vismia cayennensis</i> , <i>Vitex triflora</i> , <i>Vochysia guinanensis</i> , <i>V. tomentosa</i> , <i>Vouacapoua americana</i> , <i>Vouarana guianensis</i> , <i>Xylopia nitida</i> , <i>Xylosma benthamii</i>
	Other	<i>Acacia</i> sp., <i>A. auriculaeformis</i> , <i>Alibertia sessilis</i> , <i>Allophylus angustatus</i> , <i>A. latifolius</i> , <i>Betharocalyx salicifolius</i> , <i>Brosimum gaudichaudii</i> , <i>Buchanania arborescens</i> , <i>B. obovata</i> , <i>Byrsonima laxiflora</i> , <i>Callisthene major</i> , <i>Cassia alata</i> , <i>C. siamea</i> , <i>C. spruceana</i> , <i>Davilla elliptica</i> , <i>Denhamia obscura</i> , <i>Didymopanax macrocarpon</i> , <i>D. morototoni</i> , <i>Drypetes fanshawei</i> , <i>D. variabilis</i> , <i>Eremanthus glomerulatus</i> , <i>Erythroxylum daphnites</i> , <i>E. suberosum</i> , <i>Grevillea decurrens</i> , <i>Guapira areolata</i> , <i>G. graciflora</i> , <i>Hymenaea courbaril</i> , <i>H. martiana</i> , <i>H. stigonocarpa</i> , <i>Inga laurina</i> , <i>Machaerium acuminata</i> , <i>M. opacum</i> , <i>Matayba guianensis</i> , <i>Maytenus floribunda</i> , <i>Miconia pohliana</i> , <i>Myrcia deflexa</i> , <i>M. rostrata</i> , <i>Myrsine guianensis</i> , <i>M. umbellatum</i> , <i>Ouratea castaneaegolia</i> , <i>O. hexasperma</i> , <i>Piptocarpha macropoda</i> , <i>P. rotundifolia</i> , <i>Pouteria arnhemica</i> , <i>P. sericea</i> , <i>Pseudolmedia cf marginatum</i> , <i>Qualea dichotoma</i> , <i>Salacia crassifolia</i> , <i>Sophora chrysophylla</i> , <i>Styrax camporum</i> , <i>S. ferrugineus</i> , <i>Symplocos lanceolata</i> , <i>S. mosenii</i> , <i>Vochysia tucanorum</i>
TBD	RS	<i>Acosmum bijugum</i> , <i>Alphitonia excelsa</i> , <i>Brachystegia longifolia</i> , <i>B. spicaeformis</i> , <i>B. utilis</i> , <i>Burkea africana</i> , <i>Corymbia foelscheana</i> , <i>C. grandifolia</i> , <i>C. polycarpa</i> , <i>C. porrecta</i> , <i>C. ptychocarpa</i> , <i>Gardenia resinosa</i> , <i>Isoberlinia paniculata</i> , <i>Petalostigma pubescens</i> , <i>Strychnos lucida</i> , <i>Swartzia arborescens</i> , <i>Tabebuia serratifolia</i> , <i>Terminalia carpentariae</i> , <i>T. ferdinandiana</i> , <i>T. latipes</i> , <i>Vitex glabrata</i>
NR		<i>Adenanthera macrocarpa</i> , <i>A. microperma</i> , <i>A. pavonina</i> , <i>Adenocarpus viscosus</i> , <i>Aeschynomene elaphroxylon</i> , <i>A. pfundii</i> , <i>Affonsea bahiensis</i> , <i>Afzelia quanzensis</i> , <i>Andira anthelmia</i> , <i>A. fraxinifolia</i> , <i>A. inermis</i> , <i>A. laurifolia</i> , <i>A. nitida</i> , <i>A. paniculata</i> , <i>Antiaris toxicaria</i> , <i>Apeiba glabra</i> , <i>A. petoumo</i> , <i>Aspidosperma discolor</i> , <i>Bauhinia candicans</i> , <i>B. purpurea</i> , <i>Bombacopsis nervosa</i> , <i>Bombax</i> sp., <i>Butea frondosa</i> , <i>Byrsonima laevigata</i> , <i>Caesalpinia decapetala</i> , <i>C. myabensis</i> , <i>C. velutina</i> , <i>Caryocar glabrum</i> , <i>Cedrelinga cateniformis</i> , <i>Chrysophyllum</i> sp., <i>C. argenteum</i> , <i>C. cuneifolium</i> , <i>C. eximium</i> , <i>C. lucentifolium</i> , <i>C. prieurii</i> , <i>C. sanguinolentum</i> , <i>Clitoria brachystegia</i> , <i>Copaifera trapezifolia</i> , <i>Cordia</i> sp., <i>C. sagotii</i> , <i>Couepia bracteosa</i> , <i>C. caryophylloides</i> , <i>C. guianensis</i> , <i>C. habrantha</i> , <i>C. joaquiniae</i> , <i>C. magnoliifolia</i> , <i>C. parillo</i> , <i>Couma guianensis</i> , <i>Cyathostegia matthewsii</i> , <i>Cylista scariosa</i> , <i>Delonix regia</i> , <i>Dialium guianense</i> , <i>Dimorphandra mollis</i> , <i>Dussia discolor</i> , <i>Eriotheca</i> sp., <i>E. longitubulosa</i> , <i>Erythrina aurantiaca</i> , <i>Erythrophleum guineense</i> , <i>E. lasianthum</i> , <i>Glycydendron amazonicum</i> , <i>Gouania glabra</i> , <i>Guettarda acreana</i> , <i>Himatanthus</i> sp., <i>Hirtella bicornis</i> , <i>H. bicornis</i> var <i>bicornis</i> , <i>H. bicornis</i> var <i>pubescens</i> , <i>H. glandistipula</i> , <i>H. glandulosa</i> , <i>H. macrosepala</i> , <i>H. suffulta</i> , <i>Hoffmannseggia intricata</i> , <i>Hymenolobium janeirensense</i> , <i>Isertia spiciformis</i> , <i>Jacaranda copaia</i> , <i>Laetia procera</i> , <i>Lecythis aurantiaca</i> , <i>Lonchocarpus capassa</i> , <i>L. floribundus</i> , <i>L. guatemalensis</i> , <i>L. leucanthus</i> , <i>Macrolobium bifolium</i> , <i>M. latifolium</i> , <i>M. palisoti</i> , <i>M. zenkeri</i> , <i>Matayba inelegans</i> , <i>M. laevigata</i> , <i>Miliusa brahei</i> , <i>Mimosa caesalpiniifolia</i> , <i>M. scabrella</i> , <i>Myrospermum balsamiferum</i> , <i>M. frutescens</i> , <i>Ormosia nitida</i> , <i>Ostryocarpus riparius</i> , <i>Ouratea melinonii</i> , <i>Parapiptadenia pterosperma</i> , <i>Parinari campestris</i> , <i>P. excelsa</i> , <i>P. montana</i> , <i>Parkia velutina</i> , <i>Peltogyne</i> sp., <i>P. nitens</i> , <i>P. paniculata</i> , <i>Peltophorum africanum</i> , <i>P. pterocarpum</i> , <i>Phylloxylon perrieri</i> , <i>P. spinosa</i> , <i>Piptadenia buchanani</i> , <i>P. obliqua</i> , <i>P. viridiflora</i> , <i>Piscidia carthaginensis</i> , <i>Pithecellobium selen</i> , <i>P. dulce</i> , <i>Platymiscium obtusifolium</i> , <i>P. pinnatum</i> , <i>P. zehntneri</i> , <i>Poepigia procera</i> , <i>P. prosera</i> , <i>Poinciana regia</i> , <i>Pongamia exerocarpa</i> , <i>P. pinncta</i> , <i>Pourouma melinonii</i> , <i>P. villosa</i> , <i>Pterocarpus</i>

IMPROVED SIMULATION OF FIRE-VEGETATION INTERACTIONS IN THE LAND  
SURFACE PROCESSES AND EXCHANGES DYNAMIC GLOBAL VEGETATION MODEL  
(LPX-Mv1)

PFT	Type	Species
TBD	NR	<i>angolensis</i> , <i>P. marsupium</i> , <i>P. osun</i> , <i>P. rohrii</i> , <i>P. rotundifolius</i> , <i>P. santalinus</i> , <i>Pterodon abruptus</i> , <i>Pterogyne nitens</i> , <i>Rhynchosia clivorum</i> , <i>Sabinea carinalis</i> , <i>Schizolobium parahybum</i> , <i>Senna angulata</i> , <i>S. cana</i> , <i>Sterculia pruriens</i> , <i>S. speciosa</i> , <i>S. villosa</i> , <i>Stryphnodendron moricolor</i> , <i>S. polystachyum</i> , <i>Swartzia</i> sp., <i>S. acutifolia</i> , <i>S. amshoffiana</i> , <i>S. apetala</i> , <i>S. benthamiana</i> , <i>S. canescens</i> , <i>S. grandifolia</i> , <i>S. leblondii</i> , <i>S. oblanceolata</i> , <i>S. panacoco</i> , <i>S. panacoco</i> var. <i>panacoco</i> , <i>S. polyphylla</i> , <i>Tabebuia</i> sp., <i>T. capitata</i> , <i>Tarenna australis</i> , <i>Terminalia</i> sp., <i>T. guianensis</i> , <i>T. microcarpa</i> , <i>Tetrapleura thonningii</i> , <i>Tipuana speciosa</i> , <i>Trattinnickia demerarae</i> , <i>Vantanea parviflora</i> , <i>Xylopia frutescens</i> , <i>Zygia racemosa</i> , <i>Z. tetragona</i>
	Other	<i>Acacia kamerunensis</i> , <i>A. pennata</i> , <i>A. picachensis</i> , <i>A. tucumanensis</i> , <i>A. velutina</i> , <i>A. welwitschii</i> , <i>Aegiphila lhotskiana</i> , <i>A. sellowiana</i> , <i>Albizia adianthifolia</i> , <i>A. adinocephala</i> , <i>A. antunesiana</i> , <i>A. caribaea</i> , <i>A. forbesii</i> , <i>A. guachapele</i> , <i>A. petersiana</i> , <i>A. purpusii</i> , <i>A. sinaloensis</i> , <i>A. thompsoni</i> , <i>A. tomentosa</i> , <i>A. benthamiana</i> , <i>Aspidosperma subincanum</i> , <i>A. tomentosum</i> , <i>Astrocaryum rodriquesii</i> , <i>A. sciophilum</i> , <i>Bauhinia cunninghamii</i> , <i>B. forficata</i> , <i>Blepharocarya depauperata</i> , <i>Brachychiton diversifolius</i> , <i>Byrsinima crassa</i> , <i>Canarium australianum</i> , <i>Capparis leprieurii</i> , <i>C. maroniensis</i> , <i>Caryocar brasiliense</i> , <i>Cassia afrofistula</i> , <i>C. emarginata</i> , <i>C. fistula</i> , <i>C. laevigata</i> , <i>C. tomentosa</i> , <i>Centrolobium tomentosum</i> , <i>Dalbergia miscolobium</i> , <i>Eriotheca pubescens</i> , <i>Erythrophleum chlorostachys</i> , <i>Guapira noxia</i> , <i>Guettarda vibrinoides</i> , <i>Hymenolobium</i> sp., <i>Hymenolobium flavum</i> , <i>Leucaena shannonii</i> , <i>Owenia vernicosa</i> , <i>Platypodium elegans</i> , <i>Pouteria ramiflora</i> , <i>Qualea parviflora</i> , <i>Tabebuia impetiginosa</i> , <i>T. ochracea</i> , <i>T. roseo-alba</i>
tNE	N/A	<i>Abies alba</i> , <i>A. balsamea</i> , <i>A. cephalonica</i> , <i>A. cilicica</i> , <i>A. concolor</i> , <i>A. delavayi</i> , <i>A. grandis</i> , <i>A. lasiocarpa</i> , <i>A. lowiana</i> , <i>A. nordmanniana</i> , <i>A. recurvata</i> , <i>A. religiosa</i> , <i>A. sibirica</i> , <i>A. veitchii</i> , <i>Actinostrobus pyramidalis</i> , <i>Agathis australis</i> , <i>Agathis philippinensis</i> , <i>Araucaria angustifolia</i> , <i>A. bidwillii</i> , <i>A. columnaris</i> , <i>A. excelsa</i> , <i>Arthrotaxis cupressoides</i> , <i>Callitris cupressiformis</i> , <i>C. intratropica</i> , <i>C. macleayana</i> , <i>C. preissii</i> , <i>Calocedrus decurrens</i> , <i>Cedrus atlantica</i> , <i>C. deodara</i> , <i>Chamaecyparis lawsoniana</i> , <i>C. pisifera</i> , <i>Cryptomeria japonica</i> , <i>Cupressus arizonica</i> , <i>C. goveniana</i> , <i>C. guadalupensis</i> , <i>Dacrycarpus dacryoides</i> , <i>Dacrydium cupressinum</i> , <i>D. excelsium</i> , <i>Fitzroya cupressoides</i> , <i>Fokienia hodginsii</i> , <i>Glyptostrobus lineatus</i> , <i>Juniperus californica</i> , <i>J. cedrus</i> , <i>J. communis</i> , <i>J. deppeana</i> , <i>J. monosperma</i> , <i>J. occidentalis</i> , <i>J. osteosperma</i> , <i>J. oxycedrus</i> , <i>J. scopolorum</i> , <i>Picea</i> sp., <i>P. engelmannii</i> , <i>P. glauca</i> , <i>P. mariana</i> , <i>Pinus aristata</i> , <i>P. bahamensis</i> , <i>P. banksiana</i> , <i>P. canariensis</i> , <i>P. caribaea</i> , <i>P. coulteri</i> , <i>P. edulis</i> , <i>P. flexilis</i> , <i>P. halepensis</i> , <i>P. inops</i> , <i>P. muricata</i> , <i>P. nigra</i> , <i>P. palustris</i> , <i>P. pinea</i> , <i>P. ponderosa</i> , <i>P. pungens</i> , <i>P. radiata</i> , <i>P. rigida</i> , <i>P. strobiformis</i> , <i>P. strobus</i> , <i>P. tabuliformis</i> , <i>P. taeda</i> , <i>Podocarpus blumei</i> , <i>P. falcata</i> , <i>P. falcatus</i> , <i>P. ferruginea</i> , <i>P. junghuhniana</i> , <i>P. latifolius</i> , <i>P. macrophylla</i> , <i>P. milaniana</i> , <i>P. milanjanus</i> , <i>P. nagi</i> , <i>P. salignus</i> , <i>P. spicatus</i> , <i>P. totara</i> , <i>P. transiens</i> , <i>Prumnopitys ferruginea</i> , <i>P. taxifolia</i> , <i>Pseudolarix amabilis</i> , <i>Pseudotsuga menziesii</i> , <i>Saxegothaea conspicua</i> , <i>Sciadopitys verticillata</i> , <i>Sequoioideae</i> , <i>Sequoiadendron giganteum</i> , <i>Serruria glomerata</i> , <i>Taxodium distichum</i> , <i>Taxus baccata</i> , <i>T. brevifolia</i> , <i>Thuja occidentalis</i> , <i>T. orientalis</i> , <i>T. plicata</i> , <i>T. standishii</i>
tBE	RS	<i>Acacia karroo</i> , <i>A. luederitzii</i> , <i>Corymbia gummifera</i> , <i>Elaeocarpus reticulatus</i> , <i>E. amygdalina</i> , <i>E. bridgesiana</i> , <i>E. prava</i> , <i>E. saligna</i> , <i>E. botryoides</i> , <i>E. cameronii</i> , <i>E. nobilis</i> , <i>Leucospermum conocarpodendron</i> , <i>Mimetes fimbriifolius</i> , <i>Orites excelsa</i> , <i>Protea nitida</i> , <i>Ulex europaeus</i> , <i>Vesselowskyia rubiflora</i>
	NR	<i>Acacia</i> sp., <i>A. baileyana</i> , <i>A. decurrens</i> , <i>A. maidenii</i> , <i>A. verticillata</i> , <i>Ammodendron karelinii</i> , <i>Androstachys johnsonii</i> , <i>Anopterus glandulosus</i> , <i>Aristotelia serrata</i> , <i>Ateleia tomentosa</i> , <i>Aulax umbellata</i> , <i>Banksia integrifolia</i> ssp. <i>monticola</i> , <i>Bauhinia galpinii</i> , <i>Beilschmiedia tawa</i> , <i>Cadia ellistiana</i> , <i>Caesalpinia arenosa</i> , <i>C. cacalaco</i> , <i>C. caladenia</i> , <i>C. californica</i> , <i>C. episanioi</i> , <i>C. eriostachys</i> , <i>C. exostemma</i> ,

PFT	Type	Species
tBE	NR	<i>C. gaumeri, C. glabrata, C. gracilis, C. hilderbrandtii, C. hintonii, C. hughesii, C. madagascariensis, C. melanadenia, C. mexicana, C. nipensis, C. palmeri, C. pannosa, C. placida, C. standleyi, C. violacea, C. yucatanensis, Callistachys lanceolata, Carpodetus serratus, Chamaecytisus palmensis, C. proliferus, Chloroleucon confine, Cordeauxia edulis, Cytisus battandieri, Dalbergia hupeana, Dendrochnide excelsa, Elaeodendron transvaalense, Eucalyptus regans, Eucalyptus cf. marginata, Gymnocladus dioica, Harpaluce arborescens, Hebestigma cubense, Hoheria cf. sexstylosa, Hybosoma ehrenbergii, Laurelia novae-zelandiae, Leucadendron argenteum, L. laureolum, L. xanthoconus, Lonchocarpus acuminatus, Naucleopsis guianensis, Neea sp., Pickeringia montana, Plinia rivularis, Podocarpus elatus, Poralyria calyprata, Prosopis glandulosa, Prostanthera sp. aff. lasianthos, Protea coronata, P. lepidocarpodendron, P. repens, P. roupelliae, Pseudopanax arboreus, P. crassifolius, Raukawa edgerleyi, Sassafras albidum, Schotia brachypetala, S. capitata, Spartocytisus nubigenus, S. supranubius, Sterculia quadrifida, Styrax pallidus, Syzygium maire, Warburgia salutaris, Weinmannia racemosa, Xanthocercis zambesiaca</i>
Other		<i>Acacia brandegeana, A. choriophylla, A. coulteri, A. dealbata, A. eburnea, A. ehrenbergiana, A. farnesiana, A. floribunda, A. huarango, A. laeta, A. longifolia, A. macracantha, A. mammifera, A. melanoxyton, A. mellifera, A. nerifolia, A. nubica, A. pataczekii, A. pennivenia, A. pterygocarpa, A. radiana, A. senegal, A. seyal, A. sieberana, A. sowdenii, A. spirocarpa, A. swazica, A. willardiana, Acmena smithii, Atherosperma moschatum, Aulax pallasia, Caldcluvia paniculata, Callicoma serratifolia, Calycotome villosa, Cassia montana, C. polyantha, C. pringlei, C. skinneri, Cerratopetalum apetaum, Cordyline australis, Cryptocaria nova-anglica, C. meisneriana, Doryphora sassafrass ssp. montane, Elaeocarpus holopetalus, E. dentatus, E. australe, Endiandra sieberi, Eucalyptus coccifera, E. obliqua, E. rubida, E. pauciflora, Eucryphia lucida, Glochidion ferdinandii, Guioa semiglaucia, Hedycarya arborea, Indigofera marmorata, I. oblongifolia, I. teysmanni, Kunzea ericoides, Leucadendron salignum, Leucaena diversifolia, Lophostemon confertus, Mimetes cucullatus, Nothofagus cunninghamii, N. moorei, Notolaea sp. aff. venosa, Phyllocladus aspleniifolius, Pittosporum undulatum, Pomaderis apetala, Pomaderris apetala, Protea caffra, P. cynaroides, Quintinia sieberi, Rapanea variabilis, Schizomeria ovata, Sophora affinis, S. microphylla, S. tetraptera, S. tomentosa, Tasmania stipitata, Trichilia emetica, Trochocarpa montana</i>
tBD	RS	<i>Acacia gerrardii, A. grandicornuta, A. nigrescens, A. tortilis, Acer glabrum, A. grandidentatum, Betula papyrifera, Brachystegia boehmii, Cercis siliquastrum, Colophospermum mopane, Corymbia polysciada, Genista acanthoclada, Populus angustifolia, P. balsamifera, P. tremuloides, Sclerocarya birrea, Toona ciliata, Ziziphus mucronata</i>
NR		<i>Acacia xanthophloea, Acer negundo, Alnus oblongifolia, Apoplanesia paniculata, Balanites maughamii, Bauhinia roxburghiana, B. subrotundifolia, Brya ebenus, Caesalpinia platyloba, C. sclerocarpa, Calliandra houstoniana, Carmichaelia australis, Cercidium floridum ssp. peninsulare, C. microphyllum, C. peninsulare, C. praecox, C. texanum, Colvillea racemosa, Conzzattia multiflora, Coursetia glandulosa, Cytisus candicans, C. proliferus, Dalbergia melanoxyton, Desmanthus fruticosus, Desmodium tiliaefolium, Diphysa americana, Elephantorrhiza burkei, Enterolobium contortisiliquum, Enterolobium cyclocarpum, Eysenhardtia amorphoides, Fordia cf. brachybotrys, Fraxinus velutina, Fuchsia excorticata, Genista benehoavensis, G. cinerea, G. virgata, Geoffroea decorticans, Goodia lotifolia, Gymnocladus canadensis, Juglans major, Kirkia acuminata, Lemnopisum edule, Lysiloma aurita, L. candida, Mimosia benthamii, Mimosa falcata, Olneya tesota, Peltophorum dubium, Phyllocarpus septentrionalis, Piscidia mollis, P. piscipula, Pithecellobium glaucum, P. unguis-cati, Platanus wrightii, Populus fremontii</i>

IMPROVED SIMULATION OF FIRE-VEGETATION INTERACTIONS IN THE LAND  
SURFACE PROCESSES AND EXCHANGES DYNAMIC GLOBAL VEGETATION MODEL  
(LPX-Mv1)

---

PFT	Type	Species
tBD	NR	<i>Prunus emarginata, Retama monosperma, Rhus chirindensis, R. glabra, Robinia x holtii britzensis, Salix sp., S. babylonica, S. bebbiana, Sesbania sesban, Spartium junceum, Teline stenopetala</i>
	Other	<i>Acacia albida, A. angustissima, A. caffra, A. chameleensis, A. davyi, A. exuvialis, A. horrida, A. nilotica, A. robusta, Albizia anthelmintica, A. occidentalis, A. plurijuga, A. versicolor, Calycotome spinosa, Cassia abbreviata, C. wislizenii, Celtis reticulata, Combretum hereroense, C. imberbe, Cytisus scoparius, Dichrostachys cinerea, Gleditsia triacanthos, Laburnum anagyroides, Leucaena confertiflora, L. esculenta, L. esculenta x leucocephala, L. macrophylla, L. pulverulenta, Quercus gambelii, Robinia neomexicana, R. pseudoacacia, Sophora japonica, S. secundiflora, Terminalia prunioides, T. sericea</i>
BNE	N/A	<i>Picea abies, P. jezoensis, P. likiangensis, P. obovata, P. omorica, P. orientalis, P. pungens, P. schrenkiana, P. spinulosa, Pinus cembra, P. cembroides, P. gerardiana, P. koraiensis, P. laticio, P. longifolia, Tsuga canadensis, T. dumosa, T. heterophylla</i>

**Table S3.** Information used to calculate recovery time at sites with different fire-response adaptations. The dominant fire responses (Dominant adaptation) are AR: aerial resprouters (RS), BR: basal RS, OS: obligate seeder, and R: RS of unknown type. NR indicates vegetation with no specific fire adaptation. AR and BR sites are used to represent RS in Fig. 7, while UR, R and OS are grouped together as OS in Fig. 7. Med stands for Mediterranean-type climate. The proportion decrease (%) in the vegetation index of a site after fire is given in Impact. The vegetation indices (Veg Index) are NDVI: Normalised Difference Vegetation Index, NDVI anomalies: the deviation of NDVI from the expected value; EVI: the Enhanced vegetation index; or a site-specific index as described in the original publication. The impact of fire was expressed either with respect to local sites that were not burnt (control) or to pre-fire values at the burnt site (pre-fire), or to the maximum annual cycle value found in pre-fire years (gorgeous years – see Gouveia et al. 2010). The time to recovery is the length of time required before the Veg Index reaches 90% of the pre-fire cover. Where this is based on an extrapolation beyond the years of observation, the number of extrapolated years is given (Extrapolated Years).

Dominant Adaptation	Dominant Species	Location	Climate	Impact (%)	Veg Index	Comparison	Interpolate to recovery (yr)	Time to recovery (yr months)	Reference
AR	<i>Quercus suber</i>	Catalonia, Spain	Med	47	NDVI	control	6	13 yr 6 m	Díaz-Delgado et al. (1998)
	<i>Quercus suber</i>	Catalonia, Spain	Med	44	NDVI	control	0	5 yr 2 m	Díaz-Delgado et al. (1998)
	<i>Quercus suber</i>	Catalonia, Spain	Med	78	NDVI	control	0	7 yr 3 m	Díaz-Delgado et al. (2002)
	<i>Eucalyptus</i> sp.	Portugal	Med	27	NDVI	gorgeous years	8	10 yr 2 m	Gouveia et al. (2010)
	<i>Jameson catchment, California, USA</i>				NDVI	pre-fire	0	4 yr 4 m	Hope et al. (2007)

IMPROVED SIMULATION OF FIRE-VEGETATION INTERACTIONS IN THE LAND  
SURFACE PROCESSES AND EXCHANGES DYNAMIC GLOBAL VEGETATION MODEL  
(LPX-Mv1)

Dominant Adaptation	Dominant Species	Location	Climate	Impact (%)	Veg Index	Comparison	Interpolate to recovery (yr)	Time to recovery (yr)	Reference months)
AR/BR	<i>Adenostoma fasciculatum;</i> <i>Ceanothus</i> sp.; <i>Arcostaphylos</i> sp.; <i>Quercus dumosa</i> ; <i>Rhus ovata</i> ; <i>Heteromeles arbutifolia</i>	Santa Monica Mountains, California, USA	Med	58	NDVI	control	7	8 yr 3 m	Riaño et al. (2002)
	<i>Santa Monica Mountains, California, USA</i>	coastal sage scrub	Med	43	NDVI	control	0	0 yr 2 m	Riaño et al. (2002)
	<i>Arcostaphylos glauca;</i> <i>Ceanothus megacarpus;</i> <i>Cercocarpus betuloides;</i> <i>Rhamnus ilicifolia;</i> <i>Eriogonum fasciculatum;</i> <i>Ceanothus thyrsiflorus;</i> <i>Adenostoma fasciculatum;</i> <i>Ceanothus greggii;</i> <i>Arcostaphylos glandulosa;</i> <i>Ceanothus crassifolius;</i> <i>Ceanothus cuneatus;</i> <i>Ceanothus leucodermis;</i> <i>Prunus ilicifolia</i> ssp. <i>ilicifolia</i>	Jameson catchment, California, USA	Med	72	NDVI	pre-fire	0	5 yr 10 m	Hope et al. (2007)

Dominant Adaptation	Dominant Species	Location	Climate	Impact (%)	Veg Index	Comparison	Interpolate to recovery (yr)	Time to recovery (yr months)	Reference
AR/BR	<i>Arcostaphylos glauca;</i> <i>Ceanothus megacarpus;</i> <i>Cercocarpus betuloides;</i> <i>Rhamnus ilicifolia;</i> <i>Eriogonum fasciculatum;</i> <i>Ceanothus thyrsiflorus;</i> <i>Adenostoma fasciculatum;</i> <i>Ceanothus greggii;</i> <i>Arcostaphylos glandulosa;</i> <i>Ceanothus crassifolius;</i> <i>Ceanothus cuneatus;</i> <i>Ceanothus leucodermis;</i> <i>Prunus ilicifolia</i> ssp. <i>ilicifolia</i>	Jameson catchment, CA, USA	Med	60	NDVI	pre-fire	0	4 yr 0 m	Hope et al. (2007)
BR	<i>Sahvia apiana;</i> <i>Salvia leucophylla;</i> <i>Sahvia mellifera;</i> <i>Artemisia californica;</i> <i>Eriogonum cinereum;</i> <i>Eriogonum elongatum;</i> <i>Eriogonum fasciculatum;</i> <i>Encelia californica;</i> <i>Lotus sp.;</i> <i>Lupinus</i> sp.; <i>Mimulus</i> sp.	Santa Monica Mountains, California, USA	Med	33	NDVI	control	6	10 yr 0 m	Riaño et al. (2002)

IMPROVED SIMULATION OF FIRE-VEGETATION INTERACTIONS IN THE LAND  
SURFACE PROCESSES AND EXCHANGES DYNAMIC GLOBAL VEGETATION MODEL  
(LPX-Mv1)

Dominant Adaptation	Dominant Species	Location	Climate	Impact (%)	Veg Index	Comparison	Interpolate to recovery (yr)	Time to recovery (yr months)	Reference
BR	<i>Salvia apiana</i> ; <i>Salvia leucophylla</i> ; <i>Salvia mellifera</i> ; <i>Artemisia californica</i> ; <i>Eriogonum cinereum</i> ; <i>Eriogonum elongatum</i> ; <i>Eriogonum fasciculatum</i> ; <i>Encelia californica</i> ; <i>Lotus sp.</i> ; <i>Lupinus sp.</i> ; <i>Mimulus sp.</i>	Santa Monica Mountains, California, USA	Med	48	NDVI	control	8	11 yr 7 m	Riaño et al. (2002)
	<i>Quercus ilex</i> ; <i>Pinus halepensis</i>	Catalonia, Spain	Med	46	NDVI	control	6	14 yr 5 m	Díaz-Delgado et al. (1998)
	<i>Adenostoma fasciculatum</i> ; <i>Salvia mellifera</i> ; <i>Salvia apiana</i>	Jameson catchment, CA, USA	Med	70	NDVI	pre-fire	0	5 yr 10 m	Hope et al. (2007)
	<i>Eriogonum fasciculatum</i> ; <i>Salvia apiana</i>	Jameson catchment, CA, USA	Med	67	NDVI	pre-fire	0	7 yr 2 m	Hope et al. (2007)



**Table S4.** Extended version of Table 4 in main text. Scores obtained using the mean of the data (Data mean), and the mean and standard deviation of the scores obtained from bootstrapping experiments (Bootstrap mean, Bootstrap SD). Step 1 is a straight comparison; 2 is a comparison with the influence of the mean removed; 3 is with mean and variance removed. Step 2 and 3 have been included for inter-annual variability (IAV) and Seasonal concentration, and full scores have been included for each burnt area dataset.

Variable	Step	Measure	time period	mean	bootstrap mean	bootstrap SD
fAPAR	1	Annual average	1997-2005	1.00	1.33	0.015
	2			1.00	1.33	0.015
	3			1.00	1.32	0.014
	2	Inter-annual variability		1.00	1.23	0.32
	3			1.00	1.35	0.36
	1	Seasonal concentration		1.00	1.46	0.014
	2			1.00	1.46	0.014
	3			1.00	1.45	0.014
	N/A	Phase	1992-1993	0.30	0.38	0.0033
	N/A	life forms		0.71	0.89	0.0018
Veg cover	N/A	tree cover		0.43	0.54	0.0015
	N/A	herb cover		0.49	0.66	0.0017
	N/A	bare ground		0.46	0.56	0.0017
	N/A	broadleaf		0.83	0.96	0.0041
	N/A	evergreen		0.70	0.87	0.0032
fine litter NPP 1	Annual average	1997-2005	1.00	1.44	0.21	
	2		1.00	1.44	0.22	
	3		1.00	1.43	0.095	
	1	Annual average	2005	1.00	1.32	0.016
Height	2			1.00	1.32	0.016
	3			1.00	1.31	0.016

<b>Variable</b>	<b>Step</b>	<b>Measure</b>	<b>time period</b>	<b>Mean</b>	<b>bootstrap mean</b>	<b>bootstrap SD</b>
Fire: GFED3	1	Annual average	1997-2006	1.00	1.25	0.015
	2			1.00	1.26	0.015
	3			1.00	1.28	0.016
	2	Inter-annual variability		1.00	1.31	0.36
	3			1.00	1.25	0.33
	1	Seasonal Conc		1.00	1.36	0.020
	2			1.00	1.36	0.020
	3			1.00	1.36	0.018
	N/A	Phase		0.39	0.44	0.0046
Fire: GFED3 SE	1	Annual average	1997-2006	1.00	1.19	0.024
	2			1.00	1.19	0.024
	3			1.00	1.21	0.024
	2	Inter-annual variability		1.00	1.26	0.33
	3			1.00	1.41	0.54
	1	Seasonal Conc		1.00	1.31	0.053
	2			1.00	1.31	0.052
	3			1.00	1.31	0.045
	N/A	Phase		0.47	0.47	0.011
Fire: GFED4	1	Annual average	1997-2006	1.00	1.14	0.0028
	2			1.00	1.24	0.0037
	3			1.00	1.30	0.0053
	2	Inter-annual variability		1.00	1.50	0.34
	3			1.00	1.28	0.27
	1	Seasonal Conc		1.00	1.32	0.0073
	2			1.00	1.33	0.0071
	3			1.00	1.34	0.0061
	N/A	Phase		0.45	0.47	0.0015

Variable	Step	Measure	time period	mean	bootstrap mean	bootstrap SD
Fire: GFED4 SE	1	Annual average		1.00	1.18	0.024
	2			1.00	1.18	0.024
	3			1.00	1.20	0.025
	2	Inter-annual variability		1.00	1.24	0.34
	3			1.00	1.52	0.67
	1	Seasonal Conc		1.00	1.33	0.043
	2			1.00	1.33	0.043
	3			1.00	1.33	0.038
	N/A	Phase	1996.5-2005.5	0.44	0.47	0.010
	1	Annual average		1.00	1.13	0.026
Fire: Ground Observation	2			1.00	1.15	0.027
	3			1.00	1.10	0.025
	2	Inter-annual variability		1.00	1.32	0.37
	3			1.00	1.34	0.36

**Table S5.** Comparison metric scores for model simulations against observations. Mean and variance rows show mean and variance of simulation for annual average values, by the ratio of the mean/variance with observed mean or variance. Numbers in bold indicates if the model performs better than the original LPX model. Italic indicates model scores better than the mean of the data score listed in Table S4. Asterisks indicate model scores that are significantly better than randomly resampling listed in Table S4. S1 are step 1 comparisons, S2 are step 2; and S3 are step 3. All metrics defined in Kelley et al. (2013). Lightn column give the scores for lightning parametrisations to LPX; Drying for fuel drying time parametrisation; Roots for deep rooting fraction; Litter for litter decomposition; and Bark for the inclusion of adaptive bark. LPX-M-v1-nr incorporates all parametrisations and LPX-M-v1-rs incorporates resprouting into LPX-Mv1-nr. fAPAR is the fraction of absorbed photosynthetically active radiation, NPP is net primary productivity.

Variable	Metric used	Measure	LPX	Lightn	Drying	Roots	Litter	bark thickness	LPX-Mv1-nr	LPX-Mv1-rs
Burnt area: GFED3	Mean	Annual Average	0.082	0.12	0.084	0.086	0.02	0.003	0.049	0.050
	Mean ratio		1.13	1.64	1.15	1.18	0.28	0.039	0.67	0.69
	Variance		0.047	0.049	0.046	0.047	0.025	0.005	0.041	0.041
	Variance ratio		0.56	0.59	0.54	0.55	0.29	0.061	0.48	0.48
	NME S1	Annual Average	1.00*	1.24*	1.00*	1.00*	<b>0.90*</b>	<b>0.88*</b>	<b>0.89*</b>	<b>0.85*</b>
	NME S2		<i>0.97*</i>	<i>1.06*</i>	<i>0.97*</i>	<b>0.97*</b>	1.03*	1.02*	<b>0.94*</b>	<b>0.93*</b>
	NME S3		1.22*	1.32	1.23*	1.23*	1.22*	1.38	<b>1.12*</b>	<b>1.09*</b>
	NME S2	Inter-annual variability	0.94	1.06	0.97	0.97	<b>0.89</b>	1.00	<b>0.66*</b>	<b>0.68*</b>
	NME S3		<i>0.91</i>	<i>0.97</i>	<b>0.93</b>	<b>0.87</b>	1.09	1.02	<b>0.78</b>	<b>0.83</b>
	NME S1	Seasonal Conc.	1.39	<b>1.30*</b>	1.39	1.41	1.44	<b>1.35*</b>	<b>1.31 *</b>	<b>1.32*</b>
	NME S2		1.36	<b>1.27*</b>	1.37	1.37	<b>1.14*</b>	<b>1.09*</b>	<b>1.29 *</b>	<b>1.32*</b>
	NME S3		1.24*	1.46	<b>1.24*</b>	<b>1.23*</b>	1.33*	1.40	1.31*	1.32*
MPD	Phase		0.44	<b>0.38*</b>	0.44	0.44	0.57	0.53	0.49	0.49

IMPROVED SIMULATION OF FIRE-VEGETATION INTERACTIONS IN THE LAND  
SURFACE PROCESSES AND EXCHANGES DYNAMIC GLOBAL VEGETATION MODEL  
(LPX-Mv1)

Variable	Metric used	Measure	LPX	Lightn	Drying	Roots	Litter	bark thickness	LPX-Mv1-nr	LPX-Mv1-rs
Burnt area: GFED3 SE Aus	Mean	Annual	0.048	0.099	0.053	0.051	0.012	0.002	0.024	0.024
	Mean ratio	Average	6.69	13.1	7.34	7.02	1.63	0.25	3.33	3.38
	Variance		0.023	0.054	0.041	0.041	0.018	0.003	0.026	0.026
	Variance ratio		2.17	5.05	3.84	3.85	1.66	0.31	2.46	2.49
	NME S1	Annual average	4.03	8.41	4.75	4.64	<b>1.64</b>	<b>0.81*</b>	<b>2.43</b>	<b>2.46</b>
	NME S2		3.58	5.07	3.93	3.97	<b>1.85</b>	<b>1.05*</b>	<b>2.66</b>	<b>2.69</b>
	NME S3		2.07	<b>1.34</b>	<b>1.37</b>	<b>1.38</b>	<b>1.23</b>	<b>1.22*</b>	<b>1.29</b>	<b>1.30</b>
	NME S2	Inter-annual variability	12	14.5	14.1	15.8	<b>5.21</b>	<b>1.52</b>	<b>8.05</b>	<b>8.00</b>
	NME S3		1.74	<b>1.54</b>	<b>1.47</b>	<b>1.46</b>	<b>1.36</b>	<b>1.45</b>	<b>1.47</b>	<b>1.50</b>
	NME S1	Seasonal Conc.	1.15	1.3	1.15	<b>1.14</b>	<b>1.08</b>	1.25	<b>0.95</b>	<b>0.96</b>
Burnt area: GFED4	NME S2		1.17	<b>1.10</b>	<b>1.16</b>	<b>1.16</b>	<b>0.98</b>	<b>1.06</b>	<b>0.97</b>	<b>0.98</b>
	NME S3		1.41	<b>1.32</b>	<b>1.33</b>	<b>1.35</b>	<b>1.22</b>	1.44	<b>1.26</b>	<b>1.25</b>
	MPD		0.47	0.52	0.47	0.48	0.52	0.57	0.50	0.50
	Mean	Annual	0.083	0.12	0.084	0.086	0.02	0.003	0.049	0.050
	Mean ratio	Average	1.21	1.77	1.24	1.27	0.29	0.043	0.72	0.74
	Variance		0.047	0.049	0.046	0.047	0.025	0.005	0.041	0.041
	Variance ratio		0.60	0.63	0.58	0.6	0.32	0.068	0.53	0.53
	NME S1	Annual average	1.01*	1.29	1.02*	1.02*	<b>0.93*</b>	<b>0.9*</b>	<b>0.88*</b>	<b>0.88*</b>
Burnt area: GFED4	NME S2		0.97*	1.09*	0.98*	0.97*	1.04*	1.02*	0.93*	<b>0.93*</b>
	NME S3		1.2*	1.32	1.21*	1.2*	1.23*	1.39	1.10	<b>1.09*</b>
	NME S2	Inter-annual variability	1.05	1.05	1.08	1.17	<b>1.03</b>	<b>1.03</b>	<b>0.91</b>	<b>0.90</b>
	NME S3		1.26*	<b>1.21*</b>	1.25*	1.29*	1.33	1.60	1.23	<b>1.25*</b>

Variable	Metric used	Measure	LPX	Lightn	Drying	Roots	Litter	bark thickness	LPX-Mv1-nr	LPX-Mv1-rs	
Burnt area: GFED4	NME S1	Seasonal Conc.	1.43	<b>1.33</b>	1.43	1.44	1.49	1.44	1.32	<b>1.31*</b>	
	NME S2		1.41	<b>1.3*</b>	1.42	1.41	<b>1.16*</b>	<b>1.03*</b>	<b>1.31*</b>	<b>1.3*</b>	
	NME S3		1.26*	1.47	1.26*	<b>1.24*</b>	1.33*	1.31*	1.29*	1.29*	
	MPD	Phase	0.5	<b>0.46</b>	0.5	<b>0.49</b>	0.57	0.59	0.52	0.52	
	Burnt area: GFED4 SE Aus	Mean	Annual Average	0.048	0.099	0.053	0.051	0.012	0.002	0.024	0.025
		Mean ratio		6.00	12.4	6.68	6.37	1.55	0.27	3.07	3.12
		Variance		0.04	0.056	0.041	0.041	0.019	0.004	0.027	0.027
		Variance ratio		3.43	4.74	3.47	3.48	1.6	0.33	2.28	2.31
	NME S1	Annual average	4.03	7.97	4.35	4.23	<b>1.59</b>	<b>0.83*</b>	<b>2.29</b>	<b>2.33</b>	
Burnt area: Ground Obs.	NME S2		3.58	4.8	3.6	3.61	<b>1.78</b>	<b>1.05*</b>	<b>2.50</b>	<b>2.53</b>	
	NME S3		1.39	<b>1.35</b>	<b>1.37</b>	<b>1.38</b>	<b>1.22</b>	<b>1.21</b>	<b>1.30</b>	<b>1.30</b>	
	NME S2	Inter-annual variability	8.59	10.1	9.05	10.1	<b>3.83</b>	<b>1.27</b>	<b>5.56</b>	<b>5.71</b>	
	NME S3		1.3	1.32	1.29	1.26	<b>1.20-</b>	<b>1.41</b>	<b>1.17</b>	<b>1.24</b>	
	NME S1	Seasonal Conc.	1.29	1.38	1.29	<b>1.25*</b>	<b>1.20*</b>	1.50	<b>1.04*</b>	<b>1.04*</b>	
	NME S2		1.29	<b>1.20*</b>	<b>1.28</b>	<b>1.24*</b>	<b>1.08*</b>	<b>0.98*</b>	<b>1.06*</b>	<b>1.05*</b>	
	NME S3		1.41	1.39	1.38	1.37	1.29	1.28	1.33	1.32	
	MPD	Phase	0.53	0.57	<b>0.52</b>	<b>0.52</b>	0.57	0.62	0.56	0.55	
	Burnt area: Ground Obs.	Mean	Annual Average	0.048	0.099	0.053	0.051	0.012	0.002	0.029	0.025
Burnt area: Ground Obs.	Mean ratio		10.9	22.6	12.2	11.6	2.83	0.49	6.61	5.68	
	Variance		0.04	0.056	0.041	0.041	0.019	0.004	0.039	0.027	
	Variance ratio		5.96	8.23	6.03	6.05	2.77	0.58	3.12	4.01	
	NME S1	Annual average	7.19	14	7.67	7.59	<b>2.4</b>	<b>0.92*</b>	<b>4.27</b>	<b>3.67</b>	
	NME S2		6.13	7.91	<b>6.06</b>	6.21	<b>2.99</b>	<b>1.08*</b>	<b>4.75</b>	<b>4.20</b>	
	NME S3		1.41	<b>1.23</b>	<b>1.35</b>	<b>1.4</b>	<b>1.25</b>	<b>1.18</b>	<b>1.29</b>	<b>1.28</b>	
	NME S2	Inter-annual variability	16.6	19.3	17.5	19.4	<b>7.65</b>	<b>2.33</b>	<b>11.5</b>	<b>11.2</b>	
	NME S3		1.88	<b>1.83</b>	<b>1.86</b>	1.88	<b>1.84</b>	<b>1.83</b>	<b>1.78</b>	<b>1.84</b>	

IMPROVED SIMULATION OF FIRE-VEGETATION INTERACTIONS IN THE LAND  
SURFACE PROCESSES AND EXCHANGES DYNAMIC GLOBAL VEGETATION MODEL  
(LPX-Mv1)

Variable	Metric used	Measure	LPX	Lightn	Drying	Roots	Litter	bark thickness	LPX-Mv1-nr	LPX-Mv1-rs
fAPAR	Mean	Annual	0.19	0.12	0.19	0.18	0.24	0.26	0.22	0.22
	Mean ratio	Average	1.59	1.02	1.56	1.55	2.02	2.18	1.83	1.87
	Variance		0.076	0.034	0.073	0.074	0.099	0.11	0.11	0.092
	Variance ratio		0.95	0.42	0.91	0.92	1.24	1.35	1.34	1.16
	NME S1	Annual Average	1.11*	<b>0.98*</b>	1.11*	<b>1.07*</b>	1.61	1.8	1.31	1.35
	NME S2		0.69*	0.97*	0.72*	<b>0.68*</b>	0.7*	<b>0.69*</b>	<b>0.61*</b>	<b>0.61*</b>
	NME S3		0.71*	1.21*	0.76*	0.71*	<b>0.57*</b>	<b>0.51*</b>	<b>0.57*</b>	<b>0.54*</b>
	NME S2	Inter-annual variability	1.01	1.11	1.01	<b>0.97</b>	2.44	2.86	1.83	1.85
	NME S3	Inter-annual variability	0.67	1	<b>0.64*</b>	<b>0.63*</b>	<b>0.65*</b>	<b>0.66</b>	<b>0.66</b>	0.74
	NME S1	Seasonal Conc.	1.34*	1.44	1.35*	1.36*	<b>1.31*</b>	<b>1.31*</b>	<b>1.32*</b>	<b>1.33*</b>
Veg cover	NME S2		1.02*	1.05*	1.03*	1.02*	1.02*	1.03*	1.02*	<b>1.00*</b>
	NME S3		1.23*	1.27*	1.24*	1.23*	<b>1.21*</b>	<b>1.21*</b>	<b>1.21*</b>	<b>1.21*</b>
	MPD	Phase	0.25*	0.25*	0.25*	<b>0.24*</b>	0.25*	0.25*	<b>0.24*</b>	<b>0.24*</b>
	Mean	Trees	0.034	0.011	0.022	0.034	0.059	0.075	0.042	0.049
		Mean ratio	0.4	0.13	0.26	0.4	0.69	0.88	0.49	0.58
	Mean	Herb	0.44	0.34	0.45	0.44	0.55	0.57	0.55	0.55
		Mean ratio	0.65	0.5	0.65	0.65	0.81	0.84	0.80	0.81
	Mean	Bare ground	0.52	0.65	0.53	0.52	0.39	0.35	0.41	0.40
		Mean ratio	2.79	3.45	2.83	2.77	2.08	1.88	2.18	2.12
	Mean	Phenology	0.066	0.014	0.042	0.063	0.12	0.15	0.10	0.12
		Mean ratio	0.13	0.026	0.081	0.12	0.23	0.28	0.20	0.22
	Mean	Leaf type	0.055	0.01	0.035	0.056	0.10	0.14	0.096	0.11
		Mean ratio	0.094	0.018	0.059	0.096	0.18	0.24	0.17	0.18
	Variance	Trees	0.066	0.021	0.042	0.066	0.11	0.14	0.11	0.084
		ratio	0.64	0.21	0.41	0.64	1.07	1.33	1.03	0.82
	Variance	Herb	0.26	0.21	0.26	0.25	0.28	0.28	0.28	0.25
		ratio	1.78	1.46	1.77	1.73	1.9	1.94	1.9	1.69
	Variance	Bare ground	0.26	0.21	0.26	0.25	0.26	0.26	0.26	0.24

Variable	Metric used	Measure	LPX	Lightn	Drying	Roots	Litter	bark thickness	LPX-Mv1-nr	LPX-Mv1-rs
Veg cover	Variance ratio		1.8	1.48	1.79	1.74	1.8	1.77	1.76	1.65
	Variance Phenology		0.062	0.014	0.041	0.06	0.11	0.13	0.099	0.11
	Variance ratio		0.2	0.043	0.13	0.19	0.33	0.41	0.32	0.33
	Variance Leaf type		0.051	0.01	0.033	0.052	0.092	0.12	0.093	0.1
	Variance ratio		0.15	0.029	0.094	0.15	0.26	0.33	0.27	0.29
MM	Life Form		0.77*	0.96	0.79*	<b>0.76*</b>	<b>0.59*</b>	<b>0.56*</b>	<b>0.59*</b>	<b>0.58*</b>
	Trees		<i>0.16*</i>	<i>0.17*</i>	<i>0.17*</i>	<i>0.17*</i>	<i>0.17*</i>	<i>0.19*</i>	<i>0.17*</i>	<i>0.17*</i>
	Herb		0.66	0.77	0.67	<b>0.65*</b>	<b>0.53*</b>	<b>0.52*</b>	<b>0.51*</b>	<b>0.51*</b>
	Bare ground		0.72	0.95	0.73	<b>0.71</b>	<b>0.49*</b>	<b>0.42*</b>	<b>0.51*</b>	<b>0.51*</b>
	Phenology		0.29*	0.33*	<b>0.24*</b>	0.29*	0.61*	0.81*	0.72*	0.46*
	Leaf type		0.51*	1.01	0.62*	<b>0.46*</b>	<b>0.34*</b>	<b>0.27*</b>	<b>0.15*</b>	<b>0.15*</b>
Fine NPP	Mean	Annual	628	112	192	180	177	176	181	202
	Mean ratio	Average	2.67	0.5	0.85	0.8	0.78	0.80	0.82	0.90
	Variance		270	44.5	53.1	69.2	54.5	29.1	56.9	83.9
	Variance ratio		1.61	0.34	0.4	0.52	0.41	0.22	0.43	0.64
NME S1	Annual average		2.62	<b>0.96</b>	<b>0.79</b>	<b>0.78</b>	<b>0.82</b>	<b>1.13*</b>	<b>0.80*</b>	<b>0.73*</b>
	NME S2			1.47	<b>0.83</b>	<b>0.79</b>	<b>0.78</b>	<b>0.83</b>	<b>1.22*</b>	<b>0.79*</b>
	NME S3			0.97	<b>0.91</b>	1.01	<b>0.89</b>	1.01	2.00	<b>0.99*</b>
height	Mean	Annual	0.5	0.2	0.29	0.5	0.84	1.03	0.39	0.63
	Mean ratio	Average	0.056	0.022	0.033	0.057	0.096	0.12	0.045	0.072
	Variance		0.91	0.35	0.52	0.92	1.5	1.81	0.94	1.22
	Variance ratio		0.12	0.045	0.067	0.12	0.19	0.23	0.13	0.16
NME S1	Annual average		1.07*	1.1*	1.09*	1.07*	<b>1.02*</b>	<b>1.01*</b>	<b>1.08*</b>	<b>1.05*</b>
	NME S2			<i>0.94*</i>	<i>0.98*</i>	<i>0.97*</i>	<i>0.94*</i>	<i>0.91*</i>	<i>0.9*</i>	<i>0.96*</i>
	NME S3			1.25*	1.39	1.31*	1.26*	<i>1.11*</i>	<i>1.08*</i>	<i>1.18*</i>

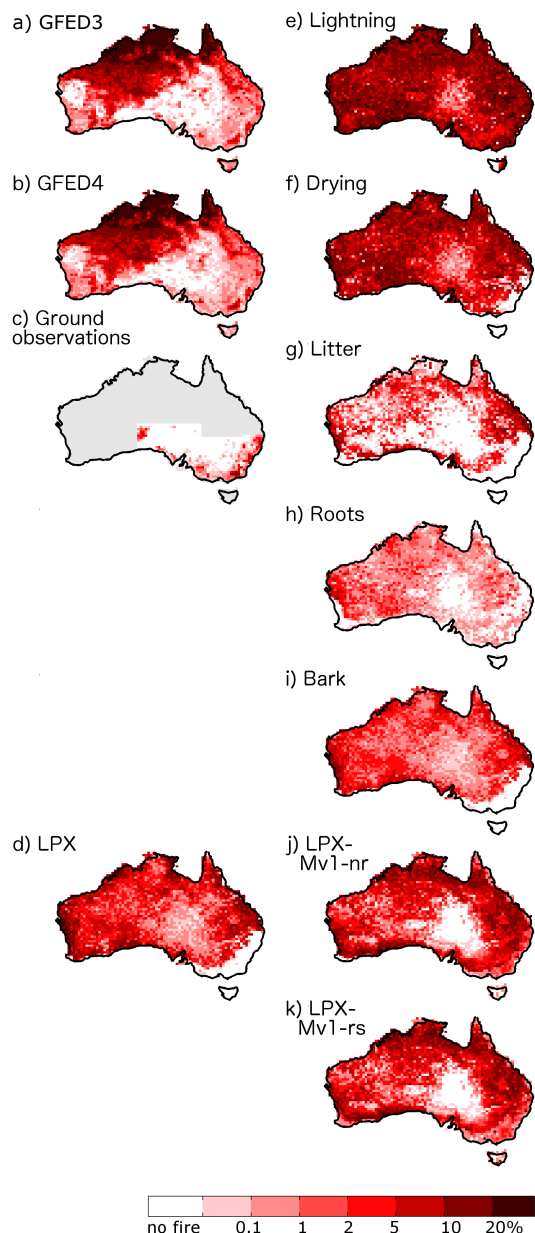


**Figure S1.** Annual average burnt area between 1997-2006 based on observations from (a) GFED3 (Giglio et al., 2010) ; b) GFED4 (Giglio et al., 2013); c) based on ground data (Bradstock, et al.

2014); and as simulated by d) LPX; and by each new parameterisation: e) lightning described in section 3.1 in the main text; f) fuel drying rates described in section 3.2; g) fuel decomposition rate in section 3.3; h) rooting depth in section 3.4; i) adaptive bark thickness in section 3.5; j) LPX-Mv1--nr; k) LPX-Mv1-rs.

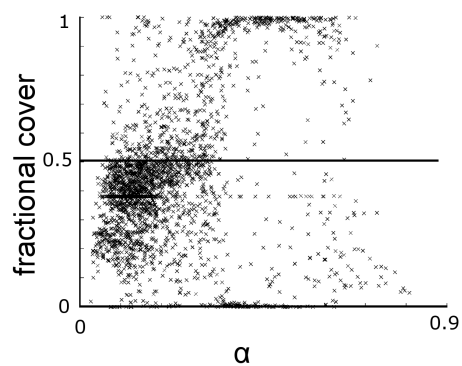


**Figure S2.** Comparison of the simulated abundance of resprouting (RS) tree PFTs and their non-resprouting (NR) equivalent PFTs along the climatic gradient in moisture, as measured by alpha (x-axis). Y-axis shows ratio of  $RS/(RS+NR)$ . Values  $>0.5$  are when RS has a competitive advantage over NR and values  $<0.5$  is when NR has a competitive advantage of RS.

**Wet day lighting sensitivity analysis**

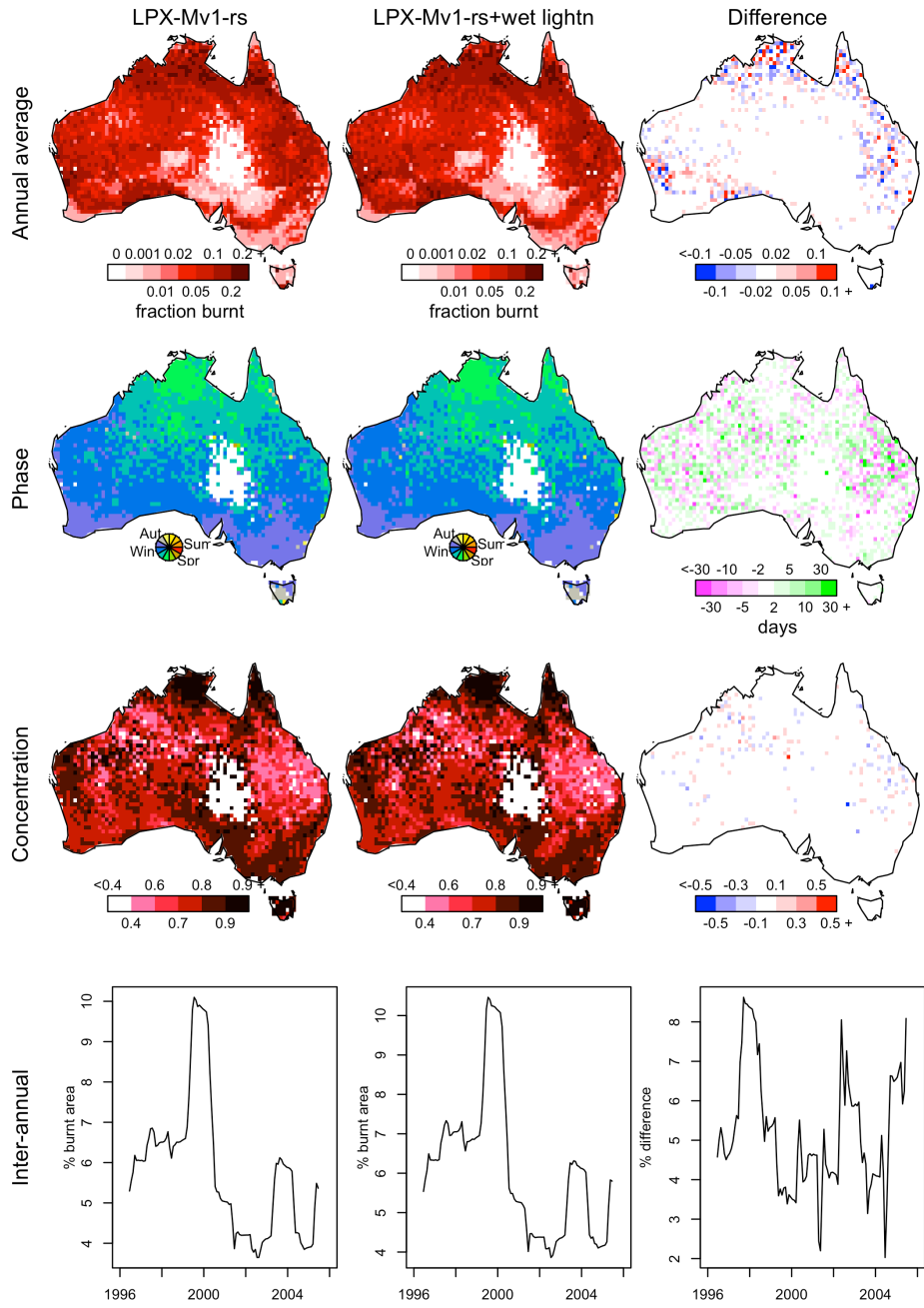


**Figure S3.** Impact of allowing lightning ignitions on wet days. The first column shows results from the standard LPX-Mv1-rs simulations, while the second column shows simulations when lighting is

allowed to occur on wet days. The third column shows the difference between the two simulations.

We show annual average burnt area (first row), seasonal timing (phase) of the fire season (second row) and concentration of the fire season (third row). The final row shows inter-annual changes in burnt area for the whole of Australia.

**Table S6.** Comparison metric scores for LPX-Mv1-rs and LPX-v1-rs incorporating wet day lighting against burnt area observations taken from GFED4 (Giglio et al. 2013). Mean and variance rows show mean and variance of simulation for annual average burnt area, by the ratio of the mean/ variance with observed mean or variance. Numbers in bold indicates if the model performs better than the original LPX model. Italic indicates model scores better than the mean of the data score listed in Table S4. Asterisks indicate model scores that are significantly better than randomly resampling listed in Table S4. S1 are step 1 comparisons, S2 are step 2; and S3 are step 3. All metrics defined in Kelley et al. (2013).

Measure	Metric used	LPX-Mv1-rs	LPX-Mv1-rs
Annual Average	Mean	0.050	0.052
	Mean ratio	0.74	0.75
	Variance	0.041	0.042
	Variance ratio	0.53	0.55
Annual average	NME S1	<b>0.88*</b>	<i>0.90*</i>
	NME S2	<b>0.93*</b>	<i>0.94*</i>
	NME S3	<b>1.09*</b>	<b>1.09*</b>
Inter-annual variability	NME S2	<b>0.90</b>	<b>0.90</b>
	NME S3	<b>1.25*</b>	<b>1.25*</b>
Seasonal Conc.	NME S1	1.31*	<b>1.30*</b>
	NME S2	<b>1.3*</b>	<b>1.3*</b>
	NME S3	1.29*	1.29*
Phase	MPD	<b>0.52</b>	0.53

**Derivation of parameter for grass in Eq. 36**

Foliage Projected Cover ( $FPC$ ) can be derived from the Normalised Difference Vegetation Index ( $NDVI$ ) using the following relationship, described in full by Lu & Shuttleworth (2002) and Sellers et al. (1996):

$$FPC \approx LAI_{pft,max} \frac{fAPAR}{fAPAR_{max}} \quad (S1)$$

where:

$$fAPAR \approx \frac{(SR - SR_{pft,min})(fAPAR_{max} - fAPAR_{min})}{(SR_{pft,max} - SR_{pft,min})} \quad (S2)$$

$fAPAR_{max}$  and  $fAPAR_{min}$  are the PFT-independent, maximum and minimum possible fraction of absorbed photosynthetic radiation ( $fAPAR$ ),  $SR$  is the ‘Simple Ratio’ and  $SR_{pft,min}$  and  $SR_{pft,max}$  are PFT specific parameters.  $SR$  is related to  $NDVI$  using the following relationship from Lu & Shuttleworth (2002):

$$SR = (1 + NDVI)/(1 - NDVI) \quad (S3)$$

Here, we are interested in the contribution of grass pfts to NDVI compared to temperate broadleaf evergreen trees (tbe – denoted ‘tree’ in the following equations), the dominant tree pft in the study area. According to Sellers et al. (1996),  $SR_{pft,min}$  is the same for tbe and grass. Re-arranging Eq. (S1) and (S2), we get:

$$P_{grass} = \frac{FPC_{grass}}{FPC_{tree}} \approx \frac{LAI_{grass,max}}{LAI_{tree,max}} \frac{(SR_{tree,max} - SR_{min})}{(SR_{grass,max} - SR_{min})} \quad (S4)$$

Using the parameters for biome 1 (tbe) for wood and biome 6-other and 9 ( $C_3/C_4$  grass and cropland) for grass from Sellers et al. (1996) in Eq. (S3) and (S4), we obtain the value of 0.32 used in Eq. 36 in the main manuscript.

**References for data used to parameterize adaptive bark thickness vs diameter at breast height.**

- Abbott, I. and Loneragan, O.: Ecology of Jarrah (*Eucalyptus marginata*) in the northern jarrah forest of Western Australia, Department of Conservation and Land Management, Perth, 1986.
- Baker, T. and Phillips, O.: Do species traits determine patterns of wood production in Amazonian forests?, *Biogeosciences*, 6, 297–307, available at: <http://www.biogeosciences.net/6/297/>, 2009.
- Baraloto, C., Bonal, D., Chave, J., Héault, B., Patiño, S., and Timothy Paine, C.E.: Functional trait variation and sampling strategies in species-rich plant communities, *Funct. Ecol.*, 24, 208–216, available at: <http://doi.wiley.com/10.1111/j.1365-2435.2009.01600.x>, 2010.
- Barlow, J., Lagan, B. O., and Peres, C. A.: Morphological correlates of fire-induced tree mortality in a central Amazonian forest, *J. Trop. Ecol.*, 19, 291–299, available at: [http://www.journals.cambridge.org/abstract\\_S0266467403003328](http://www.journals.cambridge.org/abstract_S0266467403003328), 2003.
- Brando, P. M., Balch, J. K., Bolker, B., Christman, M. C., Coe, M., Nepstad, D. C., and Putz, F. E.: Fire-induced tree mortality in a neotropical forest: the roles of bark traits, tree size, wood density and fire behavior, *Glob. Chang Biol.*, 18, 630–641, doi:10.1111/j.1365-2486.2011.02533.x, 2012.
- Bradstock R, Penman T, Boer M, Price O, Clarke H. Divergent responses of fire to recent warming and drying across south-eastern Australia. *Glob Chang Biol.* 20(5):1412-28. doi:10.1111/gcb.12449. 2014
- Chatto, K., Bell, T., and Kellas, J.: Effects of repeated low-intensity fire on tree growth and bark in a mixed eucalypt foothill forest in south-eastern Australia, *Res. Rep.* 66, 2003.
- Climent, J., Gil, L., Pardos, J. A., and Tapias, R.: Fire adaptations in the Canary Islands pine (*Pinus canariensis*), *Plant Ecol. (formerly Vegetatio)*, 171, 185–196, available at: <http://link.springer.com/article/10.1023%2FB%3AVEGE.0000029374.64778.68>, 2004.
- Cochrane, M. A.: Fire science for rainforests, *Nature*, 421, 913–9, available at: <http://www.ncbi.nlm.nih.gov/pubmed/12606992>, 2003.
- Lawes, M. J., Dathe, J., Midgley, J. J., and Richards, A.: Bark thickness determines fire resistance of selected tree species from fire-prone tropical savanna in north Australia, *Plant Ecol.*, 212, 2057–2069, available at: <http://www.springerlink.com/index/10.1007/s11258-011-9954-7>, 2011b.
- Marshall, H. D., Lachenbruch, B., and Murphy, G. E.: Effects of bark thickness estimates on optimal log merchandising, *Forest Prod. J.*, 56, 87–92, available at: <http://hdl.handle.net/1957/17956>, 2006.
- Paine, C. E. T., Baraloto, C., Courtois, E. A., Patiño, S., Sarmiento, C., and Stahl, C.: Functional explanations for variation in bark thickness in tropical rain forest trees, *Funct. Ecol.*, 24, 1202–1210, available at: <http://doi.wiley.com/10.1111/j.1365-2435.2010.01736.x>, 2010.
- Paine, C. E. T., Baraloto, C., Chave, J., and Héault, B.: Functional traits of individual trees reveal ecological constraints on community assembly in tropical rain forests, *Oikos*, 120, 720–727, available at: <http://doi.wiley.com/10.1111/j.1600-0706.2010.19110.x>, 2011.
- Patiño, S., Aguilar, A., Alvarez, E., Arroyo, L., Baker, T.R., Baraloto, C., Bonal, D., Chave, J., Costa,

A.C.L., Czimczik, C.I., Gallo, J., Herrera, R., Higuchi, N., Horna, V., Hoyos, E.J., Jimenez, E.M., Killeen, T., Leal, E., Lloyd, J., Luizão, F., Malhi, Y., Meir, P., Mercado, L.M., Monteagudo, A., Neill, D., Núñez-Vargas, P., Paiva, R., Palomino, W., Panfil, S.N., Peacock, J., Peña-Cruz, A., Peñuela, M.C., Phillips, O.L., Pitman, N., Priante Filho, N., Prieto, A., Quesada, C.A., Rudas, A., Salomão, R., Santos, A.J.B., Sarmiento, C., Schmerler, J., Schwarz, M., Silva, N., Silveira, M., Soares deAlmeida, S., Sota, A., Torres-Lezama, A., Turriago, J.D., Vásquez-Martínez, R., Vieira, I., Villanueva, B., and Vitzthum, P.: Branch xylem density variations across the Amazon Basin, *Biogeosciences*, 6, 545–568, available at: <http://eprints.jcu.edu.au/17986/>, 2009.

Pompa-Garc, M., Cruz-Cobos, F., Soto-Gutie, R., Trincado, G., and Vega-Munoz, J.: Estimates of the Bark Thickness in Bole Profiles of Oak in Northern Mexico, *Res. J. Forest.*, 6, 32–40, available at: <http://www.scialert.net/abstract/?doi=rjf.2012.32.40>, 2012.

Swaine: Ecological and evolutionary drivers of plant community assembly in a Bornean rain forest., PhD Thesis, University of Aberdeen, available at: <http://www.try-db.org>, 2007.

Uhl, C. and Kauffman, J.: Deforestation, fire susceptibility, and potential tree responses to fire in the eastern Amazon, *Ecol.*, 71, 437–449, available at: <http://www.esajournals.org/doi/abs/10.2307/1940299>, 1990.

### References

- Biganzoli, F., Wiegand, T., and Batista, W. B.: Fire-mediated interactions between shrubs in a South American temperate savannah, *Oikos*, 118, 1383–1395, doi:10.1111/j.1600-0706.2009.17349.x, 2009.
- Casady, G. M., van Leeuwen, W. J. D., and Marsh, S. E.: Evaluating post-wildfire vegetation regeneration as a response to multiple environmental determinants, *Environ. Model. Assess.*, 15, 295–307, doi:10.1007/s10666-009-9210-x, 2009.
- Cuevas-González, M., Gerard, F., Balzter, H., and Riaño, D.: Analysing forest recovery after wildfire disturbance in boreal Siberia using remotely sensed vegetation indices, *Glob. Change Biol.*, 15, 561–577, doi:10.1111/j.1365-2486.2008.01784.x, 2009.
- Díaz-Delgado, R., Salvador, R., and Pons, X.: Monitoring of plant community regeneration after fire by remote sensing, *Fire Manage. Landsc. Ecol.*, 315–324, 1998.
- Díaz-Delgado, R., Loreto, F., Pons, X., and Terradas, J.: Satellite evidence of decreasing resilience in mediterranean plant communities after recurrent wildfires, *Ecol. Soc. Am.*, 83, 2293–2303, 2002.
- Díaz-Delgado, R., Lloret, F., and Pons, X.: Influence of fire severity on plant regeneration by means of remote sensing imagery, *J. Remote Sens.*, 24, 1751–1763, 2003.
- Enright, N. J. and Goldblum, D.: Demography of a non-sprouting and resprouting Hakea species (Proteaceae) in fire-prone Eucalyptus woodlands of southeastern Australia in relation to stand age, drought and disease, *Plant Ecol.*, 144, 71–82, 1999.
- Enright, N. J. and Lamont, B. B.: Seed banks, fire season, safe sites and seedling recruitment in five co-occurring Banksia species, *J. Ecol.*, 77, 1111–1122, 1989.
- Epting, J. and Verbyla, D.: Landscape-level interactions of prefire vegetation, burn severity, and postfire vegetation over a 16-year period in interior Alaska, *Can. J. Forest Res.*, 1377, 1367–1377, doi:10.1139/X05-060, 2005.
- Giglio, L. and Randerson, J.: Assessing variability and long-term trends in burned area by merging multiple satellite fire products, *Biogeosciences*, 7, 1171–1186, available at: <http://www.biogeosciences.net/7/1171/>, 2010.
- Giglio, L., Randerson, J. T., and Werf, G. R.: Analysis of daily, monthly, and annual burned area using the fourth-generation global fire emissions database (GFED4), *J. Geophys. Res.: Biogeosciences*, 118, 317-328, doi:10.1002/jgrg.20042, 2013.
- Goetz, S. J., Fiske, G. J., and Bunn, A. G.: Using satellite time-series data sets to analyze fire disturbance and forest recovery across Canada, *Remote Sens. Environ.*, 101, 352–365, doi:10.1016/j.rse.2006.01.011, 2006.
- Gouveia, C., DaCamara, C. C., and Trigo, R. M.: Post-fire vegetation recovery in Portugal based on spot/vegetation data, *Nat. Hazards Earth Syst. Sci.*, 10, 673–684, doi:10.5194/nhess-10-673-2010, 2010.

Hope, A., Tague, C., and Clark, R.: Characterizing post fire vegetation recovery of California chaparral using TM and ETM timeseries data, *Int. J. Remote Sens.*, 28, 1339–1354, doi:10.1080/01431160600908924, 2007.

Kelley, D. I., Fisher, J. B., Harrison, S. P., Prentice, I. C., Simard, M., Wang, H., and Willis, K. O.: A comprehensive benchmarking system for evaluating global vegetation models, *Biogeosciences*, 10, 3313–3340, available at: <http://www.biogeosciences.net/10/3313/2013/>, 2013.

Lu, L. and Shuttleworth, J. W.: Incorporating NDVI-Derived LAI into the Climate Version of RAMS and its Impact on Regional Climate, *Journal of Hydrometeorology*, 3, 347–362, 2002.

Maier, S. W. and Russell-Smith, J.: Measuring and monitoring of contemporary fire regimes in Australia using satellite remote sensing, in: *Flammable Australia: the fire regimes and biodiversity and ecosystems in a changing world*, edited by Bradstock, R. A., Gill, A.M., and Williams, J. A., CSIRO Publishing, Melbourne, 79–95, 2012.

Riaño, D., Chuvieco, E., and Ustin, S.: Assessment of vegetation regeneration after fire through multitemporal analysis of AVIRIS images in the Santa Monica Mountains, *Remote Sens. Environ.*, 79, 60–71, 2002.

Sellers, P. J., Tucker, C. J., Collatz, G. J., Los, S. O., Justice, C. O., Dazlich, D. A., and Randall, D. A.: A revised land surface parameterization (SiB2) for atmospheric GCMs. Part II: The generation of global fields of terrestrial biophysical parameters from satellite data, *Journal of Climate*, 4, 706–737, 1996.

Silva-Matos, D. M., Fonseca, G. D. F. M., and Silva-Lima, L.: Differences on post-fire regeneration of the pioneer trees *Cecropia glazioui* and *Trema micrantha* in a lowland Brazilian Atlantic forest, *Revista de biología tropical*, 53, 1–4, 2005.

Solans Vila, J. P. and Barbosa, P.: Post-fire vegetation regrowth detection in the Deiva Marina region (Liguria-Italy) using Landsat TM and ETM+ data, *Ecol. Model.*, 221, 75–84, doi:10.1016/j.ecolmodel.2009.03.011, 2010.

van Leeuwen, W. J. D.: Monitoring the effects of forest restoration treatments on post-fire vegetation recovery with MODIS multitemporal data, *Sensors*, 8, 2017–2042, doi:10.3390/s8032017, 2008.

van Leeuwen, W. J. D., Casady, G. M., Neary, D. G., Bautista, S., Alloza, J. A., Carmel, Y., Wittenberg, L., Malkinson, D., and Orr, B. J.: Monitoring post-wildfire vegetation response with remotely sensed time-series data in Spain, USA and Israel, *Int. J. Wildland Fire*, 19, 75–93, doi:10.1071/WF08078, 2010.

Vivian, L. M., Cary, G. J., Bradstock, R. A., and Gill, A. M.: Influence of fire severity on the regeneration, recruitment and distribution of eucalypts in the Cotter River Catchment, Australian Capital Territory, *Aust. Ecol.*, 33, 55–67, doi:10.1111/j.1442-9993.2007.01790.x, 2008.



IMPROVED SIMULATION OF FIRE-VEGETATION INTERACTIONS IN THE LAND  
SURFACE PROCESSES AND EXCHANGES DYNAMIC GLOBAL VEGETATION MODEL  
180 (LPX-Mv1)

---



*Post fire — 6 months post fire*

# 5

## Enhanced Australian carbon sink despite increased wildfire during the 21<sup>st</sup> century

---

D. I. Kelley <sup>1</sup>, S. P. Harrison <sup>1,2</sup>

<sup>1</sup>Biological Sciences, Macquarie University, North Ryde, NSW 2109, Australia

<sup>2</sup>Geography & Environmental Sciences, School of Archaeology, Geography and Environmental Sciences, University of Reading, Whiteknights, Reading, RG6 6AB, UK.

---

**This chapter has been submitted for publication:**

Kelley, D. I., Harrison, S. P.: Enhanced Australian carbon sink despite increased wildfire during the 21<sup>st</sup> century., Environmental Research Letters. 9.10, 104015, 2014

---

OPEN ACCESS

IOP Publishing

Environ. Res. Lett. 9 (2014) 104015 (10pp)

Environmental Research Letters

doi:10.1088/1748-9326/9/10/104015

# Enhanced Australian carbon sink despite increased wildfire during the 21st century

D I Kelley<sup>1</sup> and S P Harrison<sup>1,2</sup>

<sup>1</sup> School of Biological Sciences, Macquarie University, North Ryde, NSW 2109, Australia

<sup>2</sup> School of Archaeology, Geography and Environmental Sciences, Reading University, Whiteknights, Reading, RG66AH, UK

E-mail: [douglas.kelley@students.mq.edu.au](mailto:douglas.kelley@students.mq.edu.au)

Received 12 June 2014, revised 2 September 2014

Accepted for publication 9 September 2014

Published 14 October 2014

## Abstract

Climate projections show Australia becoming significantly warmer during the 21st century, and precipitation decreasing over much of the continent. Such changes are conventionally considered to increase wildfire risk. Nevertheless, we show that burnt area increases in southern Australia, but decreases in northern Australia. Overall the projected increase in fire is small (0.72–1.31% of land area, depending on the climate scenario used), and does not cause a decrease in carbon storage. In fact, carbon storage increases by 3.7–5.6 Pg C (depending on the climate scenario used). Using a process-based model of vegetation dynamics, vegetation–fire interactions and carbon cycling, we show increased fire promotes a shift to more fire-adapted trees in wooded areas and their encroachment into grasslands, with an overall increase in forested area of 3.9–11.9%. Both changes increase carbon uptake and storage. The increase in woody vegetation increases the amount of coarse litter, which decays more slowly than fine litter hence leading to a relative reduction in overall heterotrophic respiration, further reducing carbon losses. Direct CO<sub>2</sub> effects increase woody cover, water-use efficiency and productivity, such that carbon storage is increased by 8.5–14.8 Pg C compared to simulations in which CO<sub>2</sub> is held constant at modern values. CO<sub>2</sub> effects tend to increase burnt area, fire fluxes and therefore carbon losses in arid areas, but increase vegetation density and reduce burnt area in wooded areas.

 Online supplementary data available from [stacks.iop.org/ERL/9/104015/mmedia](http://stacks.iop.org/ERL/9/104015/mmedia)

Keywords: carbon cycle, fire regimes, CO<sub>2</sub> fertilization, water-use efficiency, dynamic vegetation modeling, future environmental changes

## 1. Introduction

Emissions from biomass burning are a significant contribution to the atmospheric carbon burden. Current estimates suggest that pyrogenic emissions are about 2.8 Pg C yr<sup>-1</sup> (van der Werf *et al* 2006, van der Werf *et al* 2010) but may be as much as 3.4 Pg C yr<sup>-1</sup> if small fires are included (Randerson *et al* 2012). For comparison, fossil fuel emissions and cement production contributed  $8.3 \pm 0.4$  Pg C yr<sup>-1</sup> to the atmospheric burden between 2002 to 2011 (Le Quéré *et al* 2014).

 Content from this work may be used under the terms of the Creative Commons Attribution 3.0 licence. Any further distribution of this work must maintain attribution to the author(s) and the title of the work, journal citation and DOI.

Interannual variability in wildfire contributes about one third of the variability in atmospheric CO<sub>2</sub> growth rate (Prentice *et al* 2011), and is driven by variability in climate—primarily caused by the El Nino Southern Oscillation (ENSO)—and its effect on the balance of fuel availability and combustibility (van der Werf *et al* 2006). Only about a fifth of the pyrogenic emissions globally are associated with deforestation fires (Bowman *et al* 2009, van der Werf *et al* 2010), and thus included in land-use for global budgeting purposes (Le Quéré *et al* 2014). Emissions from wildfires are not generally included in such budgets, because it is assumed that biomass-burning losses are compensated by post-fire uptake. If climate and fire regimes are in equilibrium, fire-induced atmospheric CO<sub>2</sub> emissions are approximately balanced by subsequent CO<sub>2</sub> uptake by surviving vegetation or via regeneration (Le

Quéré *et al* 2014). However, the uptake of carbon depends on how fast vegetation recovers versus fire frequency and intensity, and vegetation uptake will not necessarily balance pyrogenic emissions when climate is changing.

Climate projections for the 21st century (Collins *et al* 2013, Kirtman *et al* 2013) indicate that increases in temperature combined with reduced precipitation will increase fire risk in subtropical regions, precisely those areas most prone to wildfire today. Statistical modeling suggests that increased fire risk may not translate into increased burning because low fuel loads limit the amount of fire in some regions (Moritz *et al* 2012). However, statistical models do not account for potential changes in vegetation and their impact on fire regimes under a changing climate. Although fire-enabled vegetation models have been used to examine the impact of projected climate changes on the terrestrial biosphere (see e.g. Scholze *et al* 2006, Harrison *et al* 2010, Kloster *et al* 2012), there has been no vegetation model-based assessment of how changing climate will affect fire regimes, and hence the pyrogenic contribution to the carbon cycle, over the 21st century using the most recent climate scenarios.

Here we examine changes in the carbon cycle over the 21st century using a state-of-the art dynamic global vegetation model, LPX-Mv1 (Kelley *et al* 2014), driven by outputs from nine coupled ocean-atmosphere models in response to changes in forcing using the RCP4.5 and RCP8.5 scenarios, and focusing on Australia. Although Australia represents only about 6% of the global annual burnt area and contributes only about 5% of the total global emissions, most of these emissions (98%) are from wildfires in natural vegetation (Giglio *et al* 2013). This contrasts with other, more fire-prone continents such as Africa or Asia, where agricultural and deforestation fires contribute about 9% and 56% respectively of the fire-related emissions. Thus, Australia provides a good focus to examine the potentially complex interactions between vegetation and fire with changing climate and how these interactions could influence the regional carbon budget during the 21st century.

## 2. Methods

We examined the changes in the carbon cycle over the 21st century, driven by outputs from nine coupled ocean-atmosphere models in response to changes in forcing using two Representative Concentration Pathway (RCP) scenarios: RCP4.5 and RCP8.5. RCP4.5 is an intermediate radiative forcing (RF) scenario which stabilizes at  $4.5 \text{ W m}^{-2}$  by 2100. RCP8.5 is an extreme RF scenario where RF reaches  $8.5 \text{ W m}^{-2}$  by 2100 (see SI). In addition to the transient climate forcing, LPX-Mv1 is driven by atmospheric CO<sub>2</sub>, which changes in the RCP4.5-driven simulations from 380.8 in 2006 to 576 ppm by 2080 CE and stabilizes thereafter (figure S3). In the RCP8.5 simulations, CO<sub>2</sub> concentrations increase throughout the 21st century to reach 1231 ppm by 2100. The robustness of the simulated changes is assessed by the agreement of the change between models using a one-sample *t*-test. The significance is measured by the strength of the

change relative to interannual variability in the historic period (1997–2006), as determined by the two-sample *t*-test. A change is described as ‘robust’ or ‘significant’ if the *t*-test *p*-value is  $<0.05$  (see table S3 and S4). Changes in fluxes are assessed based on the averages for the last decade of the 21st century (2090–2099) compared to the last decade of the historical run (1997–2006), except that the carbon store is a measure of the accumulated change over the 21st century. The length of the comparison period was largely determined by the availability of burnt-area observations to evaluate the historical run. While a decade is sufficient to examine changes in the mean state, it precludes any consideration of the impact of longer-term (decadal) climate variability, which could nevertheless be important for understanding changes in Australian fire regimes.

Changes in the carbon cycle are simulated using the latest version of the land surface processes and exchanges dynamic global vegetation model (LPX-Mv1 DGVM: Kelley *et al* 2014. See SI for more information). This version of the model is a state-of-the-art process-based DGVM, which includes an adaptive treatment of bark thickness and of vegetation recovery after fire through resprouting. The improved treatment of vegetation responses to fire, makes LPX-Mv1 more suitable for analyses of climate-induced changes in the carbon cycle than the previously published version (Prentice *et al* 2011) which tended to over-predict burnt area in non-forest vegetation and to under-predict burnt area in forests.

LPX-Mv1 simulates vegetation dynamics using a set of 13 plant functional types (PFTs), defined by life form (tree, grass), where trees represent all woody plants (i.e. trees *sensu stricto* and shrubs), with the tree PFT further subdivided by leaf type, (broadleaf, needleleaf), phenological response to drought or cold (evergreen or deciduous), ability to resprout (resprouting, non-resprouting) and bioclimatic tolerance (tropical, temperate, boreal), and grasses subdivided by photosynthetic pathway (C<sub>3</sub>, C<sub>4</sub>). Fire is explicitly simulated as a function of lightning ignitions and fire susceptibility, calculated from fuel amount, fuel properties and fuel moisture content. The model does not simulate anthropogenic ignitions: except for deforestation fire, anthropogenic ignitions are not important for the large fires and hence burnt area which is the major determinant of the impact of fire on the carbon cycle. Fire spread, intensity and residence time are dependent on weather conditions (including wind speed) and fuel moisture, and calculated using the Rothermel equations (Rothermel 1972). The effective wind speed that influences fire spread is modulated by vegetation density in wooded areas, using a simple empirical relationship (Rothermel 1972). Thus, despite the fact that lightning ignitions are the sole source of fire starts, the timing of the fire season is predominantly determined by weather conditions. Burnt area is calculated as the product of the number of fires and fire spread. Mortality occurs through crown scorching or cambial death. Cambial damage is determined by fire intensity and residence time in relation to the bark thickness of local vegetation. The model includes a PFT-specific adaptive representation of bark thickness, in which the distribution of

bark thickness within an ecosystem changes in response to previous fire history. Fire fluxes are calculated using a standard emission factor for each trace gas species multiplied by the total amount of biomass burnt, which is the sum of dead and live fuel consumption as the result of surface fire and crown scorching. LPX-Mv1 uses a photosynthesis-water balance scheme that explicitly couples CO<sub>2</sub> assimilation with transpiration (see SI), where increased CO<sub>2</sub> leads to a fertilization effect that increases production in drier conditions. In common with most other vegetation models, LPX-Mv1 does not consider the effects of nutrient limitation on CO<sub>2</sub> fertilization.

LPX-Mv1 is run using monthly climate (maximum and minimum temperature, precipitation, cloud cover and number of wet days) from the CRU TS3.1 data set (Harris *et al* 2013) and wind speed from the National Center for Environmental Prediction (NCEP) reanalysis data (Kalnay *et al* 1996), interpolated to a daily timestep. Atmospheric CO<sub>2</sub> concentration is prescribed annually. The model was spun up using constant CO<sub>2</sub> (286 ppm), detrended climate data, and the cropland area of 1850 (table S1 in the supplementary data, available at [stacks.iop.org/ERL/9/104015/mmedia](http://stacks.iop.org/ERL/9/104015/mmedia)), until the carbon pools were in equilibrium. The historical run used transient CO<sub>2</sub> from 1850 onwards. Detrended climate was used for all climate variables until 1900. From 1901 onwards, transient CRU TS3.1 was used for all climate variables except windspeed. Detrended wind speed is used until 1948 and transient values thereafter.

LPX-Mv1 was run from 2006 to 2100 using multiple climate realizations from climate model outputs in the CMIP5 database (table S2) forced by two alternative RCP scenarios (van Vuuren *et al* 2011): RCP4.5 and RCP8.5 (figure S1, figure S2). In the baseline runs, CO<sub>2</sub> was also allowed to vary (figure S3). Additional simulations were made in which climate was allowed to vary but CO<sub>2</sub> was held constant at the 2006 level of 380.8 ppm (fixed-CO<sub>2</sub> experiment). We made a further set of simulations with a version of the model in which resprouting was disabled (LPX-Mv1-nr: see Kelley *et al* 2014) in order to diagnose the impact of incorporating resprouting as a post-fire response (non-resprouting experiment). Ensemble averages of the outputs were created by simple averaging of the results of the appropriate set of individual simulations. The regional contributions to the overall changes shown in each experiment were diagnosed using geographic regions with similar vegetation types (figure S4), defined using k-means clustering.

The realism of the historic simulations was evaluated by comparing simulated and observed above-ground carbon (Ruesch and Gibbs 2008) and burnt area (GFED4: Giglio *et al* 2013). None of the simulations take account of land-use changes. However, for comparison of simulated and observed burnt area, cropland areas were masked out. Mapped values of observed above-ground biomass carbon ([http://cdiac.ornl.gov/epubs/ndp/global\\_carbon/](http://cdiac.ornl.gov/epubs/ndp/global_carbon/)) are based on site-based measurements of above-ground biomass carbon. These are interpolated to land-cover types using a continent-specific interpolation based on vegetation composition and bioclimate.

The average carbon biomass for a land-cover type in a specific continent was extrapolated over the GLC2000 5×5' land cover map (Bartholomé and Belward 2005). We excluded land areas described as swamps or anthropogenically-altered (e.g. urban or cropland) in GLC2000, and aggregated the remaining grid cells onto the 0.5° grid of LPX-Mv1. Aggregation was performed using the raster package in R (Hijmans 2014). We also compared the simulated net primary productivity (NPP), heterotrophic respiration (R<sub>h</sub>) and fire fluxes during the historical periods with reconstructions of these fluxes derived from Haverd *et al* (2013) and GFED4 (Giglio *et al* 2013).

### 3. Results

#### 3.1. Simulation of present-day carbon budget of Australia

Natural changes in the carbon stock are given by changes in NPP, heterotrophic respiration (R<sub>h</sub>) and fire. Haverd *et al* (2013) have estimated the carbon budget of Australia between 1990 and 2011 by tuning a regional biosphere model (BIOS2) using observations of carbon and water fluxes, streamflow, and data on soil and vegetation carbon pools (Haverd *et al* 2013). Fire emissions for the period 1997–2009 were taken from GFED3 (van der Werf *et al* 2010), on the assumption that these values were representative of the longer period. Similarly, an estimate of harvest for 2004 was assumed to be representative for the whole period. Haverd *et al* (2013) estimated gross primary productivity as  $4110 \pm 740 \text{ Tg C yr}^{-1}$  and NPP as  $2210 \text{ Tg C yr}^{-1}$ . Losses are dominated by heterotrophic respiration ( $1997 \pm 383 \text{ Tg C yr}^{-1}$ ), with smaller losses due to fire ( $127 \pm 22 \text{ Tg C yr}^{-1}$ , which includes a component due to fires associated with land-use and clearing of  $23 \pm 4 \text{ Tg C yr}^{-1}$ ), harvest ( $29 \pm 7 \text{ Tg C yr}^{-1}$ ), land-use change ( $18 \pm 7 \text{ Tg C yr}^{-1}$ ), and riverine and dust transport ( $3 \pm 1 \text{ Tg C yr}^{-1}$ ). This budget suggests the continent gained carbon at an average rate of  $36 \pm 29 \text{ Tg C yr}^{-1}$  (net biosphere production) between 1990 and 2011. The gain in carbon is dominated by the effect of rising CO<sub>2</sub> ( $68 \pm 7 \text{ Tg C yr}^{-1}$ ; Haverd *et al* 2013). Increasing CO<sub>2</sub> directly influences the carbon cycle through CO<sub>2</sub> fertilization *sensu stricto*, improved water-use efficiency, and shifting the competitive balance of trees against grasses. Fire and land-use changes cause net respective losses of  $26 \pm 4 \text{ Tg C yr}^{-1}$  and  $18 \pm 7 \text{ Tg C yr}^{-1}$ .

LPX-Mv1 reproduces the terms of the Australian carbon budget, within the limits of the estimation errors of each component and given uncertainties associated with differences in the time periods considered (figure 1). Our estimate of NPP ( $2029 \text{ Tg C yr}^{-1}$ ), based on the period 1997–2006, is comparable to Haverd *et al*'s estimate for 1990–2011 of  $2210 \pm 398 \text{ Tg C yr}^{-1}$  excluding the terms for harvest and land use, which are not simulated by our model. Our estimate for fire flux between 1997–2006 is slightly higher than that given by Haverd *et al* (2013) for the period 1997–2009 because the last three years of this period have low fire emissions. LPX-Mv1 also reproduces (figure 1) the large-scale geographic

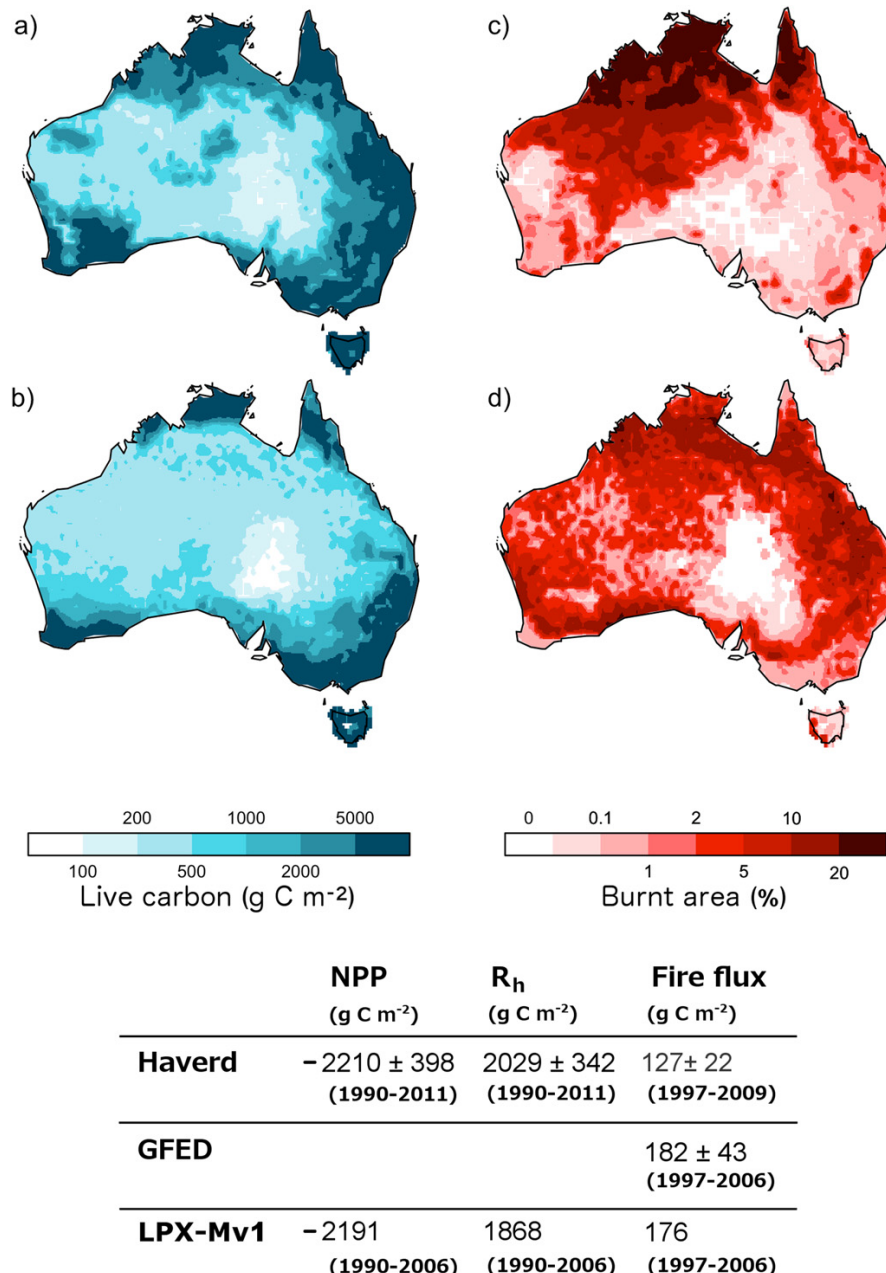


**Figure 1.** Comparison of observed (a), (c) and simulated (b), (d) components of the carbon cycle during the recent period. Observed values for (a) above-ground biomass carbon for Australia were obtained from the Ruesch and Gibbs (2008) dataset ([http://cdiac.ornl.gov/epubs/ndp/global\\_carbon/carbon\\_documentation.html](http://cdiac.ornl.gov/epubs/ndp/global_carbon/carbon_documentation.html)). Observed average burnt area (c) for the period 1997 to 2006 is from GFED4 (Giglio *et al* 2013). Net primary productivity (NPP) and heterotrophic respiration ( $R_h$ ) are averaged estimates for the period 1990 to 2011 from Haverd *et al* (2013). Observed fire flux is an average for the period 1997 to 2006 from GFED3 (van der Werf *et al* 2010). The simulated values are from the historic simulation, and are extracted for the appropriate years.

patterns of live carbon (Ruesch and Gibbs 2008), and burnt area from GFED4 (Giglio *et al* 2013); remaining biases in the simulated vegetation patterns or burnt area (Kelley *et al* 2014; see SI for further details) are small compared to simulated changes between the historic period and the end of the 21st century.

### 3.2. Response to RCP4.5 climate scenarios

The ensemble average climate shows a robust and significant increase in temperature over the 21st century, with an average increase of  $2^\circ\text{C}$  and increases of  $>5^\circ\text{C}$  in northwestern Australia (figure S5). There is a robust and marginally

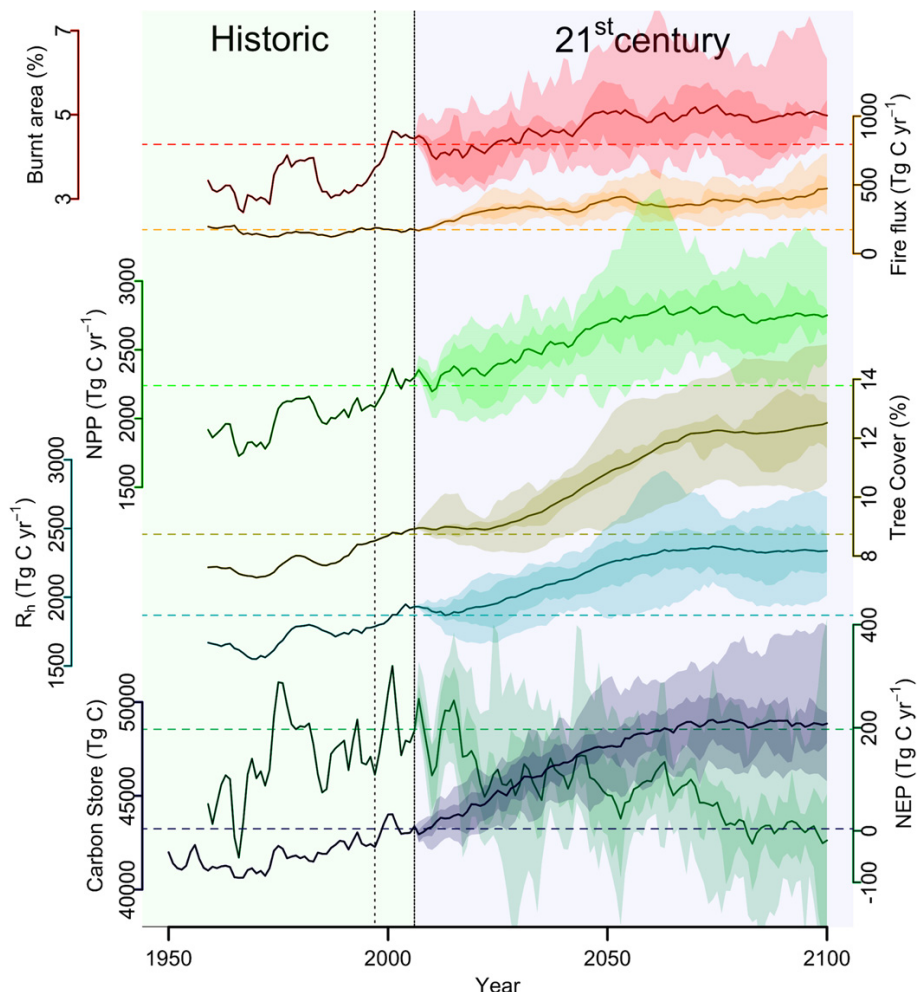


**Figure 2.** Changes in the carbon cycle over Australia through the 21st century in response to climate changes driven by the RCP4.5 scenario. The time series (bold lines) are ensemble averages of the model results for (a) burnt area (%), (b) fire flux ( $\text{Tg C yr}^{-1}$ ), (c) net primary productivity (NPP) ( $\text{Tg C yr}^{-1}$ ), (d) tree cover (%), (e) heterotrophic respiration ( $R_h$ ) ( $\text{Tg C yr}^{-1}$ ), (f) net ecosystem productivity (NEP) ( $\text{Tg C yr}^{-1}$ ), and (g) carbon store (Pg C). The range in the individual model simulations is indicated by the shaded bands. The dashed horizontal lines indicate the average value of each variable during the last decade of the historic simulation.

**Table 1.** Summary of changes in individual components of the carbon cycle for Australia over the 21st century, based on ensemble averages of the simulations driven by the RCP4.5 and RCP8.5 climate scenarios. Robust changes are in bold, whilst significant changes are in italics.

Variable	Baseline			Fixed CO <sub>2</sub>		Without resprouting		
	Historic	RCP 4.5	RCP 8.5	RCP 4.5	RCP 8.5	Historic	RCP 4.5	RCP 8.5
MAT ( $^{\circ}\text{C}$ )	22	<b>24</b>	<b>26</b>	<b>24</b>	<b>26</b>	22	<b>24</b>	<b>26</b>
MAP ( $\text{mm m}^{-2} \text{yr}^{-1}$ )	524	491	485	491	485	524	491	485
Burnt area (%)	5.32	<b>6.04</b>	<b>6.63</b>	4.74	<b>3.77</b>	5.66	<b>6.48</b>	<b>7.02</b>
Fire flux ( $\text{Tg C yr}^{-1}$ )	169	<b>449</b>	<b>941</b>	166	141	120	<b>238</b>	<b>534</b>
NPP ( $\text{Tg C yr}^{-1}$ )	2214	<b>2650</b>	<b>3448</b>	1982	<b>1706</b>	2190	<b>2559</b>	<b>3262</b>
Tree cover (%)	9.81	<b>13.71</b>	<b>21.75</b>	<b>8.29</b>	<b>6.32</b>	7.32	<b>10.07</b>	<b>16.77</b>
$R_h$ ( $\text{Tg C yr}^{-1}$ )	1858	<b>2232</b>	<b>2709</b>	1756	<b>1606</b>	1857	<b>2263</b>	<b>2731</b>
NEP ( $\text{Tg C yr}^{-1}$ )	189	-28	-202	62	-40	213	58	-3
Carbon store (Pg C)	41 607	<b>45 326</b>	<b>47 243</b>	<b>36 842</b>	<b>32 453</b>	33 972	<b>36 048</b>	<b>38 183</b>

significant decrease in precipitation in northern Australia of about 200 mm. Precipitation increases along the eastern coastal plains, in southeastern Australia and Tasmania, and also in southwestern Australia, but the changes are small, not robust and not significant. These climate changes drive an overall increase in burnt area, from  $41 \text{ Mkm}^2 \text{ yr}^{-1}$  in the historic simulation to a multi-model mean value of  $46 \text{ Mkm}^2 \text{ yr}^{-1}$  at the end of the century (table 1; figure 2). The change in burnt area leads to a 166% increase in fire flux, from  $169 \text{ Tg C yr}^{-1}$  in the historic simulations to  $449 \text{ Tg C yr}^{-1}$  by the end of the century. The increase in fire flux reflects an overall increase in biomass and particularly in woody biomass: NPP increases by  $436 \text{ Tg C yr}^{-1}$  over the 21st century and tree cover increases by 39%. However, net ecosystem productivity (NEP) remains largely positive (figure 2). Despite the increase in fire and the temperature-driven increase in heterotrophic respiration, there is an increase in the terrestrial carbon store, from  $4.2 \text{ Pg C}$  in the historic period to a multi-model mean value of  $4.5 \text{ Pg C}$  at the end of the 21st century (table 1; figure 2), with all but one of the simulations (MRI-CGCM3) showing an increase in carbon storage (table S3).

The regional contributions to this increase in carbon storage, and the pathways by which the increase occurs, vary. There is a significant decrease in fire in northern Australia because, despite the overall decrease in rainfall, more rain occurs in the fire season (May–October). Wetter fuels limit fire spread, an effect that is further enhanced by decreased wind speeds during the fire season. The reduction in fire is accompanied by an increase in tree cover, from 29% during the historic period to 56% by the end of the 21st century, and an increase in NPP by  $28 \text{ Tg C yr}^{-1}$ . This increase in woody vegetation means that when fires do occur they release more carbon. Fire flux increases from  $18 \text{ Tg C yr}^{-1}$  to  $124 \text{ Tg C yr}^{-1}$  by the end of the century. As a result of this increase, northern ecosystems are converted from a sink before 2060 to a source after 2060 CE. Despite carbon losses in the latter part of the century, carbon storage is still  $284 \text{ Tg C}$  higher than during the historic period.

The interior of the continent is occupied by shrubland and open savanna, and experiences a large increase in fire over the 21st century. NPP increases from  $1418 \text{ Tg C yr}^{-1}$  to  $1753 \text{ Tg C yr}^{-1}$  and there is an increase in tree cover from 2% to 6% by the end of the century. Much of this region is fuel limited today, and the increased production and tree cover result in an increase in burnt area from 5% to 7%. However, the low biomass means the total increase in fire flux is small, from  $52 \text{ Tg C yr}^{-1}$  to  $135 \text{ Tg C yr}^{-1}$ . This increase, combined with increased  $R_h$  (from  $1222 \text{ Tg C yr}^{-1}$  to  $1522 \text{ Tg C yr}^{-1}$ ) leads to a decrease in NEP during the century, although the region remains a sink throughout. As a result, there is an overall increase in the carbon stock, from  $1.9 \text{ Pg C}$  to  $2.3 \text{ Pg C}$ .

The southern part of the continent experiences both increased and decreased fire, but the decreases are more important in magnitude and area. Much of this region is forested, with tree cover of >50%, and comparatively small changes in fire therefore have a large impact on the carbon

cycle. In areas characterized by small increases in fire, NPP increases during the first part of the century, from  $311 \text{ Tg C yr}^{-1}$  to  $386 \text{ Tg C yr}^{-1}$  by 2060, but then remains stable. Similarly, tree cover increases initially, reaching a maximum of 80% by 2060, and then decreases to 73% by the end of the century. Fire fluxes increase throughout the century, reaching  $71 \text{ Tg C yr}^{-1}$  by 2060 and  $139 \text{ Tg C yr}^{-1}$  by the end of the century. This region is a sink during the first half of the century, but NEP declines after 2060 because of increased fire and the shift towards less wooded biomes. Although the change in carbon stock between the end of the century and the historic period is small ( $2.3 \text{ Tg C}$ ), this reflects a large initial increase in carbon stock followed by a decrease of  $1000 \text{ Tg C}$  in the last 40 years. This large decline helps to explain why the continental budget shows little change in carbon stock during the latter part of the century. Only a comparatively small part of southern Australia experiences a decrease in burnt area over the 21st century. This decrease is not directly related to climate, since precipitation changes are not correlated with the change in fire, but results from increases in tree cover from 63% in the historic period to 79% by the end of the century. The increase in woody cover affects the ratio of fine to coarse fuel, which in turn affects fuel-drying properties resulting in an increase in fuel moisture throughout the year that limits fire spread. However, the increase in productivity and tree cover means that more carbon is released when fires do occur, so there is an overall increase in fire flux from  $72 \text{ Tg C yr}^{-1}$  to  $101 \text{ Tg C yr}^{-1}$ . The combination of increased NPP (from  $137 \text{ Tg C yr}^{-1}$  to  $157 \text{ Tg C yr}^{-1}$ ) and decreased fires lead to a small increase in carbon store, from  $4970 \text{ Tg C}$  to  $5105 \text{ Tg C}$ . These regions are a minor source today and become a net carbon sink from 2030 onwards.

Thus, although continental carbon stocks increase by  $3.7 \text{ Pg C}$ , there are significant changes in regional sources and sinks over the 21st century. Regions characterized by an overall decrease in fire during the 21st century (i.e. northern Australia and parts of southern Australia) are sinks initially but become important sources in the latter part of the century. The continental interior is a sink throughout the 21st century. Although uptake is limited, the extent of this region means it contributes significantly to the end-of-century budget. Those parts of southern Australia where fire increases during the 21st century become a major source by the end of the century.

### 3.3. Response to RCP8.5 climate scenarios

The changes in climate in the RCP8.5 simulations are more extreme than in the RCP4.5 simulations. The ensemble average increase in MAT by the end of the 21st century is  $4^\circ\text{C}$ , with larger changes in northwestern Australia. Although the average change in MAP is small, there is nevertheless a robust decrease in precipitation in northern and western Australia (ca  $125 \text{ mm yr}^{-1}$ ). The changes in burnt area are larger than in the RCP4.5 simulations. Fire flux increases from  $169 \text{ Tg C yr}^{-1}$  in the historic period to  $941 \text{ Tg C yr}^{-1}$  by the last decade of the 21st century (table 1; figure 3), more than double that of the RCP4.5 simulations. This increase in

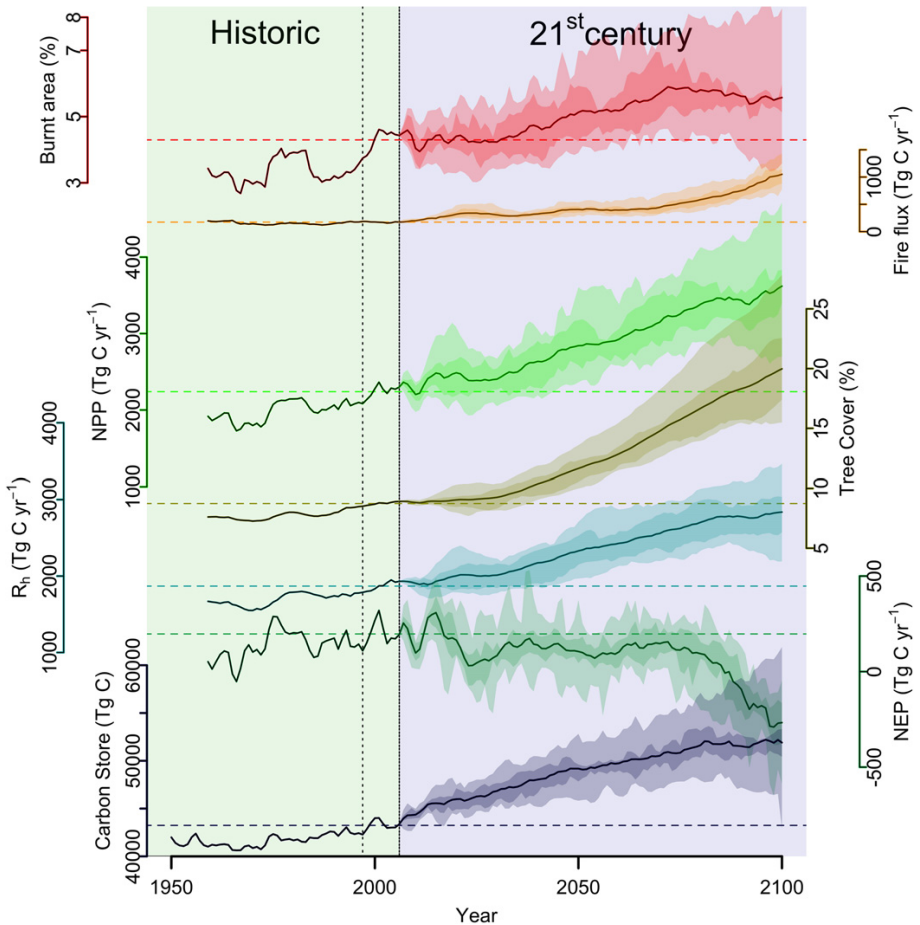


**Figure 3.** Changes in the carbon cycle over Australia through the 21st century in response to climate changes driven by the RCP8.5 scenario. The time series (bold lines) are ensemble averages of the model results for (a) burnt area (%), (b) fire flux ( $\text{Tg C yr}^{-1}$ ), (c) net primary productivity (NPP) ( $\text{Tg C yr}^{-1}$ ), (d) tree cover (%), (e) heterotrophic respiration ( $R_h$ ) ( $\text{Tg C yr}^{-1}$ ), (f) net ecosystem productivity (NEP) ( $\text{Tg C yr}^{-1}$ ), and (g) carbon store (Pg C). The range in the individual model simulations is indicated by the shaded bands. The dashed horizontal lines indicate the average value of each variable during the last decade of the historic simulation.

fire flux is driven by a large increase in biomass and particularly woody biomass: NPP increases by  $1234 \text{ Tg C yr}^{-1}$  over the 21st century and tree cover increases by 122% compared to the historic run (table 1; figure 3). Although NEP is negative by the end of the century, the overall carbon store is increased by  $5.6 \text{ Pg C}$  at the end of the 21st century, a gain of  $1.9 \text{ Pg C}$  compared to the RCP4.5 simulations, and with all models showing an increase in carbon stores (figure S6; table S4).

The overall increase in carbon storage in these simulations is driven by changes in central Australia, where stocks increase by  $7.1 \text{ Pg C}$  by the end of the century. This increase reflects large increases in tree cover (14%) and NPP ( $950 \text{ Tg C yr}^{-1}$ ) and the fact that burnt area is only very slightly greater than in the RCP4.5 simulations (6.63% compared to 6.04%). Tree cover and NPP also increase in northern Australia. However, the reduction in fire compared to the historic period is less than in the RCP4.5 simulations,

because the decrease in precipitation is smaller, and as a result fire fluxes are large ( $233 \text{ Tg C yr}^{-1}$  compared to  $123 \text{ Tg C yr}^{-1}$  in the RCP4.5 simulations). Thus, although northern Australia is characterized by an increase in carbon storage of  $216 \text{ Tg C}$ , this is less than in the RCP4.5 simulations. Those regions of southern Australia which experience increased fire during the 21st century, and thus increased fire fluxes, nevertheless also experience a significant increase in NPP. In contrast to the RCP4.5 simulations, carbon stocks increase throughout the century leading to an overall increase of  $3.3 \text{ Tg C}$ . The area of southern Australia that experiences reduced fire during the 21st century is smaller. The increase in NPP compared to the historic baseline is comparatively small ( $30 \text{ Tg C yr}^{-1}$ ) and these regions show a reduction in carbon stock ( $1 \text{ Pg C}$ ) by the end of the century. Although the continental interior is a sink throughout the 21st century in the RCP8.5 simulations, both southern and northern Australia are sources by the end of the century.

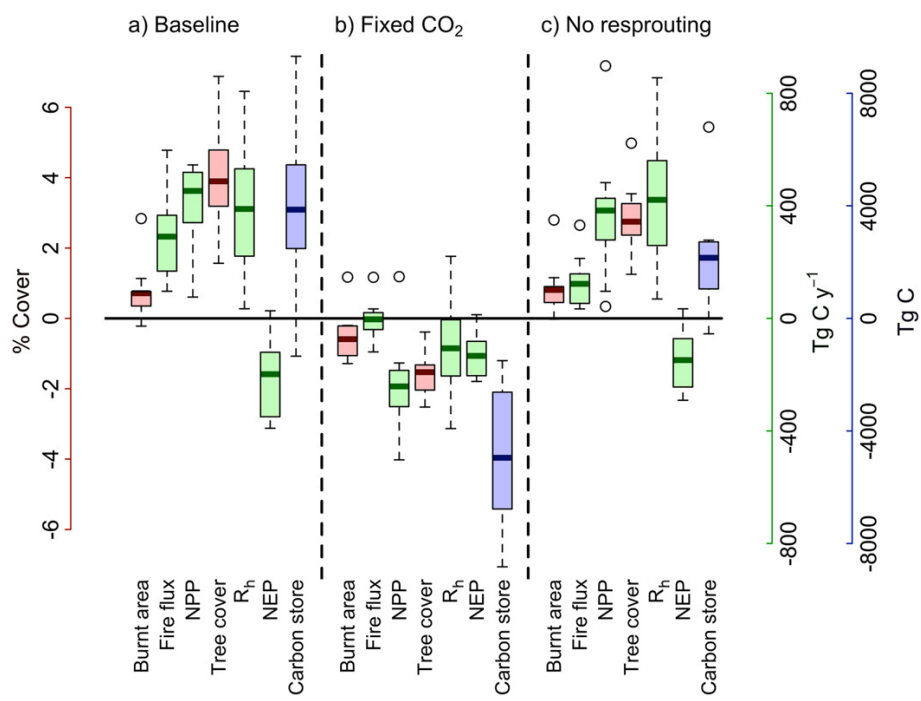


**Figure 4.** Contribution of CO<sub>2</sub> fertilization and resprouting to the simulated changes in the carbon cycle over the 21st century. The baseline plots (a) show the average changes in the last decade of the 21st century simulations relative to the 1997–2006 average from the historic simulation. The CO<sub>2</sub> plots (b) show the difference between the baseline 21st century run and a run in which CO<sub>2</sub> was fixed at 380.8 ppm (fixed CO<sub>2</sub>). The no resprouting plots (c) shows the difference between the baseline 21st century run and the run in which resprouting was disabled. In the box-and-whisker plots, the solid lines show the mean value for the ensemble of simulations, the boxes show the interquartile range and the whiskers show the 5–95% confidence limits, and outliers are shown by an open circle. Note that the scale for carbon store is 10x that of the individual carbon components.

#### 3.4. Impact of direct CO<sub>2</sub> effects on the 21st century carbon cycle

The inferred increase in carbon storage in Australia during the past two decades has been dominated by the effect of rising CO<sub>2</sub> (Haverd *et al* 2013). We evaluated the likely impact of rising CO<sub>2</sub> during the 21st century (figure S3), by running additional simulations in which CO<sub>2</sub> was held constant at 380.8 ppm (the 2006 value). We compare these simulations with the baseline simulation, in which both climate and CO<sub>2</sub> vary. NPP is decreased in the fixed-CO<sub>2</sub> RCP4.5 simulations compared to the historic period in all regions of the continent, and in contrast to the baseline simulations where NPP increases in all regions (figure 4, table 1). The impact of this difference varies regionally, reflecting the effects of the change on tree cover and fuel loads. Thus, in the continental interior, the increase in CO<sub>2</sub> produces increased vegetation cover and fuel loads, leading to an increase in burnt area and fire flux because of the removal of fuel limitations. A similar pattern is seen in regions in the south where changing climate reduces fire during the 21st century: the reduction in burnt area is smaller in the baseline simulations than in the fixed-CO<sub>2</sub> simulations because of additional production. Additionally, the CO<sub>2</sub>-induced increase in NPP and in tree cover results in larger fire flux. In northern Australia, and those southern regions where 21st century climate changes reduce

fire, the increase in CO<sub>2</sub> increases both production and tree cover. This change in tree cover leads to an increase in coarse fuel, which in turn leads to slower fuel-drying times and an overall reduction in burnt area. Nevertheless, the fire flux is higher in both areas because the direct impact of CO<sub>2</sub> produces more material to burn. The overall and regional responses to CO<sub>2</sub> are similar and somewhat larger in the RCP8.5 simulations compared to the RCP4.5 simulations (table 1).

#### 3.5. Impact of resprouting on the 21st century carbon cycle

The impact of fire on the carbon cycle and particular on carbon stocks is significantly different depending on whether the woody vegetation is fire-adapted. Most Australian ecosystems contain a significant proportion of trees that resprout after fire (Clarke *et al* 2013, Harrison *et al* 2014), ensuring rapid biomass recovery and persistence of woody vegetation in fire-prone regions. To examine the impact of resprouting on the Australian carbon budget, we ran both 21st century and historic simulations in which fire-affected trees were not allowed to resprout. The absence of resprouting leads to an overall decrease in carbon stock of 7.6 Pg C in the historic period compared to the standard run, which is unrealistically low. By the end of the 21st century, the carbon stock is 1.6 Pg C higher in the baseline RCP4.5 simulation than in the

simulation without resprouting (figure 4). The baseline simulation shows an increase in tree cover by the end of the 21st century, but despite the larger increase in burnt area in the baseline simulations, this increase is less without resprouting because fire-adapted trees are more likely to survive and indeed encroach into fire-prone areas. Except in the fuel-limited interior of the continent, the increased presence of trees reduces burnt area in the baseline simulations compared to the simulations without resprouting. This reflects the higher proportion of coarse fuel, which in turn increases fuel wetness. Although there are higher fire fluxes in the baseline simulations than in the simulations with no resprouting, because the amount of biomass is higher, the small increase in NPP associated with increased trees and the reduction in burnt area results in higher overall carbon storage when resprouting trees are present. Most of the additional carbon stock is in central (64%) and northern (22%) Australia: in the first case reflecting tree encroachment and in the second an increase in the abundance of resprouting trees. The regional impact of fire-adapted trees in southern Australia is less easy to diagnose because of the variability in the initial conditions between the baseline and non-resprouting simulations, coupled with the nonlinear nature of the carbon-cycle responses to changes in climate and fire, and the fact that a smaller proportion of species that occur today in the southern woodlands and forests are resprouters (Clarke *et al* 2013, Harrison *et al* 2014). Nevertheless, 13% of the overall increase in carbon storage is accounted for by the occurrence of fire-adapted trees in this region.

Similar results are shown in the RCP8.5 simulations (figure S6). In the absence of resprouting, with similar levels of burning overall, tree cover and NPP are reduced and the overall carbon stock at the end of the 21st century is 1.4 Pg C less than in the baseline RCP8.5 simulation. Thus, the presence of resprouting vegetation is important in maintaining high levels of tree cover and productivity in fire prone areas, and directly contributes to the overall increased carbon stock during the 21st century.

#### 4. Discussion and conclusions

Our simulations show that fire will likely increase in Australia during the 21st century. This is consistent with the generally-accepted assumption that warmer and drier conditions will lead to an increase in fire risk (Williams *et al* 2001, Pitman *et al* 2007), although the increase in burnt area is perhaps less than might be expected because increased risk does not always translate into increased fire. The signal of increased fire is opposite to that predicted by Krawchuk *et al* (2009) using statistical modeling with a previous generation of climate projections, but similar in magnitude and pattern to predictions by Moritz *et al* (2012) using a similar approach and climate inputs to Krawchuk *et al* (2009).

Despite the increase in fire flux, and heterotrophic respiration, there is a large increase in carbon storage by the end of the 21st century. The general increase in NPP as a result of the direct impacts of CO<sub>2</sub> makes a significant

contribution to the increase in carbon stocks but the importance of fire-adapted trees in Australian ecosystems is also a contributing factor. Haverd *et al* (2013) have shown that CO<sub>2</sub> fertilization caused a  $68 \pm 15 \text{ Tg C yr}^{-1}$  increase in carbon stock between 1990 and 2011. The rate simulated by LPX-Mv1 is slightly higher but nevertheless within the uncertainties of the estimated rate. One impact of increased CO<sub>2</sub> is to allow woody encroachment into semi-arid areas (Buitenhof *et al* 2012, Bragg *et al* 2013, Donahue *et al* 2013), but these areas are fire prone and persistence of trees in these regions is only possible when they can resprout. Resprouting also affects fire regimes directly because the increased tree cover that such fire-adaptations permit in fire-prone regions leads to increases in the amount of coarse fuel, and therefore of fuel moisture, and decreased effective wind speed. Other things being equal, both of these will decrease fire spread and hence burnt area.

Our simulations suggest that the carbon cycle will be more vigorous over Australia during through the 21st century, with both increased uptake and increased fluxes. In the RCP4.5 simulations, NEP is positive during the first part of the century but shows no net change (NEP  $\approx 0$ ) during the last 20 years. As a result, although the carbon cycle is in equilibrium by the end of the century, carbon stock is increased by 10% compared to today. NEP is also positive during the first part of the century in the RCP8.5 simulations, but becomes negative after 2080 CE. Because the carbon sink in the first part of the century is much larger than in the RCP4.5 simulations, carbon stock is still larger than in the RCP4.5 simulations (14%) in the last decade of the century despite the fact that the continent becomes a significant carbon source.

The simulations presented here must be considered indicative rather than definitive statements about future fire-related changes in the carbon cycle. Clearly, the trajectory of future forcing is uncertain and our focus on the RCP4.5 and RCP8.5 scenarios therefore arbitrary. Furthermore, there are non-negligible inter-model differences in the climate response to these scenarios, particularly in interannual variability for key climate drivers of fire flux (figure S1). Further uncertainty is added by the use of a single fire-enabled DGVM, which has its own, known biases in the simulation of vegetation, fuel load and burnt area. Estimates of long term CO<sub>2</sub> fertilization maybe be reduced if nutrient limitation were considered, especially under the more extreme RCP8.5 scenario (Flato *et al* 2013). The point that we wish to emphasize is that the interaction between climate, fire and carbon dynamics is complex and nonlinear and not amenable to simple statements that increased fire (or fire risk) will reduce the terrestrial carbon sink.

#### Acknowledgements

We acknowledge the World Climate Research Programme's Working Group on Coupled Modelling, which is responsible for CMIP, and the climate modeling groups for producing and making available their model output. (For CMIP the US Department of Energy's Program for Climate Model

Diagnosis and Intercomparison provides coordinating support and led development of software infrastructure in partnership with the Global Organization for Earth System Science Portals.) The analyses and figures are based on data archived by 18 June 2013. DIK is supported by an iMQRES at Macquarie University. We thank IC Prentice for comments on an earlier draft.

## References

- Bartholomé E M and Belward A S 2005 GLC2000: a new approach to global land cover mapping from Earth Observation data *Int. J. Remote Sens.* **26** 1959–77
- Bowman D M J S *et al* 2009 Fire in the Earth system *Science* **324** 481–4
- Bragg F *et al* 2013 n-Alkane stable isotope evidence for CO<sub>2</sub> as a driver of vegetation change *Biogeosciences* **10** 2001–10
- Buitewerf R, Bond W J, Stevens N and Trollope W S W 2012 Increased tree densities in South African savannas: >50 years of data suggests CO<sub>2</sub> as a driver *Glob. Change Biol.* **18** 675–84
- Clarke P J *et al* 2013 Resprouting as a key functional trait: how buds, protection and resources drive persistence after fire *New Phytol.* **197** 19–35
- Collins M *et al* 2013 Long-term climate change: projections, commitments and irreversibility *Climate Change 2013: The Physical Science Basis. Contribution of Working Group I to the Fifth Assessment Report of the Intergovernmental Panel on Climate Change* ed T F Stocker *et al* (Cambridge: Cambridge University Press) [www.ipcc.ch/report/ar5/wg1/](http://www.ipcc.ch/report/ar5/wg1/)
- Donohue R J, Roderick M L, McVicar T R and Farquhar G D 2013 Impact of CO<sub>2</sub> fertilisation on maximum foliage cover across the globe's warm, arid environments *Geophys. Res. Lett.* **40** 3031–5
- Flato G *et al* 2013 Evaluation of climate models *Climate Change 2013: The Physical Science Basis* 5th edn T F Stocker, D Qin, G-K Plattner *et al* (Cambridge: Cambridge University Press) pp 741–866 [www.ipcc.ch/report/ar5/wg1/](http://www.ipcc.ch/report/ar5/wg1/)
- Giglio L, Randerson J T and van der Werf G R 2013 Analysis of daily, monthly, and annual burned area using the fourth-generation global fire emissions database (GFED4) *J. Geophys. Res.-Biogeo.* **118** 317–28
- Harris I, Jones P D, Osborn T J and Lister D H 2013 Updated high-resolution grids of monthly climatic observations—the CRU TS3.10 dataset *Int. J. Climatol.* **34** 623–42
- Harrison S P, Marlon J R and Bartlein P J 2010 Fire in the Earth system *Changing climates, earth systems and society* ed J Dodson (Dordrecht: Springer) pp 21–48
- Harrison S P *et al* 2014 Patterns in the abundance of post-fire resprouting in Australia based on plot-level measurements *Glob. Ecol. Biogeogr.* submitted
- Haverd V *et al* 2013 The Australian terrestrial carbon budget *Biogeosciences* **10** 851–69
- Hijmans R J 2014 Raster: geographic data analysis and modeling. R package version 2.2-31 <http://CRAN.R-project.org/package=raster>
- Kalnay E *et al* 1996 The NCEP/NCAR 40-year reanalysis project *Bull. Am. Meteorol. Soc.* **77** 437–71
- Kelley D I, Harrison S P and Prentice I C 2014 Improved simulation of fire–vegetation interactions in the Land surface Processes and eXchanges Dynamic Global Vegetation Model (LPX-Mv1) *Geosci. Model. Dev.* in press
- Kirtman B *et al* 2013 Near-term climate change: Projections and predictability *Climate Change 2013: The Physical Science Basis. Contribution of Working Group I to the Fifth Assessment Report of the Intergovernmental Panel on Climate Change* ed T F Stocker *et al* (Cambridge: Cambridge University Press) [www.ipcc.ch/report/ar5/wg1/](http://www.ipcc.ch/report/ar5/wg1/)
- Kloster S, Mahowald N M, Randerson J T and Lawrence P J 2012 The impact of climate, land use, and demography on fires during the 21st century simulated by CLM-CN *Biogeosciences* **9** 509–25
- Krawchuk M A *et al* 2009 Global pyrogeography: the current and future distribution of wildfire *PloS one* **4** e5102
- Le Quéré C *et al* 2014 Global carbon budget 2013 *Earth Syst. Sci. Data* **6** 1 235–63
- Moritz M A *et al* 2012 Climate change and disruptions to global fire activity *Ecosphere* **3** 1–22
- Pitman A J, Narisma G T and McAneney J 2007 The impact of climate change on the risk of forest and grassland fires in Australia *Clim. Change* **84** 383–401
- Prentice I C *et al* 2011 Modeling fire and the terrestrial carbon balance *Glob. Biogeochem. Cycles* **25** 1–13
- Randerson J T *et al* 2012 Global burned area and biomass burning emissions from small fires *J. Geophys. Res.* **117** G04 012
- Rothermel R C 1972 *A Mathematical Model for Predicting Fire Spread in Wildland Fuels* USDA Forest Service Research Paper INT-115 (Ogden, UT: Department of Agriculture, Intermountain Forest and Range Experiment Station)
- Ruesch A and Gibbs H K 2008 *New IPCC tier-1 global biomass carbon map for the year 2000* (Oak Ridge, TN: Oak Ridge National Laboratory) Available online from the carbon dioxide information analysis center (<http://cdiac.ornl.gov>)
- Scholze M, Knorr W, Arnell N W and Prentice I C 2006 A climate-change risk analysis for world ecosystems *Proc. Natl. Acad. Sci.* **103** 116–20
- van der Werf G R *et al* 2006 Interannual variability of global biomass burning emissions from 1997 to 2004 *Atmos. Chem. Phys.* **6** 3423–41
- van der Werf G R *et al* 2010 Global fire emissions and the contribution of deforestation, savanna, forest, agricultural, and peat fires (1997–2009) *Atmos. Chem. Phys.* **10** 11707–35
- van Vuuren D P *et al* 2011 The representative concentration pathways: an overview *Clim. Change* **109** 5–31
- Williams A, Karoly D and Tapper N J 2001 The sensitivity of Australian fire danger to climate change *Clim. Change* **49** 171–91

ENHANCED AUSTRALIAN CARBON SINK DESPITE INCREASED WILDFIRE DURING  
192 THE 21<sup>ST</sup> CENTURY

---

## 5.S1 Supplementary Information: Enhanced Australian carbon sink despite increased wildfire during the 21<sup>st</sup> century

This SI contains descriptions of (a) the LPX-Mv1 dynamic global vegetation model, (b) the inputs used for the historical simulations, (c) the inputs for the future simulations, (d) the protocol for the diagnostic simulations using fixed CO<sub>2</sub> and without resprouting, (e) the data sources for the evaluation of the historic simulations, (f) the procedure for deriving regional averages, (g) the results of the individual climate simulations used to produce ensemble results for the future simulations, (h) results from the RCP8.5 simulations.

### 5.S1.1 The LPX-Mv1 DGVM

The Land surface Processes and exchanges Macquarie Version 1 (LPX-Mv1) dynamic global vegetation model (DGVM) is a coupled, process based fire-enabled model (Prentice et al., 2011; Kelley et al., 2014). The model simulates ecosystem structure (e.g. height, biomass, leaf area index and foliage projective cover) and function (e.g. gross and net primary production, evapotranspiration, competition and disturbance) with vegetation parameterized via a small number of Plant Functional Types. Plant Functional Types (PFTs) are defined life form (tree, grass), with trees further defined by climate range (tropical, temperate, boreal) leaf type (broadleaf, evergreen), and phenological response to drought or cold (evergreen, raingreen, summergreen) and grasses defined by photosynthetic pathway (C<sub>3</sub>, C<sub>4</sub>).

LPX-Mv1 uses a photosynthesis-water balance scheme that explicitly couples CO<sub>2</sub> assimilation with transpiration. Available CO<sub>2</sub> reduces potential water stress on a plant by lowering the required stomatal conductance ( $gc$ ) for a given photosynthetic rate. The maximum potential stomatal conductance ( $gcMax$ ) when water is not limiting is determined by the maximum potential day-time photosynthetic assimilation rate ( $A_{max}$ ), prescribed ambient CO<sub>2</sub> concentration, a PFT-specific minimum canopy conductance parameter and photosynthetic pathway (all woody PFTs use the C<sub>3</sub> pathway, but grasses can either use the C<sub>3</sub> or C<sub>4</sub> pathway). If  $gcMax$  results in a maximum transpiration rate ( $D$ ) that is less than the supply of water ( $S$ : a function of soil water content and soil properties), then there is no water stress and plants respire (and therefore photosynthesize) at their maximum rate. If  $D$  is greater than  $S$ , then  $gc$  (and therefore photosynthesis and production) is reduced in such a way as to be consistent with an empirical formulation (derived from Monteith, 1995) of the relationship between  $S$  and  $gc$ . When CO<sub>2</sub> is increased,  $gcMax$  decreases even if  $A_{max}$  remains the same, and the value of  $S$  that induces water stress is lowered. Thus, under these conditions, maximum production rates can occur at lower moisture availability. If  $S$  is less than  $D$ , there is still water stress but  $gc$  (and therefore production) requires less down-regulation in water stressed conditions. Increased CO<sub>2</sub> thus leads to a fertilization effect, with increases production in drier conditions.

LPX-M-v1 includes a process-based fire model (Kelley et al., 2014). In this model, the occurrence of fires is a product of ignition rate, represented by dry day lightning strikes, multiplied by a probability of ignition and fire susceptibility. The probability of ignitions is dependent on local fuel and atmospheric moisture content. Fire susceptibility is calculated from fuel amount, fuel properties and fuel moisture content. Fire spread, flame height and residence time are based on weather conditions and fuel moisture, and calculated using the Rothermel equations (Rothermel, 1972). The area affected by fire (i.e. the burnt area) is the product of the number of fires and the spread of fire LPX-M-v1 simulates fire mortality through two pathways: crown scorching and cambial damage. Crown scorching is determined by the height and intensity of the fire in relation to the height of the local vegetation, where vegetation height is represented by an average height for each PFT. The probability of mortality from crown scorch increases as flame height increases beyond the canopy height of each PFT. Cambial damage is determined by fire intensity and residence time in relation to the bark thickness: thicker-barked trees survive longer, more intense fires. Bark thickness within a PFT is represented as a simple triangular distribution, with minimum, mean and maximum thickness specified from observations. Fire preferentially kills thinner-barked trees. After a fire, the newly-established trees will have the same bark thickness distribution as the pre-fire assemblage, but the overall distribution of bark thickness will represent a weighted average of the bark thickness of the individuals that were not killed by fire and the newly-established individuals.

LPX-Mv1 includes four PFTs which can resprout from above-ground meristem tissue after a fire: tropical broadleaf evergreen resprouting tree, tropical broadleaf deciduous resprouting tree, temperate broadleaf evergreen resprouting tree, temperate broadleaf deciduous resprouting tree. Resprouting PFTs lose all above-ground productive biomass during a fire and a fraction of ‘scorched’ structural biomass, but retain plant height and root mass. As a result of this, they recover a substantial proportion of the material lost through burning in the year after the fire. However, resprouting PFTs are less successful in regenerating from seed (see review of literature, Table S2 in Kelley et al. 2014), which is simulated through implementing a reproduction penalty such that they regenerate from seed at 10% of the rate of non-resprouting equivalents. Resprouting trees also tend to have thicker bark than their non-resprouting equivalent, which means they are less likely to be damaged by fire.

A full description of the LPX-Mv1 model is given in Kelley et al. (2014).

LPX-Mv1 has been benchmarked against observations for burnt area, vegetation cover, fine fuel production and live carbon stores (Kelley et al., 2014). The model shows a significant improvement compared to previous versions of the model, particularly with respect to vegetation composition, the development of vegetation gradients in areas transitional between forest and grassland, and burnt area. However, there are still some regional discrepancies between the simulated and observed burnt area. The simulated burnt area in southeastern Australia is too large, in part because the simulation predicts fire in potential vegetation and does not account for the suppression of fire in agricultural lands. LPX-Mv1 simulates too little fire in northern Australia because it does not simulate large enough fuel loads in this region.

TABLE 5.S1: Summary of the simulation protocol for model spin-up and the baseline simulations.

Time period	CO <sub>2</sub>	Maximum & minimum temperature, precipitation, rain days, and sunshine hours	Wind speed	Lightning
Spin-up	286 ppm	detrended CRU TS3.1	detrended NCEP	climatology LIS-OTD
1850–1900	transient	detrended CRU TS3.1	detrended NCEP	climatology LIS-OTD
1901–1947	transient	transient CRU TS3.1	detrended NCEP	climatology LIS-OTD
1948–1979	transient	transient CRU TS3.1	transient NCEP	climatology LIS-OTD
1980–2006	transient NOAA	transient CRU TS3.1	transient NCEP	climatology LIS-OTD

### 5.S1.2 Historical simulations

LPX-Mv1 is run on a 0.5° resolution grid using monthly climate (maximum and minimum temperature, precipitation, cloud cover and number of wet days) from the CRU TS3.1 data set (Harris et al., 2013) and wind speed from the National Center for Environmental Prediction (NCEP) reanalysis data (Kalnay et al, 1996). Monthly input data are converted to a pseudo-daily time step by interpolation or, in the case of precipitation, using a weather generator (Gerten et al., 2004) based on monthly precipitation and the fraction of wet days each month (defined as the number of days per month with precipitation >0.1mm (New et al., 2002) to create pseudo-daily values. The CRU TS3.1 data are already on a 0.5° resolution grid; the NCEP data were interpolated from the original 1.875° resolution grid to the LPX-Mv1 grid using bilinear interpolation. Lightning is prescribed as a monthly lightning climatology from the Lightning Imaging Sensor Optical Transient Detector High Resolution flash count ([http://gcmd.nasa.gov/records/GCMD\\_lohrmc.html](http://gcmd.nasa.gov/records/GCMD_lohrmc.html)). Atmospheric CO<sub>2</sub> concentration is prescribed annually. CO<sub>2</sub> concentrations were derived from a combination of ice core and atmospheric measurements from Mauna Loa and South Pole (Rayner et al., 2005) supplemented by data from NOAA-CMDL (<http://www.esrl.noaa.gov/gmd/>) global averaged concentrations for the period from 1980–2006.

The model was spun up using constant CO<sub>2</sub> (286 ppm), and detrended climate data until the carbon pools were in equilibrium. The historical run used transient CO<sub>2</sub> from 1850 to 2005. Detrended climate was used for all climate variables until 1900. From 1901 onwards, transient CRU TS3.1 was used for all climate variables except wind speed. Detrended wind speed is used until 1948 and transient values thereafter. Table 5.S1 summarises the modelling procedure for the spin-up and historical simulations. Mean values for the historical simulations are averages of the period 1997 to 2006.

TABLE 5.S2: Information on the models from the CMIP5 database used to provide future climate scenarios. OA models are coupled ocean-atmosphere models; OAC models include a marine and terrestrial carbon cycle. The resolution (number of grid cells by latitude and longitude) is that of the atmospheric and land-surface components of each model.

<b>Code</b>	<b>Centre</b>	<b>Type</b>	<b>Original resolution</b>
CNRM-CM5	Centre National de Recherches Meteorologique	OA	128, 256
GISS-CM5	NASA Goddard Institute for Space Studies	OA	90, 144
HadGEM2-CC	Hadley Centre, UK Meteorological Office	OA	145, 192
MRI-CGCM3	Meteorological Research Institute	OA	160,320
HadGEM2-ES	Hadley Centre, UK Meteorological Office	OAC	145, 192
IPSL-CM5a-LR	Institut Pierre-Simon Laplace	OAC	96, 96
MIROC-ESM	Japan Agency for Marine-Earth Science and Technology	OAC	64, 128
MPI-ESM-LR	Max Planck Institute for Meteorology	OAC	96, 192
BCC-CSM1-1	Beijing Climate Center	OAC	64, 128

### 5.S1.3 Inputs for the 21<sup>st</sup> century climate simulations

LPX-Mv1 was run from 2006 onwards using multiple climate realizations from climate model outputs in the CMIP5 database (Table 5.S2) forced by two alternative Representative Concentration Pathway (RCP) scenarios (van Vuuren et al., 2011): RCP4.5 and RCP8.5. RCP4.5 is an intermediate radiative forcing (RF) scenario that stabilizes at 4.5 Wm<sup>-2</sup> by 2100 (Taylor et al. 2012). RCP8.5 is an extreme RF scenario where RF reaches 8.5 Wm<sup>-2</sup> by 2100.

In order to derive inputs for LPX-Mv1, we calculated climate anomalies between the simulated climate from the RCP-driven run and the simulated climate of the historic baseline period (January 1961 to December 1990). The resolution of the climate models differs (Table 5.S2). The anomalies were therefore regridded to the 0.5° resolution grid of LPX-Mv1 using bilinear interpolation. The regridded anomalies were then added to the observed climate for the January 1961 to December baseline period. For unbounded variables (e.g. temperature) this procedure is straightforward, but many variables have either a natural upper and/or lower bound (e.g. precipitation, number of wet days, wind speed, percentage cloud cover). If the result of adding anomalies to the observed climate resulted in values that exceeded these natural bounds (e.g. negative precipitation, number of wet days, wind speed, or cloud cover less than 0% or greater than 100%) then the individual climate plus anomaly values were set to

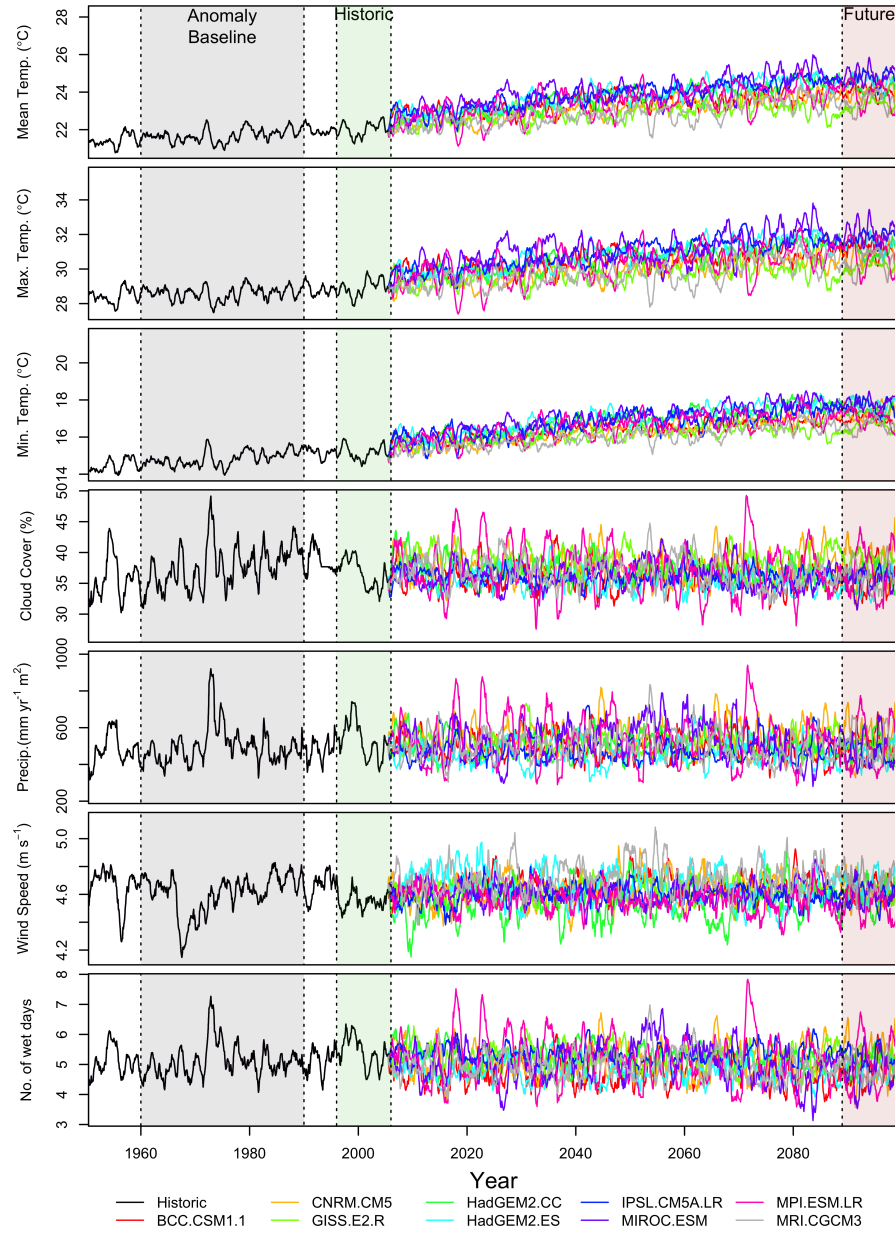


FIGURE 5.S1: Climate inputs used to drive the LPX-Mv1 simulations, averaged for Australia, showing the smooth transition between the climate used for the historic simulations and the future simulations. The twelve-month running means are shown (top to bottom) for mean temperature (°C); maximum temperature (°C); minimum temperature (°C); percentage (%) cloud cover; precipitation (mm  $\text{yr}^{-1}$   $\text{m}^{-2}$ ); wind speed ( $\text{m s}^{-1}$ ); and number of wet days. The values for 1950–2006 are from CRU TS3.1 or NCEP, post-2006 values are taken from coupled ocean-atmosphere simulations driven by the RCP4.5 scenario as described above. The coloured lines show the different ocean-atmosphere models.

the appropriate bounded values. Application of the anomaly procedure resulted in a smooth transition between the climate used for the historic simulations and the future simulations (Figures S1-S2), whilst maintaining the interannual variability of each climate model. In Australia, ENSO is a dominant influence on regional climate interannual variation (Clark et al. 2013). CMIP5 models represent an improvement on earlier CMIPs in their simulation of ENSO (Flato et al., 2013), with more accurate representation of amplitudes of temperature changes, if not period and timing. The CO<sub>2</sub> inputs from 2006 to 2100 (Figure 5.3) were calculated from the RCP monthly concentration pathway.

### 5.S1.4 Sensitivity Experiments

The 21<sup>st</sup> century RCP4.5 simulations are the baseline simulations for our analyses. In order to separate the impact of CO<sub>2</sub> fertilisation from the impact of climate changes, we ran a further set of simulations (fixed-CO<sub>2</sub> experiment) in which LPX-Mv1 was forced by 21<sup>st</sup> century climate scenario only. CO<sub>2</sub> was held constant in these runs at 380.8 ppm, the CO<sub>2</sub> value for 2006.

We also made a set of simulations to diagnose the impact of including resprouting PFTs. The vegetation distribution and carbon balance during the historic period would be different in the absence of resprouting vegetation, with total NPP being for example lower in the absence of resprouting. Thus, it was necessary to run both the historic and future simulations with the version of LPX-Mv1 in which resprouting was disabled (LPX-Mv1-nr). The impact of resprouting can be diagnosed by comparing the outputs of these simulations with the 21<sup>st</sup> century resprouting simulations, taking into account the differences between the two control (historic) simulations thus:

$$(F_{rs} - H_{rs}) - (F_{nr} - H_{nr}) \quad (5.1)$$

where  $H_{nr}$  is the historic run with no resprouting,  $F_{nr}$  is the 21<sup>st</sup> century run with no resprouting,  $H_{rs}$  is the historic run with resprouting and  $F_{rs}$  is the 21<sup>st</sup> century run with resprouting.

### 5.S1.5 Evaluation of the historical simulations

We obtained observed biomass carbon from the Ruesch and Gibbs (2008) dataset ([http://cdiac.ornl.gov/epubs/ndp/global\\_carbon/carbon\\_documentation.html](http://cdiac.ornl.gov/epubs/ndp/global_carbon/carbon_documentation.html)). These estimates are derived from site-based measurements of living carbon, which are allocated to specific land-cover types by continent based on vegetation composition and bioclimatic information. Land-cover types are based on the GLC2000 5x5 land cover map (Bartholomé and Belward, 2005). The average value of carbon biomass for a land-cover type is attributed to all cells of that land cover type. For comparison with simulated biomass carbon (Figure 5.1, main text) cells defined as swamps or as anthropogenically altered (e.g. urban or cropland) in the GLC2000 data sets were

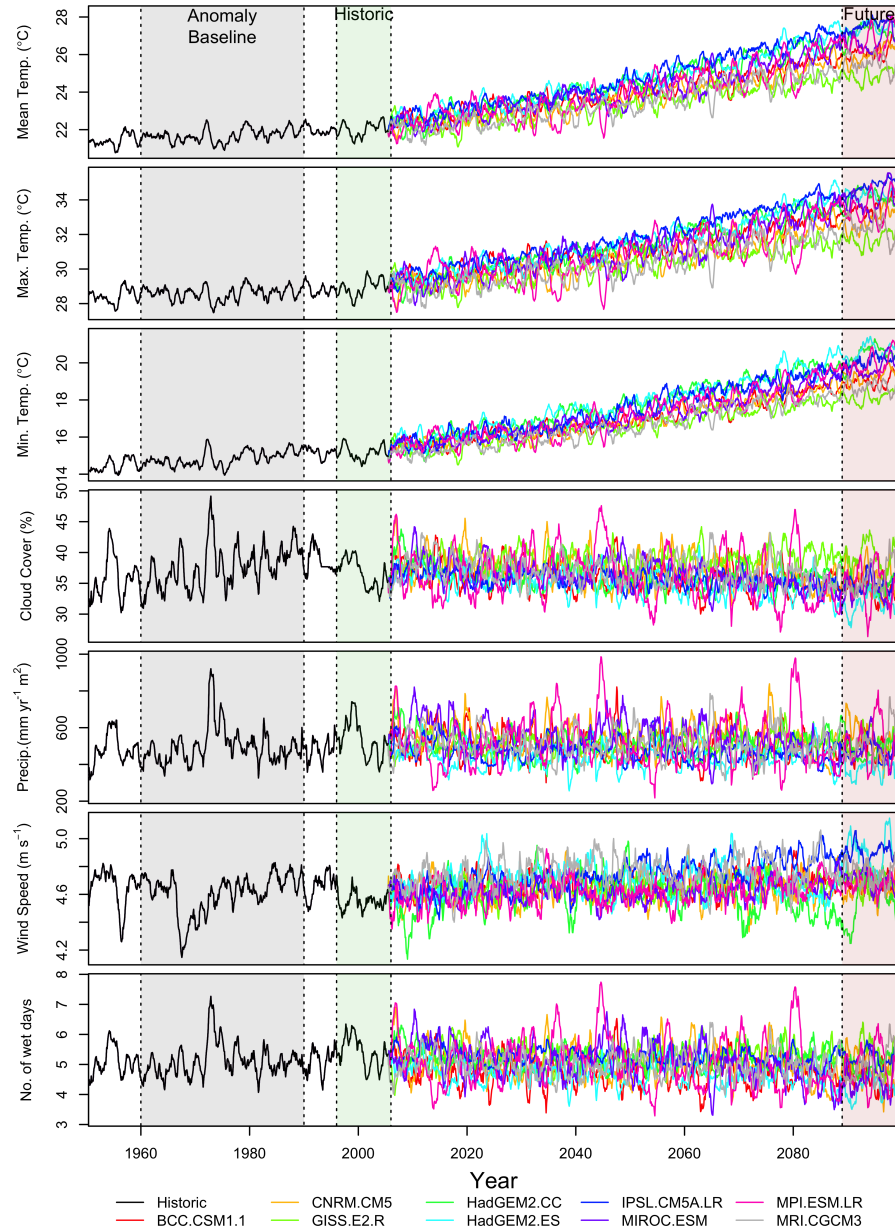


FIGURE 5.S2: Climate inputs used to drive the LPX-Mv1 simulations, averaged for Australia, showing the smooth transition between the climate used for the historic simulations and the future simulations. The twelve-month running means are shown (top to bottom) for mean temperature (°C); maximum temperature (°C); minimum temperature (°C); percentage (%) cloud cover; precipitation ( $\text{mm yr}^{-1} \text{m}^{-2}$ ); wind speed ( $\text{m s}^{-1}$ ); and number of wet days. The values for 1950–2006 are from CRU TS3.1 or NCEP, post-2006 values are taken from coupled ocean-atmosphere simulations driven by the RCP8.5 scenario as described above. The coloured lines show the different ocean-atmosphere models.

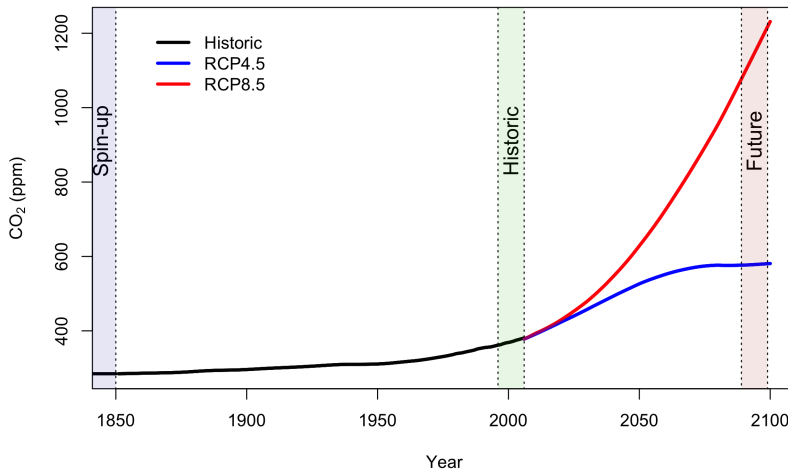


FIGURE 5.S3: Annual CO<sub>2</sub> concentrations used as input to the LPX-Mv1 model. The black line shows CO<sub>2</sub> values used for the historic run (pre-2006), and the red and blue shows CO<sub>2</sub> concentrations consistent with the RCP8.5 and RCP4.5 runs respectively, used for the 21<sup>st</sup> century simulation with LPX-Mv1.

excluded. We aggregated the remaining grid cells to a 0.5° LPX-Mv1 grid using the raster package in R (Hijmans, 2014).

Evaluation of simulated burnt area, and the timing and concentration of fire, was made using the fourth version of the Global Fire Database (GFED4: Giglio et al., 2013). GFED4 provides data from the mid-1995 to 2012. We re-gridded the data for the period 1997–2006 (i.e. the period that overlaps with the climate drivers) to a 0.5° LPX-Mv1 grid using the raster package in R (Hijmans, 2014).

Estimates of the carbon budget of Australia between 1990 and 2011 have been obtained by Haverd et al. (2013), by tuning a regional biosphere model (BIOS2) using observations from multiple sources. Essentially BIOS2 is a modification of the CABLE land-surface scheme (Wang et al., 2011) that includes improved soil treatment (Haverd and Cuntz, 2010) and the CASA-CNP biogeochemical model (Wang et al., 2010). BIOS2 parameters were constrained using observational data sets, including eddy flux data (CO<sub>2</sub> and H<sub>2</sub>O) from 12 OzFlux tower sites, streamflow, and data on soil, litter and biomass carbon pools (Haverd et al., 2012). Haverd et al. (2013) used fire emissions for the period 1997–2009 from GFED3 (van der Werf et al., 2010), on the assumption that the average values were representative of the whole period. Haverd et al. (2013) used estimates of harvest from 2004, and assumed these were representative for the whole period. However, since we do not simulate harvest, we ignore this term in our comparisons.

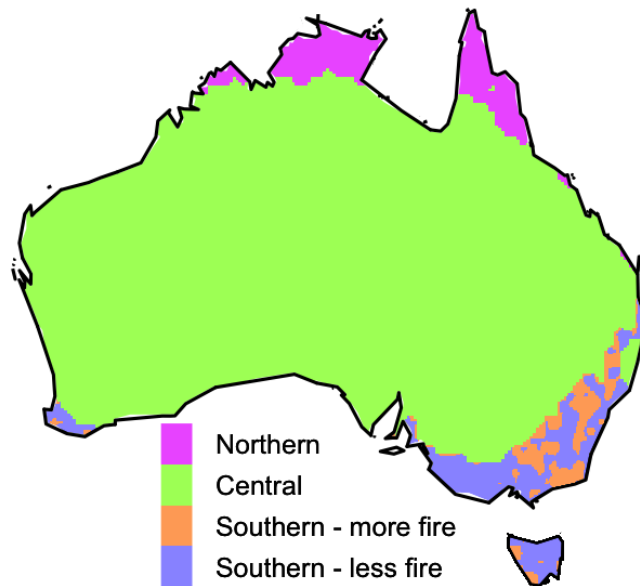
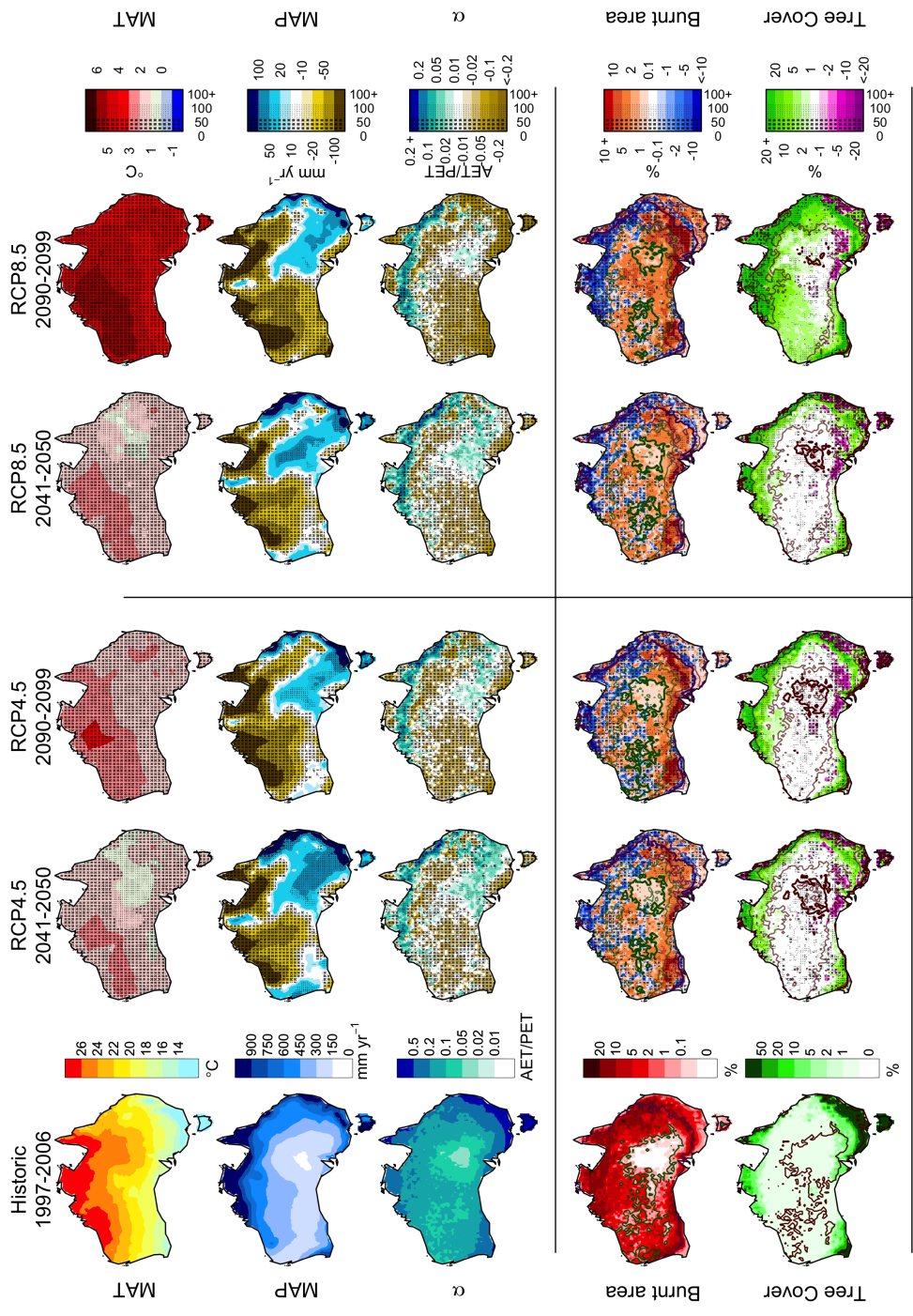


FIGURE 5.S4: Map showing the four regions used in the final analyses. In addition to the primary regions (northern, central) the southern region is subdivided into southern, more fire (where fire increases in the 21<sup>st</sup> century) and southern, less fire (where fire decrease in the 21<sup>st</sup> century).

### 5.S1.6 Definition of regions

Selection of regions was based on vegetation cover simulated by LPX-Mv1 during the period 1997–2006 and geographic location using k-means partitioning in R (Oksanen et al., 2013; R Core Team, 2013). Vegetation cover was defined in terms of proportions of tree cover, grass cover; and bare ground, and geographic location was defined by longitude and latitude. The 5 predictor variables were scaled between 0 and 1 so as to assign equal weight to each. Although the variance ratio criterion (Calinski and Harabasz, 1974) suggested that six was the optimal number of clusters, we combined the southeastern and southwestern clusters into a single region (southern) for the purposes of our analyses. Similarly, we combined the interior southern grassland and interior western and eastern desert and grassland clusters into a single region (central). Thus for the purposes of our analyses we defined three basic regions (northern, central, southern: see Figure 5.S4) although we divided the southern region into areas experiencing an increase and areas experiencing a decrease in fire for the baseline run during the 21<sup>st</sup> century.

## 5.S1.7 Results of the individual RCP4.5 simulations



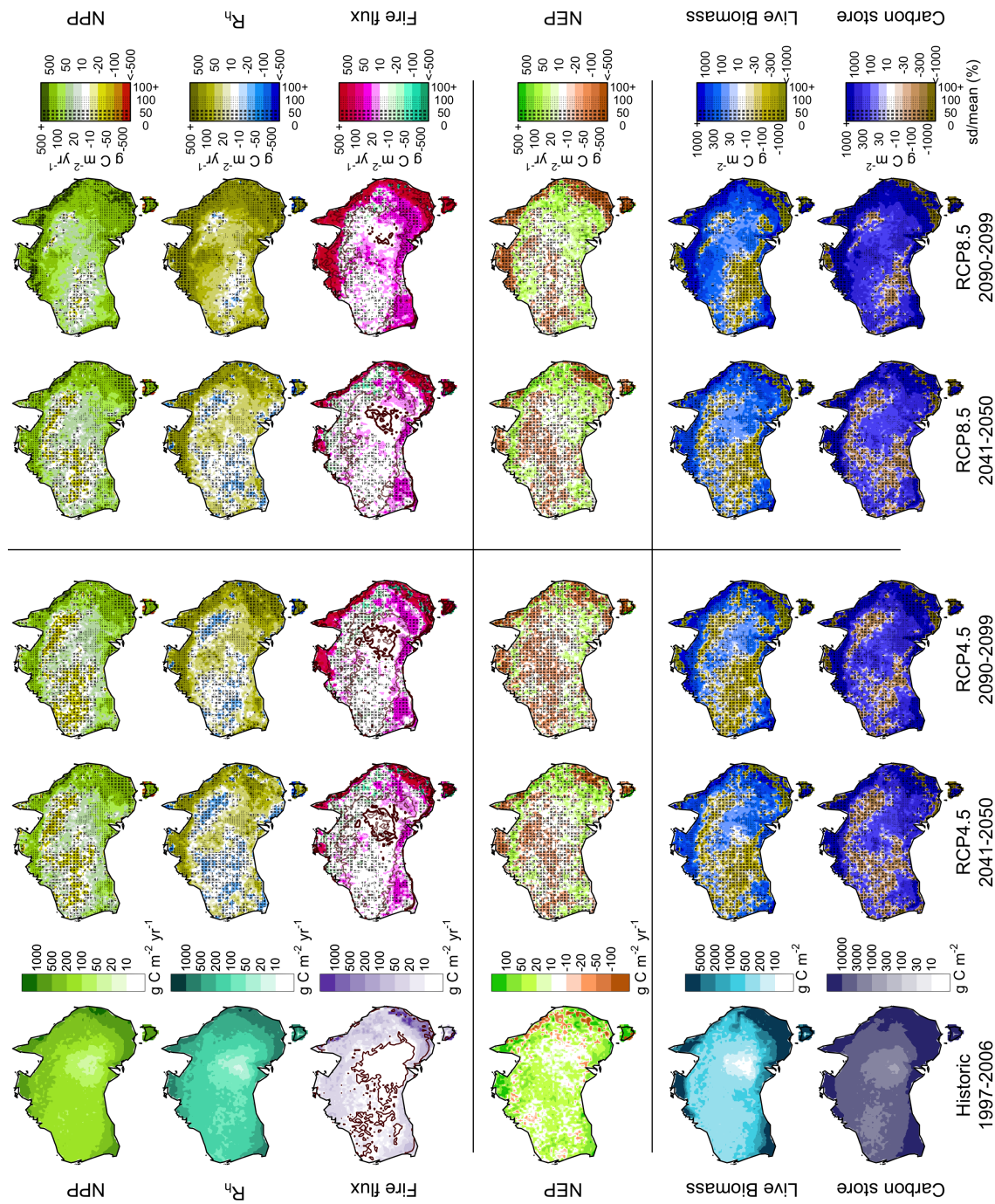


FIGURE 5.S5: Maps of the ensemble changes in climate, vegetation and carbon cycle from the RCP4.5 and RCP8.5 experiments compared to the historic period (1997–2006). We show ensemble averages for two periods, 2041–2050 and 2090–2099. The climate variables are mean annual temperature (MAT), mean annual precipitation (MAP) and the ratio of actual to potential evapotranspiration (AETPET,  $\alpha$ ). The vegetation parameters are burnt area and tree cover. The carbon cycle terms are net primary productivity (NPP), respiration ( $R_h$ ), fire flux, net ecosystem productivity (NEP), live biomass and carbon storage. Colours show the absolute change and stippling shows the robustness of the signal (as measured by the standard deviation, sd, of the model results divided by the ensemble mean for each grid cell). Thick contour guides show ensemble mean and thin contour guides show ensemble range for (fire map - green) simulated fine fuel loads of 200gC/m<sup>2</sup>; (fire map - purple) fuel moisture content of 20%; and (Tree cover and Fire flux - red) 0.1% annual burnt area.

TABLE 5.S3: Summary of changes in carbon budget terms as simulated using RCP4.5 outputs from individual climate models. The model codes are given in Table 5.S2. The changes are averages for the period 2090–2099 compared to the 1997–2006 period from the historic simulation. *Italicized* values give the p-value for testing the significance of the change (see methods in main text for details). The final column lists the p-value for the test in robustness and (in italics) significance of the model ensemble change.

Variable	Historic	BCC-CSM1-1	CNRM-CM5	GISS-E2-R	HadGEM2-CC	HadGEM2-ES	IPSL-CM5A-LR	MIROC-ESM	MPI-ESM-LR	MRI-GCM3	Robust/ <i>significant</i>
Burnt area (%)	41	44	50	63	44	39	45	44	47	43	0.059
Fire flux (Tg C yr <sup>-1</sup> )	169	262	521	744	494	331	597	6604	0.316	0.950	0.304
NPP (Tg C yr <sup>-1</sup> )	2214	2287	2696	3171	2681	0.007	0	0.064	0.007	0	0.001
Tree cover (%)	9.81	11	15	17	14	12	15	13	14	13	0
$R_h$ (Tg C yr <sup>-1</sup> )	1858	1890	2369	2634	2268	1995	2373	2303	0.023	0.15	0
NEP (Tg C yr <sup>-1</sup> )	189	136	-191	-205	-80	33	-231	21	0.29	0.317	0
Carbon store (Tg C)	41607	43997	45801	50569	46857	0.878	0.045	0.984	0.087	0.959	0.119
	0	0	0	0	0	0	46870	45931	44282	40315	0.405
							0	0	0	0	0

### 5.S1.8 Ensemble and individual results of the individual RCP8.5 simulations

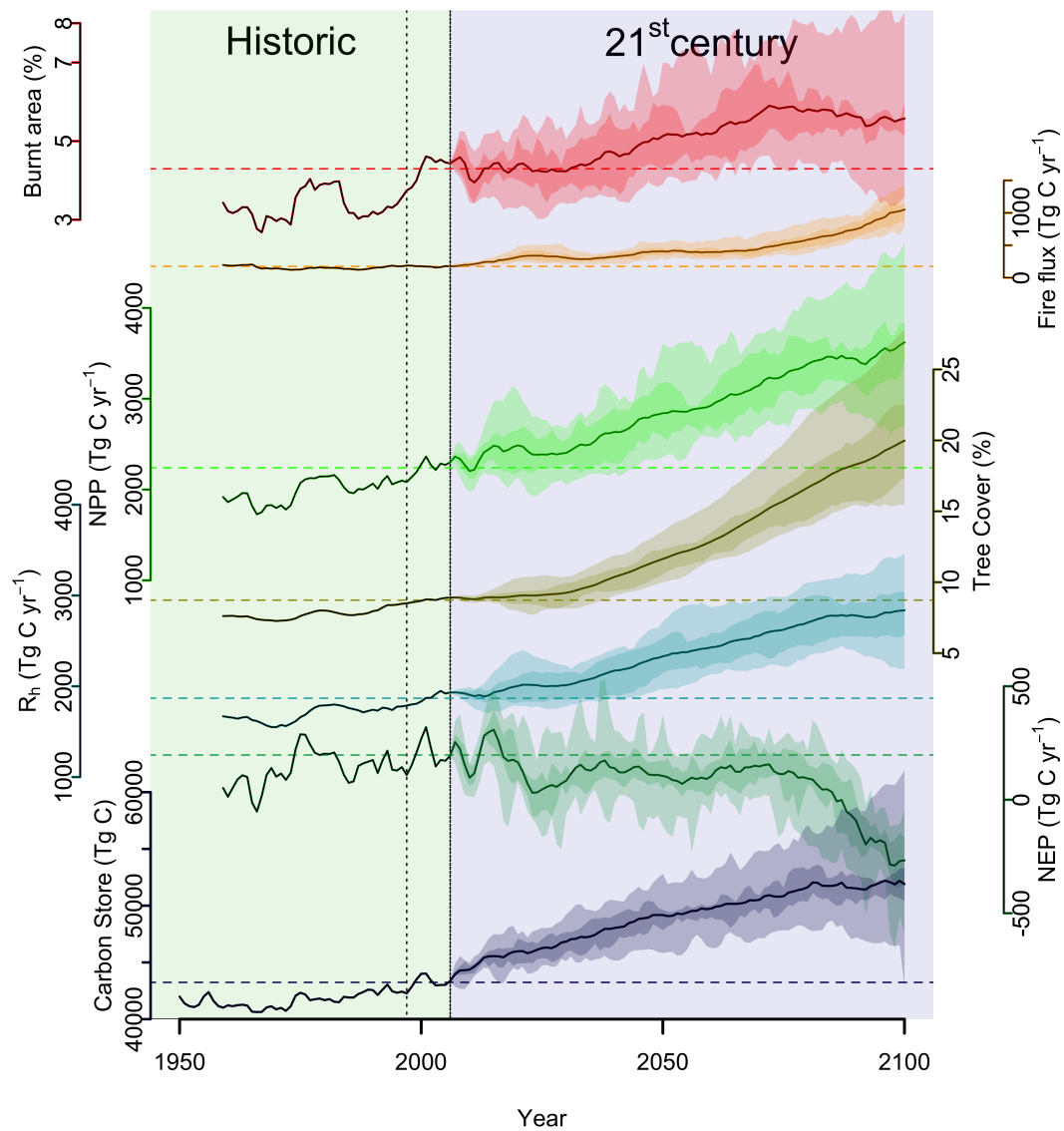


FIGURE 5.S6: Changes in the carbon cycle over Australia through the 21<sup>st</sup> century based on the RCP8.5 scenarios. The time series (bold lines) are ensemble averages of the model results for (a) burnt area (Mkm<sup>2</sup>), (b) fire flux (Tg C yr<sup>-1</sup>), (c) net primary productivity (NPP) (Tg C yr<sup>-1</sup>), (d) tree cover (%), (e) heterotrophic respiration ( $R_h$ ) (Tg C yr<sup>-1</sup>), (f) net ecosystem productivity (NEP) Tg C yr<sup>-1</sup>), and (g) carbon store (Pg C). The range in the individual model simulations is indicated by the shaded bands. The dashed horizontal lines indicate the average value of each variable during the last decade of the historic simulation.

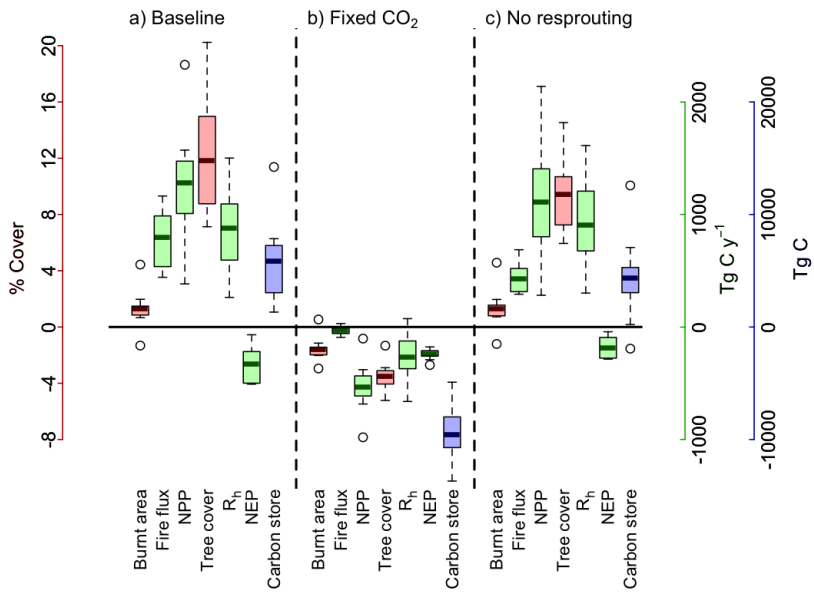


FIGURE 5.S7: Contribution of direct CO<sub>2</sub> effects and resprouting to the simulated changes in the carbon cycle over the 21<sup>st</sup> century based on the RCP8.5 scenarios. The baseline plots (a) show the average changes in the last decade of the 21<sup>st</sup> century simulations relative to the 1997–2006 average from the historic simulation. The CO<sub>2</sub> plots (b) show the difference between the baseline 21<sup>st</sup> century run and a run in which CO<sub>2</sub> was fixed at 380.8 ppm. The no resprouting plots (c) shows the difference between the baseline 21<sup>st</sup> century run and a run in which resprouting was disabled. In the box-and-whisker plots, the solid lines show the mean value for the ensemble of simulations, the boxes show the interquartile range and the whiskers show the 5–95% confidence limits. Outliers are shown by an open circle. Note that the scale for carbon store is 10x that of the individual carbon components.

TABLE 5.S4: Summary of changes in carbon budget terms as simulated using RCP8.5 outputs from individual climate models. The model codes are given in Table 5.S2. The changes are averages for the period 2090–2099 compared to the 1997–2006 period from the historic simulation. The ensemble average values are also given for comparison. The final column lists the p-value for the test in robustness and (in italics) significance of the model ensemble change.

Variable	Historic	BCC-CSM1-1	CNRM-CM5	GISS-E2-R	HadGEM2-CC	HadGEM2-ES	IPSL-CM5A-LR	MIROC-ESM	MPI-ESM-LR	MRCM3	Robust/ significance
Burnt area (%)	41	47	56	75	51	31	50	49	46	52	0.048
Fire flux (Tg C yr <sup>-1</sup> )	169	594	0.014	0.037	0.001	0.237	0.053	0.132	0.864	0.372	0.200
NPP (Tg C yr <sup>-1</sup> )	2214	3042	0	926	1289	1045	640	1174	1119	997	0.054
Tree cover (%)	9.81	19	22	30	25	17	25	20	19	18	0
R <sub>h</sub> (Tg C yr <sup>-1</sup> )	1858	2422	2752	3302	2858	2111	2948	2910	2649	2430	0
NEP (Tg C yr <sup>-1</sup> )	189	26	0	0.001	0	0	0.027	0	0.001	0.006	0.004
Carbon store (Tg C)	41607	0.196	46592	0.314	0.295	0.078	0.132	0.007	0	0.268	0.025

## 5.S2 References

Bartholom E.M and Belward, A.S. GLC2000: a new approach to global land cover mapping from Earth Observation data. *Int. J. Remote Sensing* 26, 1959–1977 (2005).

Calinski, T. & Harabasz, J. A dendrite method for cluster analysis. *Commun. Stat.* 3, 1–27 (1974).

Clarke, H., Lucas, C. and Smith, P.: Changes in Australian fire weather between 1973 and 2010, *Int. J. Climatol.*, 33(4), 931944 (2013).

Flato G, Marotzke J, Abiodun B, et al. Evaluation of Climate Models. In: Stocker TF, Qin D, Plattner G-K, et al., eds. *Climate Change 2013: The Physical Science Basis*. 5th ed. Cambridge, UK and New You, NY, USA.: Cambridge University Press; 2013:741–866.

Gerten, D., Schaphoff , S., Haberlandt, U., Lucht, W. & Sitch, S. Terrestrial vegetation and water balance - hydrological evaluation of a dynamic global vegetation model. *J. Hydrol.* 286, 249–270, doi:10.1016/j.jhydrol.2003.09.029 (2004).

Giglio, L., Randerson, J. T. & van der Werf, G. R. Analysis of daily, monthly, and annual burned area using the fourth-generation Global Fire Emissions Database (GFED4). *J. Geophys. Res.-Biogeo.* 118, 317–328 (2013).

Harris, I., Jones, P. D., Osborn, T. J. & Lister, D. H. Updated high-resolution grids of monthly climatic observations — the CRU TS3.10 Dataset. *Int. J. Climatol.*, doi:10.1002/joc.3711 (2013).

Haverd, V. & Cuntz, M. Soil-Litter-Iso: A one-dimensional model for coupled transport of heat, water and stable isotopes in soil with a litter layer and root extraction. *J. Hydrol.* 388, 438–455 (2010).

Haverd, V. et al. Multiple observation types reduce uncertainty in Australias terrestrial carbon and water cycles, *Biogeosciences Discuss.* 9, 12181–12258, doi:10.5194/bgd-9–12181–2012 (2012).

Haverd, V. et al. The Australian terrestrial carbon budget. *Biogeosciences* 10, 851–869 (2013).

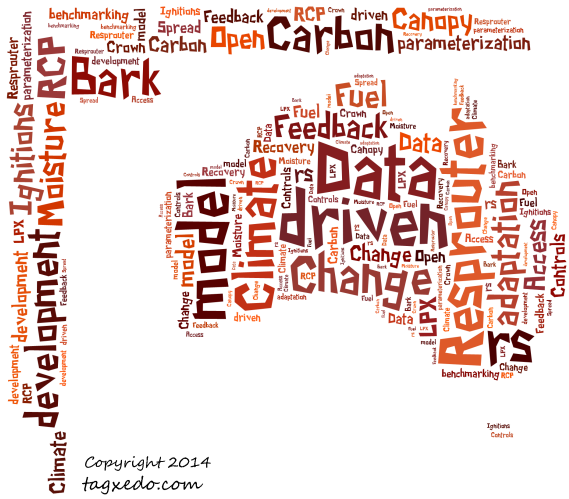
Hijmans, R.J. Raster: Geographic data analysis and modeling. R package version 2.2–31. <http://CRAN.R-project.org/package=raster> (2014) Kalnay, E. et al. The NCEP/NCAR 40-year reanalysis project. *Bull. Amer. Meteor. Soc.* 77, 437–471 (1996).

- Kelley, D.I., Harrison, S.P. & Prentice, I.C., 2014. Improved simulation of fire-vegetation interactions in the Land surface Processes and eXchanges Dynamic Global Vegetation Model (LPX-Mv1). *Geosci. Model Devel. Discussions* 7: 1–70.
- Monteith, J.L. A reinterpretation of stomatal responses to humidity. *Plant, Cell & Environment* 18, 357–364 (1995).
- New, M., Lister, D., Hulme, M. & Makin, I. A highresolution data set of surface climate over global land areas. *Clim. Res.* 21, 1–25, doi:10.3354/cr021001 (2002).
- Oksanen, J. et al. Vegan: Community Ecology Package. R package version 2.0–10. <http://CRAN.R-project.org/package=vegan> (2013).
- Prentice, I.C., Kelley, D.I., Foster, P.N., Friedlingstein, P., Harrison, S.P. & Bartlein, P.J. Modeling fire and the terrestrial carbon balance. *Glob. Biogeochem. Cy.* 25, 1–13 (2011).
- R Core Team. R: A language and environment for statistical computing. R Foundation for Statistical Computing, Vienna, Austria. URL <http://www.R-project.org/> (2013).
- Rayner, N.A. et al. Improved analyses of changes and uncertainties in sea surface temperature measured in situ since the mid-nineteenth century: The HadSST2 Dataset. *J. Clim* 19, 446–469 (2005).
- Rothermel, R.C. A Mathematical Model for Predicting Fire Spread in Wildland Fuels. USFS (1972).
- Ruesch, A. & Gibbs, H.K. New IPCC Tier-1 Global Biomass Carbon Map For the Year 2000. Available online from the Carbon Dioxide Information Analysis Center [<http://cdiac.ornl.gov>], Oak Ridge National Laboratory, Oak Ridge, Tennessee (2008).
- Taylor, K. E., Stouffer, R. J. & Meehl, G. A. An overview of CMIP5 and the experiment design. *Bull. Am. Meteorol. Soc.* <http://dx.doi.org/BAMS-D-11-00094.1> (2012).
- van der Werf, G.R. et al. Global fire emissions and the contribution of deforestation, savanna, forest, agricultural, and peat fires (1997–2009). *Atmos. Chem. Phys.* 10, 11707–11735 (2010).
- van Vuuren, D.P. et al. The representative concentration pathways: an overview. *Clim. Change* 109, 5–31 (2011).
- Wang, Y.P., Law, R.M. & Pak, B. A global model of carbon, nitrogen and phosphorus cycles for the terrestrial biosphere. *Biogeosci.* 7, 2261–2282, doi:10.5194/bg-7-2261–2010 (2010).

Wang, Y. P. et al. Diagnosing errors in a land surface model (CABLE) in the time and frequency domains. *J. Geophys. Res.-Biogeosci.* 116, G01034, doi:10.1029/2010JG001385 (2011).

# 6

## Conclusion



In this thesis, I have adopted an explicit iterative approach to model development in the Land Processes and eXchanges (LPX: Prentice et al., 2011) dynamic global vegetation model (DGVM), in which benchmarking against observations is used to identify areas for new data-driven parameterizations and then subsequently used to evaluate whether the implementation of these new parameterizations produces an overall improvement in model performance. This approach contrasts with the general tendency to focus evaluation on new components, for example the evaluation of fire treatments within DGVMs using only observations of burnt area and/or fire carbon fluxes (see e.g. Li et al., 2012; Pfeiffer et al., 2013). One reason for this partial approach to evaluation is the lack of a comprehensive benchmarking system (Luo et al., 2012). Existing attempts to develop benchmarks for the evaluation of DGVMs and land-surface surface models have focused on a limited number of processes, generally related to energy and carbon fluxes (e.g. Randerson et al., 2009; Blyth et al., 2010; Beer et al., 2010; Cadule et al., 2010; Blyth et al., 2011). Furthermore, they make use of a limited number of metrics which are difficult to compare across processes and do not yield results that are easily interpreted in terms of the causes of model errors. As part of this thesis (Chapter 2), I have developed a comprehensive benchmarking system which allows evaluation of spatial and temporal patterns of multiple aspects of the simulated vegetation, hydrology, fire regimes and ecosystem fluxes as well as allowing the impact of specific types of bias to be taken into account. This benchmarking system serves several purposes: (1) it quantifies how well a model performs across a comprehensive range of important processes; (2) it allows the identification of model weaknesses through comparison of the performance with respect to different benchmarks and thus facilitates the identification of processes that require improvement; (3) it quantifies the differences between model

versions, which allows assessment of the overall impact of new parameterizations. Application of this benchmarking system to LPX identified Australia as a region that was poorly simulated compared to other parts of the world. One reason for this was the sharp, fire-controlled boundaries between grassland and forest. Through benchmarking, I identified that the sharp boundaries between regions experiencing no fire and those experiencing fire resulted from an unrealistic sensitivity to lightning ignitions. This led to the re-examination of lightning parameterization (Chapter 4). The sharp grassland/forest boundaries resulted because of high mortality rates for woody plants in areas with fire. This led to a re-examination of the realism of the PFT-specific treatment of bark thickness in the model and the subsequent inclusion of an adaptive parameterization of bark thickness as well as fire recovery through resprouting in the model (Chapter 4).

The implementation of individual data-driven parameterizations can degrade model performance, particularly when the original parameterization was tuned to produce a reasonable simulation of an emergent property of the model. For example, in the original version of LPX, the parameterization of lighting distribution on wet and dry days was tuned to produce a good simulation of burnt area (Prentice et al., 2011). The implementation of a new treatment based on analyses of the actual occurrence of lightning on days with/without rain resulted in a significant increase in the amount of fire and led to a 24% degradation in the simulated annual average burnt area in Australia. However, benchmarking showed that the new parameterization resulted in a 7-8% improvement in the seasonal pattern of fire and a more realistic timing of the peak fire season by between 15-22 days. The fact that the benchmarking system was specifically set up to measure different aspects of the fire regime meant that it was possible to distinguish between the bias in total fire and the simulation of a more realistic temporal pattern of fire, and thus to isolate the causes of the overall bias as resulting from poor simulation of burnt area rather than ignitions. Once new parameterizations effecting fuel loads and moisture were implemented, the bias in total burnt area was reduced, resulting in a 19% overall improvement in model performance.

The model development described in this thesis was driven by extensive data analysis, and can be seen as part of a wider movement towards data-driven parameterization of a wide range of fundamental vegetation processes (see e.g. Brovkin et al., 2012; Smith et al., 2012; Wang et al., 2012, 2013; Verheijen et al., 2013; Prentice et al., 2014; Wang et al., 2014). The initial development of DGVMs and fire-enabled DGVMs occurred when access to large-scale or multi-year data sets was limited. Many of the early models were developed using studies from specific regions: MC-FIRE (Lenihan et al., 1998) for example was initially developed using data from studies in South Dakota, while GLOBFIRM (Thonicke et al., 2001) was parameterized using data from 31 sites from Portugal, California and northern Australia. However, the increasing availability of remotely-sensed data sets or GIS-based data products provide a fantastic opportunity for data-driven model development. The parameterization of lightning ignitions in this thesis provides an example, since it was based on an analysis of remotely-sensed lightning observations (LIS; Christian et al., 1999; Christian, 1999), together with extensive ground-based observations of lightning (NDLN; Cummins and Murphy, 2009) and daily

precipitation data (CPC; Higgins et al., 1996; Higgins and Climate Prediction Centre, 2000) at a continental scale over the USA.

The collation of site-based or field data in databases provides another source of information for data-driven model development. In this thesis, I made use of the TRY database of plant traits (Kattge et al., 2011), for example, to obtain data on bark thickness for individual species. However, data syntheses of this sort are relatively new and existing databases do not cover all areas of interest for model development. In this thesis, I present an analysis of a new database of fire-response traits (Chapter 3). This work was a contribution to the Australian Centre for Ecological Analysis and Synthesis (ACEAS) working group on ‘Using plant functional traits to predict ecosystem vulnerability to changing fire regimes’ ([www.aceas.org.au/index.php?option=com\\_content&view=article&id=114&Itemid=115](http://www.aceas.org.au/index.php?option=com_content&view=article&id=114&Itemid=115)), part of the aim of which is to synthesise data about fire-related plant traits. This effort could provide a rich source of information that could be used in future model development. There are many other areas where synthesis of site-based data could potentially be useful for model development. One example would be the synthesis of site-based data on fuel loads, which could be used to characterize the relationship between fuel limitation and fire — something that fire-enabled DGVMs handle very differently (see Table 1.1). Similarly, data on wind profiles in different vegetation types could help improve the scaling of wind speed data to take account of the presence of vegetation in models.

One novel aspect of the model development undertaken in this thesis is the inclusion of within-PFT variability in bark thickness in LPX (Chapter 4). In many DGVMs the basic vegetation unit is a PFT, with PFT-specific values for individual parameters and simulated vegetation represented by an average individual plant per PFT within a given grid cell. However, there is considerable variability in the characteristics of the individual plant species that are grouped together, for simplicity, within any PFT. This variability underpins species selection in response to changing environmental conditions. Bark thickness is a classic example of this: thicker-barked species are more likely to survive a fire and thus there is selective pressure toward these species in fire prone regions such that the average bark thickness within a population increases with fire frequency (Fig. 1.7 Lawes et al., 2011). Here, I have adopted the method for incorporating within-PFT trait variability described by Verheijen et al. (2013) and applied it to bark thickness (Fig. 4.5). Bark thickness within each PFT is initially represented by a simple data-derived distribution. Fire preferentially kills the thinner barked individuals within this distribution. The post-fire distribution is calculated based on the average bark thickness of surviving and re-establishing individuals. This scheme allows representation of the full range of bark thickness found within each PFT, and allows the PFT-averaged bark thickness to adapt to changes in fire regime, but does not increase model complexity excessively and avoids the need to add additional computationally expensive PFTs in order to describe the range of trait variability better. Within-PFT variability exists in other simulated traits (e.g. the fraction of deep roots: Fig 4.3) and field observations suggest that these characteristics can also be adaptive (e.g. the increase in average rooting depth along aridity gradients Schenk and Jackson, 2002b,a, 2005). Adaptive parameterization of such traits could provide substantial improvements to the simulation of vegetation responses to climate change. However, the

design of such a parameterization requires an understanding of the adaptive benefit conferred by changes in the trait, as well as the existence of site-based data syntheses in order to develop well-founded parameterizations.

Another novel aspect of this thesis is the incorporation of resprouting PFTs in order to improve the post-fire response of woody vegetation (Chapter 4). The initial suite of PFTs in DGVMs was chosen to allow the representation of climate and environmental controls on vegetation distribution and carbon cycling. Additional PFTs have been added as new processes were incorporated in the DGVM framework. For example, the inclusion of wetlands in LPJ in order to improve the simulation of the terrestrial carbon and methane cycles necessitated the creation of two new PFTs, specifically mosses and flood tolerant grasses (LPJ-WhyMe: Wania, 2007; Wania et al., 2010). Similarly, crop PFTs were incorporated into LPJ in order to simulate human land use (LPJ-ml: Bondeau et al., 2007) and a shrub PFT was included in CLM-DGVM to improve the simulation of arid/semi-arid shrublands (Zeng et al., 2008). Despite the fact that many vegetation types are maintained by regular fire (e.g. savannas: Cochrane et al., 1999; Beckage et al., 2009; Lehmann et al., 2011) and that plants in fire-prone ecosystems display adaptations to survive or recover quickly after fire (Clarke et al., 2013), there has been no consideration of the need to include fire-related PFTs in a DGVM framework until now. Resprouting, the ability to regenerate from meristems in wood, bark or underground organs, is typical of fire-adapted vegetation. This behavior has a significant implication for the carbon cycle. Post-fire recovery rates in the current generation of DGVMs and land-surface models are slow because plants have to regenerate from seed. The ability to resprout means that ecosystem recovery takes place much faster (Fig. 4.7). I used analyses of site-based abundance data on resprouting (Chapter 3) to identify which PFTs included both resprouters and non-resprouters. This led to the definition of for new PFTs: resprouting tropical broadleaf evergreen trees, resprouting tropical broadleaf deciduous trees, resprouting temperate broadleaf evergreen trees, resprouting temperate broadleaf deciduous trees. Further data analyses allowed me to derive a cost for resprouting in terms of a reduction in reproductive success and establishment from seeds (Chapter 4). This treatment leads to a situation in which resprouting is favoured in fire-prone areas but resprouting trees are less successful after other forms of disturbance. Thus, the relative abundance of resprouting trees and non-resprouting trees is responsive to changes in fire regimes. The inclusion of resprouting PFTs and adaptive bark thickness in LPX produces a 33% improvement in the simulated vegetation distribution across Australia (Chapter 4).

The reduced re-seeding rate in resprouting pfts compared to their non-resprouting counterparts represents an initial attempt to model a resprouting trade-off - regeneration via resprouting is at the expense of new seedling establishment. Another important consideration, which we have not attempted to model, is the cost in carbon for building and maintaining resprouting and thick bark adaptations. Thicker bark requires greater carbon investment and resprouters have a higher allocation to roots than shoots (see e.g. Knox and Morrison, 2005) and non-structural carbohydrate stores in order to fund resprouting (Clarke et al., 2013). This carbon must be diverted from other plant structures, which is likely to cause decrease juvenile growth rates

---

and increase the time for plants to reach sexual maturity (Bell and Ojeda, 1999; Lamont and Wiens, 2003; Lawes et al., 2011; Clarke et al., 2013) as well as decreasing reproductive success. Including these costs in a modelling framework would improve the representation of competition between fire adaptive (thick barked/resprouting) and non-fire adapted (thin barked/non-resprouting) PFTs. However, as of yet, there have been very few attempts to quantify these costs in a way that would allow them to be modelled.

The overarching goal of this thesis was to produce a model that provides a good representation of fire across Australia in order to be able to use it for future prediction. LPX-Mv1 incorporates improvements to the simulation of ignitions, fuel loads, fuel drying rates, fire resistance, and fire recovery rates (Chapter 4). The simulated distribution of vegetation and fire is significantly improved compared to the original version of LPX. I have applied this model to examine changes in fire regimes over the 21<sup>st</sup> century in response to projections of future climate changes (Chapter 5). Previous studies, based on calculation of some form of Fire Danger Index (FDI), have shown that the risk of fire increases across the whole of Australia in the 21<sup>st</sup> century (Beer and Williams, 1995; Williams et al., 2001; McGregor and Dix, 2001; Pitman et al., 2007). However, FDIs only take account of the prevalence of climate conditions that favour burning. They do not take account of the potential for CO<sub>2</sub> fertilization or climate-induced changes in vegetation on fuel production or structure. The LPX-Mv1 simulations show that climate-induced increases in fire risk do not necessarily translate into increases in biomass burning. The simulations imply that fire will decrease in northern Australia and increase in the interior and southeastern parts of the continent. The reduction of fire in northern Australia occurs because of increased fuel moisture and decreases in wind speed during the fire season. The increase of fire in southeastern Australia occurs because of an increase in fuel dryness in a region where fires are currently moisture-limited. The increase in fire in the interior of the continent reflects increases in fuel load in an area that is currently fuel-limited. Some of these changes reflect changes in vegetation productivity as a result of CO<sub>2</sub> fertilization. Thus, despite an increase in aridity, grass productivity is enhanced in the interior and this leads to greater fuel production and reduction of the area that is fuel limited. CO<sub>2</sub> fertilization is also responsible for the expansion of woody resprouting PFTs into relatively dry environments, which affects fuel load, structure and moisture conditions. However, the simulated expansion of woody vegetation is only possible because of the inclusion of resprouting PFTs in the model. In the absence of these fire-adapted trees, increased productivity would lead to increased fire and the replacement of trees by grasses. The maintenance of a significant tree cover, and indeed expansion of tree cover into many fire-prone regions, combined with the rapid recovery of biomass after fire due to resprouting, results in a 10% increase in carbon sequestration by the biosphere over the 21<sup>st</sup> century despite an increase in the overall amount of fire at a continental scale. This is a novel result which runs counter to inferences that might be made about the carbon budget of Australia based on changing fire danger indices or indeed DGVMs that lack realistic treatments of vegetation adaptations to fire.

## 6.1 References

- Beckage, B., Platt, W. J., and Gross, L. J.: Vegetation, Fire, and Feedbacks: A Disturbance-Mediated Model of Savannas, *The American Naturalist*, 174, 805–818, 2009.
- Beer, C., Reichstein, M., Tomelleri, E., Ciais, P., Jung, M., Carvalhais, N., Rödenbeck, C., Arain, M. A., Baldocchi, D., Bonan, G. B., Bondeau, A., Cescatti, A., Lasslop, G., Lindroth, A., Lomas, M. R., Luyssaert, S., Margolis, H., Oleson, K. W., Roupsard, O., Veenendaal, E., Viovy, N., Williams, C., Woodward, F. I., and Papale, D.: Terrestrial gross carbon dioxide uptake: global distribution and covariation with climate, *Science*, 329, 834–8, doi:10.1126/science.1184984, 2010.
- Beer, T. and Williams, A.: Estimating Australian forest fire danger under conditions of doubled carbon dioxide concentrations, *Climatic change*, 29, 169–188, 1995.
- Bell, T. L. and Ojeda, F.: Underground starch storage in Erica species of the Cape Floristic Region—differences between seeders and resprouters, *The New Phytologist*, 144, 143–152, 1999.
- Blyth, E., Gash, J., Lloyd, A., Pryor, M., Weedon, G. P., and Shuttleworth, J.: Evaluating the JULES land surface model energy fluxes using FLUXNET data, *Journal of Hydrometeorology*, 11, 509–519, 2010.
- Blyth, E., Clark, D. B., Ellis, R., Huntingford, C., Los, S., Pryor, M., Best, M., and Sitch, S.: A comprehensive set of benchmark tests for a land surface model of simultaneous fluxes of water and carbon at both the global and seasonal scale, *Geoscientific Model Development*, 4, 255–269, 2011.
- Bondeau, A., Smith, P. C., Zaehle, S., Schaphoff, S., Lucht, W., Cramer, W., Gerten, D., Lotze-Campen, H., Müller, C., Reichstein, M., and Smith, B.: Modelling the role of agriculture for the 20th century global terrestrial carbon balance, *Global Change Biology*, 13, 679–706, doi:10.1111/j.1365-2486.2006.01305.x, 2007.
- Brovkin, V., van Bodegom, P. M., Kleinen, T., Wirth, C., Cornwell, W. K., Cornelissen, J. H. C., and Kattge, J.: Plant-driven variation in decomposition rates improves projections of global litter stock distribution, *Biogeosciences*, 9, 565–576, doi:10.5194/bg-9-565-2012, 2012.
- Cadule, P., Friedlingstein, P., Bopp, L., Sitch, S., Jones, C. D., Ciais, P., Piao, S. L., and Peylin, P.: Benchmarking coupled climate-carbon models against long-term atmospheric CO<sub>2</sub> measurements, *Global Biogeochemical Cycles*, 24, GB2016, 2010.
- Christian, H. J.: Optical Detection of Lightning from Space, in: *Proceedings of the 11th International Conference on Atmospheric Electricity*, pp. 715–718, Guntersville, Alabama, 1999.

- Christian, H. J., Blakeslee, R. J., Goodman, S. J., Mach, D. A., Stewart, M. F., Buechler, D. E., Koshak, W. J., Hall, J. M., Boeck, W. L., Driscoll, K. T., and Bocippio, D. J.: The Lightning Imaging Sensor, in: Proceedings of the 11th International Conference on Atmospheric Electricity, pp. 746–749, Guntersville, Alabama, 1999.
- Clarke, P. J., Lawes, M. J., Midgley, J. J., Lamont, B. B., Ojeda, F., Burrows, G. E., Enright, N. J., and Knox, K. E. J.: Resprouting as a key functional trait: how buds, protection and resources drive persistence after fire., *The New Phytologist*, 197, 19–35, doi:10.1111/nph.12001, 2013.
- Cochrane, M. A., Alencar, A., and Schulze, M.: Positive feedbacks in the fire dynamic of closed canopy tropical forests, *Science*, 284, 1832–1835, 1999.
- Cummins, K. and Murphy, M.: An overview of lightning locating systems: History, techniques, and data uses, with an in-depth look at the US NLDN, *Electromagnetic Compatibility*, IEEE ..., 51, 499–518, 2009.
- Higgins, R. W. and Climate Prediction Centre, U.: Improved United States precipitation quality control system and analysis, in: NCEP/Climate Prediction Center ATLAS No. 6, NOAA, National Weather Service, National Centers for Environmental Prediction, Climate Prediction Center, Camp Springs, Md, 2000.
- Higgins, R. W., Janowiak, J. E., and Yao, Y.-P.: A gridded hourly precipitation data base for the United States (1963-1993), in: NCEP/Climate Prediction Center Atlas 1, p. 46, NOAA, National Weather Service, National Centers for Environmental Prediction, Climate Prediction Center, Camp Springs, Md, 1996.
- Kattge, J., Diaz, S., Lavorel, S., Prentice, I. C., Leadley, P., Bonisch, G., Garnier, E., Westoby, M., Reich, P. B., Wright, I. J., Cornelissen, J. H. C., Violette, C., Harrison, S. P., Van Bodegom, P. M., Reichstein, M., Enquist, B. J., Soudzilovskaia, N. A., Ackerman, D. D., Anand, M., Atkin, O., Bahn, M., Baker, T. R., Baldocchi, D., Bekker, R., Blanco, C. C., Blonder, B., Bond, W. J., Bradstock, R. A., Bunker, D. E., Casanoves, F., Cavender-Bares, J., Chambers, J. Q., Chapin III, F. S., Chave, J., Coomes, D., Cornwell, W. K., Craine, J. M., Dobrin, B. H., Duarte, L., Durka, W., Elser, J., Esser, G., Estiarte, M., Fagan, W. F., Fang, J., Fernandez-Mendez, F., Fidelis, A., Finegan, B., Flores, O., Ford, H., Frank, D., Freschet, G. T., Fyllas, N. M., Gallagher, R. V., Green, W. A., Gutierrez, A. G., Hickler, T., Higgins, S. I., Hodgson, J. G., Jalili, A., Jansen, S., Joly, C. A., Kerkhoff, A. J., Kirkup, D., Kitajima, K., Kleyer, M., Klotz, S., Knops, J. M. H., Kramer, K., Kuhn, I., Kurokawa, H., Laughlin, D. C., Lee, T. D., Leishman, M., Lens, F., Lenz, T., Lewis, S. L., Lloyd, J., Llusia, J., Louault, F., Ma, S., MAHECHA, M. D., Manning, P., Massad, T., Medlyn, B. E., Messier, J., Moles, A. T., Muller, S. C., Nadrowski, K., Naeem, S., Niinemets, U., Nollert, S., Nuske, A., Ogaya, R., Oleksyn, J., Onipchenko, V. G., Onoda, Y., Ordonez, J., Overbeck, G., Ozinga, W. A., Patino, S., Paula, S., Pausas, J. G., Penuelas, J., Phillips, O. L., Pillar, V., Poorter, H., Poorter, L., Poschlod, P., Prinzing, A., Proulx, R., Rammig, A., Reinsch, S., Reu, B., Sack, L., Salgado-Negret, B., Sardans, J., Shiodera, S., Shipley, B., Siefert, A., Sosinski, E., Soussana, J.-F., Swaine, E., Swenson, N., Thompson, K.,

Thornton, P., Waldram, M., Weiher, E., White, M., White, S., Wright, S. J., Yguel, B., Zaehle, S., Zanne, A. E., and Wirth, C.: TRY – a global database of plant traits, *Global Change Biology*, 17, 2905–2935, doi:10.1111/j.1365-2486.2011.02451.x, 2011.

Knox, K. J. and Morrison, D. A.: Effects of inter-fire intervals on the reproductive output of resprouters and obligate seeders in the Proteaceae, *Austral Ecology*, 30, 407–413, 2005.

Lamont, B. B. and Wiens, D.: Are seed set and speciation rates always low among species that resprout after fire, and why?, *Evolutionary Ecology*, 17, 277–292, 2003.

Lawes, M. J., Richards, A., Dathe, J., and Midgley, J. J.: Bark thickness determines fire resistance of selected tree species from fire-prone tropical savanna in north Australia, *Plant Ecology*, 212, 2057–2069, doi:10.1007/s11258-011-9954-7, 2011.

Lehmann, C. E. R., Archibald, S., Hoffmann, W. A., and Bond, W. J.: Deciphering the distribution of the savanna biome., *The New Phytologist*, 191, 197–209, doi:10.1111/j.1469-8137.2011.03689.x, 2011.

Lenihan, J. M., Daly, C., Bachelet, D., and Neilson, R. P.: Simulating broad-scale fire severity in a dynamic global vegetation model, *Northwest Science*, 72, 91–103, 1998.

Li, F., Zeng, X. D., and Levis, S.: A process-based fire parameterization of intermediate complexity in a Dynamic Global Vegetation Model, *Biogeosciences*, 9, 2761–2780, doi:10.5194/bg-9-2761-2012, 2012.

Luo, Y. Q., Randerson, J. T., Abramowitz, G., Bacour, C., Blyth, E., Carvalhais, N., Ciais, P., Dalmonech, D., Fisher, J. B., Fisher, R., Friedlingstein, P., Hibbard, K., Hoffman, F. M., Huntzinger, D., Jones, C. D., Koven, C., Lawrence, D. M., Li, D. J., Mahecha, M., Niu, S. L., Norby, R., Piao, S. L., Qi, X., Peylin, P., Prentice, I. C., Riley, W., Reichstein, M., Schwalm, C., Wang, Y. P., Xia, J. Y., Zaehle, S., and Zhou, X. H.: A framework for benchmarking land models, *Biogeosciences*, 9, 3857–3874, doi:10.5194/bg-9-3857-2012, 2012.

Mcgregor, J. L. and Dix, M. R.: The CSIRO conformal-cubic atmospheric GCM, in: IUTAM Symposium on Advances in Mathematical Modelling of Atmosphere and Ocean Dynamics, pp. 197–202, Springer, 2001.

Pfeiffer, M., Spessa, A., and Kaplan, J. O.: A model for global biomass burning in preindustrial time: LPJ-LMfire (v1.0), *Geoscientific Model Development*, 6, 643–685, doi:10.5194/gmd-6-643-2013, 2013.

Pitman, A. J., Narisma, G. T., and McAneney, J.: The impact of climate change on the risk of forest and grassland fires in Australia, *Climatic Change*, 84, 383–401, doi:10.1007/s10584-007-9243-6, 2007.

Prentice, I. C., Kelley, D. I., Foster, P. N., Friedlingstein, P., Harrison, S. P., and Bartlein, P. J.: Modeling fire and the terrestrial carbon balance, *Global Biogeochemical Cycles*, 25, 1–13, doi:10.1029/2010GB003906, 2011.

Prentice, I. C., Dong, N., Gleason, S. M., Maire, V., and Wright, I. J.: Balancing the costs of carbon gain and water transport: testing a new theoretical framework for plant functional ecology., *Ecology letters*, 17, 82–91, doi:10.1111/ele.12211, 2014.

Randerson, J. T., Hoffman, F. M., Thornton, P. E., Mahowald, N. M., Lindsay, K., Lee, Y.-H., Nevison, C. D., Doney, S. C., Bonan, G. B., Stöckli, R., Covey, C., Running, S. W., and Fung, I. Y.: Systematic assessment of terrestrial biogeochemistry in coupled climate-carbon models, *Global Change Biology*, 15, 2462–2484, doi:10.1111/j.1365-2486.2009.01912.x, 2009.

Schenk, H. J. and Jackson, R.: Rooting depths, lateral root spreads and below-ground/aboveground allometries of plants in waterlimited ecosystems, *Journal of Ecology*, pp. 480–494, 2002a.

Schenk, H. J. and Jackson, R.: The global biogeography of roots, *Ecological monographs*, 72, 311–328, 2002b.

Schenk, H. J. and Jackson, R. B.: Mapping the global distribution of deep roots in relation to climate and soil characteristics, *Geoderma*, 126, 129–140, doi:10.1016/j.geoderma.2004.11.018, 2005.

Smith, M. J., Vanderwel, M. C., Lyutsarev, V., Emmott, S., and Purves, D. W.: The climate dependence of the terrestrial carbon cycle; including parameter and structural uncertainties., *Biogeosciences Discussions*, 9, 2012.

Thonicke, K., Venevsky, S., Sitch, S., and Cramer, W.: The role of fire disturbance for global vegetation dynamics: coupling fire into a Dynamic Global Vegetation Model, *Global Ecology and Biogeography*, 10, 661–677, doi:10.1046/j.1466-822X.2001.00175.x, 2001.

Verheijen, L. M., Brovkin, V., Aerts, R., Bönisch, G., Cornelissen, J. H. C., Kattge, J., Reich, P. B., Wright, I. J., and van Bodegom, P. M.: Impacts of trait variation through observed traitclimate relationships on performance of an Earth system model: a conceptual analysis, *Biogeosciences*, 10, 5497–5515, doi:10.5194/bg-10-5497-2013, 2013.

Wang, H., Prentice, I. C., and Ni, J.: Primary production in forests and grasslands of China: contrasting environmental responses of light- and water-use efficiency models, *Biogeosciences*, 9, 4689–4705, doi:10.5194/bg-9-4689-2012, 2012.

Wang, H., Prentice, I. C., and Ni, J.: Data-based modelling and environmental sensitivity of vegetation in China, *Biogeosciences*, 10, 5817–5830, doi:10.5194/bg-10-5817-2013, 2013.

Wang, H., Prentice, I. C., and Davis, T. W.: Biophysical constraints on gross primary production by the terrestrial biosphere, *Biogeosciences Discussions*, 11, 3209–3240, doi:10.5194/bgd-11-3209-2014, 2014.

Wania, R.: Modelling northern peatland land surface processes, vegetation dynamics and methane emissions, Phd, University of Bristol, 2007.

Wania, R., Ross, I., and Prentice, I. C.: Implementation and evaluation of a new methane model within a dynamic global vegetation model: LPJ-WHyMe v1.3.1, Geoscientific Model Development, 3, 565–584, doi:10.5194/gmd-3-565-2010, 2010.

Williams, A., Karoly, D., and Tapper, N. J.: The sensitivity of Australian fire danger to climate change, Climatic change, pp. 171–191, 2001.

Zeng, X., Zeng, X., and Barlage, M.: Growing temperate shrubs over arid and semiarid regions in the Community Land Model-Dynamic Global Vegetation Model, Global Biogeochemical Cycles, 22, GB3003, doi:10.1029/2007GB003014, 2008.